

COUPLED-CLUSTER STUDIES OF QUANTUM DOTS

Magnus Pedersen Lohne



THESIS SUBMITTED FOR THE DEGREE OF
MASTER OF SCIENCE IN COMPUTATIONAL PHYSICS

Department of Physics
University of Oslo

June 2010

Acknowledgements

Abstract

Contents

1	Introduction	1
I	THEORY	3
2	Quantum Mechanics	5
2.1	Postulates of Quantum Mechanics	6
2.2	Single-Particle Quantum Mechanics	8
2.2.1	Coordinate Representation	9
2.2.2	Intrinsic Spin	11
2.2.3	Total Wavefunction	13
3	Many-Body Theory	15
3.1	The Many-Body Problem	15
3.2	The Non-Interacting System	17
3.3	Identical Particles	18
3.4	The Interacting Many-Body System	20
3.4.1	Hilbert Space of Distinguishable Particles	20
3.4.2	Hilbert Space of Bosons and Fermions	21
3.5	Second Quantization	22
3.5.1	Creation and Annihilation Operators	22
3.5.2	Operators in Second Quantization	23
3.5.3	Wick's Theorem	25
3.5.4	Particle-Hole Formalism	27
4	Theoretical Description of Quantum Dots	31
4.1	Approximations	31
4.2	Schrödinger Equation for Spherically Symmetric Potentials	32
4.3	Solutions for the Single-Electron Parabolic Quantum Dot	34
4.4	N -Electron Model Hamiltonian	40
4.5	Scaling the Model Hamiltonian	41
II	MANY-BODY METHODS	43
5	Hartree-Fock Method	45
5.1	Introduction	45
5.2	Basic Ideas	46
5.3	Derivation of the Hartree-Fock Equations	47

6 Coupled-Cluster Method	51
6.1 Introduction and Fundamental Ideas	51
6.1.1 Notation	54
6.2 Fundamental Concepts	55
6.3 Formal Coupled-Cluster Theory	59
6.4 Coupled-Cluster Singles and Doubles Equations	60
6.4.1 Normal-Ordered Form of the Hamiltonian	60
6.4.2 The Campbell-Baker-Hausdorff Expansion	62
6.4.3 Energy Equation - An Algebraic Approach	63
6.4.4 Coupled-Cluster Diagrams	68
6.4.5 Energy Equation on Diagrammatic Form	73
6.4.6 Amplitude Equations on Diagrammatic Form	74
6.4.7 Amplitude Equations on Algebraic Form	80
III IMPLEMENTATIONS AND RESULTS	87
7 Implementation	89
7.1 Implementation of the Hartree-Fock Method	89
7.1.1 Overview	90
7.1.2 Validation of the Code	90
7.1.3 Code Structure and Class Implementation	91
7.2 Implementation of the Coupled-Cluster method	94
7.2.1 Overview	95
7.2.2 Validation of the Code	96
7.2.3 Code Structure and Class Implementation	98
7.2.4 Implementation of the CCSD Algorithm	100
7.2.5 F-matrix and Interaction Elements	103
7.2.6 Implementation of the Amplitude Equations	106
8 Numerical Results and Analysis	125
8.1 Standard interaction	125
8.1.1 Tables of Numerical Results	127
8.1.2 General Analysis and Discussion	135
8.1.3 Full Correlation Energy	139
8.1.4 Correlation Energy	140
8.1.5 CCSD Correlation Energy	141
8.1.6 Analysis of the Amplitudes	142
8.1.7 Analysis of Basis Size	143
8.1.8 Hartree-Fock Basis	153
8.2 Effective Interaction	153
8.2.1 Tables of Numerical Results	156
A Mathematical Derivations	157
A.1 Solution of the Single-Electron Schrödinger Equation	157

Chapter 1

Introduction

Part I

THEORY

Chapter 2

Quantum Mechanics

Mechanics is the field of physics concerned with the behaviour of physical bodies when subjected to forces, and the effect of the bodies on the environment. We have two major sub-fields in the science of mechanics. *Classical Mechanics* is used for describing the dynamics of macroscopic objects, while *Quantum Mechanics* is used for describing the dynamics of microscopic objects. Quantum Mechanics is a theoretical description of Nature that was created by European researchers in 1925-28. The theory contained elements that were completely unknown in classical mechanics:

- Quantization: Many physical quantities can only have certain discrete values.
- Wave-particle duality: Both particles and fields (for example electromagnetic fields) have wave properties and particle properties.
- Probability interpretation: The quantum mechanical description can only give the probability to find a particle at a certain location.
- Uncertainty principle: Nature puts fundamental limits on the precision that some physical variables can be measured by.
- Annihilation and creation: Any particle can be destroyed or created.

Quantum Mechanics was created because many experimental results were totally inconsistent with classical physics. Already in 1752, Thomas Melvill observed the characteristic sodium line. Frauenhofers measurements of the spectrum of the sunlight in 1814 served as a basis for many spectroscopic experiments. Johann Balmer discovered in 1885 an empirical equation that determines the wavelength of the emitted light from a hydrogen gas. It is given as

$$\lambda_n = 3.6456 \cdot 10^{-7} \frac{n^2}{n^2 - 4} \text{m}, \quad (2.1)$$

where $n = 3, 4, 5, 6$. None of these experiments could be understood with classical physics. However, the *real* crisis in physics came with the photoelectric effect, the Compton effect, and diffraction experiments with electrons. See [1] for a brief overview.

Put simply, Quantum Mechanics is the theoretical framework within which it has been found possible to describe, correlate and predict the behaviour of a vast range of physical systems: from systems containing elementary particles, through nuclei and atoms, to molecules and solids. This chapter aims to give a short review of Quantum Mechanics. It is assumed that the reader is well acquainted with the fundamental theory. The focus in the presentation will be on parts that are directly relevant for this thesis. The first section is devoted to the general postulates of Quantum Mechanics. In the second chapter we present basic concepts of single-particle Quantum Mechanics, with an emphasize on the time-independent Schrödinger equation, coordinate representation, intrinsic spin, and the total wavefunction of a particle. We refer to [1] and [2] for a complete introduction to the field. For a more profound presentation, we refer to [3].

2.1 Postulates of Quantum Mechanics

Every fundamental physical theory is based on postulates. We will in the following present the postulates of Quantum Mechanics.

- [1] A quantum state of an isolated system is described by a vector in a complex (finite/infinite) linear vector space, called Hilbert space.

Comments: In the bra-ket formalism (see [3]), for every quantum quantum state $|\Psi\rangle$ in the Hilbert space (called “ket”), there exists a dual state $\langle\Psi|$ in a dual vector space (called “bra”). The Hilbert space \mathcal{H} is a complex inner product space [4], meaning that \mathcal{H} is a complex vector space on which there exists an inner product. An inner product is a function that, to each pair of vectors $|\alpha\rangle$ and $|\beta\rangle$ in \mathcal{H} , associates a complex number

$$\langle\alpha|\beta\rangle. \quad (2.2)$$

It satisfies

$$\langle\alpha|\beta\rangle = \langle\beta|\alpha\rangle^* \quad (2.3)$$

$$\langle c_1\alpha_1 + c_2\alpha_2|\beta\rangle = c_1\langle\alpha_1|\beta\rangle + c_2\langle\alpha_2|\beta\rangle \quad (2.4)$$

$$\langle c\alpha|\beta\rangle = c\langle\alpha|\beta\rangle \quad (2.5)$$

$$\langle\alpha|\alpha\rangle \geq 0, \quad (2.6)$$

where $*$ is the complex conjugate, and c , c_1 and c_2 are complex numbers. We refer to [4] for a more profound discussion of complex vector spaces. For any finite/infinite dimensional Hilbert space, we can find a basis set. Assume a discrete basis with orthonormality relation

$$\langle i|j\rangle = \delta_{ij}, \quad (2.7)$$

and completeness relation

$$\hat{I} = \sum_i |i\rangle\langle i|, \quad (2.8)$$

where δ_{ij} is the Kronecker delta, and \hat{I} is the identity operator. The quantum state can then be written as

$$|\Psi\rangle = \sum_i |i\rangle\langle i|\Psi\rangle = \sum_i c_i|i\rangle, \quad (2.9)$$

where $c_i = \langle i|\Psi\rangle$. When the basis is continuous, the orthonormality relation is given as

$$\langle x|x'\rangle = \delta(x - x'), \quad (2.10)$$

and the completeness relation as

$$\hat{I} = \int dx |x\rangle\langle x|, \quad (2.11)$$

where $\delta(x - x')$ is the Dirac delta function. The quantum state then reads

$$|\Psi\rangle = \int dx |x\rangle\langle x|\Psi\rangle = \int dx c(x)|x\rangle, \quad (2.12)$$

where $c(x) = \langle x|\Psi\rangle$.

- [2] To every physical observable of a quantum system corresponds a linear, hermitian operator acting on vectors in the Hilbert space. Operators representing the generalized coordinate q_n and the corresponding generalized momentum p_n satisfy the commutation relation

$$[\hat{q}_n, \hat{p}_n] = i\hbar, \quad (2.13)$$

here i is the imaginary unit, and \hbar is the (reduced) Planck constant.

Comments: A hermitian operator is defined as

$$\hat{A} = \hat{A}^\dagger, \quad (2.14)$$

where \hat{A}^\dagger is the hermitian conjugate of \hat{A} . The eigenstates $|a_i\rangle$ and eigenvalues a_i of \hat{A} are given by the eigenvalue equation

$$\hat{A}|a_i\rangle = a_i|a_i\rangle. \quad (2.15)$$

The set of eigenfunctions $\{|a_i\rangle\}_{i=1}^d$, where d is the dimension of the Hilbert space, form a complete set of vectors, i.e.

$$\hat{I} = \sum_i^d |a_i\rangle\langle a_i|. \quad (2.16)$$

Furthermore, the spectral decomposition of any hermitian operator is given as

$$\hat{A} = \sum_i^d a_i |a_i\rangle\langle a_i|. \quad (2.17)$$

- [3] The time evolution of the quantum state is (in the Schrödinger picture) represented by a time-dependent state vector $|\Psi(t)\rangle$ that satisfies the fundamental Schrödinger equation

$$i\hbar \frac{d}{dt} |\Psi(t)\rangle = \hat{H} |\Psi(t)\rangle, \quad (2.18)$$

with \hat{H} as the Hamiltonian of the system.

Comments: Since the Schrödinger equation is a linear differential equation with a first order time derivative, the quantum state $|\Psi(t)\rangle$ is uniquely determined by $|\Psi(t_0)\rangle$ for $t_0 \neq t$. Thus

$$|\Psi(t)\rangle = \hat{\mathcal{U}}(t, t_0) |\Psi(t_0)\rangle, \quad (2.19)$$

where $\hat{\mathcal{U}}(t, t_0)$ is the time evolution operator determined by \hat{H} . We have that $\hat{\mathcal{U}}(t, t_0)$ must be linear and unitary, i.e.

$$\hat{\mathcal{U}}\hat{\mathcal{U}}^\dagger = \hat{\mathcal{U}}^\dagger\hat{\mathcal{U}} = \hat{I}, \quad (2.20)$$

where \hat{I} is the identity operator. Inserting Eq. (2.19) into Eq. (2.18) yields the following equation for the time evolution operator,

$$i\hbar \frac{\partial}{\partial t} \hat{\mathcal{U}}(t, t_0) = \hat{H}(t) \hat{\mathcal{U}}(t, t_0). \quad (2.21)$$

When the Hamiltonian is time-independent, we obtain

$$\hat{\mathcal{U}}(t, t_0) = e^{-i\hat{H}(t-t_0)/\hbar}. \quad (2.22)$$

Thus, given an initial quantum state $|\Psi(t_0)\rangle$, the quantum state (for an isolated system) at $t > t_0$ is given as

$$|\Psi(t)\rangle = e^{-i\hat{H}(t-t_0)/\hbar} |\Psi(t_0)\rangle. \quad (2.23)$$

- [4] In any measurement of the observable associated with the operator \hat{A} , the measured value will *always* be an eigenvalue of \hat{A} . The eigenvalue equation is given as

$$\hat{A}|a_i\rangle = a_i|a_i\rangle, \quad (2.24)$$

where a_i is the eigenvalue and $|a_i\rangle$ is the corresponding eigenvector.

Comments: For a system in quantum state $|\Psi\rangle$, the measured eigenvalue a_i will appear with probability

$$p_i = \sum_{n=1}^l |\langle a_{in}|\Psi\rangle|^2, \quad (2.25)$$

where $l = 1, 2, 3, \dots$, and

$$\hat{A}|a_{in}\rangle = a_i|a_{in}\rangle, \quad (2.26)$$

where $\{|a_{in}\rangle\}_{n=1}^l$ are possible degenerate eigenfunctions. When the energy level is degenerate, i.e. several eigenfunctions have the same energy, $l > 1$. In the non-degenerate case we have that $l = 1$. The eigenvalues a_i and eigenvectors $|a_{in}\rangle$ are given by

$$\hat{A}|a_{in}\rangle = a_i|a_{in}\rangle. \quad (2.27)$$

When the eigenvalue x of an operator \hat{x} is a continuous variable, the orthonormality relation reads

$$\langle x|x'\rangle = \delta(x - x'). \quad (2.28)$$

In this case, p_i (in Eq. 2.25) is a probability density.

- [5] In an ideal measurement, when the measured value of an observable \hat{A} is a_i , the quantum state immediately changes to the corresponding eigenstate, i.e.

$$|\Psi\rangle \rightarrow |a_i\rangle. \quad (2.29)$$

Comments: This is called the collapse of the wavefunction. When a measurement of \hat{A} gives a_i , measurements at all later times will with certainty yield a_i .

2.2 Single-Particle Quantum Mechanics

Consider a single-particle system with Hamiltonian

$$\hat{H} = \hat{T} + \hat{U}, \quad (2.30)$$

where \hat{T} is the kinetic energy operator, and \hat{U} is the potential energy operator. The dynamics of the system is provided by the time-dependent Schrödinger equation, which in bra-ket notation reads

$$i\hbar \frac{d}{dt} |\Psi(t)\rangle = \hat{H}|\Psi(t)\rangle, \quad (2.31)$$

where $|\Psi(t)\rangle$ is the quantum state of the system at time t , i is the standard imaginary unit with the property $i^2 = -1$, and \hbar is the (reduced) Planck constant. When the Hamiltonian is time-independent, the time evolution of the state vector reads (see Postulate C in Sec. 2)

$$|\Psi(t)\rangle = \hat{\mathcal{U}}(t, t_0)|\Psi(t_0)\rangle, \quad (2.32)$$

where

$$\hat{U}(t, t_0) = e^{i\hat{H}(t-t_0)/\hbar}, \quad (2.33)$$

and $|\Psi(t_0)\rangle$ is the initial state vector. Since the time evolution of the state vector is totally determined by the Hamiltonian, the solutions of the energy eigenvalue equation,

$$\hat{H}|\phi_j\rangle = \epsilon_j|\phi_j\rangle, \quad (2.34)$$

can be used to obtain an analytical expression of $|\Psi(t)\rangle$. This equation is called the time-independent Schrödinger equation. When the eigenvalues ϵ_j and eigenvectors $|\phi_j\rangle$ are determined, the initial state vector can be written as

$$|\Psi(t_0)\rangle = \sum_{j=1}^d \langle \phi_j | \Psi(t_0) \rangle |\phi_j\rangle, \quad (2.35)$$

since

$$\hat{I} = \sum_{j=1}^d |\phi_j\rangle \langle \phi_j|, \quad (2.36)$$

where d is the dimension of the Hilbert space. See Postulate A in Sec. 2. The quantum state at time $t > t_0$ then reads

$$|\Psi(t)\rangle = e^{i\hat{H}(t-t_0)/\hbar} \sum_{j=1}^d \langle \phi_j | \Psi(t_0) \rangle |\phi_j\rangle = \sum_{j=1}^d \langle \phi_j | \Psi(t_0) \rangle e^{i\epsilon_j(t-t_0)/\hbar} |\phi_j\rangle. \quad (2.37)$$

Provided an initial state vector and a time-independent Hamiltonian, the state vector at time $t > t_0$ can in principle always be determined by solving the time-independent Schrödinger equation in (2.34). In addition, the energy spectrum is often the main interest in quantum mechanical calculations. We will therefore in the following consider the time-independent Schrödinger equation.

2.2.1 Coordinate Representation

The time-independent Schrödinger equation in (2.34) is written in the bra-ket formalism. This formalism offers a general and concise notation. When we want to do explicit calculations, we often transform the time-independent Schrödinger equation to the coordinate representation. In the 1-dimensional case, the eigenvalue equation of the position operator \hat{x} reads

$$\hat{x}|x\rangle = x|x\rangle, \quad (2.38)$$

where $|x\rangle$ is the eigenvector and x is the corresponding eigenvalue. The completeness relation reads

$$\hat{I} = \int_{-\infty}^{\infty} dx |x\rangle \langle x|. \quad (2.39)$$

The energy eigenfunctions in Eq. (2.34) can then be written as (suppressing the j -index)

$$|\phi\rangle = \int_{-\infty}^{\infty} dx \phi(x) |x\rangle, \quad (2.40)$$

where we have defined

$$\phi(x) \equiv \langle x | \phi \rangle. \quad (2.41)$$

We multiply Eq. (2.34) with $\langle x|$ from the left, yielding

$$\langle x|\hat{H}|\phi\rangle = \epsilon\langle x|\phi\rangle. \quad (2.42)$$

Using the completeness relation in Eq. (2.39) we obtain

$$\int_{-\infty}^{\infty} dx' \langle x|\hat{H}|x'\rangle \langle x'|\phi\rangle = \epsilon\langle x|\phi\rangle, \quad (2.43)$$

leading to

$$\int_{-\infty}^{\infty} dx' \langle x|\hat{H}|x'\rangle \phi(x') = \epsilon\phi(x), \quad (2.44)$$

where we have used the definition in Eq. (2.41). In the 1-dimensional case, the momentum operator is given as [1]

$$\hat{p} = -i\hbar \frac{\partial}{\partial x}. \quad (2.45)$$

When $\hat{H} = \hat{H}(\hat{x}, \hat{p})$,

$$\langle x|\hat{H}(\hat{x}, \hat{p})|x'\rangle = \hat{H}(x, -i\hbar \frac{\partial}{\partial x})\delta(x - x'), \quad (2.46)$$

where $\delta(x - x')$ is the Dirac delta function. See [1] for a derivation. Inserting this expression into Eq. (2.44) yields

$$\hat{H}(x, -i\hbar \frac{\partial}{\partial x})\phi(x) = \epsilon\phi(x), \quad (2.47)$$

which is nothing but the time-independent Schrödinger equation in the coordinate representation. Suppressing the parenthesis in the Hamiltonian, the 3-dimensional time-independent Schrödinger equation reads

$$\hat{H}\phi(x, y, z) = \epsilon\phi(x, y, z), \quad (2.48)$$

where x, y and z are cartesian coordinates. In classical mechanics, the kinetic energy of a particle is given as

$$T = \frac{p^2}{2m}, \quad (2.49)$$

where $p = mv$ is the momentum, and m is the mass of the particle. The quantum mechanical kinetic energy thus reads

$$\hat{T} = \frac{\hat{p}^2}{2m}, \quad (2.50)$$

where T and p are changed to \hat{T} and \hat{p} . In 3-dimensions, the momentum operator is given as

$$\hat{p} = i\hbar\nabla, \quad (2.51)$$

where ∇ is the gradient. The Hamiltonian in Eq. (2.30) thus reads

$$\hat{H} = \frac{\hat{p}^2}{2m} + u(x, y, z) = -\frac{\hbar^2}{2m}\nabla^2 + u(x, y, z), \quad (2.52)$$

leading to the most common form of the time-independent Schrödinger equation,

$$\left(-\frac{\hbar^2}{2m}\nabla^2 + u(x, y, z)\right)\phi(x, y, z) = \epsilon\phi(x, y, z), \quad (2.53)$$

where $\phi(x, y, z)$ is the eigenfunction with corresponding eigenvalue ϵ , m is the mass of the particle, and $u = u(x, y, z)$ is the potential.

2.2.2 Intrinsic Spin

In classical mechanics, an object admits two kinds of angular momentum. The first is the orbital momentum defined as

$$\mathbf{L} = \mathbf{r} \times \mathbf{p}, \quad (2.54)$$

where \mathbf{r} is the position vector and \mathbf{p} is the momentum vector. The second is the spin momentum

$$\mathbf{S} = I\omega, \quad (2.55)$$

where I is the moment of inertia, and ω is the angular velocity. While the angular momentum is associated with the motion of the center of mass, the spin momentum is associated with motion about the center of mass. In quantum mechanics, angular momentum is also associated with the motion of particles in space. The particles also carry another form of angular momentum, which has nothing to do with motion in space. This angular momentum is somewhat analogous to the classical spin, and we therefore use the same word. We say that the particles carry *intrinsic spin*. In quantum mechanics, observables are represented by operators. Since S and L are observable quantities,

$$S \rightarrow \hat{S} \quad (2.56)$$

$$L \rightarrow \hat{L}. \quad (2.57)$$

The algebraic theory of spin is identical to the theory of orbital angular momentum [1]. The fundamental commutation relations reads

$$[\hat{S}_x, \hat{S}_y] = i\hbar\hat{S}_z \quad [\hat{S}_y, \hat{S}_z] = i\hbar\hat{S}_x \quad [\hat{S}_z, \hat{S}_x] = i\hbar\hat{S}_y, \quad (2.58)$$

where \hat{S}_x , \hat{S}_y and \hat{S}_z are the components of \hat{S} . The eigenvectors of \hat{S}^2 and \hat{S}_z satisfy [1]

$$\hat{S}^2|s m_s\rangle = \hbar s(s+1)|s m_s\rangle \quad (2.59)$$

$$\hat{S}_z|s m_s\rangle = \hbar m_s|s m_s\rangle, \quad (2.60)$$

where s is the principal spin quantum number, and m_s is the quantum number associated with the z-projection of the spin. Since the components of the spin do not have a common set of eigenfunctions, they are incompatible observables. This means that we cannot determine two components, say \hat{S}_z and \hat{S}_x , at the same time. However, we can determine *one* of the components and \hat{S}^2 simultaneously. Standard textbooks in quantum mechanics often choose the z-component of the spin (see for example [1], [2] and [5]), and we therefore also do so. Since the intrinsic spin cannot be associated with motion in space, the eigenfunctions of \hat{S}_z and \hat{S}^2 cannot be written down as analytical functions. The spin quantum numbers are given as [2]

$$s = 0, \frac{1}{2}, 1, \frac{3}{2}, 2, \frac{5}{2}, \dots \quad (2.61)$$

$$m_s = -s, -s+1, \dots, s-1, s. \quad (2.62)$$

Each elementary particle has a specific and immutable value of s . Often we call s the *spin* of the particle. Electrons have spin $\frac{1}{2}$, photons have spin 1, gravitons have spin 2, and so forth. The measured value of \hat{S}^2 for a certain elementary particle will therefore *always* be $\hbar s(s+1)$.

We will now consider the spin $\frac{1}{2}$ case, i.e.

$$s = \frac{1}{2}, \quad (2.63)$$

which is by far the most important case. This is the spin of electrons, protons, neutrons, quarks, and leptons. The measured value of \hat{S}^2 will in this case be $3\hbar^2/4$. Since $s = 1/2$, the quantum number associated with the z-projection of the spin can have two values,

$$m_s = \pm \frac{1}{2}. \quad (2.64)$$

The measured value of \hat{S}_z (or another component of the spin) will therefore be either $\hbar/2$ or $-\hbar/2$. The eigenfunctions of \hat{S}^2 and \hat{S}_z are given as

$$\left| \frac{1}{2}, \frac{1}{2} \right\rangle \equiv |+\rangle \quad (2.65)$$

$$\left| \frac{1}{2}, -\frac{1}{2} \right\rangle \equiv |-\rangle \quad (2.66)$$

which are often referred to as *spin up* and *spin down*, respectively. Thus, when $s = 1/2$, the Hilbert space of the spin is 2-dimensional. Using the eigenstates of \hat{S}^2 and \hat{S}_z in Eqs. (2.65) and (2.66) as basis vectors, the general state of a spin 1/2 particle reads

$$|\chi\rangle = a|+\rangle + b|-\rangle, \quad (2.67)$$

where a and b are the weights. We often call $|\chi\rangle$ a spinor. The spinor must be normalized, i.e. $\sqrt{a^2 + b^2} = 1$. The measured value of the z-component of the spin for a particle in state $|\chi\rangle$ will be $\hbar/2$ with probability $|a|^2$, and $-\hbar/2$ with probability $|b|^2$. Since the Hilbert space is 2-dimensional, we can represent spinors by [1]

$$|\chi\rangle = \begin{pmatrix} a \\ b \end{pmatrix}, \quad (2.68)$$

and operators by

$$\hat{A} = \begin{pmatrix} c & d \\ e & f \end{pmatrix}. \quad (2.69)$$

The basis is thus given as

$$|+\rangle = \begin{pmatrix} 1 \\ 0 \end{pmatrix} \quad |-\rangle = \begin{pmatrix} 0 \\ 1 \end{pmatrix}. \quad (2.70)$$

The matrix representation of \hat{S}^2 and \hat{S}_z are determined by considering the eigenvalue equation for $|+\rangle$ and $|-\rangle$, yielding

$$\hat{S}^2 = \frac{3}{4}\hbar^2 \begin{pmatrix} 1 & 0 \\ 0 & 1 \end{pmatrix}, \quad (2.71)$$

and

$$\hat{S}_z = \frac{\hbar}{2} \begin{pmatrix} 1 & 0 \\ 0 & -1 \end{pmatrix}. \quad (2.72)$$

In the basis of $|+\rangle$ and $|-\rangle$, we have the following matrix representation of \hat{S}_x and \hat{S}_y ,

$$\hat{S}_x = \frac{\hbar}{2} \begin{pmatrix} 0 & 1 \\ 1 & 0 \end{pmatrix} \quad \hat{S}_y = \frac{\hbar}{2} \begin{pmatrix} 0 & -i \\ i & 0 \end{pmatrix}, \quad (2.73)$$

where i is the imaginary unit. Defining the so-called *Pauli spin matrices*

$$\hat{\sigma}_x \equiv \begin{pmatrix} 0 & 1 \\ 1 & 0 \end{pmatrix} \quad \hat{\sigma}_y \equiv \begin{pmatrix} 0 & -i \\ i & 0 \end{pmatrix} \quad \hat{\sigma}_z \equiv \begin{pmatrix} 1 & 0 \\ 0 & -1 \end{pmatrix}, \quad (2.74)$$

we obtain

$$\hat{S}_x = \frac{\hbar}{2}\hat{\sigma}_x \quad \hat{S}_y = \frac{\hbar}{2}\hat{\sigma}_x \quad \hat{S}_z = \frac{\hbar}{2}\hat{\sigma}_z. \quad (2.75)$$

2.2.3 Total Wavefunction

Consider the time-independent Schrödinger equation in (2.53). Since the intrinsic spin of a particle has nothing to do with motion in space, the spin degree of freedom cannot be included directly in the energy eigenfunctions $\phi(x, y, z)$. However, the spin degree of freedom must be included in some way. First we note that the Hilbert space of the spin, and the Hilbert space spanned by the energy eigenfunctions, are two distinct spaces. The solution to include the spin is to divide the wavefunction into two parts that exist in different spaces. Operators must also be modified in order to reflect which space they act in. Mathematically, this is obtained by the so-called tensor product [6]. We now define the *total* energy eigenfunctions of the time-independent Schrödinger equation as

$$\psi(\mathbf{r}) \equiv \phi(x, y, z) \otimes |\chi\rangle, \quad (2.76)$$

where \mathbf{r} include the spin degree of freedom, $\phi(x, y, z)$ is the spatial part, and $|\chi\rangle = |\pm\rangle$ (see Eqs. 2.65 and 2.66) is the spin part. An operator \hat{A} acting in the “spatial” Hilbert space is given as

$$\hat{A} \otimes \hat{I}, \quad (2.77)$$

where \hat{I} is the identity matrix. An operator \hat{B} that acts in the spin space is given as

$$\hat{I} \otimes \hat{B}. \quad (2.78)$$

For example, given an operator $\hat{A} \otimes \hat{B}$ acting on the total wavefunction $\psi(\mathbf{r})$ yields

$$(\hat{A} \otimes \hat{B}) \psi(\mathbf{r}) = \hat{A}\phi(x, y, z) \otimes \hat{B}|\chi\rangle. \quad (2.79)$$

We will in the following drop the tensor product sign when expressing operators. It will be obvious in which space the operator act. We finally obtain the time-independent Schrödinger equation for a single-particle system with Hamiltonian given by Eq. (2.52),

$$\left(-\frac{\hbar^2}{2m} \nabla^2 + u(x, y, z) \right) \psi(\mathbf{r}) = \epsilon \psi(\mathbf{r}), \quad (2.80)$$

where $\psi(\mathbf{r})$ is the total wavefunction in Eq. (2.76). Our aim is to solve the time-independent Schrödinger equation and determine the eigenvectors $\psi(\mathbf{r})$ and eigenvalues ϵ . However, this is as far as we can go before a specific potential u is provided.

Chapter 3

Many-Body Theory

Single-particle quantum mechanics deals with systems consisting of only *one* particle. This is of course a natural and necessary starting point for all quantum mechanical considerations, where fundamental postulates, formalism, quantization effects, and so forth, can be introduced and discussed in peace and quiet without considering the implications of interacting particles. When this done, it is natural to move over to systems consisting of more than one particle. These systems are often called many-body or many-particle systems in the literature, and provide a breeding ground for many-body theory and many approximation schemes and methods.

In this chapter we present the basic quantum mechanics of many-body systems. We will focus on the parts that are directly relevant for this thesis. In the first section we present the "many-body problem", which refers to the N -particle Schrödinger equation. We will then consider the non-interacting system and the implications of identical particles on the solutions. Then we turn to the interacting system and discuss important properties of the solutions. In the last section we present the formalism of second quantization, including definitions of creation and annihilation operators, Wick's theorem and a presentation of the particle-hole formalism.

3.1 The Many-Body Problem

Consider an isolated system consisting of N particles that can be treated non-relativistic. The properties of the system are given by the Schrödinger equation. In bra-ket notation, the equation reads (see Sec. 2.1, Postulate C)

$$i\hbar \frac{\partial}{\partial t} |\Psi(t)\rangle = \hat{H} |\Psi(t)\rangle, \quad (3.1)$$

where $|\Psi(t)\rangle$ is the N -particle wavefunction at time t , and \hat{H} is the Hamiltonian of the system. The Hamiltonian is defined as

$$\hat{H} = \hat{T} + \hat{V}, \quad (3.2)$$

where \hat{T} is the total kinetic energy operator, and \hat{V} is the total potential energy operator. The kinetic energy operator reads

$$\hat{T} = \sum_{k=1}^N \hat{t}_k, \quad (3.3)$$

where \hat{t}_k is the kinetic energy of electron k . Since \hat{T} is the sum of \hat{t}_k , it is a one-body operator. Furthermore, in the general case, the potential energy operator is given as

$$\hat{V} = \hat{V}_1 + \hat{V}_2 + \hat{V}_3 + \dots + \hat{V}_N \quad (3.4)$$

$$= \sum_{k=1}^N \hat{v}_k^{(1)} + \frac{1}{2!} \sum_{kl}^N \hat{v}_{kl}^{(2)} + \frac{1}{3!} \sum_{klm}^N \hat{v}_{klm}^{(3)} + \dots + \frac{1}{N!} \sum_{klm..p}^N \hat{v}_{klm..p}^{(N)} \quad (3.5)$$

where

$$\widehat{V}_n = \frac{1}{n!} \sum_{klm..p}^N \quad (3.6)$$

is an n -body potential operator. In electronic systems like atoms and quantum dots, the Hamiltonian is a two-body operator. However, in nuclear physics, the fundamental strong interaction seems to exhibit three-body behaviour. This is due to the fact that the exchange particles (gluons) can couple to themselves.

The quantum state at time t is given as (see Sec. 2.1)

$$|\Psi(t)\rangle = \widehat{\mathcal{U}}(t, t_0)|\Psi(t_0)\rangle, \quad (3.7)$$

where $t > t_0$, $\mathcal{U}(t, t_0)$ is the time evolution operator, and $|\Psi(t_0)\rangle$ is the quantum state at time t_0 . Inserting this expression into Eq. (3.1) yields

$$i\hbar \frac{\partial}{\partial t} \widehat{\mathcal{U}}(t, t_0) = \widehat{H} \widehat{\mathcal{U}}(t, t_0). \quad (3.8)$$

When the Hamiltonian is time-independent, the time evolution operator reads

$$\widehat{\mathcal{U}}(t, t_0) = e^{-i\widehat{H}(t-t_0)/\hbar}. \quad (3.9)$$

If we were to prepare a system in quantum state $|\Psi(t_0)\rangle$ at time t_0 , the quantum state $|\Psi(t)\rangle$ at $t > t_0$ is determined by simply letting the time evolution operator act on the initial state. Thus the Hamiltonian determines the time evolution of the system. The solution of the energy eigenvalue equation (time-independent Schrödinger equation)

$$\widehat{H}|\Psi_\lambda\rangle = E_\lambda|\Psi_\lambda\rangle, \quad (3.10)$$

where $|\Psi_\lambda\rangle$ is the eigenfunction, and E_λ is the energy eigenvalue, can be used to obtain an algebraic expression of the time evolution. Since the set of eigenfunctions spans the N -particle Hilbert space, the initial state vector can be written as a linear combinations of eigenfunctions, viz.

$$|\Psi(t_0)\rangle = \sum_\lambda C_\lambda |\Psi_\lambda\rangle, \quad (3.11)$$

yielding the following analytical expression of the time evolution,

$$|\Psi(t)\rangle = e^{-i\widehat{H}(t-t_0)/\hbar}|\Psi_0\rangle = \sum_\lambda C_\lambda |\Psi_\lambda\rangle e^{-iE_\lambda(t-t_0)/\hbar}. \quad (3.12)$$

Moreover, the energy eigenvalues and eigenfunctions are often the main target in many-body calculations. The time-independent Schrödinger equation in (3.10) is usually called the quantum mechanical many-body problem. This is a nontrivial problem due to the interaction between the particles. In Nature, particles interact with each other, and realistic Hamiltonians are at least two-body operators. Even for the simplest case when the Hamiltonian is a two-body operator, the many-body problem can in general not be solved exactly. For example, the Hamiltonian for the helium atom reads (in atomic units)

$$\widehat{H} = -\frac{1}{2}\nabla_1^2 - \frac{1}{2}\nabla_2^2 - \frac{2}{r_1} - \frac{2}{r_2} + \frac{1}{r_{12}}, \quad (3.13)$$

where ∇_1 and ∇_2 is the gradient of electron 1 and 2, r_1 is the distance between electron 1 and the nucleus, r_2 is the distance between electron 2 and the nucleus, and r_{12} is the distance between the electrons. This many-body problem cannot be solved exactly. In quantum mechanical treatment of many-body systems we are therefore forced to utilize approximation schemes and complex techniques. In Part 2, we will present two important many-body methods: The Hartree-Fock and the Coupled-Cluster method.

We will in the following consider the non-interacting many-body system. This system serves as a starting point for most many-body methods such as Hartree-Fock method and Coupled-Cluster.

3.2 The Non-Interacting System

The non-interacting system consists of N non-interacting particles. This system is also called the unperturbed system. The Hamiltonian reads

$$\hat{H}_0 = \hat{T} + \hat{U}, \quad (3.14)$$

where \hat{T} is the total kinetic energy operator (given in Eq. 3.3), and \hat{U} is a possible external one-body potential given as

$$\hat{U} = \sum_{k=1}^N \hat{u}_k, \quad (3.15)$$

where \hat{u}_k is the potential energy of particle k . Defining

$$\hat{h} = \hat{T} + \hat{u}, \quad (3.16)$$

we obtain that

$$\hat{H}_0 = \sum_{k=1}^N \hat{h}_k. \quad (3.17)$$

The time-independent Schrödinger equation reads (in bra-ket notation)

$$\hat{H}_0 |\Phi_a\rangle = E_a |\Phi_a\rangle, \quad (3.18)$$

where $|\Phi\rangle$ is the energy eigenvector, and E_a is the energy eigenvalue. We now assume the particles are distinguishable. Since the Hamiltonian is a one-body operator, Eq. (3.18) is separable. The energy eigenfunctions are given as

$$|\Phi_a\rangle = |\psi_\alpha\rangle \otimes |\psi_\beta\rangle \otimes |\psi_\gamma\rangle \otimes \dots \otimes |\psi_\delta\rangle, \quad (3.19)$$

where a denotes the set of quantum numbers $(\alpha, \beta, \gamma, \dots, \delta)$. The single-particle energy eigenfunctions are determined by

$$\hat{h} |\psi_\alpha\rangle = \varepsilon_\alpha |\psi_\alpha\rangle, \quad (3.20)$$

where ε_α is the energy eigenvalue. We note that $|\psi_\alpha\rangle$ is the total single-particle wavefunction, i.e. it includes the spin. See Secs. 2.2.2 and 2.2.3. The energy eigenvalues of the non-interacting system are thus given as

$$E_a = \sum_{\alpha \in a} \varepsilon_\alpha. \quad (3.21)$$

The simple product form in Eq. (3.19) assumes that we can tell the particles apart. It would otherwise make no sense to claim that particle 1 is in state ψ_α , particle 2 is in state ψ_β , and so forth. On the macroscopic scale, we can in principle always distinguish particles from each other. However, on microscopic scale, the situation is fundamentally different. Considering for example a system of electrons, we will never be able to tell them apart. Moreover, it is not just that we do not happen to know. There is no such thing as “this” or “that” electron. Electrons are *identical* in a way classical objects will never be. The solution in Eq. (3.19) can therefore not be used for systems consisting of identical particles.

3.3 Identical Particles

Consider a non-interacting system consisting of N identical particles. We will now utilize the coordinate representation. The single-electron energy eigenfunctions (see Eq. 3.20) reads

$$\psi_\alpha(\mathbf{r}) = \langle \mathbf{r} | \psi_\alpha \rangle, \quad (3.22)$$

where \mathbf{r} includes the spin. We start our discussion by investigating the permutation operator \hat{P} . It is defined through its action on the N -particle product state,

$$\hat{P}_{ij}\psi_\alpha(\mathbf{r}_1)\dots\psi_\beta(\mathbf{r}_i)\dots\psi_\gamma(\mathbf{r}_j)\dots\psi_\delta(\mathbf{r}_N) = \psi_\alpha(\mathbf{r}_1)\dots\psi_\beta(\mathbf{r}_i)\dots\psi_\gamma(\mathbf{r}_j)\dots\psi_\delta(\mathbf{r}_N), \quad (3.23)$$

i.e. it interchanges the coordinates of particle i and j . When the particles are identical, this should not affect their probability distribution. We define

$$\Phi_a(\mathbf{r}_1, \mathbf{r}_2, \dots, \mathbf{r}_N) = \langle \mathbf{r}_1 \mathbf{r}_2 \dots, \mathbf{r}_N | \Phi_a \rangle \quad (3.24)$$

as the eigenfunction of N non-interacting and identical particles. Thus we obtain that

$$|\Phi_a(\mathbf{r}_1, \dots, \mathbf{r}_i, \dots, \mathbf{r}_j, \dots, \mathbf{r}_N)|^2 = |\Phi_a(\mathbf{r}_1, \dots, \mathbf{r}_j, \dots, \mathbf{r}_i, \dots, \mathbf{r}_N)|^2, \quad (3.25)$$

leading to

$$\Phi_a(\mathbf{r}_1, \dots, \mathbf{r}_i, \dots, \mathbf{r}_j, \dots, \mathbf{r}_N) = \pm \Phi_a(\mathbf{r}_1, \dots, \mathbf{r}_j, \dots, \mathbf{r}_i, \dots, \mathbf{r}_N). \quad (3.26)$$

The wavefunction is therefore either antisymmetric or symmetric with respect to the interchange of two particles. The non-interacting Hamiltonian is invariant under the interchange of particles. It follows that

$$[\hat{H}_0, \hat{P}_{ik}] = 0, \quad (3.27)$$

i.e. \hat{H}_0 and \hat{P} are compatible observables. Thus there exist eigenfunctions \hat{H}_0 that are also eigenfunctions of \hat{P}_{ij} (see [7]). The eigenvalue equation of the permutation operator reads

$$\hat{P}_{ij}\Phi_a(\mathbf{r}_1, \dots, \mathbf{r}_i, \dots, \mathbf{r}_j, \dots, \mathbf{r}_N) = \beta\Phi_a(\mathbf{r}_1, \dots, \mathbf{r}_i, \dots, \mathbf{r}_j, \dots, \mathbf{r}_N). \quad (3.28)$$

Since

$$\hat{P}_{ij}^2 = 1, \quad (3.29)$$

it follows that

$$\beta = \pm 1, \quad (3.30)$$

leading to Eq. (3.26). Particles with a symmetric wavefunction ($\beta = +1$) are called bosons, while particles with an antisymmetric wavefunction ($\beta = -1$) are called fermions. Depending on whether the system consists of identical bosons or fermions, the eigenfunctions of Eq. (3.18) are either symmetric or antisymmetric. Consider now a two-particle system. We can construct the following normalized symmetric (S) and antisymmetric (AS) wavefunctions

$$\Phi_S(\mathbf{r}_1, \mathbf{r}_2) = \frac{1}{\sqrt{2}} [\phi_\alpha(\mathbf{r}_1)\phi_\beta(\mathbf{r}_2) + \phi_\alpha(\mathbf{r}_2)\phi_\beta(\mathbf{r}_1)], \quad (3.31)$$

$$\Phi_{AS}(\mathbf{r}_1, \mathbf{r}_2) = \frac{1}{\sqrt{2}} [\phi_\alpha(\mathbf{r}_1)\phi_\beta(\mathbf{r}_2) - \phi_\alpha(\mathbf{r}_2)\phi_\beta(\mathbf{r}_1)], \quad (3.32)$$

where the single-particle orbitals are given in Eq. (3.20). Both Φ_S and Φ_{AS} are eigenstates of the permutation operator with eigenvalue $+1$ and -1 , respectively. Moreover, they are also eigenstates of the non-interacting Hamiltonian \hat{H}_0 with energy eigenvalue

$$E_a = \varepsilon_\alpha + \varepsilon_\beta. \quad (3.33)$$

In the general N -particle case, symmetric and antisymmetric wavefunctions are constructed by the so-called symmetrizer and antisymmetrizer operators acting on product states, respectively. The symmetrizer is defined as

$$\hat{\mathcal{S}} = \frac{1}{N!} \sum_p \hat{P}, \quad (3.34)$$

and the antisymmetrizer as

$$\hat{\mathcal{A}} = \frac{1}{N!} \sum_p (-1)^p \hat{P}, \quad (3.35)$$

where p is the permutation number. Normalized symmetric and antisymmetric states are then given by

$$\Phi_S(\mathbf{r}_1, \mathbf{r}_2, \dots, \mathbf{r}_N) = \sqrt{\frac{N!}{n_\alpha! n_\beta! \dots n_\gamma!}} \hat{\mathcal{S}} \psi_\alpha(\mathbf{r}_1) \psi_\beta(\mathbf{r}_2) \dots \psi_\delta(\mathbf{r}_N) \quad (3.36)$$

and

$$\Phi_{AS}(\mathbf{r}_1, \mathbf{r}_2, \dots, \mathbf{r}_N) = \sqrt{N!} \hat{\mathcal{A}} \psi_\alpha(\mathbf{r}_1) \psi_\beta(\mathbf{r}_2) \dots \psi_\delta(\mathbf{r}_N), \quad (3.37)$$

respectively. The antisymmetric wavefunction can be written as a determinant, viz.

$$\Phi_{\alpha\beta\dots\delta}(\mathbf{r}_1, \mathbf{r}_2, \dots, \mathbf{r}_N) = \frac{1}{\sqrt{N!}} \begin{vmatrix} \psi_\alpha(\mathbf{r}_1) & \psi_\beta(\mathbf{r}_1) & \dots & \psi_\delta(\mathbf{r}_1) \\ \psi_\alpha(\mathbf{r}_2) & \psi_\beta(\mathbf{r}_2) & \dots & \psi_\delta(\mathbf{r}_2) \\ \vdots & \vdots & \ddots & \vdots \\ \psi_\alpha(\mathbf{r}_N) & \psi_\beta(\mathbf{r}_N) & \dots & \psi_\delta(\mathbf{r}_N) \end{vmatrix}, \quad (3.38)$$

called a Slater determinant. We observe that a single-particle state can only be occupied by *one* fermion. If we were to put two fermions in the same state, the antisymmetric wavefunction would be equal to zero. This is completely nonsense. In 1925, Wolfgang Pauli formulated the so-called Pauli exclusion principle: Two identical fermions cannot occupy the same single-particle state simultaneously. However, bosons may occupy the same single-particle state. In Nature, bosons have integer spin, and fermions have half integer spin. This can be proven in relativistic quantum field theory [8].

Bosons and fermions turn out to behave quite differently. For example, the so-called Bose-Einstein Condensate (BEC) is a state of matter of a dilute gas of weakly interacting bosons cooled down to temperatures close to absolute zero. At these temperatures, a large fraction of the particles occupy the single-particle state with the lowest energy. Obviously, this would not be the case if the system consisted of fermions. An other example is that bosons tend to be somewhat closer together than fermions. This is shown by calculating the expectation value $\langle(x_1 - x_2)^2\rangle$ for a two-particle system in 1 dimension. After some tedious algebra (see [2]), the expectation value reads

$$\langle(x_1 - x_2)^2\rangle_{\pm} = \langle(x_1 - x_2)^2\rangle \mp 2 |\langle x \rangle_{\alpha\beta}|^2, \quad (3.39)$$

where $+$ denotes bosons, $-$ denotes fermions, $\langle(x_1 - x_2)^2\rangle$ is expectation value for distinguishable particles, and

$$\langle x \rangle_{\alpha\beta} = \int x \phi_\alpha^*(x) \phi_\beta(x) dx. \quad (3.40)$$

Note that we have omitted the spin. When the single-particle functions overlap, there is an “attraction force” between bosons, and a “repulsion force” between fermions. This is the so-called exchange force. It is important to note that this is not a physical force, but a geometrical consequence of the symmetrization requirement.

3.4 The Interacting Many-Body System

In this section we consider the interacting many-body system. We limit the discussion to systems consisting of N fermions. In the coordinate representation, the Schrödinger equation reads

$$\hat{H}\Psi_\lambda(\mathbf{r}_1, \mathbf{r}_2, \dots, \mathbf{r}_N) = E_\lambda\Psi_\lambda(\mathbf{r}_1, \mathbf{r}_2, \dots, \mathbf{r}_N), \quad (3.41)$$

where E_λ is the energy eigenvalue, and

$$\Psi_\lambda(\mathbf{r}_1, \mathbf{r}_2, \dots, \mathbf{r}_N) = \Upsilon_\eta(\vec{r}_1, \vec{r}_2, \dots, \vec{r}_N) \otimes |\chi_\zeta\rangle \quad (3.42)$$

is the total wavefunction (see Sec. 2.2.3), where λ denote the set of quantum numbers (η, ζ) , $\Upsilon_\eta(\vec{r}_1, \vec{r}_2, \dots, \vec{r}_N)$ is the spatial part, \vec{r} is the position vector, and $|\chi_\zeta\rangle$ is the spin part. As pointed our before, the Schrödinger equation cannot in general be solved exactly. However, the symmetry properties of the Hamiltonian can be used in order to obtain important information of the eigenfunctions. The permutation symmetry is an obvious symmetry for systems consisting of identical fermions. We obtain that

$$[\hat{H}, \hat{P}] = 0, \quad (3.43)$$

where the permutation operator is defined in Eq. (3.23). Thus we can construct a set of functions that are simultaneously eigenfunctions of \hat{H} and \hat{P} . The eigenvalue equation for the permutation operator reads

$$\hat{P}_{ij}\Psi_\lambda(\mathbf{r}_1, \dots, \mathbf{r}_i, \dots, \mathbf{r}_j, \dots, \mathbf{r}_N) = \beta\Psi_\lambda(\mathbf{r}_1, \dots, \mathbf{r}_i, \dots, \mathbf{r}_j, \dots, \mathbf{r}_N), \quad (3.44)$$

where $\hat{P}^2 = 1$ leads to $\beta = \pm 1$ (symmetric/antisymmetric wavefunction). Thus the *total* wavefunction is antisymmetric with respect to the interchange of two particles. We have two possibilities,

$$\Psi(\mathbf{r}_1, \mathbf{r}_2, \dots, \mathbf{r}_N)_{\text{AS}} = \Upsilon_{\text{AS}}(\vec{r}_1, \vec{r}_2, \dots, \vec{r}_N) \otimes |\chi\rangle_{\text{S}} \quad (3.45)$$

$$\Psi(\mathbf{r}_1, \mathbf{r}_2, \dots, \mathbf{r}_N)_{\text{S}} = \Upsilon_{\text{S}}(\vec{r}_1, \vec{r}_2, \dots, \vec{r}_N) \otimes |\chi\rangle_{\text{AS}}, \quad (3.46)$$

where ‘‘AS’’ denotes antisymmetric and ‘‘S’’ denotes symmetric.

3.4.1 Hilbert Space of Distinguishable Particles

Consider a system of N distinguishable particles. The energy eigenfunctions live in the N -particle Hilbert space \mathcal{H}_N with dimension d (possible infinite). Assume we have an orthonormal set of single-particle functions

$$\mathcal{B}_1 = \{|\alpha\rangle\}_{\alpha=1}^d \quad (3.47)$$

that spans the 1-particle Hilbert space \mathcal{H}_1 . The N -particle Hilbert space can mathematically be constructed by combining N single-particle spaces with tensor products,

$$\mathcal{H}_N = \mathcal{H}_{1 \otimes 1 \otimes \dots \otimes 1} \equiv \mathcal{H}_1^{(1)} \otimes \mathcal{H}_1^{(2)} \otimes \dots \otimes \mathcal{H}_1^{(N)}. \quad (3.48)$$

This is called the direct product space. We denote $\hat{\mathcal{H}}_1^{(n)}$ as the 1-particle Hilbert space for particle n . The basis set of the N -particle product space can be constructed in a similar fashion through a tensor product,

$$|\alpha\beta..\delta\rangle \equiv |\alpha\rangle \otimes |\beta\rangle \otimes \dots \otimes |\delta\rangle, \quad (3.49)$$

where $|\alpha\beta..\delta\rangle$ is called a product state. See [3] for details. The energy eigenfunctions can be written as a linear combination of product states, viz.

$$|\Psi_D\rangle = \sum_{\{\alpha\beta..\gamma\}} c_{\alpha\beta..\gamma} |\alpha\beta..\gamma\rangle, \quad (3.50)$$

where “D” denote distinguishable. In the coordinate representation, the expression above reads

$$\Psi_D(\mathbf{r}_1, \mathbf{r}_2, \dots, \mathbf{r}_N) = \langle \mathbf{r}_1 \mathbf{r}_2 \dots \mathbf{r}_N | \Psi_D \rangle = \sum_{\alpha \beta \dots \delta} c_{\alpha \beta \dots \delta} \xi_\alpha(\mathbf{r}_1) \xi_\beta(\mathbf{r}_2) \dots \xi_\delta(\mathbf{r}_N), \quad (3.51)$$

where \mathbf{r} includes the spin, and $c_{\alpha \beta \dots \delta}$ is the expansion coefficient. Eq. (3.51) is always valid provided that the set of functions $\{\xi(\mathbf{r})\}$ are orthogonal and complete.

3.4.2 Hilbert Space of Bosons and Fermions

Consider a system of N bosons or fermions. As pointed out before, the total N -particle quantum state must either be symmetric or antisymmetric. We denote the N -particle Hilbert space of symmetric states as \mathcal{H}_N^S , and the Hilbert space of antisymmetric states as \mathcal{H}_N^{AS} . In the two-particle system, to each pair of product states $|\alpha\beta\rangle$ and $|\beta\alpha\rangle$, there exist one symmetric state and one antisymmetric state. When $\alpha = \beta$, the product state is already symmetric, and an antisymmetric state does not exist due to the Pauli exclusion principle. The two-particle Hilbert space (of distinguishable particles) has thus enough product states to form one symmetric space and one antisymmetric space, viz.

$$\mathcal{H}_2 = \mathcal{H}_2^S \otimes \mathcal{H}_2^{AS}, \quad (3.52)$$

In the general N -particle case we have that (see [3])

$$\mathcal{H}_N = \mathcal{H}_N^S \otimes \mathcal{H}_N^{AS}, \quad (3.53)$$

where \mathcal{H}_N is the Hilbert space of distinguishable particles, \mathcal{H}_N^S is the Hilbert space of bosons (symmetric states), and \mathcal{H}_N^{AS} is the Hilbert space of fermions (antisymmetric states). Defining

$$\mathcal{B}_N^S = \{|\sigma\rangle\}_{\sigma=1}^d \quad (3.54)$$

as the basis of \mathcal{H}_N^S with dimension d , and

$$\mathcal{B}_N^{AS} = \{|\varsigma\rangle\}_{\varsigma=1}^{d'} \quad (3.55)$$

as the basis of \mathcal{H}_N^{AS} with dimension d' , a symmetric and antisymmetric N -particle state can be written as

$$|\Psi_S\rangle = \sum_{\sigma}^d f_{\sigma} |\sigma\rangle \quad (3.56)$$

$$|\Psi_{AS}\rangle = \sum_{\varsigma}^{d'} g_{\varsigma} |\varsigma\rangle, \quad (3.57)$$

where f_{σ} and g_{ς} are expansion coefficients. The basis functions in \mathcal{B}_N^S and \mathcal{B}_N^{AS} must be symmetric and antisymmetric, respectively. The direct product states in Eq. (3.49) are neither symmetric nor antisymmetric. Thus they cannot constitute a basis for \mathcal{H}_N^S or \mathcal{H}_N^{AS} . In section 3.3, symmetric and antisymmetric states were constructed from product states (see Eqs. 3.36 and 3.37). These states have correct symmetry. Moreover, they are orthogonal and complete [3]. Thus,

$$|\sigma\rangle = \sqrt{\frac{N!}{n_{\alpha}! n_{\beta}! \dots n_{\delta}!}} \hat{\mathcal{S}} |\alpha\beta\dots\delta\rangle \quad (3.58)$$

$$|\varsigma\rangle = \sqrt{N!} \hat{\mathcal{A}} |\alpha\beta\dots\delta\rangle, \quad (3.59)$$

where σ and ς denote a set of quantum numbers $(\alpha, \beta, \dots, \delta)$, $|\alpha\beta\dots\delta\rangle$ is the product state, $\hat{\mathcal{S}}$ is the symmetrizer defined in Eq. (3.34), and $\hat{\mathcal{A}}$ is the antisymmetrizer defined in Eq. (3.35). This is *one* possible choice of basis functions. We emphasize that any set

$$\{|\alpha\rangle\}_{\alpha=1}^d \quad (3.60)$$

that spans the single-particle Hilbert space \mathcal{H}_1 with dimension d , can be used. A general symmetric and antisymmetric N -particle function can then be written as

$$\Psi_S(\mathbf{r}_1, \mathbf{r}_2, \dots, \mathbf{r}_N) = \sum_{\alpha\beta..\delta} f_{\alpha\beta..\delta} \sqrt{\frac{N!}{n_\alpha! n_\beta! \dots n_\gamma!}} \hat{\mathcal{S}} \xi_\alpha(\mathbf{r}_1) \xi_\beta(\mathbf{r}_2) \dots \xi_\delta(\mathbf{r}_N) \quad (3.61)$$

$$\Psi_{AS}(\mathbf{r}_1, \mathbf{r}_2, \dots, \mathbf{r}_N) = \sum_{\alpha\beta..\delta} g_{\alpha\beta..\delta} \sqrt{N!} \hat{\mathcal{A}} \xi_\alpha(\mathbf{r}_1) \xi_\beta(\mathbf{r}_2) \dots \xi_\delta(\mathbf{r}_N), \quad (3.62)$$

where

$$\xi_\alpha(\mathbf{r}) = \langle \mathbf{r} | \alpha \rangle. \quad (3.63)$$

The energy eigenfunctions of the interacting N -fermion system in Eq. (3.41) can therefore be written as a linear combination of the eigenfunctions of the non-interacting system in Eq. (3.18), viz.

$$\Psi_\lambda(\mathbf{r}_a, \mathbf{r}_2, \dots, \mathbf{r}_N) = \sum_{\alpha\beta..\delta} C_{\alpha\beta..\delta}^\lambda \Phi_{\alpha\beta..\delta}(\mathbf{r}_1, \mathbf{r}_2, \dots, \mathbf{r}_N), \quad (3.64)$$

where $C_{\alpha\beta..\delta}^\lambda$ is the expansion coefficient, and $\Phi_{\alpha\beta..\delta}(\mathbf{r}_1, \mathbf{r}_2, \dots, \mathbf{r}_N)$ is the Slater determinant given in Eq. (3.38).

3.5 Second Quantization

We have seen that the energy eigenstates of a non-interacting many-fermion system are given as Slater determinants (see Eq. 3.38). One may never assign one-to-one correspondence between single-particle states and particle coordinates. The only thing we can say is whether a single-particle orbital is occupied or not. The Slater determinant in Eq. (3.38) thus includes redundant information. It is therefore appropriate to characterize Slater determinants by single-particle orbitals only. We define

$$\Phi_{\alpha_1\alpha_2..\alpha_N} \equiv |\alpha_1\alpha_2..\alpha_N\rangle. \quad (3.65)$$

Note that we in Eq. (3.49) defined $|\alpha\beta..\delta\rangle$ as a product state. In the rest of the thesis, the context will clearly show which definition that is used. The notation in Eq. (3.65) is called the occupancy representation. This form of the Slater determinant does not explicitly reflect the antisymmetry in the particle coordinates. Nevertheless, the Slater determinant changes sign in the permutation of two columns, yielding

$$|\alpha_1..\alpha_i..\alpha_j..\alpha_N\rangle = -|\alpha_1..\alpha_i..\alpha_j..\alpha_N\rangle. \quad (3.66)$$

The full potential of this notation appears when creation and annihilation operators are introduced. A creation operator creates a fermion in single-particle state, while an annihilation operator removes a fermion from single-particle state. This formalism is called second quantization. It has not the direct physical interpretation as in relativistic quantum field theory. The formalism is utilized in non-relativistic many-body theory in order to introduce concepts and methods such as particle-hole representation, Wick's theorem, diagrams, and so forth.

3.5.1 Creation and Annihilation Operators

In this section, we will define creation and annihilation operators. These operators are mappings between the many-particle Hilbert spaces of different particle numbers, viz.

$$a_\alpha^\dagger : \mathcal{H}_N^{AS} \rightarrow \mathcal{H}_{N+1}^{AS} \quad (3.67)$$

$$a_\alpha : \mathcal{H}_N^{AS} \rightarrow \mathcal{H}_{N-1}^{AS}, \quad (3.68)$$

where

$$\alpha \in \mathcal{H}_1. \quad (3.69)$$

Creation and annihilation operators are operators that create and annihilate fermions. We define the fermionic creation operator by

$$a_\alpha^\dagger |\alpha_1 \alpha_2 .. \alpha_N\rangle \equiv |\alpha \alpha_1 \alpha_2 .. \alpha_N\rangle, \quad (3.70)$$

i.e. it adds a fermion with quantum number α to an antisymmetric state (Slater determinant) in which N fermions occupy single-particle orbitals $(\alpha_1, \alpha_2, .., \alpha_N)$. An antisymmetric $(N+1)$ -fermion state is the result. Note that if α is already occupied, the result is zero. We can now write a Slater determinant as a product of creation operators, viz.

$$|\alpha_1 \alpha_2 .. \alpha_N\rangle = a_{\alpha_1}^\dagger a_{\alpha_2}^\dagger .. a_{\alpha_N}^\dagger |0\rangle = \prod_{i=1}^N a_{\alpha_i}^\dagger |0\rangle, \quad (3.71)$$

where $|0\rangle$ is the vacuum state. Combining Eqs. (3.66) and (3.71) yields

$$a_{\alpha_1}^\dagger .. a_{\alpha_i}^\dagger .. a_{\alpha_j}^\dagger .. a_{\alpha_N}^\dagger |0\rangle = -a_{\alpha_1}^\dagger .. a_{\alpha_j}^\dagger .. a_{\alpha_i}^\dagger .. a_{\alpha_N}^\dagger |0\rangle, \quad (3.72)$$

leading to the following anticommutation relation

$$\{a_\alpha^\dagger, a_\beta^\dagger\} = a_\alpha^\dagger a_\beta^\dagger + a_\beta^\dagger a_\alpha^\dagger = 0. \quad (3.73)$$

The adjoint of a_α^\dagger is called an annihilation operator,

$$a_\alpha = (a_\alpha^\dagger)^\dagger. \quad (3.74)$$

It can be shown that its action on a Slater determinant (see [7, 9]) is given by

$$a_\alpha |\alpha_1 \alpha_2 .. \alpha_{i-1} \alpha_i \alpha_{i+1} .. \alpha_{N-1} \alpha_N\rangle = (-1)^{i-1} |\alpha_1 \alpha_2 .. \alpha_{i-1} \alpha_{i+1} .. \alpha_{N-1} \alpha_N\rangle \quad (3.75)$$

when $\alpha = \alpha_i$ is occupied by a fermion, and

$$a_\alpha |\alpha_1 \alpha_2 .. \alpha_N\rangle = 0, \quad (3.76)$$

when α is unoccupied, i.e. $\alpha \neq \alpha_i$ for $i = 1, 2, .., N$. The annihilator operator a_α has therefore the property that its action upon an antisymmetric N -fermion state (Slater determinant) produces an antisymmetric $(N-1)$ -fermion state, provided that α is occupied. The anticommutation relation reads

$$\{a_\alpha, a_\beta\} = a_\alpha a_\beta + a_\beta a_\alpha = 0. \quad (3.77)$$

Furthermore, the anticommutation relation between the creation and annihilation operator (see [7]) reads

$$\{a_\alpha^\dagger, a_\beta\} = \delta_{\alpha\beta}. \quad (3.78)$$

3.5.2 Operators in Second Quantization

We are now in a position to express many-fermion states by creation and annihilation operators. In many-body theory in general, we often need to calculate matrix elements or expectation values of operators. Consider for example the matrix element

$$\langle \alpha_1 \alpha_2 | \hat{O} | \alpha_3 \alpha_4 \rangle, \quad (3.79)$$

where $|\alpha_1\alpha_2\rangle$ and $|\alpha_3\alpha_4\rangle$ are Slater determinants. In second quantization, this element reads

$$\langle 0 | a_{\alpha_1} a_{\alpha_2} \hat{O} a_{\alpha_3}^\dagger a_{\alpha_4}^\dagger | 0 \rangle. \quad (3.80)$$

Is it possible to write \hat{O} in terms of creation and annihilation operators? The answer is yes, provided that the operators conserve the particle number. Thus we can solve the matrix element by using the anticommutation relations in Eqs. (3.78), (3.77) and (3.73).

Operators expressed in second quantization have the convenient property that they do not depend on the numbers of particles in the system. They work in the so-called Fock space (see [7]), which is the vector space constructed by the direct sum of the vacuum space, the single-particle Hilbert space, the two-particle Hilbert space, and so forth, viz.

$$\mathcal{F} \equiv \bigoplus_{n=0}^{\infty} \mathcal{H}_n^{\text{AS}}, \quad (3.81)$$

where $\mathcal{H}_n^{\text{AS}}$ is the n -fermion Hilbert space. We will in the following only consider the second quantized form of one-body and two-body operators.

Consider a one-body operator \hat{F} . It is given as

$$\hat{F} = \sum_{i=1}^N \hat{f}_i, \quad (3.82)$$

where \hat{f}_i acts on particle i , and N is the number of fermions. Given an *arbitrary* single-particle basis

$$\mathcal{B}_1 = \{|\alpha\rangle\}_{i=1}^d \quad (3.83)$$

that spans the one-fermion Hilbert space \mathcal{H}_1 with dimension d (often infinity), the second quantized form of \hat{F} reads

$$\hat{F} = \sum_{\alpha\beta} \langle \alpha | f | \beta \rangle a_\alpha^\dagger a_\beta. \quad (3.84)$$

See [7] for a deduction. Thus for every set of quantum numbers (α, β) , the operator \hat{F} annihilates a fermion in state β and creates a fermion in state α with probability amplitude $\langle \alpha | f | \beta \rangle$. Furthermore, consider a two-body operator \hat{V} . It is given as

$$\hat{V}_N = \sum_{i=1 < j}^N \hat{v}_{ij}, \quad (3.85)$$

where \hat{v}_{ij} acts on particle i and j , and N is the number of fermions in the system. Given an *arbitrary* single-particle basis (see Eq. 3.83), the second quantized form of \hat{V} reads

$$\hat{V} = \frac{1}{2} \sum_{\alpha\beta\gamma\delta} \langle \alpha\beta | v | \gamma\delta \rangle a_\alpha^\dagger a_\beta^\dagger a_\delta a_\gamma \quad (3.86)$$

$$= \frac{1}{4} \sum_{\alpha\beta\gamma\delta} \langle \alpha\beta | v | \gamma\delta \rangle_{\text{AS}} a_\alpha^\dagger a_\beta^\dagger a_\delta a_\gamma, \quad (3.87)$$

where the antisymmetrized matrix element is defined as

$$\langle \alpha\beta | v | \gamma\delta \rangle_{\text{AS}} = \langle \alpha\beta | v | \gamma\delta \rangle - \langle \alpha\beta | v | \delta\gamma \rangle. \quad (3.88)$$

See [7] for a deduction. For every set of quantum numbers $(\alpha, \beta, \gamma, \delta)$, the operator \hat{V} annihilates a fermion from states γ and δ , and creates a fermion in states α and γ , with probability amplitude $\frac{1}{4} \langle \alpha\beta | v | \gamma\delta \rangle_{\text{AS}}$.

We are now in a position to write antisymmetric wavefunctions (Slater determinants), one-body operators and two-body operators in second quantization. As pointed out before, in quantum mechanical treatment of many-body systems, we often end up with evaluating matrix elements. As an example, consider

$$\langle \alpha_1 \alpha_2 | \hat{V} | \alpha_3 \alpha_4 \rangle, \quad (3.89)$$

where $|\alpha_1 \alpha_2\rangle$ and $|\alpha_3 \alpha_4\rangle$ denote Slater determinants, and \hat{V} a two-body operator. Since

$$\langle \alpha_1 \alpha_2 | = \langle 0 | a_{\alpha_1} a_{\alpha_2} \quad (3.90)$$

$$| \alpha_3 \alpha_4 \rangle = a_{\alpha_3}^\dagger a_{\alpha_4}^\dagger | 0 \rangle, \quad (3.91)$$

we obtain that

$$\langle \alpha_1 \alpha_2 | \hat{V} | \alpha_3 \alpha_4 \rangle = \frac{1}{4} \sum_{\alpha \beta \gamma \delta} \langle \alpha \beta | v | \gamma \delta \rangle_{AS} \langle 0 | a_{\alpha_1} a_{\alpha_2} a_\alpha^\dagger a_\beta^\dagger a_\delta a_\gamma a_{\alpha_3}^\dagger a_{\alpha_4}^\dagger | 0 \rangle, \quad (3.92)$$

where the second quantized form of \hat{V} is given in Eq. (3.86). Thus we end up with evaluating the vacuum expectation value of products of creation and annihilation operators. These elements can be determined by using the anticommutation relations in Eqs. (3.73), (3.77) and (3.78). However, this approach can be quite tedious and time-consuming. Wick's theorem provides an easy, yet sophisticated, method for writing a string of creation and annihilation operators as a sum of *normal ordered* terms with all possible combinations of *contractions*. This will allow us to easily point out which terms that contribute to the expression. We will in the next section define Wick's theorem, and the concepts of normal-ordering and contractions.

3.5.3 Wick's Theorem

As pointed out in the previous section, quantum mechanical treatment of many-body systems often entails calculating matrix elements of operators between state vectors. Thus in the formalism of second quantization, we often end up with vacuum expectation values of creation and annihilation operators. We can use the anticommutation relations in Eqs. (3.73), (3.77) and (3.78) to rearrange the product into an operator string where the annihilation operators are placed to the right of the creation operators. All terms with a rightmost annihilation operator are zero, by construction. Thus, according to Eq. (3.78), every vacuum expectation value of creation and annihilation operators can be written as a sum of delta functions. Although the procedure is straightforward in itself, it becomes tedious and time-consuming even for simple cases. The so-called Wick's theorem allow us to determine these matrix elements in a simple and convenient way.

Wick's theorem is based on two fundamental concepts, viz. normal-ordering and contractions. Consider a product of creation and annihilation operators,

$$\hat{A} \hat{B} .. \hat{X} \hat{Y}. \quad (3.93)$$

Its normal-ordered form is defined as

$$\left\{ \hat{A} \hat{B} .. \hat{X} \hat{Y} \right\} \equiv (-1)^p [\text{creation operators}] \cdot [\text{annihilation operators}], \quad (3.94)$$

where p denotes the number of permutations that is needed to transform the original string into the normal-ordered form. The contraction between two operators \hat{X} and \hat{Y} is defined as

$$\overline{\hat{A} \hat{B}} \equiv \langle 0 | \hat{A} \hat{B} | 0 \rangle. \quad (3.95)$$

Furthermore, we define the contraction between two operators within a normal-ordered product as

$$\left\{ \overline{\hat{A} \hat{B} .. \hat{X} \hat{Y}} \right\} = (-1)^p \left\{ \hat{A} \hat{B} .. \hat{X} \hat{Y} \right\}, \quad (3.96)$$

where p is the number of permutations needed to bring both operator to the leftmost. In the general case when we have m contractions within a normal-ordered product, the prefactor reads

$$(-1)^{p_1+p_2+\dots+p_m}. \quad (3.97)$$

Wick's theorem states that every string of creation and annihilation operators can be written as a sum of normal-ordered products with all possible combinations of contractions. The theorem reads

$$\begin{aligned} \hat{A}\hat{B}\hat{C}\hat{D}\dots\hat{R}\hat{X}\hat{Y}\hat{Z} &= \left\{ \hat{A}\hat{B}\hat{C}\hat{D}\dots\hat{R}\hat{X}\hat{Y}\hat{Z} \right\} \\ &+ \sum_{(1)} \left\{ \overline{\hat{A}\hat{B}\hat{C}\hat{D}\dots\hat{R}\hat{X}\hat{Y}\hat{Z}} \right\} \\ &+ \sum_{(2)} \left\{ \overline{\overline{\hat{A}\hat{B}\hat{C}\hat{D}\dots\hat{R}\hat{X}\hat{Y}\hat{Z}}} \right\} \\ &+ \dots \\ &+ \sum_{(n/2)} \left\{ \overline{\overline{\overline{\hat{A}\hat{B}\hat{C}\hat{D}\dots\hat{R}\hat{X}\hat{Y}\hat{Z}}}} \right\}, \end{aligned} \quad (3.98)$$

where (m) denotes the number of contractions, and $(n/2)$ denotes the largest integer that do not exceed $n/2$ (n being the number of operators). When n is even, we obtain fully contracted terms. However, when n is odd, none of the terms in Eq. (3.98) are fully contracted. See [7] for a proof of Wick's theorem. An important extension of Wick's theorem is the so-called generalized Wick's theorem. This theorem reads

$$\begin{aligned} \left\{ \hat{A}\hat{B}\hat{C}\hat{D}\dots \right\} \left\{ \hat{R}\hat{X}\hat{Y}\hat{Z}\dots \right\} &= \left\{ \hat{A}\hat{B}\hat{C}\hat{D}\dots\hat{R}\hat{X}\hat{Y}\hat{Z} \right\} \\ &+ \sum_{(1)} \left\{ \overline{\hat{A}\hat{B}\hat{C}\hat{D}\dots\hat{R}\hat{X}\hat{Y}\hat{Z}} \right\} \\ &+ \sum_{(2)} \left\{ \overline{\overline{\hat{A}\hat{B}\hat{C}\hat{D}\dots\hat{R}\hat{X}\hat{Y}\hat{Z}}} \right\} \\ &+ \dots \end{aligned} \quad (3.99)$$

The vacuum expectation value of creation and annihilation operators can now be written as

$$\begin{aligned} \langle 0 | \hat{A}\hat{B}\hat{C}\hat{D}\dots\hat{R}\hat{X}\hat{Y}\hat{Z} | 0 \rangle &= \langle 0 | \left\{ \hat{A}\hat{B}\hat{C}\hat{D}\dots\hat{R}\hat{X}\hat{Y}\hat{Z} \right\} | 0 \rangle \\ &+ \sum_{(1)} \langle 0 | \left\{ \overline{\hat{A}\hat{B}\hat{C}\hat{D}\dots\hat{R}\hat{X}\hat{Y}\hat{Z}} \right\} | 0 \rangle \\ &+ \sum_{(2)} \langle 0 | \left\{ \overline{\overline{\hat{A}\hat{B}\hat{C}\hat{D}\dots\hat{R}\hat{X}\hat{Y}\hat{Z}}} \right\} | 0 \rangle \\ &+ \dots \\ &+ \sum_{[\frac{N}{2}]} \langle 0 | \left\{ \overline{\overline{\overline{\hat{A}\hat{B}\hat{C}\hat{D}\dots\hat{R}\hat{X}\hat{Y}\hat{Z}}}} \right\} | 0 \rangle. \end{aligned} \quad (3.100)$$

Since

$$\langle 0 | \left\{ \overline{\overline{\overline{\hat{A}\hat{B}\dots\hat{X}\hat{Y}}}} \right\} | 0 \rangle = 0, \quad (3.101)$$

by construction (see Eq. 3.96), only the fully contracted terms yield nonzero contribution. Thus we obtain

$$\begin{aligned}\langle 0 | \overbrace{\hat{A} \hat{B} \hat{C} \hat{D} \dots \hat{R} \hat{X} \hat{Y} \hat{Z}}^{\text{(fc)}} | 0 \rangle &= \sum_{(\text{fc})} \langle 0 | \left\{ \overbrace{\hat{A} \hat{B} \hat{C} \hat{D} \dots}^{\text{(fc)}}, \overbrace{\hat{R} \hat{X} \hat{Y} \hat{Z}}^{\text{(fc)}} \right\} | 0 \rangle \\ &= \sum_{(\text{fc})} \overbrace{\hat{A} \hat{B} \hat{C} \hat{D} \dots}^{\text{(fc)}}, \overbrace{\hat{R} \hat{X} \hat{Y} \hat{Z}}^{\text{(fc)}},\end{aligned}\quad (3.102)$$

where “fc” denotes fully contractions. When the number of creation and annihilation operators is odd, the vacuum expectation value is zero. However, when the number is even, the expectation value is simply the sum of fully contracted terms. We observe from the definition in Eq. (3.94) the following relations,

$$a_\alpha^\text{ } \overbrace{a_\beta^\dagger}^{\text{t}} = \delta_{\alpha\beta} \quad (3.103)$$

$$\overbrace{a_\alpha^\dagger}^{\text{t}} a_\beta = 0 \quad (3.104)$$

$$a_\alpha^\text{ } \overbrace{a_\beta}^{\text{t}} = 0 \quad (3.105)$$

$$\overbrace{a_\alpha^\dagger}^{\text{t}} \overbrace{a_\beta^\dagger}^{\text{t}} = 0. \quad (3.106)$$

Wick’s theorem can thus be used to calculate matrix elements of operators between Slater determinants.

3.5.4 Particle-Hole Formalism

We have seen that the formalism of second quantization is a convenient formalism for constructing antisymmetric wavefunctions and operators that conserves the particle-number. However, the real power of second quantization emerges when the particle-hole formalism is introduced. This is a so-called quasi-particle formalism.

In Sec. 3.5.1, we saw that antisymmetric wavefunctions can be written as

$$| \alpha_1 \alpha_2 \dots \alpha_N \rangle = a_{\alpha_1}^\dagger a_{\alpha_2}^\dagger \dots a_{\alpha_N}^\dagger | 0 \rangle, \quad (3.107)$$

where $| 0 \rangle$ is the vacuum state. The vacuum state is often called the reference state. In many-body theory we often deal with Slater determinants that have a few fermions excited relative to an other determinant. For example, the first excited energy eigenstate of the non-interacting N -fermion system (provided by the Schrödinger equation in Eq. 3.18) has one particle excited relative to the ground state. An other excited state may have two particles excited relative to the ground state, and so forth. It is therefore in many cases appropriate to introduce a new reference state. In the previous example, when we are dealing with energy eigenstates of the non-interacting system, the reference state could be the ground state. The transition from the ordinary particle representation to the particle-hole representation is shown schematically in Fig. (3.5.4). We have in the figure illustrated three antisymmetric states (Slater determinants),

$$| a \rangle = | \alpha_1 \alpha_2 \dots \alpha_{N-1} \alpha_N \rangle \in \mathcal{H}_N^{\text{AS}} \quad (3.108)$$

$$| b \rangle = | \alpha_1 \alpha_2 \dots \alpha_{N-1} \alpha_N \alpha_{N+1} \rangle \in \mathcal{H}_{N+1}^{\text{AS}} \quad (3.109)$$

$$| c \rangle = | \alpha_1 \alpha_2 \dots \alpha_{N-1} \rangle \in \mathcal{H}_{N-1}^{\text{AS}}, \quad (3.110)$$

in both the particle representation (left), and the particle-hole representation (right). Here we denote the singe-particle state by quantum numbers $\alpha_1 \alpha_2 \dots \alpha_{N+1}$. In the particle representation, the determinants are written as a product of creation operators acting on the vacuum state, viz.

$$| a \rangle_0 = | \alpha_1 \alpha_2 \dots \alpha_{N-1} \alpha_N \rangle = a_{\alpha_1}^\dagger a_{\alpha_2}^\dagger \dots a_{\alpha_{N-1}}^\dagger a_{\alpha_N}^\dagger | 0 \rangle \quad (3.111)$$

$$| b \rangle_0 = | \alpha_1 \alpha_2 \dots \alpha_{N-1} \alpha_N \alpha_{N+1} \rangle = a_{\alpha_1}^\dagger a_{\alpha_2}^\dagger \dots a_{\alpha_{N-1}}^\dagger a_{\alpha_N}^\dagger a_{\alpha_{N+1}}^\dagger | 0 \rangle \quad (3.112)$$

$$| c \rangle_0 = | \alpha_1 \alpha_2 \dots \alpha_{N-1} \rangle = a_{\alpha_1}^\dagger a_{\alpha_2}^\dagger \dots a_{\alpha_{N-1}}^\dagger | 0 \rangle, \quad (3.113)$$

where the 0-subscript denotes that the vacuum state is the reference state. By defining a new reference state

$$|r\rangle \equiv |a\rangle = a_{\alpha_1}^\dagger a_{\alpha_2}^\dagger \dots a_{\alpha_{N-1}}^\dagger a_{\alpha_N}^\dagger |0\rangle, \quad (3.114)$$

the two other determinants can be expressed as

$$|b\rangle_r = (-1)^N a_{\alpha_{N+1}}^\dagger |r\rangle \equiv (-1)^N |\alpha_{N+1}\rangle_r \quad (3.115)$$

$$|c\rangle_r = (-1)^{N-1} a_{\alpha_N}^\dagger |r\rangle \equiv (-1)^{N-1} |\alpha_N^{-1}\rangle. \quad (3.116)$$

The difference between $|b\rangle$ and the reference state is the particle occupying single-state α_{N+1} . Thus in the new representation, $|b\rangle$ is called a particle-state. Furthermore, relative to the reference state, $|c\rangle$ has a particle removed from single-particle state α_N , and is therefore called a hole-state.

The new representation is known as the particle-hole representation, and the new reference state $|r\rangle$ is the so-called particle-hole vacuum. This is a quasi-particle representation. The idea is that both holes (unoccupied single-particle states below the fermi level) and particles (occupied single-particle states above the fermi level) are treated as quasi-particles, where the fermi level denotes the single-particle state α_N . Creation of a quasi-particle means *either* creating a particle in state $\alpha > \alpha_N$, *or* creating a hole (i.e. removing a particle) in state $\alpha \leq \alpha_N$. Annihilation of a quasi-particle means *either* removing a particle from state $\alpha > \alpha_N$, *or* removing a hole (create a particle) in state $\alpha \leq \alpha_N$. The choice of reference state is in principle arbitrary, but the particle-hole formalism is only appropriate when the reference state correspond to a system which is physically steady.

When defining a new reference state, the ordinary creation and annihilation operators for particles must be replaced with corresponding operators for quasi-particles. We will denote the single-particle states that are part of the occupied space ($\alpha \leq \alpha_N$) with $ijk\dots$, and the states that are part of the unoccupied space ($\alpha > \alpha_N$) with $abc\dots$. We will refer to i as a hole state, and a as a particle state. The quasi-particle creation operator is defined as

$$b_\alpha^\dagger \equiv \begin{cases} a_\alpha^\dagger & \text{if } \alpha = a, b, c, \dots \\ a_\alpha & \text{if } \alpha = i, j, k, \dots \end{cases}, \quad (3.117)$$

and the annihilation operator

$$b_\alpha \equiv \begin{cases} a_\alpha^\dagger & \text{if } \alpha = i, j, k, \dots \\ a_\alpha & \text{if } \alpha = a, b, c, \dots \end{cases}. \quad (3.118)$$

The definitions above yield the following anticommutation relations,

$$\{b_\alpha, b_\beta\} = 0 \quad (3.119)$$

$$\{b_\alpha^\dagger, b_\beta^\dagger\} = 0 \quad (3.120)$$

$$\{b_\alpha^\dagger, b_\beta\} = \delta_{\alpha\beta}, \quad (3.121)$$

which are identical to Eqs. (3.77), (3.73) and (3.78), as expected. We can now express quasi-particle states as

$$|ijkl..abcd..\rangle_r \equiv b_i^\dagger b_j^\dagger b_k^\dagger b_l^\dagger .. b_a^\dagger b_b^\dagger b_c^\dagger b_d^\dagger .. |r\rangle, \quad (3.122)$$

where $ijkl..$ are occupied by holes, and $abcd..$ are occupied by particles. Operators can also be expressed by quasi-particle creation and annihilation operators. This is for example necessary in order to utilize the particle-hole formalism when evaluation matrix elements of operators between quasi-particle states. Moreover, Wick's theorem in Eq. (3.98) is valid for products of

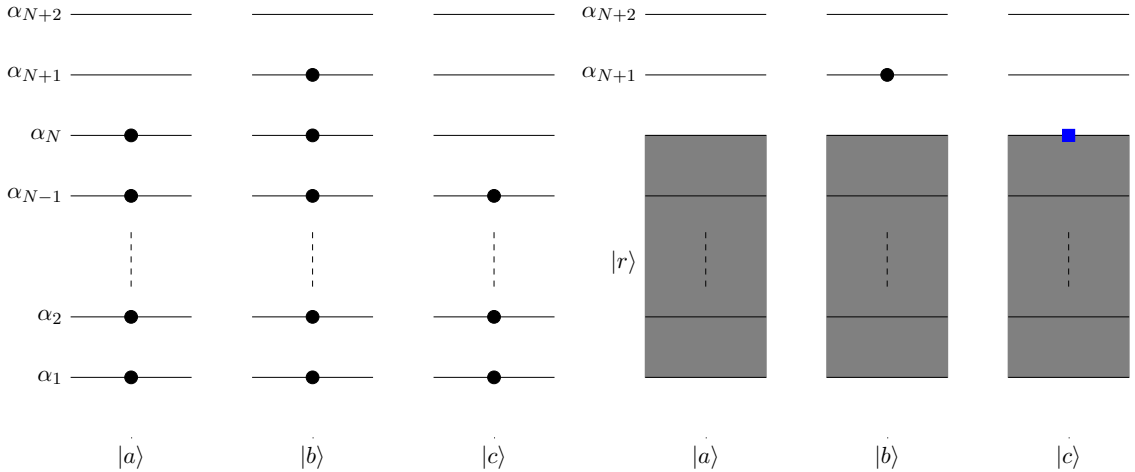


Figure 3.1: Illustration of the particle-hole representation. We have three Slater determinants: $|a\rangle \in \mathcal{H}_N^{\text{AS}}$, $|b\rangle \in \mathcal{H}_{N+1}^{\text{AS}}$ and $|c\rangle \in \mathcal{H}_{N-1}^{\text{AS}}$. To the left we have the ordinary particle representation where each occupied single-particle state is specified. The corresponding expressions are given in Eqs. (3.111), (3.111) and (3.111). To the right we have the particle-hole representation where each occupied state (by a particle or hole), that is not occupied in the reference determinant, is specified. The expressions are given in Eqs. (3.114), (3.115) and (3.115). Note that \bullet represents a particle, and \square represents a hole.

quasi-particle creation and annihilation operators, provided that the contractions are defined relative to the reference state. The only nonzero contraction is

$$b_\alpha b_\beta^\dagger = \langle r | b_\alpha b_\beta^\dagger | r \rangle = \delta_{\alpha\beta}. \quad (3.123)$$

We will omit the discussion of operators in quasi-particle representation, and evaluation of matrix elements of such operators between quasi-particle states. This is not directly relevant for this thesis.

Chapter 4

Theoretical Description of Quantum Dots

In this chapter we aim at developing a theoretical framework for the 2-dimensional quantum dot. Put simply, we want to establish a quantum mechanical description of the single-electron system, i.e. solve the time-independent Schrödinger equation in 2 dimensions. In order to achieve our goal, a model of the system must be determined. The results from this chapter will be used in the many-body treatment of quantum dots.

The first section is devoted to the theoretical model of quantum dots and the approximations that are done. We will see that the confinement potential can be approximated by the harmonic oscillator potential, which belongs to the class of spherically symmetric potentials. Therefore, the second section consider the the time-independent Schrödinger equation for a general spherically symmetric potential in 2 dimensions. For these potentials, the Schrödinger equation simplifies to two independent equations: one angular equation, and one radial equation. The angular equation can be solved without specifying the potential. Then, in the third section, we will specify the potential to the harmonic oscillator potential and solve the time-independent Schrödinger equation. Finally, we will in the last two sections develop our final model Hamilton and scale this into dimensionless form.

4.1 Approximations

As pointed out before, quantum dots are fabricated systems of trapped electrons. It is created in a semiconductor, typically gallium arsenide (GaAs). The electrons in a quantum dot are confined by either a physical barrier, typically an insulator like aluminum gallium arsenide (AlGaAs), or/and an electromagnetic field. In order to calculate properties of real life quantum dots, we obviously need a model Hamiltonian which is as close to the exact one as possible. However, quantum dots are complex devices. It is impossible to give a simple, yet totally complete, theoretical model. For example, we should determine an exact analytical expression of the confinement potential, account for edge effects, and so forth. In addition, all interactions that are present in the system should be included in our model. However, the complexity of such a model would quickly reach the limit of computational resources. Approximations are therefore necessary. In this thesis we disregard edge effects. Moreover, we only include the electron-electron interaction, which is given by the Coulomb interaction

$$v(r_{ij}) = \frac{e^2}{4\pi\epsilon_0\epsilon_r} \frac{1}{r_{ij}}, \quad (4.1)$$

where e is the electron charge, ϵ_0 is the vacuum permittivity, ϵ_r is the relative permittivity, and r_{ij} is the distance between the electrons. Numerical [10, 11, 12, 13] and experimental [14, 15, 16] studies show that the confinement potential can be approximated by the harmonic oscillator

potential

$$u(r) = \frac{1}{2}m^*\omega^2r^2, \quad (4.2)$$

where m^* is the effective mass of the electron, ω is the oscillator frequency, and r is the distance between the electron and the point in space where $u(r) = 0$. Also, theoretical simulations with this potential have predicted strong absorption of far-infrared light at the frequency corresponding to the oscillator frequency. See for example [17, 18]. This prediction is consistent with experimental results, such as [19]. Furthermore, another common approximation of quantum dots is to reduce the spatial dimensions from three to two. The third dimension is usually fixed by a manufacture technique, which force the electrons to occupy a planar region. We will in this thesis consider the 2-dimensional quantum dot. The confinement potential will be given by the harmonic oscillator potential, and the electron-electron interaction will be modeled with the Coulomb interaction. This is what we call the *parabolic* quantum dot. We will also include the effect of an electromagnetic field, where the magnetic field is constant and uniform in the z-direction, i.e. the direction that is perpendicular to the 2-dimensional electron plane.

4.2 Schrödinger Equation for Spherically Symmetric Potentials

In Nature we observe many important potentials that are spherically symmetric, i.e. they only depend on the distance from a certain point in space,

$$V = V(r). \quad (4.3)$$

The single-particle Schrödinger equation can in these cases be simplified to a set of independent equations by first introducing spherical coordinates (r, φ, θ) , and then separate the equation in these new variables. We will in the following present how we can rewrite the time-independent Schrödinger equation as a set of independent equations in 2 dimensions. The total wavefunction is given as (see Sec. 2.2.3) a tensor product between a spatial part and a spin part. Since the potential is independent of the spin of the particle, the spin part can be omitted in the calculation. We here assume that the magnetic field is zero. In the case of an electron, the eigenstates of \hat{S}_z and \hat{S}^2 is given by Eqs. (2.65) and (2.66). We will therefore in following only consider the spatial part of the total wavefunction.

In the cartesian coordinate representation, the time-independent Schrödinger equation for a single-particle system reads

$$-\frac{\hbar^2}{2m^*} \left(\frac{\partial^2}{\partial x^2} + \frac{\partial^2}{\partial y^2} \right) \phi(x, y) + u(\sqrt{x^2 + y^2})\phi(x, y) = \epsilon\phi(x, y), \quad (4.4)$$

where m is the mass of the particle, $u = u(\sqrt{x^2 + y^2})$ is a spherically symmetric potential, and $\phi(x, y)$ is the eigenfunction with corresponding eigenvalue ϵ . We now introduce spherical coordinates (r, θ) defined as

$$r \equiv \sqrt{x^2 + y^2} \quad (4.5)$$

$$\theta \equiv \arccos\left(\frac{x}{r}\right) = \arcsin\left(\frac{y}{r}\right). \quad (4.6)$$

In this representation, the time-independent Schrödinger equation reads

$$-\frac{\hbar^2}{2m^*} \left(\frac{\partial^2}{\partial r^2} + \frac{1}{r} \frac{\partial}{\partial r} + \frac{1}{r^2} \frac{\partial^2}{\partial \theta^2} \right) \phi(r, \theta) + u(r)\phi(r, \theta) = \epsilon\phi(r, \theta). \quad (4.7)$$

We are seeking the solutions that are separable in r and θ , viz.

$$\phi(r, \theta) = R(r)Y(\theta), \quad (4.8)$$

and substitute this expression into Eq. (4.7), yielding

$$-\frac{\hbar^2}{2m^*} \left(Y(\theta) \frac{\partial^2 R(r)}{\partial r^2} + \frac{Y(\theta)}{r} \frac{\partial R(r)}{\partial r} + \frac{R(r)}{r^2} \frac{\partial^2 Y(\theta)}{\partial \theta^2} \right) + u(r)R(r)Y(\theta) = \epsilon R(r)Y(\theta). \quad (4.9)$$

We multiply $-2m^*r^2/\hbar^2 R(r)Y(\theta)$ on both sides and collect the terms containing r and θ for themselves,

$$\left[\frac{r^2}{R(r)} \frac{\partial^2 R(r)}{\partial r^2} + \frac{r}{R(r)} \frac{\partial R(r)}{\partial r} - \frac{2m^*r^2}{\hbar^2} (u(r) - \epsilon) \right] + \left[\frac{1}{Y(\theta)} \frac{\partial^2 Y(\theta)}{\partial \theta^2} \right] = 0. \quad (4.10)$$

The term in the first square bracket depends only on r , whereas the second term in square bracket depends only on θ . Each term is therefore equal to a constant,

$$\frac{r^2}{R(r)} \frac{\partial^2 R(r)}{\partial r^2} + \frac{r}{R(r)} \frac{\partial R(r)}{\partial r} - \frac{2m^*r^2}{\hbar^2} (u(r) - \epsilon) = k_r \quad (4.11)$$

$$\frac{1}{Y(\theta)} \frac{\partial^2 Y(\theta)}{\partial \theta^2} = k_\theta, \quad (4.12)$$

where

$$k_r = -k_\theta. \quad (4.13)$$

We choose $k_r = m^2$. Do not confuse m with the mass of the particle m^* . Eq. (4.10) can now be written as two independent differential equations,

$$r^2 \frac{d^2 R(r)}{dr^2} + r \frac{dR(r)}{dr} - \frac{2m^*r^2 R(r)}{\hbar^2} (V(r) - \epsilon) = m^2 R(r) \quad (4.14)$$

$$\frac{d^2 Y(\theta)}{d\theta^2} = -m^2 Y(\theta). \quad (4.15)$$

The solution of the *angular equation* in (4.15) is

$$Y(\theta) = C e^{im\theta}, \quad (4.16)$$

where C is a constant, and i is the imaginary unit. Actually, there is also another solution: $e^{-im\theta}$. This is covered by allowing m to run negative. Since the spatial wavefunction must be normalized, i.e.

$$\int_0^\infty \int_0^{2\pi} |R(r)Y(\theta)|^2 r dr d\theta = 1, \quad (4.17)$$

the angular solution must satisfy

$$\int_0^{2\pi} |Y(\theta)|^2 d\theta = 1, \quad (4.18)$$

yielding $C^2 = 1/2\pi$. The normalized solution of the angular equation thus reads

$$Y(\theta) = \frac{1}{\sqrt{2\pi}} e^{im\theta}. \quad (4.19)$$

At this point, there are no mathematical restrictions on m . Since the system is invariant under 2π -rotation, we demand that

$$Y(\theta + 2\pi) = Y(\theta). \quad (4.20)$$

This imply that

$$e^{im\theta} = 1, \quad (4.21)$$

leading to the following allowed values of m ,

$$m = 0, \pm 1, \pm 2, \pm 3, \dots \quad (4.22)$$

We now turn to Eq. (4.14). In order to simplify the equation, we define

$$\rho(r) \equiv \sqrt{r}R(r) \quad \Rightarrow \quad R(r) = \frac{\rho(r)}{\sqrt{r}}, \quad (4.23)$$

and substitute this expression into Eq. (4.14), yielding

$$-\frac{\hbar^2}{2m^*} \frac{d^2\rho(r)}{dr^2} + \left[u(r) + \frac{\hbar^2}{2m^*} \frac{m^2 - \frac{1}{4}}{r^2} \right] \rho(r) = \epsilon \rho(r). \quad (4.24)$$

This is called the *radial equation*. It is identical to the 1-dimensional Schrödinger equation with an effective potential

$$u_{\text{eff}}(r) = u(r) + \frac{\hbar^2}{2m^*} \frac{m^2 - \frac{1}{4}}{r^2}. \quad (4.25)$$

Just like the centrifugal pseudo-force in classical mechanics, the second term in the above expression can be characterized as a centrifugal term which tends to throw the particle outwards. The radial part of the wavefunction must satisfy the normalization condition

$$\int_0^\infty |R(r)|^2 r dr = \int_0^\infty |\rho(r)|^2 dr = 1 \quad (4.26)$$

This is as far as we can go before we specify the potential. Given a spherically symmetric potential $u(r)$, the solution of the single-particle Schrödinger equation is found by solving the radial equation in (4.24), yielding $R(r)$ (through Eq. 4.23) and the eigenvalues ϵ . The normalized form of $R(r)$ is found by Eq. (4.26). The final spatial solution reads

$$\phi_m(r, \theta) = \frac{1}{\sqrt{2\pi}} R(r) e^{im\theta}, \quad (4.27)$$

with m given in Eq. (4.22).

4.3 Solutions for the Single-Electron Parabolic Quantum Dot

We will in this section solve the Schrödinger equation for the single-electron parabolic quantum dot in 2 dimensions. The potential is given by Eq. (4.2). In the absence of an electromagnetic field, the hamiltonian of the single-electron system reads

$$\hat{H} = -\frac{\hat{p}^2}{2m^*} + \frac{1}{2} m^* \omega^2 r^2, \quad (4.28)$$

where

$$\hat{p} = -i\hbar\nabla = -i\hbar \left(\frac{\partial}{\partial x} \mathbf{i} + \frac{\partial}{\partial y} \mathbf{j} \right) \quad (4.29)$$

is the momentum operator, m^* is the effective mass of the electron, ω is the oscillator frequency, r is the distance between the electron and the point where $1/2m^*\omega^2r^2 = 0$, and \mathbf{i} and \mathbf{j} are the cartesian unit vectors. We now introduce an electromagnetic field. The classical Hamiltonian of a charged electron in an electromagnetic field reads [20]

$$H = \frac{1}{2m} (\mathbf{p} - e\mathbf{A})^2 + e\Omega, \quad (4.30)$$

with Ω and \mathbf{A} as the electromagnetic potentials, m as the mass, e as the charge, and $\mathbf{p} = m\mathbf{v}$ is the classical momentum vector. The electromagnetic potentials are related to electromagnetic field by the equations

$$\mathbf{E} = -\frac{\partial \mathbf{A}}{\partial t} - \nabla \Omega \quad (4.31)$$

$$\mathbf{B} = \nabla \times \mathbf{A}, \quad (4.32)$$

where t is the time. In quantum mechanics, electrons carry intrinsic spin (see Sec. 2.2.2). This leads to an additional energy contribution, $-\hat{\mu} \cdot \mathbf{B}$, where $\hat{\mu}$ is the magnetic moment of the electron. The Hamiltonian of a single-electron parabolic quantum dot subjected to an electromagnetic field then reads

$$\hat{H} = \frac{1}{2m^*} (\hat{p} - e\mathbf{A})^2 + e\Omega - \hat{\mu} \cdot \mathbf{B} + \frac{1}{2}m^*\omega_0^2 r^2, \quad (4.33)$$

where \hat{p} is given by Eq. (4.29). For reasons that will appear later, the oscillator frequency is changed from ω to ω_0 . We are seeking the solution of the time-independent Schrödinger equation,

$$\left(\frac{1}{2m^*} (\hat{p} - e\mathbf{A})^2 + e\Omega - \hat{\mu} \cdot \mathbf{B} + \frac{1}{2}m^*\omega_0^2 r^2 \right) \psi(\mathbf{r}) = \epsilon \psi(\mathbf{r}), \quad (4.34)$$

where ϵ is the energy eigenvalue, and \mathbf{r} includes the spin degree of freedom. The total wavefunction (energy eigenfunction) $\psi(\mathbf{r})$ (see Sec. 2.2.3) is defined as

$$\psi(\mathbf{r}) = \phi(x, y) \otimes |\chi\rangle, \quad (4.35)$$

where $\phi(x, y)$ is the spatial part, and $|\chi\rangle$ is the spin part. We observe that the Hamiltonian contains a spin dependent part and two parts that depend on the position of the electron, i.e. parts that act in different spaces (see Sec. 2.2.3). Inserting the total wavefunction in Eq. (4.35) into the Schrödinger equation (4.34), yields

$$\frac{1}{\phi(x, y)} \left[\frac{1}{2m^*} (\hat{p} - e\mathbf{A})^2 + \frac{1}{2}m^*\omega_o^2 (x^2 + y^2) \right] \phi(x, y) - \frac{1}{|\chi\rangle} (\mu \cdot \mathbf{B}) |\chi\rangle + e\Omega = \epsilon. \quad (4.36)$$

The term in the square bracket depends only on the cartesian coordinates x and y , whereas the term in the parenthesis depends only on the spin. Therefore, each term must be equal to a constant. Eq. (4.36) can then be re-written as two independent differential equations, one for the spatial part and one for the spin part,

$$\left(\frac{1}{2m^*} [\hat{p} - e\mathbf{A}]^2 + \frac{1}{2}m^*\omega_o^2 (x^2 + y^2) \right) \phi(x, y) = \epsilon_r \phi(x, y) \quad (4.37)$$

$$- (\mu \cdot \mathbf{B}) |\chi\rangle = \epsilon_s |\chi\rangle. \quad (4.38)$$

The total energy is given as

$$\epsilon = \epsilon_r + \epsilon_s + e\Omega. \quad (4.39)$$

We first consider the spatial equation in (4.37). The equation can be simplified by writing out the first term on the left hand side,

$$\frac{1}{2m^*} (\hat{p} - e\mathbf{A})^2 = \frac{1}{2m^*} \left(\hat{p}^2 + e^2 \mathbf{A}^2 - e\mathbf{B} \cdot \hat{L} \right), \quad (4.40)$$

where \hat{L} is the angular momentum operator [1] defined as

$$\hat{L} = (x \mathbf{i} + y \mathbf{j}) \times \hat{p}, \quad (4.41)$$

where \hat{p} is given in Eq. (4.29). Furthermore, we are working in the Coulomb gauge [20], i.e.

$$\nabla \cdot \mathbf{A} = 0. \quad (4.42)$$

One possible solution is

$$\mathbf{A} = \frac{1}{2}\mathbf{B} \times (x\mathbf{i} + y\mathbf{j}). \quad (4.43)$$

The Hamiltonian can then be written in the following form,

$$\hat{H} = \frac{1}{2m^*} \left[\hat{p}^2 + \frac{e^2}{4} \left(\mathbf{B} \times (x\mathbf{i} + y\mathbf{j}) \right)^2 - e\mathbf{B} \cdot \hat{\mathbf{L}} \right] + \frac{1}{2}m^*\omega_o^2(x^2 + y^2). \quad (4.44)$$

We now consider the special case of a constant and uniform magnetic field in the z-direction, i.e.

$$\mathbf{B} = B_0\mathbf{k}, \quad (4.45)$$

where \mathbf{k} is the unit vector in the z-direction, and B_0 is a constant. The Hamiltonian then reads

$$\hat{H} = \frac{1}{2m^*} \left[\hat{p}^2 + \frac{e^2B_0^2}{4} (x^2 + y^2) - eB_0(x\hat{p}_y - y\hat{p}_x) \right] + \frac{1}{2}m^*\omega_o^2(x^2 + y^2). \quad (4.46)$$

Defining

$$\omega_B \equiv \frac{eB_0}{2m^*}, \quad (4.47)$$

and

$$\omega^2 \equiv \omega_0^2 + \omega_B^2, \quad (4.48)$$

the Hamiltonian can be written as

$$\hat{H} = \frac{1}{2m^*} \left[\hat{p}^2 - eB_0(x\hat{p}_y - y\hat{p}_x) \right] + \frac{1}{2}m^*\omega^2(x^2 + y^2). \quad (4.49)$$

We identify

$$x\hat{p}_y - y\hat{p}_x = \hat{L}_z, \quad (4.50)$$

i.e. the z-projection of the angular momentum $\hat{\mathbf{L}}$. Thus we obtain

$$\hat{H} = \frac{1}{2m^*} \left(\hat{p}^2 - eB_0\hat{L}_z \right) + \frac{1}{2}m^*\omega^2(x^2 + y^2). \quad (4.51)$$

We now introduce spherical coordinates (see Eqs. 4.5 and 4.6). In this representation, the z-projection of the angular momentum reads

$$\hat{L}_z = -i\hbar \frac{\partial}{\partial\theta}. \quad (4.52)$$

The Hamiltonian is now given as

$$\hat{H} = -\frac{\hbar^2}{2m^*} \left(\frac{\partial^2}{\partial r^2} + \frac{1}{r} \frac{\partial}{\partial r} + \frac{1}{r^2} \frac{\partial^2}{\partial\theta^2} - \frac{ieB_0}{\hbar} \frac{\partial}{\partial\theta} \right) + \frac{1}{2}m^*\omega^2r^2. \quad (4.53)$$

We are seeking the solution of the time-independent Schrödinger equation,

$$\left[-\frac{\hbar^2}{2m^*} \left(\frac{\partial^2}{\partial r^2} + \frac{1}{r} \frac{\partial}{\partial r} + \frac{1}{r^2} \frac{\partial^2}{\partial\theta^2} - \frac{ieB_0}{\hbar} \frac{\partial}{\partial\theta} \right) + \frac{1}{2}m^*\omega^2r^2 \right] \phi(r, \theta) = \epsilon_r \phi(r, \theta). \quad (4.54)$$

We observe that the time-independent Schrödinger equation for a general spherically symmetric potential (4.7) is almost identical to the equation above. The magnetic field provides an additional term,

$$-\frac{ieB_0}{\hbar} \frac{\partial}{\partial\theta}. \quad (4.55)$$

Since it only depends on the angle ϕ , the solution of Eq. (4.54) is separable. In the previous section we found that the solution of the angular equation in (4.15) is given as $\exp(im\theta)/\sqrt{2\pi}$. We therefore make the following ansatz

$$\phi(r, \theta) = R(r)e^{im\theta}, \quad (4.56)$$

where m is given by Eq. (4.22) since we demand $e^{im\theta} = 1$. Substituting the ansatz into Eq. (4.54), yields

$$\left[-\frac{\hbar^2}{2m^*} \left(\frac{d^2}{dr^2} + \frac{1}{r} \frac{d}{dr} - \frac{m^2}{r^2} + \frac{emB_0}{\hbar} \right) + \frac{1}{2} m^* \omega^2 r^2 \right] R(r) = \epsilon_r R(r). \quad (4.57)$$

The normalized energy eigenfunctions are given as

$$\phi_{nm}(r, \theta) = \sqrt{\frac{n!}{\pi(n+|m|)!}} \beta^{\frac{1}{2}(1+|m|)} r^{|m|} e^{-\frac{1}{2}\beta r^2} L_n^{|m|}(\beta r^2) e^{im\theta}, \quad (4.58)$$

where $L(\beta r^2)_n^{|m|}$ is the associated Laguerre polynomials, and β is defined as

$$\beta \equiv \frac{m^* \omega}{\hbar}. \quad (4.59)$$

The eigenvalues are given as

$$\epsilon_{r,nm} = (1 + |m| + 2n) \hbar\omega + m\hbar\omega_B, \quad (4.60)$$

where ω_B is defined in Eq. (4.47), and $n = 0, 1, 2, 3, \dots$ See App. (A.1) for the full derivation of Eq. (4.58) and Eq. (4.60).

We now consider the spin equation in (4.38). The magnetic moment is given as

$$\hat{\mu} = \frac{eg}{2m^*} \hat{S}, \quad (4.61)$$

where g is the g -factor of the electron, e is the charge, m^* is the effective mass, and \hat{S} is the spin operator. Since $\mathbf{B} = B_0 \mathbf{k}$, the spin equation reads

$$-\frac{egB_0}{2m^*} S_z |\chi\rangle = \epsilon_s |\chi\rangle, \quad (4.62)$$

where \hat{S}_z is the z-projection of the spin. The eigenvectors are given by Eqs. (2.65) and (2.66). The eigenvalues are (see Sec 2.2.2)

$$\epsilon_{s,m_s} = -\frac{eg\hbar B_0}{2m^*} m_s = g m_s \hbar \omega_B. \quad (4.63)$$

Collecting all terms that contribute to the *total* energy ϵ in Eq. (4.39), yields

$$\epsilon_{nmm_s} = (1 + |m| + 2n) \hbar\omega + m\hbar\omega_B + g m_s \hbar\omega_B + e\Omega. \quad (4.64)$$

The *total* energy eigenfunctions are given as

$$\psi_{nmm_s}(r, \theta) = \sqrt{\frac{n!}{\pi(n+|m|)!}} \beta^{\frac{1}{2}(1+|m|)} r^{|m|} e^{-\frac{1}{2}\beta r^2} L_n^{|m|}(\beta r^2) e^{im\phi} \otimes |\chi_{m_s}\rangle, \quad (4.65)$$

where $|\chi_{m_s}\rangle$ is given in Eqs. (2.65) and (2.66).

When the electromagnetic field vanishes, i.e. $\omega_B = 0$ and $\Omega = 0$, the energy is given as

$$\epsilon_{nm}^0 = (1 + |m| + 2n) \hbar\omega_0, \quad (4.66)$$

where 0 denote the absence of an electromagnetic field. This is the energy spectrum we would have obtained by directly solving the radial equation in (4.24) with the harmonic oscillator potential. Since

$$n = 0, 1, 2, 3, \dots \quad (4.67)$$

$$m = 0, \pm 1, \pm 2, \pm 3, \dots \quad (4.68)$$

$$m_s = -\frac{1}{2}, \frac{1}{2}, \quad (4.69)$$

the total degeneracy of energy level ϵ_{nm}^0 is given as

$$D = 2d = 2(1 + |m| + 2n), \quad (4.70)$$

where the factor of 2 comes from the spin degree of freedom (spin up/down). This is what we call a *shell structure*. In Nature, we often observe this feature. The most well-known case is perhaps the Hydrogen atom. The energy eigenvalues are given as (Bohr formula)

$$E_n = -\frac{1}{2\hbar^2} \left(\frac{e^2}{4\pi\epsilon_0} \right)^2 \frac{1}{n^2}, \quad (4.71)$$

where n is the so-called principal quantum number. The quantum state is characterized by four quantum numbers n, l, m_l and m_s , where l is the orbital quantum numbers, m_l is the magnetic quantum number, and m_s is the quantum number associated with the z-projection of the spin. Since the energy only depends on n , each energy level has degeneracy. Turning back to the quantum dot system, we define the shell number as

$$R \equiv (1 + |m| + 2n). \quad (4.72)$$

The shell structure is shown in Table 4.1 and illustrated in Figure 4.1. For each shell number

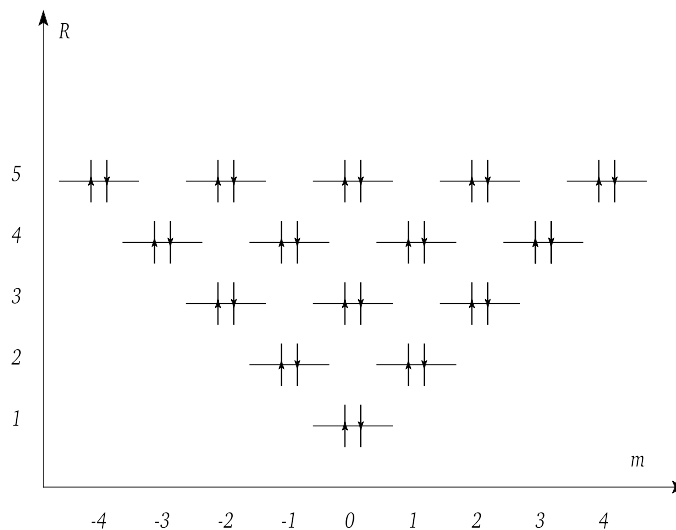


Figure 4.1: Shell structure of a single-electron parabolic quantum dot, where R is the shell number defined in Eq. (4.72), m is the angular quantum number, and $\uparrow\downarrow$ denote $m_s = \pm 1/2$ (spin quantum number).

R	$D = 2d$	Shell-filling
1	2	2
2	4	6
3	6	12
4	8	20
5	10	30
6	12	42
7	14	56

Table 4.1: Shell structure of the single-electron parabolic quantum dot, where R is the shell number (energy level) defined in Eq. (4.72), D is the degeneracy for each level, and “shell-filling” is the number of orbitals from shell 1 up to shell R .

R , we associate D orbitals. Also, for a given shell R , there are

$$D + (D - 2) + (D - 4) + \dots + 2 \quad (4.73)$$

orbitals associated with shells $R' \leq R$. We have in Table 4.1 tabulated this value for each R (Shell-filling). These are the so-called *magic numbers*, which represents the number of non-interacting electrons that are needed to obtain a closed-shell ground state. These numbers are important for many-body calculations of interacting systems. We will come back to this later.

Consider Eqs. (4.66) and (4.65). We see that the presence of magnetic field makes the energy depend on m_s and the sign of m . When the strength of the magnetic field increases, the degenerate states for $\mathbf{B} = 0$ will separate more and more. In order to illustrate this feature, we set $\Omega = 0$ (this is just a constant) and remove the spin contribution $gm_s\hbar\omega_B$. By substituting Eq. (4.48) into Eq. (4.60) and divide by $\hbar\omega_0$, we obtain

$$\frac{\epsilon_{nm}}{\hbar\omega_0} = (1 + |m| + 2n) \sqrt{1 + \frac{\omega_B^2}{\omega_0^2} + m \frac{\omega_B}{\omega_0}}. \quad (4.74)$$

This leads to the so-called Fock-Darwin energy spectrum shown in Fig. (4.2). Including the

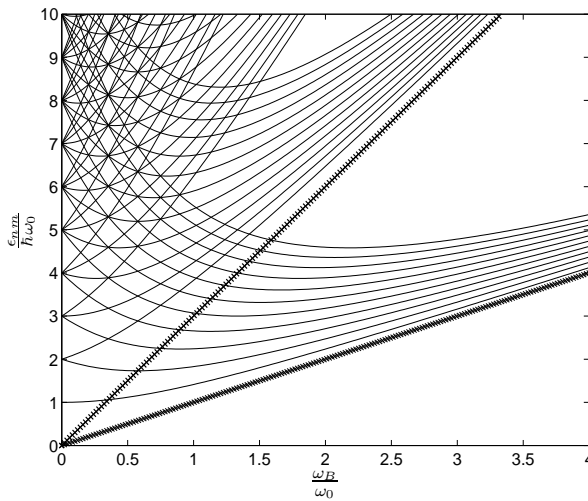


Figure 4.2: The 2-dimensional Fock-Darwin energy spectrum for a single-electron quantum dot. For $\omega_B = 0$, the energy levels are degenerate. When ω_B increases, the energy levels split due to the contribution from $m\hbar\omega_B$. Sudden degeneracy occur, with subsequent splitting. If we were to follow the “energy history” of an electron when ω_B increases, we would observe a zig-zag line since it chooses the state with the most favorable energy (after a sudden degeneracy). We clearly observe that the energy levels converge to the high field limits in Eq. (4.79), forming Landau bands.

spin part would split up each energy line and result in an even more complicated Fock-Darwin diagram. When $\omega_B = 0$, the energy levels are degenerate, as discussed above. When the magnetic field is turned on, the degenerate states separate due to the $m\hbar\omega_B$ term. Further increment of the magnetic field leads to sudden degeneracies with other states, i.e. states belonging to different shells. When the magnetic field increases even more (after a sudden degeneracy), an electron in a degenerate state will choose the state (if available) with the most favorable energy. Further increment leads to more sudden degeneracies. In Fig. (4.2) we clearly observe that the energy lines congregate into bands when the magnetic field increases. These bands are often called Landau bands. In the limit when $\omega_B \rightarrow \infty$, the energy eigenvalues (4.74) reads

$$\lim_{\omega_B \rightarrow \infty} \epsilon_{nm} = (1 + |m| + m + 2n) \hbar\omega_B. \quad (4.75)$$

When $m \geq 0$ we obtain

$$\lim_{\omega_B \rightarrow \infty} \epsilon_{nm} = (1 + 2(m + n)) \hbar\omega_B. \quad (4.76)$$

In the other case, when $m < 0$, the expression reads

$$\lim_{\omega_B \rightarrow \infty} \epsilon_{nm} = (1 + 2n) \hbar\omega_B. \quad (4.77)$$

It is natural to define the Landau number

$$N_L \equiv 0, 1, 2, 3, \dots \quad (4.78)$$

Therefore, for a sufficient strong magnetic field, the energy eigenvalues are approximately given as

$$\epsilon_L \approx (1 + 2N_L) \hbar\omega_B. \quad (4.79)$$

In Fig. (4.2), the Landau bands for $N_L = 0$ and $N_L = 1$ are shown as cross-lines. We clearly observe that when the magnetic field increases, the energy spectrum form Landau bands which converges to the Landau energies in Eq. (4.79).

4.4 N-Electron Model Hamiltonian

When the quantum dot contains more than one electron, the time-independent Schrödinger equation must be solved numerically. In order to do numerical simulations, a Hamiltonian must be provided. The Hamiltonian of an N -electron parabolic quantum dot in an electromagnetic field with $\mathbf{B} = B_0 \mathbf{k}$ reads (see Secs. 4.2 and 4.3)

$$\begin{aligned} \hat{H} = & \sum_{i=1}^N \left(-\frac{\hbar^2}{2m^*} \nabla_i^2 + \frac{1}{2} m^* \omega_0^2 r_i^2 \right) + \frac{e^2}{4\pi\epsilon_0\epsilon_r} \sum_{i=1 < j}^N \frac{1}{r_{ij}} \\ & + \sum_{i=1}^N \left(\frac{1}{2} m^* \omega_B^2 r_i^2 - \omega_B \hat{L}_z^{(i)} - g\omega_B \hat{S}_z^{(i)} \right), \end{aligned} \quad (4.80)$$

where \hbar is the Planck constant, m^* is the effective mass of the electron, $-\imath\hbar\nabla_i^2/2m^*$ is the kinetic energy of electron i , ω_0 is the oscillator frequency, r_i is the distance between electron i and the point where the harmonic oscillator potential is zero, e is the electron charge, ϵ_0 is the vacuum permittivity, ϵ_r is the relative permittivity, r_{ij} is the distance between electron i and j , ω_B is the cyclotron frequency defined in Eq. (4.47), g is the g -factor of the electron, $\hat{L}_z^{(i)}$ is the z-component

of the angular momentum, and $\hat{S}_z^{(i)}$ is the z-component of the spin. The Hamiltonian can be simplified to the following form by defining the total frequency ω in Eq. (4.48),

$$\begin{aligned}\hat{H} = & \sum_{i=1}^N \left(-\frac{\hbar^2}{2m^*} \nabla_i^2 + \frac{1}{2} m^* \omega^2 r_i^2 \right) + \frac{e^2}{4\pi\epsilon_0\epsilon_r} \sum_{i=1<j}^N \frac{1}{r_{ij}} \\ & - \sum_{i=1}^N \left(\omega_B \hat{L}_z^{(i)} + g\omega_B \hat{S}_z^{(i)} \right).\end{aligned}\quad (4.81)$$

Since both \hat{L}_z and \hat{S}_z commute with the Hamiltonian, we can perform the calculations separately in subspaces of given m and m_s [21]. We can therefore rewrite the Hamiltonian,

$$\begin{aligned}\hat{H} = & \sum_{i=1}^N \left(-\frac{\hbar^2}{2m^*} \nabla_i^2 + \frac{1}{2} m^* \omega^2 r_i^2 \right) + \frac{e^2}{4\pi\epsilon_0\epsilon_r} \sum_{i=1<j}^N \frac{1}{r_{ij}} \\ & - \sum_{i=1}^N \left(\omega_B m^{(i)} + g\omega_B m_s^{(i)} \right).\end{aligned}\quad (4.82)$$

Since the angular-part and the spin-part of the Hamiltonian only involve the good quantum numbers and not the operators themselves, one merely needs to solve the problem without the magnetic field [21], but with $\omega_0 \rightarrow \omega$. The contributions from these terms can be added after the simulation. Our final model Hamiltonian thus reads

$$\hat{H} = \sum_{i=1}^N \left(-\frac{\hbar^2}{2m^*} \nabla_i^2 + \frac{1}{2} m^* \omega^2 r_i^2 \right) + \frac{e^2}{4\pi\epsilon_0\epsilon_r} \sum_{i=1<j}^N \frac{1}{r_{ij}}.\quad (4.83)$$

4.5 Scaling the Model Hamiltonian

In order to simplify the computations, the Hamiltonian in Eq.(4.83) can be scaled into a dimensionless form. We will in the following present the scaling used by for example [22, 23, 24]. First we define

$$\begin{aligned}\omega &\equiv \omega_k \omega' \\ \mathbf{r} &\equiv l_0 \mathbf{r}' = l_0 (x' \mathbf{i} + y' \mathbf{j} + z' \mathbf{k}) \\ \nabla'^2 &\equiv \frac{\partial^2}{\partial x'^2} + \frac{\partial^2}{\partial y'^2} + \frac{\partial^2}{\partial z'^2},\end{aligned}\quad (4.84)$$

where ω_k and l_0 are constants. We then obtain

$$\begin{aligned}\nabla_i^2 &= \frac{1}{l_0^2} \nabla'^2 \\ r_i^2 &= l_0^2 r_i'^2 \\ r_{ij} &= l_0 r_{ij}'\end{aligned}\quad (4.85)$$

Inserting these expression into Eq. (4.83), yields

$$\hat{H} = -\frac{\hbar^2}{2m^* l_0^2} \sum_{i=1}^N \nabla_i'^2 + \frac{1}{2} m^* \omega_k^2 \omega'^2 l_0^2 \sum_{i=1}^N r_i'^2 + \frac{\hbar}{\kappa l_0} \sum_{i<j}^N \frac{1}{r_{ij}'},\quad (4.86)$$

where

$$\kappa \equiv \frac{4\pi\epsilon_0\epsilon_r\hbar}{e^2}.\quad (4.87)$$

Since $e^2/4\pi\epsilon_0\epsilon_r$ is units of Jm, κ is written in units of s/m. Furthermore, we define

$$l_0 \equiv \sqrt{\frac{\hbar}{m^*\omega}} = \sqrt{\frac{\hbar}{m^*\omega_k\omega'}}. \quad (4.88)$$

We observe that l_0 is in units of m. We now substitute this expression into Eq. (4.86),

$$\hat{H} = -\frac{\omega_k\omega'\hbar}{2} \sum_{i=1}^N \nabla_i'^2 + \frac{\hbar}{2}\omega_k\omega' \sum_{i=1}^N r_i'^2 + \frac{\hbar}{\kappa} \sqrt{\frac{m^*\omega_k\omega'}{\hbar}} \sum_{i < j}^N \frac{1}{r_{ij}'}. \quad (4.89)$$

We want to express the energy in units of effective Hartrees,

$$\begin{aligned} E_H^* &\equiv m^* \left(\frac{e^2}{4\pi\epsilon_0\epsilon_r\hbar} \right)^2 \\ &= \frac{m^*}{\kappa^2}, \end{aligned} \quad (4.90)$$

which is in units of J . We divide Eq. (4.89) by E_H^* , i.e. multiply with $\kappa^2\hbar/m^*$, yielding

$$\hat{H}' = -\frac{\omega_k\omega'\hbar\kappa^2}{2m^*} \sum_{i=1}^N \nabla_i'^2 + \frac{\hbar\kappa^2}{2m^*}\omega_k\omega' \sum_{i=1}^N r_i'^2 + \frac{\kappa\hbar}{m^*} \sqrt{\frac{m^*\omega_k\omega'}{\hbar}} \sum_{i < j}^N \frac{1}{r_{ij}'}, \quad (4.91)$$

where $\hat{H}' \equiv \hat{H}/E_H^*$. We now define

$$\omega_k \equiv \frac{m^*}{\hbar\kappa^2},$$

and observe that ω_k is in units of 1/s. Inserting this expression into the above equation finally yields

$$\hat{H}' = -\frac{\omega'}{2} \sum_{i=1}^N \nabla_i'^2 + \frac{1}{2}\omega' \sum_{i=1}^N r_i'^2 + \sqrt{\omega'} \sum_{i < j}^N \frac{1}{r_{ij}'}. \quad (4.92)$$

This is the dimensionless model Hamiltonian which we have performed all of our numerical calculations with. Energy is measured in units of effective Hartrees E_H^* , lengths in units of l_0 and oscillator frequencies in units of ω_k .

We now define the one-body and two-body part of the Hamiltonian as

$$\hat{h}'_i \equiv -\frac{\omega'}{2} \nabla_i'^2 + \frac{1}{2}\omega' r_i'^2 \quad (4.93)$$

$$\hat{v}'_i \equiv \sqrt{\omega'} \sum_{i < j}^N \frac{1}{r_{ij}'}, \quad (4.94)$$

leading to the following simplified form,

$$\hat{H}' = \sum_{i=1}^N \hat{h}'_i + \sum_{i < j}^N \hat{v}'_{ij}. \quad (4.95)$$

Part II

MANY-BODY METHODS

Chapter 5

Hartree-Fock Method

In this chapter we present the Hartree-Fock (HF) method for a closed-shell system [25], called the Restricted Hartree-Fock method (RHF). The aim of the chapter is to give a brief overview of the theory and a derivation of the HF equations that is implemented in this thesis. In the first section we give an introduction to the method. Then we present the basic ideas of HF and the variational principle. Thereafter, we derive the Hartree-Fock equations.

5.1 Introduction

The Hartree-Fock (HF) method is an approximate method to determine the ground state energy and wavefunction of a many-fermion system. Its origin dates back to the end of 1920s, just after the Schrödinger equation saw daylight in 1926 [26]. One year later, in 1927, D.R. Hartree introduced the self-consistent field method, which we today know as the Hartree method. This was a method to calculate approximate ground state energies and wavefunctions for atoms and ions. One of Hartrees main objectives behind the development of the Hartree method was to solve the many-body Schrödinger equation from fundamental physical principles alone. Such methods are today called *ab initio* methods. Many of Hartrees competitors did not understand the physical reasoning behind the Hartree equations and the self-consistent procedure. Furthermore, the connection to the time-independent Schrödinger equation was unclear to many people. In 1928, J. C. Slater showed that the Hartree equations can be derived by applying the quantum mechanical variational principle on a trial wavefunction (ansatz) which consists of products of single-particle functions. A few years earlier, in 1925, W. Pauli formulated the important Pauli exclusion principle stating that fermions cannot occupy identical single-particle states. In 1929, J. C. Slater published that determinants ensure the antisymmetry requirement of fermionic wavefunction and the Pauli exclusion principle [27]. V. A. Fock and J. C. Slater pointed out that the Hartree method did not respect the antisymmetry requirement of the wavefunction. Thus a more correct ansatz would be the Slater determinants. Applying the variational principle on a Slater determinant ansatz leads to the so-called Hartree-Fock method. The Hartree method can be regarded as an approximation to the Hartree-Fock method, where the exchange term is removed. Despite the physical and intuitive picture of the Hartree-Fock method, it was infrequently used until 1950s when electronic computers saw daylight.

The HF method is often called a mean-field approximation [7]. The main idea of HF is that the interactions in the system are replaced by an effective (averaged) interaction. The result is essentially that the many-body Schrödinger equation reduces to a one-body problem. Such a description means that we potentially loose important information in the system. We can only *hope* that most of the correlations in the system are well-described in this approximation. It turns out that HF calculations often give important information of the system. As an example we compare the ground state energy for the beryllium atom calculated by the Hartree-Fock method [28] and the Variational Monte Carlo method [29]. See [25] for an introduction the VMC method. Table 5.1 shows the HF results. The VMC result is $-14.4900 \pm 2.82 \cdot 10^{-4}$ (atomic

Number s-waves	Energy [E_H]
2	-13.7159
3	-14.5082
4	-14.5115
5	-14.5141
6	-14.5156
7	-14.5165
8	-14.5171
9	-14.5175
10	-14.5178
11	-14.5181
12	-14.5183
15	-14.5186

Table 5.1: Hartree-Fock results for the beryllium atom [28]. The table shows the ground state energy for different numbers of s-waves.

units). From Table (5.1) we observe that the HF method gives a better energy than VMC for $s \geq 3$. When $s = 15$, the HF energy is -14.5186 . The difference is approximately 0.03. Thus in the case of the beryllium atom, the HF method describes the correlations in the system better than the VMC ansatz (see [29]). This example illustrates that HF can sometimes yield good energy estimates despite its single-particle picture.

5.2 Basic Ideas

The basic idea of HF is the following. First we approximate the ground state wavefunction by a Slater determinant. Then we vary the single-particle orbitals in order to determine the best estimate of the ground state energy. The fundamental of HF is the variational principle of Rayleigh and Ritz (RR) (see for example [30]). This is one of the oldest and most powerful tools in quantum mechanical theory. The Rayleigh Ritz principle forms the basis of other important many-body methods such as Density Functional Theory (DFT) [9, 31]. It states that given an (in principle arbitrary) ansatz ψ_T for the ground state wavefunction, the expectation value of \hat{H} in state ψ_T is certain to overestimate the exact ground state energy. This can be verified by the following proof,

$$\begin{aligned}
 \langle \hat{H} \rangle &\equiv \langle \psi_{\text{HF}} | \hat{H} | \psi_{\text{HF}} \rangle \\
 &= \left\langle \sum_n c_n \psi_n | \hat{H} | \sum_m c_m \psi_m \right\rangle \\
 &= \left\langle \sum_n c_n \psi_n | \sum_m c_m E_m \psi_m \right\rangle \\
 &= \sum_{n,m} c_n^* E_m c_m \langle \psi_n | \psi_m \rangle \\
 &= \sum_{n,m} c_n c_m E_m \delta_{mn} \\
 &= \sum_n |c_n|^2 E_n \\
 &\leq E_0 \sum_n |c_n|^2 = E_0,
 \end{aligned}$$

where E_0 is the exact ground state energy. Our goal is to minimize $\langle \hat{H} \rangle$ in order to obtain an approximation of the ground state energy.

5.3 Derivation of the Hartree-Fock Equations

The HF ansatz reads

$$\Psi_{\text{HF}}(\mathbf{r}_1, \mathbf{r}_2, \dots, \mathbf{r}_N) = \frac{1}{\sqrt{N!}} \sum_p (-1)^p \hat{P} \varphi_a(\mathbf{r}_1) \varphi_b(\mathbf{r}_2) \dots \varphi_d(\mathbf{r}_N), \quad (5.1)$$

where $\varphi_a(\mathbf{r})$ is a so-called HF orbital. In order to minimize the energy expectation value, we have two possibilities. The first is to vary the HF orbitals directly, leading to the so-called Roothaan-Hartree-Fock [32] method. Another opportunity, which we have chosen in this thesis, is to expand the orbitals in well known single-particle functions and vary the expansion coefficients. We define the HF orbital as

$$\varphi_a(\mathbf{r}) = \sum_{\alpha}^{d_b} C_{a\alpha} \psi_{\alpha}(\mathbf{r}), \quad (5.2)$$

where $C_{a\alpha}$ is an expansion coefficient, and

$$\mathcal{B}_{\text{HF}} = \{\psi\}_{\alpha=1}^{d_b} \quad (5.3)$$

is an orthonormal set of single-particle functions spanning our model space with dimension d_b . The basis set can in principle be chosen arbitrary. We now limit the discussion to two-body Hamiltonians. Consider the Hamiltonian

$$\hat{H} = \hat{H}_0 + \hat{V}$$

where

$$\hat{H}_0 = \sum_{i=1}^N \hat{h}_i$$

is the Hamiltonian of the non-interacting system, and

$$\hat{V} = \sum_{i=1 < j}^N \hat{v}_{ij}$$

is the interaction potential between the particles. In the formalism of second quantization (see Sec. 3.5), the Hamiltonian reads

$$\hat{H} = \sum_{ab} \langle a|h|b\rangle a_a^\dagger a_b + \frac{1}{2} \sum_{abcd} \langle ab|v|cd\rangle a_a^\dagger a_b^\dagger a_d a_c,$$

where a_b^\dagger is the creation operator and a_b is the annihilation operator. We have here chosen the Hartree-Fock orbitals in Eq. (5.2) as basis functions. Using Wick's theorem (see Sec. 3.5.3), the energy expectation value reads

$$\begin{aligned} E[\Psi_{\text{HF}}] &\equiv \langle \Psi_{\text{HF}} | \hat{H} | \Psi_{\text{HF}} \rangle \\ &= \langle \Psi_{\text{HF}} | \hat{H}_0 | \Psi_{\text{HF}} \rangle + \langle \Psi_{\text{HF}} | \hat{V} | \Psi_{\text{HF}} \rangle \\ &= \sum_{ab} \langle a|h|b\rangle \langle \Psi_{\text{HF}} | a_a^\dagger a_b | \Psi_{\text{HF}} \rangle + \frac{1}{2} \sum_{abde} \langle ab|v|de\rangle \langle \Psi_{\text{HF}} | a_a^\dagger a_b^\dagger a_d a_c | \Psi_{\text{HF}} \rangle. \\ &= \sum_a^N \langle a|h|a\rangle + \frac{1}{2} \sum_{ab}^N \left[\langle ab|v|ab\rangle - \langle ab|v|ba\rangle \right]. \end{aligned} \quad (5.4)$$

Inserting Eq. (5.2) into this expression yields

$$E[\Psi_{\text{HF}}] = \sum_a^N \sum_{\alpha\beta}^{d_b} C_{a\alpha}^* C_{a\beta} \langle \alpha|h|\beta\rangle + \frac{1}{2} \sum_{ab}^N \sum_{\alpha\beta\gamma\delta}^{d_b} C_{a\alpha}^* C_{b\beta}^* C_{a\gamma} C_{b\delta} \left[\langle \alpha\beta|v|\gamma\delta\rangle - \langle \alpha\beta|v|\delta\gamma\rangle \right], \quad (5.5)$$

where N is the number of particles, the latin letters denote the new basis (Hartree-Fock orbitals), and the greek letters denote the old basis in Eq. (5.3). We now want to minimize $E[\Psi_{\text{HF}}]$ with the constraint that the Hartree-Fock orbitals are orthonormal, viz.

$$\langle a|b\rangle = \sum_{\lambda} C_{a\lambda}^* C_{b\lambda} = \delta_{ab}.$$

Thus we have to introduce Lagrangian multipliers [6]. In general, in order to find the minimum or maximum of a function $f(x, y, z, \dots, w)$ subjected to the constraints

$$g_1(x, y, z, \dots, w) = k_1 \quad (5.6)$$

$$g_2(x, y, z, \dots, w) = k_2 \quad (5.7)$$

⋮

$$g_N(x, y, z, \dots, w) = k_N, \quad (5.8)$$

we define

$$F \equiv f + \vartheta_1 g_1 + \dots + \vartheta_N g_N, \quad (5.9)$$

and set each partial derivative $\partial F / \partial x_i = 0$. The minimum or maximum is found by solving the differential equations and the constraint equations for x, y, z, \dots, w and the Lagrangian multipliers $\vartheta_1 \vartheta_2 \dots \vartheta_N$.

We define

$$\begin{aligned} F &\equiv E[\Psi_{\text{HF}}] - \sum_{a=1}^N \vartheta_a g_a \\ &= E[\Psi_{\text{HF}}] - \sum_{a=1}^N \vartheta_a \sum_{\alpha} C_{a\alpha}^* C_{a\alpha}. \end{aligned}$$

Then we take the partial derivative of F with respect to $C_{k\alpha}^*$, yielding

$$\begin{aligned} 0 &= \frac{\partial}{\partial C_{k\alpha}^*} \left(E[\Psi_{\text{HF}}] - \sum_{a=1}^N \vartheta_a \sum_{\alpha} C_{a\alpha}^* C_{a\alpha} \right) \\ &= \frac{\partial}{\partial C_{k\alpha}^*} \left(\sum_a^N \sum_{\alpha\beta} C_{a\alpha}^* C_{a\beta} \langle \alpha|h|\beta \rangle + \frac{1}{2} \sum_{ab}^N \sum_{\alpha\beta\gamma\delta} C_{a\alpha}^* C_{b\beta}^* C_{a\gamma} C_{b\delta} [\langle \alpha\beta|v|\gamma\delta \rangle - \langle \alpha\beta|v|\delta\gamma \rangle] \right. \\ &\quad \left. - \sum_{a=1}^N \vartheta_a \sum_{\alpha} C_{a\alpha}^* C_{a\alpha} \right) \\ &= \sum_{\alpha\beta} C_{k\beta} \langle \alpha|h|\beta \rangle + \sum_a^N \sum_{\alpha\beta\gamma\delta} C_{a\beta}^* C_{k\gamma} C_{a\delta} [\langle \alpha\beta|v|\gamma\delta \rangle - \langle \alpha\beta|v|\delta\gamma \rangle] - \vartheta_k \sum_{\alpha} C_{k\alpha}. \end{aligned}$$

The factor of $1/2$ disappears since $C_{a\alpha}$ and $C_{a\alpha}^*$ are independent. We simplify the expression into

$$\sum_{\alpha\beta} C_{k\beta} \langle \alpha|h|\beta \rangle + \sum_a^N \sum_{\alpha\beta\gamma\delta} C_{a\beta}^* C_{k\gamma} C_{a\delta} [\langle \alpha\beta|v|\gamma\delta \rangle - \langle \alpha\beta|v|\delta\gamma \rangle] = \vartheta_k \sum_{\alpha} C_{k\alpha}, \quad (5.10)$$

leading to

$$\sum_{\gamma} C_{k\gamma} \langle \alpha|h|\gamma \rangle + \sum_a^N \sum_{\beta\gamma\delta} C_{a\beta}^* C_{k\gamma} C_{a\delta} [\langle \alpha\beta|v|\gamma\delta \rangle - \langle \alpha\beta|v|\delta\gamma \rangle] = \vartheta_k C_{k\alpha}, \quad (5.11)$$

where we have changed the dummy index β to γ . Thus we obtain

$$\sum_{\gamma} \left(\langle \alpha | h | \gamma \rangle + \sum_a^N \sum_{\beta\delta} C_{a\beta}^* C_{a\delta} [\langle \alpha\beta | v | \gamma\delta \rangle - \langle \alpha\beta | v | \delta\gamma \rangle] \right) C_{k\gamma} = \vartheta_k C_{k\alpha}. \quad (5.12)$$

By defining the Hartree-Fock Hamiltonian as

$$h_{\alpha\gamma}^{HF} \equiv \langle \alpha | h | \gamma \rangle + \sum_a^N \sum_{\beta\delta} C_{a\beta}^* C_{a\delta} [\langle \alpha\beta | v | \gamma\delta \rangle - \langle \alpha\beta | v | \delta\gamma \rangle], \quad (5.13)$$

we finally obtain the Hartree-Fock equations,

$$\sum_{\gamma} h_{\alpha\gamma}^{HF} C_{k\gamma} = \vartheta_k C_{k\alpha}. \quad (5.14)$$

The Hartree-Fock equations are non-linear eigenvalue equations. They must be solved iteratively. Eq.(5.14) determines the expansion coefficients in Eq. (5.2) that minimizes the energy expectation value in Eq. (5.4).

Chapter 6

Coupled-Cluster Method

We will in this chapter give a presentation of the Coupled-Cluster (CC) method. The first chapter is devoted to some introductory and historical aspects of the method and motivation for what we call the Coupled-Cluster wavefunction. In the following sections we present fundamental concepts and the formal theory. The focus will be on the formal Coupled-Cluster equations, and how programmable equations are obtained. We will derive the programmable equations in detail using both an analytical and diagrammatic method. Both methods will be thoroughly presented.

6.1 Introduction and Fundamental Ideas

The CC method was introduced in the context of nuclear physics by Coester and Kümmel around 1960. In the later 1960s, the method was introduced in quantum chemistry by Čížek [33, 34] and Paldus. The community was however slow to accept the theory. The reason for this was probably that the earliest researches used elegant but unfamiliar theoretical tools such as the formalism of second quantization and Feynman-like diagrams to derive equations. Almost ten years after the important contributions from Čížek and Paldus, in 1970s, Hurley presented a re-derivation of the Coupled-Cluster Doubles (CCD) equations [35] in a framework that was more familiar to quantum chemists. Thereafter, Monkhorst [36] developed a CC response theory for calculating properties of molecular systems. In the later 1970s, computer implementations for realistic systems began to appear, with important contributions from the groups of Pople and Bartlett. Then, in 1982, Purvis and Bartlett derived the Coupled-Cluster Singles and Doubles (CCSD) equations, and implemented them in a computer program [37]. After this work, CC methods became very popular in quantum chemistry. However, in the nuclear physics community, the method gained little attention before the 1990s. Tremendous efforts has been made to construct efficient CC codes, inclusion of higher excitations (for example CCSDT), and develop methods to treat excited states (Equation of Motion Coupled-Cluster).

The CC method is a numerical method used for quantum mechanical treatment of many-body systems. The method belongs to the group of many-body methods that operates with determinantal wavefunctions. Other important members to this group are Many-Body Perturbation Theory (MBPT) and Configuration Interaction (CI) (see [38]). The CC method is today probably the most powerful *ab initio* method to obtain the ground state energy of many-body systems. The fundamental idea of the method is that the exact many-body wavefunction can be written as a linear combination of Slater determinants. The set of determinants must therefore span the whole N -electron Hilbert space. Let us now prove this. Consider a complete and orthonormal set of one-electron functions $\{\psi_\alpha(\mathbf{r})\}_{\alpha=1}^n$, where \mathbf{r} includes spin. The orthonormality is expressed as

$$\int \psi_\alpha^*(\mathbf{r}) \psi_\beta(\mathbf{r}) d\mathbf{r} = \delta_{\alpha\beta}, \quad (6.1)$$

and the completeness relation as

$$\sum_{\alpha}^n \psi_{\alpha}^{*}(\mathbf{r}') \psi_{\alpha}(\mathbf{r}) = \delta(\mathbf{r} - \mathbf{r}'). \quad (6.2)$$

We now construct an N -electron Slater determinant Φ_a from the set of single-electron functions,

$$\Phi_a(\mathbf{r}_1, \mathbf{r}_2, \dots, \mathbf{r}_N) = \frac{1}{\sqrt{N!}} \sum_p (-1)^p \widehat{P} \psi_{\alpha_1}(\mathbf{r}_1) \psi_{\alpha_2}(\mathbf{r}_2) \dots \psi_{\alpha_N}(\mathbf{r}_N), \quad (6.3)$$

where a denote the set of quantum numbers $(\alpha_1, \alpha_2, \dots, \alpha_N)$. Similarly, we construct another determinant

$$\Phi_b(\mathbf{r}_1, \mathbf{r}_2, \dots, \mathbf{r}_N) = \frac{1}{\sqrt{N!}} \sum_p (-1)^p \widehat{P} \psi_{\beta_1}(\mathbf{r}_1) \psi_{\beta_2}(\mathbf{r}_2) \dots \psi_{\beta_N}(\mathbf{r}_N), \quad (6.4)$$

where at least one function $\psi_{\beta_j} \neq \psi_{\alpha_i}$. The Slater determinants Φ_a and Φ_b are orthonormal since the set of single-electron functions are orthonormal. This is proved by

$$\begin{aligned} \int \Phi_a^{*}(\mathbf{R}) \Phi_a(\mathbf{R}) d\mathbf{R} &= \sqrt{N!} \int \Phi_a^{*}(\mathbf{R}) \psi_{\alpha_1}(\mathbf{r}_1) \dots \psi_{\alpha_N}(\mathbf{r}_N) d\mathbf{R} \\ &= \int \left[\sum_p (-1)^p \widehat{P} \psi_{\alpha_1}^{*}(\mathbf{r}_1) \dots \psi_{\alpha_N}^{*}(\mathbf{r}_N) \right] \psi_{\alpha_1}(\mathbf{r}_1) \dots \psi_{\alpha_N}(\mathbf{r}_N) d\mathbf{R} \\ &= \int |\psi_{\alpha_1}(\mathbf{r}_1)|^2 d\mathbf{r}_1 \int |\psi_{\alpha_2}(\mathbf{r}_2)|^2 d\mathbf{r}_2 \dots \int |\psi_{\alpha_N}(\mathbf{r}_N)|^2 d\mathbf{r}_N, \\ &= 1, \end{aligned} \quad (6.5)$$

and

$$\begin{aligned} \int \Phi_a^{*}(\mathbf{R}) \Phi_b(\mathbf{R}) d\mathbf{R} &= \sqrt{N!} \int \Phi_a^{*}(\mathbf{R}) \psi_{\beta_1}(\mathbf{r}_1) \dots \psi_{\beta_N}(\mathbf{r}_N) d\mathbf{R} \\ &= \int \left[\sum_p (-1)^p \widehat{P} \psi_{\alpha_1}^{*}(\mathbf{r}_1) \dots \psi_{\alpha_N}^{*}(\mathbf{r}_N) \right] \psi_{\beta_1}(\mathbf{r}_1) \dots \psi_{\beta_N}(\mathbf{r}_N) d\mathbf{R} \\ &= \int |\psi_{\alpha_1}(\mathbf{r}_1)|^2 d\mathbf{r}_1 \dots \int \psi_{\alpha_i}^{*}(\mathbf{r}_i) \psi_{\beta_i}(\mathbf{r}_i) d\mathbf{r}_i \dots \int |\psi_{\alpha_N}(\mathbf{r}_N)|^2 d\mathbf{r}_N \\ &= 0. \end{aligned} \quad (6.6)$$

The first equality in Eqs. (6.5) and (6.6) follows from the fact that given a symmetric operator \widehat{F} ,

$$\int \Phi_a^{*}(\mathbf{R}) \widehat{F} \Phi_b(\mathbf{R}) d\mathbf{R} = \sqrt{N!} \int \Phi_a^{*}(\mathbf{R}) \widehat{F} \psi_{\beta_1}(\mathbf{r}_1) \dots \psi_{\beta_N}(\mathbf{r}_N) d\mathbf{R}. \quad (6.7)$$

See [39] for proof. We conclude that Slater determinants constructed from an orthonormal set of single-electron functions, form an orthonormal set as well. We will assume that the set of Slater determinants constructed from all possible combinations of single-electron functions (that is complete and orthonormal), form a complete set, i.e. it spans the whole antisymmetric N -electron Hilbert space. In the bra-ket notation, the completeness relation reads

$$\sum_a |\Phi_a\rangle \langle \Phi_a| = 1. \quad (6.8)$$

Any N -electron wavefunction $|\Psi\rangle$ can thus be written as a linear combination of N -electron Slater determinants,

$$|\Psi\rangle = \sum_a C_a |\Phi_a\rangle, \quad (6.9)$$

where $\{C_a\}$ are the expansion coefficients. This sum goes in most cases to infinity. The expansion coefficient C_b is determined by projecting $|\Psi\rangle$ down on $|\Phi_b\rangle$,

$$\langle \Phi_b | \Psi \rangle = \sum_a C_a \langle \Phi_b | \Phi_a \rangle = \sum_a C_a \delta_{ba} = C_b. \quad (6.10)$$

The set of single-electron basis functions can in principle be chosen arbitrary. However, for a given many-electron system, the most appropriate functions (as a first step) are the solutions of the single-electron system. By “most appropriate” we mean the basis functions that allow us to truncate Eq. (6.9) without loosing important information of the system, i.e. without loosing the important correlations that are present. Assume we have solved the single-electron system and obtained a complete set of orthonormal energy eigenfunctions. As pointed out in Chapter 3, Slater determinants constructed from such a basis set are energy eigenfunctions of the non-interacting many-body system. Thus in this basis, the exact wavefunction of the interacting system (see Eq. 6.9) is the infinite sum of excited states in the non-interacting system. We have in Figure 6.1 illustrated this. The horizontal lines represents the single-electron functions

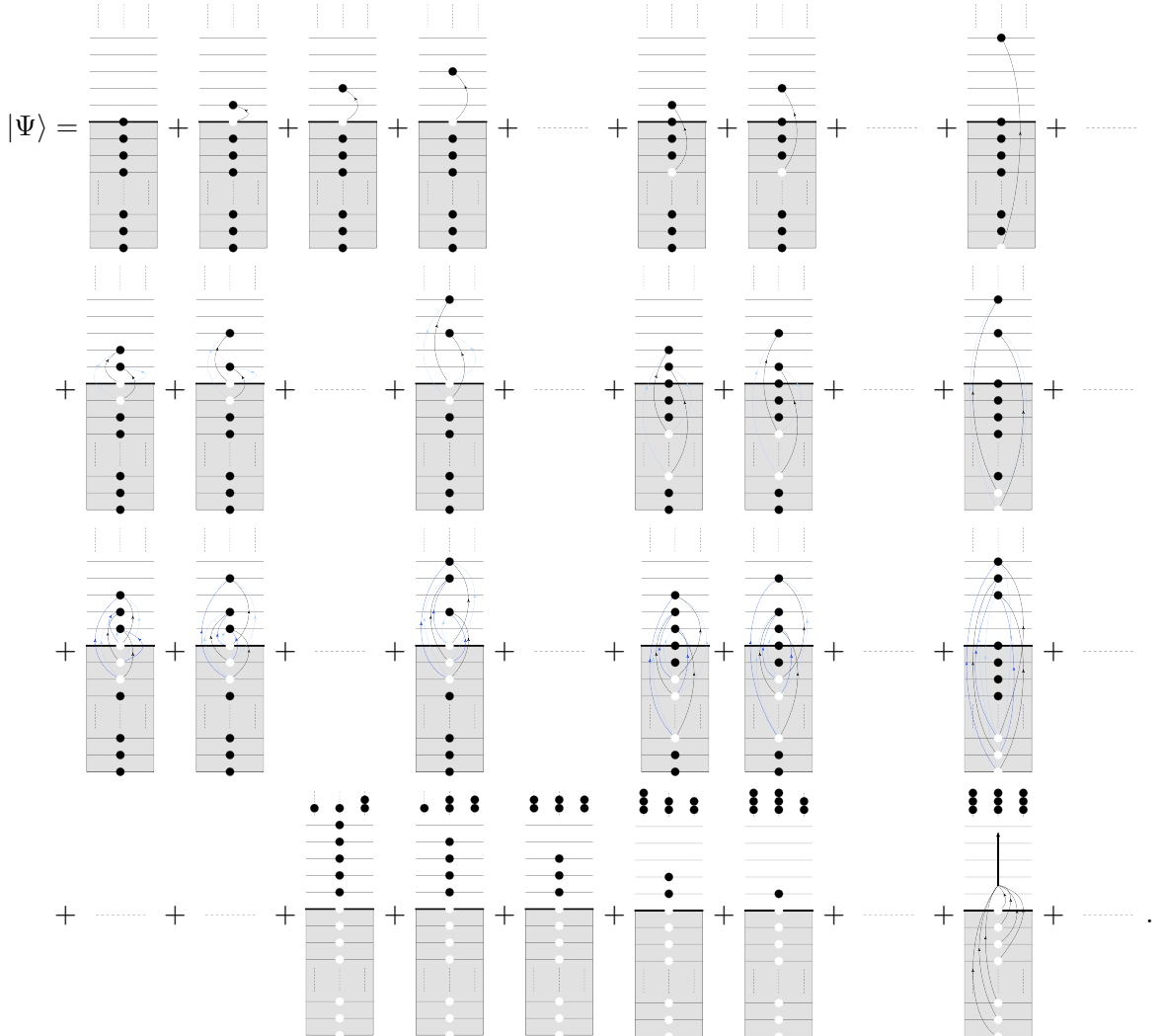


Figure 6.1: Illustration of the exact wavefunction $|\Psi\rangle$ in Eq. (6.9), written as a linear combination of eigenfunctions of the non-interacting system. The expansion coefficients are suppressed in the drawing.

(spin included). Each orbital can therefore only be occupied by one electron at most. The non-interacting ground state is represented by the shadowed area with a bold horizontal line

denoting the fermi level of the system. The black circles represent electrons, and the white ones represent holes. The define an n-particle n-hole excited state as a excited eigenfunction of the non-interacting system where n electrons are excited from below the fermi level, to orbitals above the fermi level, leaving n holes. We will in following denote n-particle n-hole excitations by the shorthand notation npnh. The 1p1h excitations are unique in the sense that given a 1p1h excited determinant, we can only obtain this state in one way. In the the 2p2h case, each excited state can be reached in two ways, indicated by the excitation lines in the figure. In the general case, one can produce each npnh excited state in $n!$ different ways. Physically, however, this is irrelevant. The physical information lies in which single-electron states that are occupied by an electron. Each diagram in Figure 6.1 therefore represents *one* Slater determinant, with its corresponding expansion coefficient suppressed.

Given the exact wavefunction $|\Psi\rangle$ and a complete set of Slater determinants, the linear combination in Eq. (6.9) is uniquely determined. However, the exact many-body wavefunction is *not* known, simply because this is the main objective in our calculation. In addition, the many-body problem can in most cases not be solved exactly. At first sight, this does not look promising. The fact is, however, that Eq. (6.9) serves as a fundamental basis for several powerful and accurate *ab initio* methods such as CC and CI. The basic idea is that the exact wavefunction is approximated with a (necessarily) truncated expansion of Slater determinants, and that the coefficients are determined by solving Schrödinger equation. When the N -electron basis is the set of eigenfunctions of the non-interacting system, the expansion coefficient C_b tells us “how much” of the correlations in the system that are represented by $|\Phi_b\rangle$. The “correct” formulation is: $|C_b|^2$ is the probability to measure the non-interacting energy eigenvalue E_b corresponding to $|\Phi_b\rangle$. Given the exact wavefunction, the coefficients are determined by Eq. (6.10). However, since the exact wavefunction is unknown, physical considerations must be build into these coefficients right from the beginning. Different approximations schemes serve as the basis for different many-body methods. Before turning to this point, we present basic notation.

6.1.1 Notation

We will in the following use the particle-hole formalism presented in Sec. 3.5.4. The reference state is defined as

$$|r\rangle = |\Phi_0\rangle, \quad (6.11)$$

where $|\Phi_0\rangle$ is the ground state of the non-interacting system,

$$|\Phi_0\rangle = a_{\alpha_1}^\dagger a_{\alpha_2}^\dagger \dots a_{\alpha_N}^\dagger |0\rangle. \quad (6.12)$$

We will denote hole states as $ijk\dots$, and particle states as $abc\dots$. Hole states are single-electron orbitals that are occupied in the reference state, while particle states are all states beyond the fermi state. These subspaces are called the occupied space and the virtual space, respectively. States that are in either of the subspaces are denoted $pqr\dots$. We will not use the standard quasi-particle creation and annihilation operators b_α^\dagger and b_α explicitly, but in an implicit way using vacuum creation and annihilation operators with quantum numbers $ij..ab..pq\dots$. This notation tells us in which subspace the operators act.

$$a_i^\dagger = b_\alpha \quad \alpha \leq \alpha_F \quad (6.13)$$

$$a_a^\dagger = b_\alpha^\dagger \quad \alpha > \alpha_F \quad (6.14)$$

$$a_i = b_\alpha \quad \alpha \leq \alpha_F \quad (6.15)$$

$$a_a = b_\alpha \quad \alpha > \alpha_F \quad (6.16)$$

We can now construct particle states, hole states and particle-hole (excited determinants) states, by acting with strings of creation and annihilation operators on the reference state:

$$\begin{aligned}
 a_a^\dagger a_b^\dagger a_c^\dagger \dots |\Phi_0\rangle &= \begin{array}{c} \text{Diagram showing three virtual orbitals (dotted lines) with particles (black dots) at positions } a, b, c. \\ \text{Below it: } \equiv |\Phi^{abc..}\rangle \end{array} \\
 a_i a_j a_k \dots |\Phi_0\rangle &= \begin{array}{c} \text{Diagram showing three occupied orbitals (solid lines) with particles (black dots) at positions } i, j, k. \\ \text{Below it: } \equiv |\Phi_{ijk..}\rangle \end{array} \\
 a_a^\dagger a_b^\dagger a_c^\dagger \dots a_k a_j a_i |\Phi_0\rangle &= \begin{array}{c} \text{Diagram showing a mix of virtual (dotted lines) and occupied (solid lines) orbitals with particles at various positions.} \\ \text{Below it: } \equiv |\Phi_{ijk..}^{abc}\rangle \end{array}
 \end{aligned}$$

Particle states will be denoted with virtual orbitals on the top right position of the ket, hole states with occupied orbitals in the lower right position, and particle-hole states with both virtual states and occupied states at their respective positions. The number of particles in a system that are represented by

$$|\Phi_{n_o}^{n_v}\rangle, \quad (6.17)$$

are given as

$$N = N' + n_v - n_o \quad (6.18)$$

where N' is the number of particles in the reference state. When $n_v = n_o \neq 0$, the state represents an excitation of the reference state.

6.2 Fundamental Concepts

We are seeking the solution of the Schrödinger equation

$$\hat{H}|\Psi\rangle = E|\Psi\rangle \quad (6.19)$$

for a system containing N interacting electrons. The Hamiltonian reads

$$\hat{H} = \hat{T} + \hat{U} + \hat{V}, \quad (6.20)$$

where

$$\hat{T} = \sum_{i=1}^N \hat{t}_i \quad (6.21)$$

$$\hat{U} = \sum_{i=1}^N \hat{u}_i \quad (6.22)$$

$$\hat{V} = \sum_{i=1}^N \hat{v}_{ij}, \quad (6.23)$$

where \hat{T} is the total kinetic energy, \hat{U} is the total potential energy, \hat{V} is the total interaction energy, \hat{t}_i is the kinetic energy of electron i , \hat{u}_i is the potential energy of electron i , and finally, \hat{v}_{ij} is the interaction energy (Coulomb interaction) between electron i and j . We define

$$\hat{h}_i \equiv \hat{t}_i + \hat{u}_i, \quad (6.24)$$

leading to

$$\hat{H}_0 \equiv \sum_{i=1}^N \hat{h}_i = \hat{T} + \hat{U}, \quad (6.25)$$

which is the Hamiltonian of the non-interacting system. In second quantization (see See 3.5), the Hamiltonian reads

$$\hat{H} = \sum_{pq} \langle p|h|q \rangle a_p^\dagger a_q + \frac{1}{4} \sum_{pqrs} \langle pq|v|rs \rangle a_p^\dagger a_q^\dagger a_s a_r, \quad (6.26)$$

where the interaction elements $\langle pq|v|rs \rangle$ are antisymmetrized.

The many-electron problem in Eq. (6.19) can in general not be solved exactly. However, as pointed out previously, given an arbitrary orthonormal and complete set of single-electron functions, the exact energy eigenfunctions of Eq. (6.19) can be written as linear combinations (see 6.9) of Slater determinants constructed from these. We now choose the single-electron basis to be the solutions of the single-electron Schrödinger equation

$$\hat{h}|\psi_\alpha\rangle = \epsilon_\alpha |\psi_\alpha\rangle, \quad (6.27)$$

with \hat{h} defined in Eq. (6.24). By using the set of Slater determinants

$$\mathcal{B}_N = \{|\Phi_a\rangle\}_{a=1}^\infty, \quad (6.28)$$

where

$$\langle \mathbf{r}_1 \mathbf{r}_2 .. \mathbf{r}_N | \Phi_a \rangle = \frac{1}{\sqrt{N!}} \sum_p (-1)^p \hat{P} \psi_{\alpha_1}(\mathbf{r}_1) \psi_{\alpha_2}(\mathbf{r}_2) .. \psi_{\alpha_N}(\mathbf{r}_N), \quad (6.29)$$

as basis functions (a running over all possible combinations of $\alpha_1 \alpha_2 .. \alpha_N$), the exact wavefunction is a linear combination of the energy eigenstates of the non-interacting system. The exact wavefunction thus reads

$$|\Psi\rangle = C_0 |\Phi\rangle + \sum_{ia} C_i^a |\Phi_i^a\rangle + \sum_{ijab} C_{ij}^{ab} |\Phi_{ij..}^{ab}\rangle + ... + \sum_{ijk..abc..} C_{ijk..}^{abc..} |\Phi_{ijk..}^{abc..}\rangle, \quad (6.30)$$

where all the electrons are excited in the last term. The first sum gives the contributions from all 1p1h excitations, the second gives the contributions from all 2p2h excitations, and so forth up to NpNh excitations. Even though the sum naturally truncates after NpNh excitations, it is still an infinite sum since the subspace containing the virtual orbitals are infinite. If the summations over single-particle orbitals are not truncated, the exact wavefunction is given by Eq. (6.30). In practice this is not possible. However, Eq. (6.30) tells us an important thing: Given the exact wavefunction, there exists a set of expansion coefficients $\{C\}$ so that the linear combination in Eq. (6.30) is equal to the exact state. The wavefunction is *not* known, meaning that the expansion coefficients are the unknowns to be determined by the Schrödinger equation. Before this can be done, we must specify the contributions to each expansion coefficient $C_{ij..}^{ab..}$. For a given excited Slater determinant $|\Phi_{ij..}^{ab..}\rangle$, the corresponding expansion coefficients $C_{ij..}^{ab..}$ gets contributions from *excitation amplitudes* with all possible couplings. As an example, consider the 3p3h-excited determinant $|\Phi_{ijk}^{abc}\rangle$. The corresponding coefficient C_{ijk}^{abc} gets contributions from excitation amplitudes with all possible couplings ,

$$C_{ijk}^{abc} = t_i^a t_j^b t_k^c + t_{ij}^{ab} t_k^c + t_i^a t_{jk}^{bc} + t_j^b t_{ik}^{ac} + t_{ijk}^{abc} \quad (6.31)$$

We thus obtain

$$C_{ijk}^{abc} |\Phi_{ijk}^{abc}\rangle = \left(t_i^a t_j^b t_k^c + t_{ij}^{ab} t_k^c + t_i^a t_{jk}^{bc} + t_j^b t_{ik}^{ac} + t_{ijk}^{abc} \right) |\Phi_{ijk}^{abc}\rangle \quad (6.32)$$

$$= \begin{array}{c} \text{Diagram 1} \\ \vdots \end{array} + \begin{array}{c} \text{Diagram 2} \\ \vdots \end{array} + \begin{array}{c} \text{Diagram 3} \\ \vdots \end{array} + \begin{array}{c} \text{Diagram 4} \\ \vdots \end{array} + \begin{array}{c} \text{Diagram 5} \\ \vdots \end{array} \quad (6.33)$$

where we have illustrated the coupling in the figures by wavy lines. Each figure in Eq. (6.33) represents the contribution from one specific coupling to the total expansion coefficient C_{ijk}^{abc} . The first figure in Eq. (6.33) represents the 3p3h determinants with three 1p1h excitations that do not couple any of the electrons. This is a crucial contribution when we consider a system consisting of two subsystems that do not interact with each other. In addition, a weakly interacting system gets important contribution from this term. The second, third and forth term in Eq. (6.33) denote 3p3h determinants where electrons in two orbitals are coupled. The fifth term denote the contribution from the 3p3h determinant where all three electrons are coupled. This example illustrates that for a certain determinant $|\Phi_{ijk..}^{abc..}\rangle$, one may divide its corresponding expansion coefficient into a sum of all possible couplings.

We now define the single-orbital excitation operator (cluster operator) as

$$\hat{t}_i \equiv \sum_a t_i^a a_a^\dagger a_i. \quad (6.34)$$

Acting with this operator on the reference state, yields

$$\hat{t}_i |\Phi\rangle = \sum_a t_i^a |\Phi_i^a\rangle. \quad (6.35)$$

Similarly, we define the two-orbital excitation operator as

$$\hat{t}_{ij}^{ab} \equiv \frac{1}{2} \sum_{ab} t_{ij}^{ab} a_a^\dagger a_b^\dagger a_j a_i. \quad (6.36)$$

Acting with this operator on the reference states, yields

$$\hat{t}_{ij}^{ab} |\Phi\rangle = \frac{1}{2} \sum_{ab} t_{ij}^{ab} |\Phi_{ij}^{ab}\rangle, \quad (6.37)$$

where the factor of 1/2 is due to two independent summations, viz. $a = c_1$ and $b = c_2$ yields the same excited state as $a = c_2$ and $b = c_1$. In general, the n -orbital excitation operator is defined as

$$\hat{t}_{ijk..}^{abc..} \equiv \frac{1}{n!} \sum_{abc..} t_{ijk..}^{abc..} a_a^\dagger a_b^\dagger a_c^\dagger \dots a_k a_j a_i. \quad (6.38)$$

When we act with this operator on the reference state, we obtain

$$\hat{t}_{ijk..}^{abc..} |\Phi\rangle = \frac{1}{n!} \sum_{abc..} t_{ijk..}^{abc..} |\Phi_{ijk..}^{abc..}\rangle. \quad (6.39)$$

These definitions allow us to produce excited determinants with all possible couplings between electrons. For example,

$$\left(\frac{1}{2} \hat{t}_i \hat{t}_j + \hat{t}_{ij} \right) |\Phi_0\rangle = \frac{1}{2} \sum_{ab} \left(t_i^a t_j^b + t_{ij}^{ab} \right) |\Phi_{ij}^{ab}\rangle, \quad (6.40)$$

produces all 2p2h excited determinants with a hole in i and j . By summing over the hole states, we obtain *all* 2p2h states

$$\frac{1}{4} \sum_{ijab} \left(t_i^a t_j^b + t_{ij}^{ab} \right) |\Phi_{ij}^{ab}\rangle, \quad (6.41)$$

with all possible couplings. We now define *total* excitation amplitudes:

$$\hat{T}_1 \equiv \sum_i \hat{t}_i = \sum_{ia} t_i^a a_a^\dagger a_i \quad (6.42)$$

$$\hat{T}_2 \equiv \frac{1}{2} \sum_{ij} \hat{t}_{ij}^{ab} = \frac{1}{4} \sum_{ijab} t_{ij}^{ab} a_a^\dagger a_b^\dagger a_j a_i \quad (6.43)$$

$$\vdots \quad \vdots$$

$$\hat{T}_n \equiv \frac{1}{n!} \sum_{ijk..} \hat{t}_{ijk..}^{abc..} a_a^\dagger a_b^\dagger a_c^\dagger ... a_k a_j a_i = \left(\frac{1}{n!} \right)^2 \sum_{ijk..abc..} t_{ijk..}^{abc..} a_a^\dagger a_b^\dagger a_c^\dagger ... a_k a_j a_i. \quad (6.44)$$

The total excitation amplitudes can be used to obtain all excitations with all possible couplings between the electrons. For example, all 3p3h determinants are obtained by using combinations of \hat{T}_1 , \hat{T}_2 and \hat{T}_3 , yielding

$$|3p3h\rangle = \left(\frac{1}{6} \hat{T}_1^3 + \hat{T}_1 \hat{T}_2 + \hat{T}_3 \right) |\Phi_0\rangle. \quad (6.45)$$

In the general case, all npnh determinants are obtained by using combinations of \hat{T}_1 , \hat{T}_2 , ..., \hat{T}_n . We thus obtain the following expression for the exact wavefunction in Eq. (6.30),

$$|\Psi\rangle = \left(1 + \hat{T}_1 + \left[\frac{1}{2!} \hat{T}_1^2 + \hat{T}_2 \right] + \left[\frac{1}{3!} \hat{T}_1^3 + \hat{T}_1 \hat{T}_2 + \hat{T}_3 \right] + \left[\frac{1}{4!} \hat{T}_1^4 + \frac{1}{2!} \hat{T}_1^2 \hat{T}_2 + \hat{T}_1 \hat{T}_3 + \frac{1}{2!} \hat{T}_2^2 + \hat{T}_4 \right] + \dots + \left[\dots + \hat{T}_N \right] \right) |\Phi_0\rangle. \quad (6.46)$$

Higher-order terms (like \hat{T}_{N+1}) do not appear since N is the number of electrons in the system. Because all excitation operators commute, i.e.

$$[\hat{T}_i, \hat{T}_j] = 0, \quad (6.47)$$

all terms in Eq. (6.46) match those from the power series expansion of an exponential function. We thus obtain that

$$|\Psi\rangle = e^{\hat{T}} |\Phi_0\rangle, \quad (6.48)$$

where

$$\hat{T} \equiv \hat{T}_1 + \hat{T}_2 + \dots + \hat{T}_N, \quad (6.49)$$

is defined as the total excitation operator. We are in practical calculation, however, forced to choose a model space, i.e. truncate the single-electron basis. Thus in practical calculations,

$$|\Psi\rangle \neq e^{\hat{T}} |\Phi_0\rangle. \quad (6.50)$$

In addition, when the system consists of many particles, the total excitation operator must also be truncated, leading to additional errors. Both truncations have consequences for the results. We therefore define the Coupled-Cluster wavefunction as

$$|\Psi\rangle_{CC} \equiv e^{\hat{T}} |\Phi_0\rangle, \quad (6.51)$$

where

$$\hat{T} = \hat{T}_1 + \hat{T}_2 + \dots + \hat{T}_i, \quad (6.52)$$

and $i \leq N$. The wavefunction in Eq. (6.51) is also called “exponential ansatz”. This is an ansatz to the exact wavefunction. Our hope is that most of the correlations in the system are baked into the CC wavefunction, viz.

$$|\Psi\rangle \approx |\Psi\rangle_{\text{CC}}. \quad (6.53)$$

How close the ansatz are to the exact wavefunction is determined by our model space and where we truncate the total excitation operator. Truncation at specific excitation levels leads to a hierarchy of CC schemes,

$$\hat{T} = \hat{T}_1 + \hat{T}_2 \rightarrow \text{CCSD} \quad (6.54)$$

$$\hat{T} = \hat{T}_1 + \hat{T}_2 + \hat{T}_3 \rightarrow \text{CCSDT} \quad (6.55)$$

$$\hat{T} = \hat{T}_1 + \hat{T}_2 + \hat{T}_3 + \hat{T}_4 \rightarrow \text{CCSDTQ} \quad (6.56)$$

$$\hat{T} = \hat{T}_1 + \hat{T}_2 + \hat{T}_3 + \hat{T}_4 + \dots + \hat{T}_N \rightarrow \text{CCSDTQ..N}$$

where S, D, T and Q denote single-, double-, triple- and quadruple-excitations, respectively. In the next section, the formal CC theory is presented.

6.3 Formal Coupled-Cluster Theory

The CC wavefunction in Eq. (6.51) is the starting point for all CC calculations. We are seeking an approximation to the exact ground state wavefunction and energy. First we assume that for a given model space and approximation scheme (CCSD, CCSDT, and so forth), the exponential ansatz is a good approximation to the wavefunction, i.e.

$$|\Psi\rangle \rightarrow |\Psi\rangle_{\text{CC}} = e^{\hat{T}}|\Phi_0\rangle. \quad (6.57)$$

This is hopefully, but not *a priori*, a good approximation. Inserting the CC wavefunction into the Schrödinger equation, yields

$$\hat{H}e^{\hat{T}}|\Phi_0\rangle = E_0e^{\hat{T}}|\Phi_0\rangle, \quad (6.58)$$

where E_0 is the ground state energy. The unknowns are the excitation amplitudes ($t_i^a, t_{ij}^{ab}, \dots, t_{ijk\dots}^{abc\dots}$) and the energy E_0 , which are determined by Eq. (6.58). The basic CC equations are the so-called energy equation and the amplitude equations. These equations constitute the basic CC machinery. The formal form of these equations are found by using a “projective” technique. The energy equation is found by multiplying the equation with the dual reference state from the left, yielding

$$\langle\Phi_0|\hat{H}e^{\hat{T}}|\Phi_0\rangle = E_0\langle\Phi_0|e^{\hat{T}}|\Phi_0\rangle = E_0. \quad (6.59)$$

The last equality follows from the fact that $\langle\Phi_0|\Psi\rangle_{\text{CC}} = 1$, by construction. Expressions for the excitation amplitudes are obtained left-multiplying the Schrödinger equation with excited determinants. For example, in order to obtain the \hat{T}_2 equation, $|\Phi_{ij}^{ab}\rangle$ must be used. The general amplitude equation reads

$$\langle\Phi_{ijk\dots}^{abc\dots}|\hat{H}e^{\hat{T}}|\Phi_0\rangle = E_0\langle\Phi_{ijk\dots}^{abc\dots}|e^{\hat{T}}|\Phi_0\rangle = E_0t_{ijk\dots}^{abc\dots}. \quad (6.60)$$

Due to the presence of $e^{\hat{T}}$, all amplitude equations are coupled, meaning that for example t_i^a depend on all other amplitudes. The CC equations must therefore be solved iteratively. Again we emphasize that the equations are formally *exact*. When \hat{T} is not truncated, and the model space is equal to the full single-electron Hilbert space, the equations are exact.

Eqs. (6.59) and (6.60) serve only as a way to get formal insight into the CC method. In practical computer implementation, however, they are not useful [40]. In order to obtain

programmable equations, the first step is to multiply Eq. (6.58) with $e^{-\hat{T}}$ from the left, and then use the “projective” technique. The modified equations are given as

$$\langle \Phi_0 | e^{-\hat{T}} \hat{H} e^{\hat{T}} | \Phi_0 \rangle = E_0 \quad (6.61)$$

$$\langle \Phi_{ijk\cdot}^{abc} | e^{-\hat{T}} \hat{H} e^{\hat{T}} | \Phi_0 \rangle = 0. \quad (6.62)$$

These equations define the conventional CC method. Furthermore, they are equivalent to the formal equations in (6.59) and (6.60), but have two important advantages. First, the amplitude equations are decoupled from the energy equation. Secondly, the similarity transformed Hamiltonian

$$e^{-\hat{T}} \hat{H} e^{\hat{T}} \quad (6.63)$$

can written as a sum of nested commutators by the so-called Campbell-Baker-Hausdorff (CBH) expansion. This sum is in principle infinite, but as we will see, it truncates naturally in our case, yielding simplified CC equations.

6.4 Coupled-Cluster Singles and Doubles Equations

We will in this section derive programmable Coupled-Cluster Singles and Doubles (CCSD) equations using both an algebraic approach, and a diagrammatic approach. In the first two subsections, we present the notion of normal-ordered form of the Hamiltonian and the Campbell-Baker-Hausdorff expansion. Thereafter, we will derive the programmable energy equation using the algebraic approach. Then we will give an introduction to CC diagrams, forming the diagrammatic approach. Both the energy and amplitude equations will be written on diagrammatic form, and then transformed to algebraic expressions using the so-called diagram rules.

In CCSD we define the total excitation operator as

$$\hat{T} \equiv \hat{T}_1 + \hat{T}_2, \quad (6.64)$$

where

$$\hat{T}_1 = \sum_{ia} t_i^a a_a^\dagger a_i \quad (6.65)$$

$$\hat{T}_2 = \frac{1}{4} \sum_{ijab} t_{ij}^{ab} a_a^\dagger a_b^\dagger a_j a_i. \quad (6.66)$$

6.4.1 Normal-Ordered Form of the Hamiltonian

The Hamiltonian is given as

$$\hat{H} = \sum_{pq} \langle p | h | q \rangle + \frac{1}{4} \sum_{pqrs} \langle pq | v | rs \rangle a_p^\dagger a_q^\dagger a_s a_r, \quad (6.67)$$

According to Wick's theorem, the two operator strings in Eq. (6.67) can be written as

$$\begin{aligned}
 a_p^\dagger a_q &= \left\{ a_p^\dagger a_q \right\} + \left\{ \overline{a_p^\dagger a_q} \right\} \\
 &= \left\{ a_p^\dagger a_q \right\} + \delta_{pq \in i} \\
 a_p^\dagger a_q^\dagger a_s a_r &= \left\{ a_p^\dagger a_q^\dagger a_s a_r \right\} + \left\{ \overline{a_p^\dagger a_q^\dagger a_s a_r} \right\} + \left\{ \overline{\overline{a_p^\dagger a_q^\dagger a_s a_r}} \right\} + \left\{ \overline{a_p^\dagger a_q^\dagger a_s a_r} \right\} \\
 &\quad + \left\{ \overline{a_p^\dagger a_q^\dagger a_s a_r} \right\} + \left\{ \overline{\overline{a_p^\dagger a_q^\dagger a_s a_r}} \right\} + \left\{ \overline{\overline{\overline{a_p^\dagger a_q^\dagger a_s a_r}}} \right\} \\
 &= \left\{ a_p^\dagger a_q^\dagger a_s a_r \right\} - \left\{ a_q^\dagger a_r \right\} \delta_{ps \in i} + \left\{ a_q^\dagger a_s \right\} \delta_{pr \in i} \\
 &\quad + \left\{ a_p^\dagger a_r \right\} \delta_{qs \in i} - \left\{ a_p^\dagger a_s \right\} \delta_{qr \in i} + \delta_{pr \in i} \delta_{qs \in j} - \delta_{ps \in i} \delta_{qr \in j},
 \end{aligned}$$

where the contraction is defined relative to the non-interacting ground state $|\Phi_0\rangle$, and $p \in i$ means that p must be contained in the set of occupied orbitals and must be equal to i . Substitute these expressions into Eq. (6.67), yields

$$\begin{aligned}
 \hat{H} &= \sum_{pq} \langle p|h|q \rangle \left\{ a_p^\dagger a_q \right\} + \sum_i \langle i|h|i \rangle \\
 &\quad + \frac{1}{4} \sum_{pqrs} \langle pq|v|rs \rangle \left\{ a_p^\dagger a_q^\dagger a_s a_r \right\} - \frac{1}{4} \sum_{qri} \langle iq|v|ri \rangle \left\{ a_q^\dagger a_r \right\} + \frac{1}{4} \sum_{qsi} \langle iq|v|is \rangle \left\{ a_q^\dagger a_s \right\} \\
 &\quad + \frac{1}{4} \sum_{pri} \langle pi|v|ri \rangle \left\{ a_p^\dagger a_r \right\} - \frac{1}{4} \sum_{psi} \langle pi|v|is \rangle \left\{ a_p^\dagger a_s \right\} + \frac{1}{4} \sum_{ij} \langle ij|v|ij \rangle - \frac{1}{4} \sum_{ij} \langle ij|v|ji \rangle.
 \end{aligned}$$

Furthermore, since the two-particle matrix element $\langle pq|v|rs \rangle$ is antisymmetrized, it satisfies the following relation,

$$\langle pq|v|rs \rangle = -\langle pr|v|sr \rangle = -\langle rp|v|rs \rangle = \langle rp|v|sr \rangle. \quad (6.68)$$

Using this relation, the Hamiltonian can then be written as

$$\hat{H} = \sum_{pq} \langle p|h|q \rangle \left\{ a_p^\dagger a_q \right\} + \sum_{pqi} \langle pi|v|qi \rangle \left\{ a_p^\dagger a_q \right\} \quad (6.69)$$

$$+ \sum_{pqrs} \langle pq|v|rs \rangle \left\{ a_p^\dagger a_q^\dagger a_s a_r \right\} + \sum_i \langle i|h|i \rangle + \frac{1}{2} \sum_{ij} \langle ij|v|ij \rangle. \quad (6.70)$$

We now define

$$f_q^p \equiv \langle p|h|q \rangle + \sum_i \langle pi|v|qi \rangle \quad (6.71)$$

$$\hat{F}_N \equiv \sum_{pq} f_q^p \left\{ a_p^\dagger a_q \right\} \quad (6.72)$$

$$\hat{V}_N \equiv \sum_{pqrs} \langle pq|v|rs \rangle \left\{ a_p^\dagger a_q^\dagger a_s a_r \right\}. \quad (6.73)$$

By identifying

$$\langle \Phi_0 | \hat{H} | \Phi_0 \rangle = \sum_i \langle i|h|i \rangle + \frac{1}{2} \sum_{ij} \langle ij|v|ij \rangle, \quad (6.74)$$

the Hamiltonian reads

$$\hat{H} = \hat{F}_N + \hat{V}_N + \langle \Phi_0 | \hat{H} | \Phi_0 \rangle \quad (6.75)$$

$$= \hat{H}_N + \langle \Phi_0 | \hat{H} | \Phi_0 \rangle, \quad (6.76)$$

where the normal-ordered Hamiltonian \hat{H}_N is defined as

$$\hat{H}_N \equiv \hat{F}_N + \hat{V}_N. \quad (6.77)$$

Note that the N -subscript indicates normal-ordering of the operator strings. We first observe that

$$\hat{H}_N = \hat{H} - \langle \Phi_0 | \hat{H} | \Phi_0 \rangle. \quad (6.78)$$

The normal-ordered form of the Hamiltonian is thus equal to the Hamiltonian itself minus its reference expectation value. It is therefore natural to consider \hat{H}_N as a correlation operator. Actually, the normal-ordered form of *any* operator is equal to the operator itself minus its reference expectation value.

At this point, the benefit of introducing the normal-ordered form of the Hamiltonian may be unclear. We will shortly see that it form the basis needed to derive programmable equations with the algebraic method.

6.4.2 The Campbell-Baker-Hausdorff Expansion

The conventional energy and amplitude equations in (6.61) and (6.62) contain the similarity transformed Hamiltonian

$$\underline{\hat{H}} \equiv e^{-\hat{T}} \hat{H} e^{\hat{T}}. \quad (6.79)$$

Inserting Eq. (6.76) into Eq. (6.79) yields

$$\underline{\hat{H}} = e^{-\hat{T}} \hat{H}_N e^{\hat{T}} + \langle \Phi_0 | \hat{H} | \Phi_0 \rangle. \quad (6.80)$$

We now insert this expression into the Eqs. (6.61) and (6.62), leading to

$$E_0 = \langle \Phi_0 | e^{-\hat{T}} \hat{H}_N e^{\hat{T}} | \Phi_0 \rangle + \langle \Phi_0 | \hat{H} | \Phi_0 \rangle \quad (6.81)$$

$$0 = \langle \Phi_i^a | e^{-\hat{T}} \hat{H}_N e^{\hat{T}} | \Phi_0 \rangle \quad (6.82)$$

$$0 = \langle \Phi_{ij}^{ab} | e^{-\hat{T}} \hat{H}_N e^{\hat{T}} | \Phi_0 \rangle. \quad (6.83)$$

Since the reference expectation value of the Hamiltonian is known, the CC problem is reduced to calculating matrix elements of the similarity transformed normal-ordered Hamiltonian. We now define the CC energy as

$$E_{\text{CC}} \equiv \langle \Phi_0 | e^{-\hat{T}} \hat{H}_N e^{\hat{T}} | \Phi_0 \rangle = E_0 - \langle \Phi_0 | \hat{H} | \Phi_0 \rangle. \quad (6.84)$$

The CCSD equations are usually written as

$$\langle \Phi_0 | e^{-\hat{T}} \hat{H}_N e^{\hat{T}} | \Phi_0 \rangle = E_{\text{CC}} \quad (6.85)$$

$$\langle \Phi_i^a | e^{-\hat{T}} \hat{H}_N e^{\hat{T}} | \Phi \rangle = 0 \quad (6.86)$$

$$\langle \Phi_{ij}^{ab} | e^{-\hat{T}} \hat{H}_N e^{\hat{T}} | \Phi \rangle = 0. \quad (6.87)$$

The next step is to find an expression for $e^{-\hat{T}} \hat{H}_N e^{\hat{T}}$. Using the well-known Campbell-Baker-Hausdorff formula, we obtain

$$e^{-\hat{T}} \hat{H}_N e^{\hat{T}} = \hat{H}_N + [\hat{H}_N, \hat{T}] + \frac{1}{2!} [[\hat{H}_N, \hat{T}], \hat{T}] + \frac{1}{3!} [[[[\hat{H}_N, \hat{T}], \hat{T}], \hat{T}] + \dots \quad (6.88)$$

The CC problem is therefore reduced to evaluating matrix elements of nested commutators. Fortunately, the sum truncates naturally.

6.4.3 Energy Equation - An Algebraic Approach

We will in this section derive the programmable form of the CCSD energy equation using the so-called algebraic approach. This equation is actually valid for all CC schemes (CCSD, CCSDT, CCSDTQ, and so forth), provided that the Hamiltonian is a two-body operator. In the CCSD scheme (see Eq. 6.64), the Hausdorff expansion in Eq. (6.88) reads

$$e^{-\widehat{T}} \widehat{H}_N e^{\widehat{T}} = \widehat{H}_N + [\widehat{H}_N, \widehat{T}_1] + [\widehat{H}_N, \widehat{T}_2] + \frac{1}{2!} [[\widehat{H}_N, \widehat{T}_1], \widehat{T}_1] + [[\widehat{H}_N, \widehat{T}_2], \widehat{T}_1] + \frac{1}{2!} [[\widehat{H}_N, \widehat{T}_2], \widehat{T}_1] + \frac{1}{2!} [[[\widehat{H}_N, \widehat{T}_1], \widehat{T}_1], \widehat{T}_1] + \frac{1}{2!} [[[\widehat{H}_N, \widehat{T}_2], \widehat{T}_1], \widehat{T}_1] + \frac{1}{3!} [[[[\widehat{H}_N, \widehat{T}_1], \widehat{T}_1], \widehat{T}_1], \widehat{T}_1] + \dots \quad (6.89)$$

We will in the following determine the contribution to the CC energy from each of the terms above. The contribution from $\langle \Phi_0 | \widehat{X} | \Phi_0 \rangle$ will be denoted as

$$E_{\text{CC}} \leftarrow \langle \Phi_0 | \widehat{X} | \Phi_0 \rangle, \quad (6.90)$$

where E_{CC} is the CC energy. We emphasize that the excitation operators are already on normal-ordered form, viz.

$$\langle \Phi_0 | \widehat{T}_k | \Phi_0 \rangle = 0. \quad (6.91)$$

Term 1

The first contribution is

$$E_{\text{CC}} \leftarrow \langle \Phi_0 | \widehat{H}_N | \Phi_0 \rangle = 0. \quad (6.92)$$

Term 2

The second contribution reads

$$E_{\text{CC}} \leftarrow \langle \Phi_0 | [\widehat{H}_N, \widehat{T}_1] | \Phi_0 \rangle = \langle \Phi_0 | [\widehat{F}_N, \widehat{T}_1] | \Phi_0 \rangle + \langle \Phi_0 | [\widehat{V}_N, \widehat{T}_1] | \Phi_0 \rangle. \quad (6.93)$$

Using Eqs. (6.72) and (6.65), we obtain the following expressions for $\widehat{F}_N \widehat{T}_1$ and $\widehat{T}_1 \widehat{F}_N$,

$$\widehat{F}_1 \widehat{T}_1 = \sum_{pqia} f_q^p t_i^a \left\{ a_p^\dagger a_q \right\} \left\{ a_a^\dagger a_i \right\} \quad (6.94)$$

$$\widehat{T}_1 \widehat{F}_1 = \sum_{pqia} f_a^p t_i^a \left\{ a_a^\dagger a_i \right\} \left\{ a_p^\dagger a_q \right\}. \quad (6.95)$$

The generalized Wick's theorem allow us to rewrite the product of normal-ordered strings of operators into

$$\begin{aligned} \left\{ a_p^\dagger a_q \right\} \left\{ a_a^\dagger a_i \right\} &= \left\{ a_p^\dagger a_q a_a^\dagger a_i \right\} + \left\{ a_p^\dagger a_q a_a^\dagger a_i \right\} + \left\{ a_p^\dagger a_q a_a^\dagger a_i \right\} + \left\{ a_p^\dagger a_q a_a^\dagger a_i \right\} \\ &= \left\{ a_p^\dagger a_q a_a^\dagger a_i \right\} + \left\{ a_q a_a^\dagger \right\} \delta_{pi} + \left\{ a_p^\dagger a_i \right\} \delta_{qa} + \delta_{pi} \delta_{qa} \\ \left\{ a_a^\dagger a_i \right\} \left\{ a_p^\dagger a_q \right\} &= \left\{ a_a^\dagger a_i a_p^\dagger a_q \right\}. \end{aligned}$$

Inserting these expressions into Eqs. (6.94) and (6.95), yields

$$[\widehat{F}_N, T_1] = \sum_{qia} f_q^i t_i^a \left\{ a_q a_a^\dagger \right\} + \sum_{pia} f_a^p t_i^a \left\{ a_p^\dagger a_i \right\} + \sum_{ia} f_a^i t_i^a. \quad (6.96)$$

Remembering that the reference expectation value of a normal-ordered string of creation and annihilation operators is zero, i.e.

$$\langle \Phi_0 | \{ \dots \} | \Phi_0 \rangle = 0, \quad (6.97)$$

yields the first non-zero contribution to the CC energy,

$$E_{\text{CC}} \leftarrow \langle \Phi_0 | [\hat{F}_N, \hat{T}_1] | \Phi_0 \rangle = \sum_{ia} f_a^i t_i^a. \quad (6.98)$$

Furthermore, using Eqs. (6.73) and (6.65), we obtain the following expression for $\hat{V}_N \hat{T}_1$ and $\hat{T}_1 \hat{V}_N$,

$$\hat{V}_N \hat{T}_1 = \frac{1}{4} \sum_{pqrsia} \langle pq|v|rs \rangle t_i^a \left\{ a_p^\dagger a_q^\dagger a_s a_r \right\} \left\{ a_a^\dagger a_i \right\} \quad (6.99)$$

$$\hat{T}_1 \hat{V}_N = \frac{1}{4} \sum_{pqrsia} \langle pq|v|rs \rangle t_i^a \left\{ a_a^\dagger a_i \right\} \left\{ a_p^\dagger a_q^\dagger a_s a_r \right\}. \quad (6.100)$$

We observe that we cannot obtain fully contracted terms, and thus the second term does not contribute to the energy, i.e.

$$E_{\text{CC}} \leftarrow \langle \Phi_0 | [\hat{V}_N, \hat{T}_1] | \Phi_0 \rangle = 0. \quad (6.101)$$

Term 3

We will now determine the contribution from

$$E_{\text{CC}} \leftarrow \langle \Phi_0 | [\hat{H}_N, \hat{T}_2] | \Phi_0 \rangle = \langle \Phi_0 | [\hat{F}_N, \hat{T}_2] | \Phi_0 \rangle + \langle \Phi_0 | [\hat{F}_N, \hat{T}_2] | \Phi_0 \rangle. \quad (6.102)$$

Eqs. (6.72) and (6.66) yield the following expressions for $\hat{F}_N \hat{T}_2$ and $\hat{T}_2 \hat{F}_N$,

$$\hat{F}_N \hat{T}_2 = \frac{1}{4} \sum_{pqijab} f_q^p t_{ij}^{ab} \left\{ a_p^\dagger a_q \right\} \left\{ a_a^\dagger a_b^\dagger a_j a_i \right\} \quad (6.103)$$

$$\hat{T}_2 \hat{F}_N = \frac{1}{4} \sum_{pqijab} f_q^p t_{ij}^{ab} \left\{ a_a^\dagger a_b^\dagger a_j a_i \right\} \left\{ a_p^\dagger a_q \right\}. \quad (6.104)$$

Using Wick's generalized theorem we observe that that $[\hat{F}_N, \hat{T}_2]$ does not include any fully contracted terms. Therefore,

$$E_{\text{CC}} \leftarrow \langle \Phi_0 | [\hat{F}_N, \hat{T}_2] | \Phi_0 \rangle = 0.$$

Furthermore, Eqs. (6.73) and (6.66) give the following expressions for $\hat{V}_N \hat{T}_2$ and $\hat{T}_2 \hat{V}_N$,

$$\hat{V}_N \hat{T}_2 = \frac{1}{16} \sum_{pqrsijab} t_{ij}^{ab} \langle pq|v|rs \rangle \left\{ a_p^\dagger a_q^\dagger a_s a_r \right\} \left\{ a_a^\dagger a_b^\dagger a_j a_i \right\} \quad (6.105)$$

$$\hat{T}_2 \hat{V}_N = \frac{1}{16} \sum_{pqrsijab} t_{ij}^{ab} \langle pq|v|rs \rangle \left\{ a_a^\dagger a_b^\dagger a_i a_j \right\} \left\{ a_p^\dagger a_q^\dagger a_s a_r \right\}. \quad (6.106)$$

Using Wick's generalized theorem, we rewrite the products of normal-ordered strings into

$$\begin{aligned} \left\{ a_p^\dagger a_q^\dagger a_s a_r \right\} \left\{ a_a^\dagger a_b^\dagger a_j a_i \right\} &= \left\{ \overbrace{a_p^\dagger a_q^\dagger a_s a_r a_a^\dagger a_b^\dagger a_j a_i}^{\text{string 1}} \right\} + \left\{ \overbrace{a_p^\dagger a_q^\dagger a_s a_r a_a^\dagger a_b^\dagger a_j a_i}^{\text{string 2}} \right\} \\ &\quad + \left\{ \overbrace{a_p^\dagger a_q^\dagger a_s a_r a_a^\dagger a_b^\dagger a_j a_i}^{\text{string 3}} \right\} + \left\{ \overbrace{a_p^\dagger a_q^\dagger a_s a_r a_a^\dagger a_b^\dagger a_j a_i}^{\text{string 4}} \right\} \\ &\quad + \left\{ a_p^\dagger a_q^\dagger a_s a_r a_a^\dagger a_b^\dagger a_j a_i \right\} + \dots \\ &= \delta_{pi} \delta_{qj} \delta_{sb} \delta_{ra} - \delta_{pi} \delta_{qj} \delta_{sa} \delta_{rb} - \delta_{pj} \delta_{qi} \delta_{sb} \delta_{ra} + \delta_{pj} \delta_{qi} \delta_{sa} \delta_{rb} \\ &\quad + \left\{ a_p^\dagger a_q^\dagger a_s a_r a_a^\dagger a_b^\dagger a_j a_i \right\} + \dots \\ \left\{ a_a^\dagger a_b^\dagger a_j a_i \right\} \left\{ a_p^\dagger a_q^\dagger a_s a_r \right\} &= \left\{ a_a^\dagger a_b^\dagger a_j a_i a_p^\dagger a_q^\dagger a_s a_r \right\}, \end{aligned}$$

where we include only fully contracted terms, and the two non-contracted terms. Inserting these expressions into Eqs. (6.106) and (6.105), yields

$$\begin{aligned} [\widehat{V}_N, \widehat{T}_2] &= \frac{1}{16} \sum_{ijab} [\langle ij|v|ab\rangle - \langle ij|v|ba\rangle - \langle ji|v|ab\rangle + \langle ji|v|ba\rangle] t_{ij}^{ab} + \dots \\ &= \frac{1}{4} \sum_{ijab} \langle ij|v|ab\rangle t_{ij}^{ab} + \dots \end{aligned} \quad (6.107)$$

We note that since

$$\left\{ a_p^\dagger a_q^\dagger a_s a_r a_a^\dagger a_b^\dagger a_j a_i \right\} = \left\{ a_a^\dagger a_b^\dagger a_j a_i a_p^\dagger a_q^\dagger a_s a_r \right\}, \quad (6.108)$$

the two non-contracted terms cancel each other in the commutator. Since only fully contracted terms give contribution to the CC energy, we finally obtain

$$E_{CC} \leftarrow \frac{1}{4} \sum_{ijab} \langle ij|v|ab\rangle t_{ij}^{ab}.$$

Term 4

The fourth contribution to the CC energy reads

$$E_{CC} \leftarrow \frac{1}{2} \langle \Phi_0 | [[\widehat{H}_N, \widehat{T}_1], \widehat{T}_1] | \Phi_0 \rangle = \frac{1}{2} \langle \Phi_0 | [[\widehat{F}_N, \widehat{T}_1], \widehat{T}_1] | \Phi_0 \rangle + \frac{1}{2} \langle \Phi_0 | [[\widehat{V}_N, \widehat{T}_1], \widehat{T}_1] | \Phi_0 \rangle.$$

Consider the first term in the above expression. Using Eqs. (6.65) and (6.96), we obtain the following expressions

$$[\widehat{F}_N, \widehat{T}_1] \widehat{T}_1 = \sum_{qijab} f_q^i t_i^a t_j^b \left\{ a_q a_a^\dagger \right\} \left\{ a_b^\dagger a_j \right\} + \sum_{pijab} f_p^i t_i^a t_j^b \left\{ a_p^\dagger a_i \right\} \left\{ a_b^\dagger a_j \right\} + \sum_{ijab} f_i^i t_i^a t_j^b \left\{ a_b^\dagger a_j \right\} \quad (6.109)$$

$$\widehat{T}_1 [\widehat{F}_N, \widehat{T}_1] = \sum_{qijab} f_q^i t_i^a t_j^b \left\{ a_b^\dagger a_j \right\} \left\{ a_q a_a^\dagger \right\} + \sum_{pijab} f_p^i t_i^a t_j^b \left\{ a_b^\dagger a_j \right\} \left\{ a_p^\dagger a_i \right\} + \sum_{ijab} f_i^i t_i^a t_j^b \left\{ a_b^\dagger a_j \right\} \quad (6.110)$$

As always, the only terms that give non-zero contribution to the CC energy are those in which all creation and annihilation operators are fully contracted. First we note that the constants terms on the right hand side of Eqs. (6.109) and (6.110) cancel each other in the full commutator expression. Moreover, all non-zero contractions are between a creation (annihilation) operator with quantum number a (i) and a annihilation (creation) operator with quantum number p , or the other way around. Thus we cannot obtain non-zero fully contracted terms in Eqs. (6.109) and (6.110). Therefore,

$$E_{CC} \leftarrow \frac{1}{2} \langle \Phi_0 | [[\widehat{F}_N, \widehat{T}_1], \widehat{T}_1] | \Phi_0 \rangle = 0.$$

Furthermore, by using Eqs. (6.99), (6.100) and (6.65), we obtain the following terms in $[[\widehat{V}_N, \widehat{T}_1], \widehat{T}_1]/2$,

$$\begin{aligned} [\widehat{V}_N, \widehat{T}_1] \widehat{T}_1 &= \frac{1}{4} \sum_{pqrsijab} \langle pq|v|rs\rangle t_i^a t_j^b \left\{ a_p^\dagger a_q^\dagger a_s a_r \right\} \left\{ a_a^\dagger a_i \right\} \left\{ a_b^\dagger a_j \right\} \\ &\quad + \frac{1}{4} \sum_{pqrsijab} \langle pq|v|rs\rangle t_i^a t_j^b \left\{ a_a^\dagger a_i \right\} \left\{ a_p^\dagger a_q^\dagger a_s a_r \right\} \left\{ a_b^\dagger a_j \right\} \\ \widehat{T}_1 [\widehat{V}_N, \widehat{T}_1] &= \frac{1}{4} \sum_{pqrsijab} \langle pq|v|rs\rangle t_i^a t_j^b \left\{ a_b^\dagger a_j \right\} \left\{ a_p^\dagger a_q^\dagger a_s a_r \right\} \left\{ a_a^\dagger a_i \right\} \\ &\quad + \frac{1}{4} \sum_{pqrsijab} \langle pq|v|rs\rangle t_i^a t_j^b \left\{ a_b^\dagger a_j \right\} \left\{ a_a^\dagger a_i \right\} \left\{ a_p^\dagger a_q^\dagger a_s a_r \right\}. \end{aligned}$$

We utilize Wick's generalized theorem in order to obtain

$$\begin{aligned} \frac{1}{2}\langle\Phi_0|[[\hat{V}_N, \hat{T}_1], \hat{T}_1]|\Phi_0\rangle &= \frac{1}{8} \sum_{pqrsijab} \langle pq|v|rs\rangle t_i^a t_j^b \\ &\quad \times (\delta_{pi}\delta_{qj}\delta_{sa}\delta_{rb} - \delta_{pi}\delta_{qj}\delta_{sb}\delta_{ra} - \delta_{pj}\delta_{qi}\delta_{sa}\delta_{rb} + \delta_{pj}\delta_{qi}\delta_{sb}\delta_{ra}) + \dots \\ &= \frac{1}{8} \sum_{ijab} (\langle ij|v|ba\rangle - \langle ij|v|ab\rangle - \langle ji|v|ba\rangle + \langle ji|v|ab\rangle) t_i^a t_j^b + \dots \\ &= \frac{1}{2} \sum_{ijab} \langle ij|v|ab\rangle t_i^a t_j^b + \dots, \end{aligned}$$

where only fully contracted terms are included. We finally obtain

$$E_{CC} \leftarrow \frac{1}{2}\langle\Phi_0|[[\hat{V}_N, \hat{T}_1], \hat{T}_1]|\Phi_0\rangle = \frac{1}{2} \sum_{ijab} \langle ij|v|ab\rangle t_i^a t_j^b.$$

We have now evaluated the first four contributions to the CC energy in Eq. (6.89). The Hausdorff expansion is in principle infinite. Fortunately, it truncates naturally. First, the examples above allow us to make an important generalization when Wick's generalized theorem is applied to the commutators: The only nonzero terms in the Hausdorff expansion are those in which the Hamiltonian has at least one contraction with every excitation operator \hat{T}_i on its right side. Thus the Hausdorff expansion reads

$$e^{-\hat{T}} \hat{H}_N e^{\hat{T}} = \left(\hat{H}_N + \hat{H}_N \hat{T} + \frac{1}{2!} \hat{H}_N \hat{T}^2 + \frac{1}{3!} \hat{H}_N \hat{T}^3 + \frac{1}{4!} \hat{H}_N \hat{T}^4 + \dots \right)_c, \quad (6.111)$$

where $\hat{T} = \hat{T}_1 + \hat{T}_2$, and the c -subscript denotes that the Hamiltonian must have *at least* one contraction with every excitation operator. Furthermore, since we are dealing with an electronic system, the Hamiltonian is a two-body operator. The Hausdorff expansion thus simplifies to

$$e^{-\hat{T}} \hat{H}_N e^{\hat{T}} = \left(\hat{H}_N + \hat{H}_N \hat{T} + \frac{1}{2} \hat{H}_N \hat{T}^2 + \frac{1}{6} \hat{H}_N \hat{T}^3 + \frac{1}{24} \hat{H}_N \hat{T}^4 \right)_c, \quad (6.112)$$

i.e. it naturally truncates. The expansion truncates when a specific Hamiltonian is determined. For example, if the Hamiltonian is a three-body operator, the sum truncates after $\hat{H}_N \hat{T}^6 / 6!$ for CCSD.

Eq. (6.112) yields the following expression for the CC energy,

$$E_{CC} = \langle\Phi_0|(\hat{H}_N + \hat{H}_N \hat{T} + \frac{1}{2} \hat{H}_N \hat{T}^2 + \frac{1}{6} \hat{H}_N \hat{T}^3 + \frac{1}{24} \hat{H}_N \hat{T}^4)_c|\Phi_0\rangle. \quad (6.113)$$

As pointed out before, only fully contracted terms give nonzero contribution. By inserting Eq. (6.64), we obtain

$$E_{CC} = \langle\Phi_0|(\hat{H}_N \hat{T}_1 + \hat{H}_N \hat{T}_2 + \frac{1}{2} \hat{H}_N \hat{T}_1^2)_{fc}|\Phi_0\rangle, \quad (6.114)$$

where the fc-subscript denotes that only the fully contracted terms are included. This expression is not limited to the CCSD scheme. It is valid for *all* CC schemes (CCSD, CCSDT, CCSDTQ, and so forth), provided that the Hamiltonian is a two-body operator. It is interesting that the energy only depends explicitly on the t_i^a and t_{ij}^{ab} amplitudes. However, in for example CCSDT, all amplitudes are coupled together yielding an implicit dependence of t_{ijk}^{abc} .

Using Eq. (6.77), we obtain the following expression for the CC energy

$$\begin{aligned} E_{CC} &= \langle\Phi_0|(\hat{F}_N \hat{T}_1 + \hat{V}_N \hat{T}_2 + \frac{1}{2} \hat{V}_N \hat{T}_1^2)_{fc}|\Phi_0\rangle \\ &= \langle\Phi_0|(\hat{F}_N \hat{T}_1)_{fc}|\Phi_0\rangle + \langle\Phi_0|(\hat{V}_N \hat{T}_2)_{fc}|\Phi_0\rangle + \frac{1}{2} \langle\Phi_0|(\hat{V}_N \hat{T}_1^2)_{fc}|\Phi_0\rangle. \end{aligned}$$

where $\widehat{V}_N \widehat{T}_1$ and $\widehat{F}_N \widehat{T}_1^2$ are removed since fully contractions are impossible. We obtain the following three contributions:

$$\begin{aligned}
 \langle \Phi_0 | (\widehat{F}_N \widehat{T}_1)_{\text{fc}} | \Phi_0 \rangle &= \sum_{pqia} f_q^p t_i^a \left\{ a_p^\dagger a_q a_a^\dagger a_i \right\} = \sum_{pqia} f_q^p t_i^a \delta_{pi} \delta_{qa} = \sum_{ia} f_a^i t_i^a \\
 \langle \Phi_0 | (\widehat{V}_N \widehat{T}_2)_{\text{fc}} | \Phi_0 \rangle &= \frac{1}{16} \sum_{pqrsijab} \langle pq | v | rs \rangle t_{ij}^{ab} \left\{ a_p^\dagger a_q^\dagger a_s a_r a_a^\dagger a_b^\dagger a_j a_i \right\} \\
 &\quad + \frac{1}{16} \sum_{pqrsijab} \langle pq | v | rs \rangle t_{ij}^{ab} \left\{ a_p^\dagger a_q^\dagger a_s a_r a_a^\dagger a_b^\dagger a_j a_i \right\} \\
 &\quad + \frac{1}{16} \sum_{pqrsijab} \langle pq | v | rs \rangle t_{ij}^{ab} \left\{ a_p^\dagger a_q^\dagger a_s a_r a_a^\dagger a_b^\dagger a_j a_i \right\} \\
 &\quad + \frac{1}{16} \sum_{pqrsijab} \langle pq | v | rs \rangle t_{ij}^{ab} \left\{ a_p^\dagger a_q^\dagger a_s a_r a_a^\dagger a_b^\dagger a_j a_i \right\} \\
 &= \frac{1}{16} \sum_{pqrsijab} \langle pq | v | rs \rangle t_{ij}^{ab} (\delta_{pi} \delta_{qj} \delta_{sb} \delta_{ra} - \delta_{pi} \delta_{qj} \delta_{sa} \delta_{rb} - \delta_{pj} \delta_{qi} \delta_{sb} \delta_{ra} + \delta_{pj} \delta_{qi} \delta_{sa} \delta_{rb}) \\
 &= \frac{1}{4} \sum_{ijab} \langle ij | v | ab \rangle t_{ij}^{ab} \\
 \frac{1}{2} \langle \Phi_0 | (\widehat{V}_N \widehat{T}_1^2)_{\text{fc}} | \Phi_0 \rangle &= \frac{1}{8} \sum_{pqrsijab} \langle pq | v | rs \rangle t_i^a t_j^b (\delta_{pi} \delta_{qj} \delta_{sa} \delta_{rb} - \delta_{pi} \delta_{qj} \delta_{sb} \delta_{ra} - \delta_{pj} \delta_{qi} \delta_{sa} \delta_{rb} + \delta_{pj} \delta_{qi} \delta_{sb} \delta_{ra}) \\
 &= \frac{1}{2} \sum_{ijab} \langle ij | v | ab \rangle t_i^a t_j^b
 \end{aligned}$$

These expression are equal to the contributions obtained from Term 1, Term 3 and Term 4. We finally arrive at the following expression for the CC energy,

$$E_{\text{CC}} = \sum_{ia} f_a^i t_i^a + \frac{1}{4} \sum_{ijab} \langle ij | v | ab \rangle t_{ij}^{ab} + \frac{1}{2} \sum_{ijab} \langle ij | v | ab \rangle t_i^a t_j^b. \quad (6.115)$$

We have now presented the algebraic approach through solving

$$E_{\text{CC}} = \langle \Phi_0 | e^{-\widehat{T}} \widehat{H}_N e^{\widehat{T}} | \Phi_0 \rangle.$$

Programmable amplitude equations can be determined in the same way by using Wick's generalized theorem and evaluate the resulting matrix elements. An important difference to the energy equation is that

$$\langle \Phi_{ijk..}^{abc..} | \widehat{X} | \Phi_0 \rangle,$$

where we have an excited determinant on the left. This means that the nonzero contributions to the amplitudes are *not* the fully contracted ones, but instead those therms with an excitation level that is equal to the excited determinant. The algebraic procedure is simple and straightforward. However, it is tedious and time-consuming even for the \widehat{T}_1 amplitude equation. The so-called diagrammatic method offers a far more convenient and practical approach to construct the programmable CC equations. We will in the next section introduce a diagrammatic approach which is particularly convenient for these equations.

6.4.4 Coupled-Cluster Diagrams

Throughout the history of many-body theory, many varieties of diagrams have been used. Depending on the mathematical context, diagrams represent wavefunctions, operators or matrix elements. Diagrams are most frequently used to represent matrix elements. For example,

$$\langle \alpha_1 \alpha_2 | \hat{O} | \alpha_1 \alpha_2 \rangle = \frac{1}{4} \sum_{pqrs} \langle pq | o | rs \rangle \langle 0 | a_{\alpha_1} a_{\alpha_2} a_p^\dagger a_q^\dagger a_s a_r a_{\alpha_1}^\dagger a_{\alpha_2}^\dagger | 0 \rangle$$

$$= \begin{array}{c} \text{Diagram 1} \\ + \end{array} \quad \begin{array}{c} \text{Diagram 2} \\ + \end{array} \quad \begin{array}{c} \text{Diagram 3} \\ + \end{array} \quad \begin{array}{c} \text{Diagram 4} \\ , \end{array} \quad (6.116)$$

where \hat{O} is a two-body operator. The standard problem is that we want to evaluate a certain matrix element, and we are seeking an algebraic expression in terms of (in our example) the matrix elements $\langle pq | v | rs \rangle$. This can obviously be done by using Wick's theorem. However, this is often a quite tedious and time-consuming procedure. Alternatively, the matrix element can be transformed into a diagrammatic expression (as we have done above), and then use so-called diagram rules in order to obtain an algebraic expression. Many varieties of diagrammatic techniques have been developed in order to give a convenient and practical approach for obtaining algebraic expressions of matrix elements. It is important to note that diagrammatic techniques are constructed and tuned to give the same results as the more “fundamental” algebraic approach using Wick's theorem.

We will in this section present the diagrammatic technique popularized by Kucharski and Bartlett [1]. This formalism allows us to construct programmable CC equations in a practical and straightforward way. We first present the diagrammatic representation of Slater determinants (particle-hole formalism) and normal-ordered operators. Then we focus on how diagrams of operators may be connected (analogous to contractions) forming operator products. This leads to a simple procedure that determines which terms contribute to the energy and amplitude equations.

Diagrams Representing Slater Determinants

Arrows constitute an important part of diagrams. They point either upwards or downwards, but will often have a tilt in the diagram. In general, arrows are used to represent Slater determinants. The particle-hole formalism, with reference determinant defined as

$$|r\rangle \equiv |\Phi_0\rangle,$$

where $|\Phi_0\rangle$ is the ground state of the non-interacting system, allow us to represent Slater determinants in a simple way. Upward and downward directed lines identify those single-particle orbitals that differ from those that are occupied in the reference determinant. We use the convention that downward directed lines represents hole states, while upward directed lines represents particle states. Thus we can represent all excited states of the non-interacting system (Slater determinants) with combinations of hole and particle lines. Figure 6.4.4 shows some examples.

Diagrams Representing Dynamical Operators

Diagrams can also represent dynamical operators. They are depicted by horizontal lines, called interaction lines, with vertical directed lines attached to it. These lines are attached to “vertices” on the interacting line. Each vertex represents the action of the operator on individual electrons. Therefore, diagrams associated with an n -body operator have n vertices. Each vertex has one

$= |\Phi_0\rangle$ (6.117)

$= |\Phi_{ij}^a\rangle$ (6.118)

$= |\Phi_{ijk}^{ab}\rangle$ (6.119)

$= |\Phi_{ijkm}^{abc}\rangle$ (6.120)

$= |\Phi_m\rangle$ (6.121)

Figure 6.2: Diagrammatic representation of Slater determinants. The non-interacting ground state is the reference state, viz. $|r\rangle = |\Phi_0\rangle$, represented by empty space. The states in the left column are excited states of the non-interacting system. They are represented with particle and hole lines (equal number) indicating which orbitals that are occupied by a particle-hole pair. In the right column are states with particles added or removed from the system.

incoming line and one outgoing line attached to it, which represents the annihilation and creation operators of the dynamical operators normal-ordered string. Since an n -body operator contains $2n$ annihilation and creation operators, diagrams representing an n -body operator contain $2n$ directed lines. The direction (upwards/downwards) is determined by in which orbital space the creation/annihilation operator acts. Operators acting in the occupied space yield downward directed lines, while operators acting in the unoccupied space yield upward directed lines. Since the orbitals in the occupied and unoccupied space are called hole states and particle states, respectively, a downward directed line is called a hole line, while an upward directed line is called a particle line. Furthermore, a directed line is placed beneath or above the interaction line depending on whether its corresponding operator is a quasi-annihilation operator or a quasi-creation operator (see Eqs. 3.118 and 3.117).

We are seeking the diagrammatic representation of \hat{F}_N , \hat{V}_N , \hat{T}_1 and \hat{T}_2 . Consider first \hat{F}_N . The second quantized form is given as

$$\hat{F}_N = \sum_{pq} f_q^p \left\{ a_p^\dagger a_q \right\}. \quad (6.122)$$

Separating the different combinations of orbitals spaces, i.e. terms with $a_i^\dagger a_j$, $a_i^\dagger a_a$, $a_a^\dagger a_i$ and $a_a^\dagger a_b$, we obtain

$$\begin{aligned} \hat{F}_N = & \sum_{ab} f_b^a \left\{ a_a^\dagger a_b \right\} + \sum_{ij} f_j^i \left\{ a_i^\dagger a_j \right\} + \sum_{ia} f_a^i \left\{ a_i^\dagger a_a \right\} + \sum_{ai} f_i^a \left\{ a_a^\dagger a_i \right\} \\ \hat{F}_N = & \text{Diagram 1} + \text{Diagram 2} + \text{Diagram 3} + \text{Diagram 4}. \end{aligned} \quad (6.123)$$

The first diagram contains one quasi-particle annihilation line (particle line) beneath the interaction line corresponding to a_i^\dagger , and one quasi-particle creation line (particle line) above corresponding to a_b . In the second diagram, we have one quasi-particle annihilation line corresponding to a_i^\dagger , and one quasi-particle creation line corresponding to a_j . In the third and fourth diagram, we have two quasi-particle annihilation lines corresponding to a_i^\dagger and a_a , and two quasi-particle creation lines corresponding to a_a^\dagger and a_i , respectively.

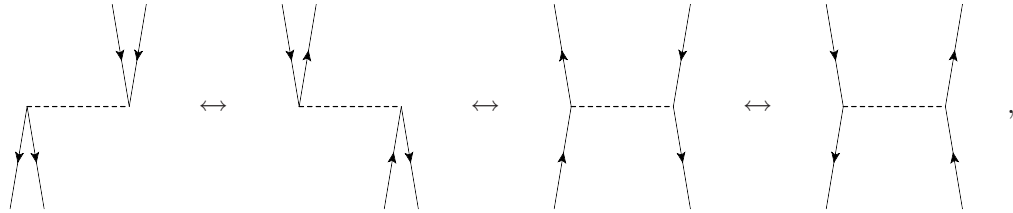
Turning to \hat{V}_N , \hat{F}_N , we partition in a similar manner as for \hat{F}_N , yielding

$$\begin{aligned} \hat{V}_N = & \frac{1}{4} \sum_{abcd} \langle ab|v|cd \rangle \left\{ a_a^\dagger a_b^\dagger a_d a_c \right\} + \frac{1}{4} \sum_{ijkl} \langle ij|v|kl \rangle \left\{ a_i^\dagger a_j^\dagger a_l a_k \right\} + \sum_{iabj} \langle ia|v|bj \rangle \left\{ a_i^\dagger a_a^\dagger a_j a_b \right\} \\ & + \frac{1}{2} \sum_{aibc} \langle ai|v|bc \rangle \left\{ a_a^\dagger a_i^\dagger a_c a_b \right\} + \frac{1}{2} \sum_{ijka} \langle ij|v|ka \rangle \left\{ a_i^\dagger a_j^\dagger a_a a_k \right\} + \frac{1}{2} \sum_{abcj} \langle ab|v|ci \rangle \left\{ a_a^\dagger a_b^\dagger a_i a_c \right\} \\ & + \frac{1}{2} \sum_{iajk} \langle ia|v|jk \rangle \left\{ a_i^\dagger a_a^\dagger a_k a_j \right\} + \frac{1}{4} \sum_{abij} \langle ab|v|ij \rangle \left\{ a_a^\dagger a_b^\dagger a_j a_i \right\} + \frac{1}{4} \sum_{ijab} \langle ij|v|ab \rangle \left\{ a_i^\dagger a_j^\dagger a_b a_a \right\}. \end{aligned}$$

The diagrammatic representation reads

$$\begin{aligned}
 \hat{V}_N = & \quad \text{Diagram 1} + \quad \text{Diagram 2} + \quad \text{Diagram 3} \\
 + & \quad \text{Diagram 4} + \quad \text{Diagram 5} + \quad \text{Diagram 6} \\
 + & \quad \text{Diagram 7} + \quad \text{Diagram 8} + \quad \text{Diagram 9}
 \end{aligned} \tag{6.124}$$

Here we have implicit antisymmetry with respect to permutation of the lines leaving or entering the vertices. For example, the sum over $\langle ia|v|bj\rangle a_i^\dagger a_a^\dagger a_j a_b$ can be transformed into the following four equivalent diagrams,



differing by a sign. Furthermore, the diagrammatic representation of \hat{T}_1 and \hat{T}_2 reads

$$\hat{T}_1 = \text{Diagram 10} \tag{6.125}$$

$$\hat{T}_2 = \text{Diagram 11} . \tag{6.126}$$

Since the second quantized form of the excitation operators in Eqs. (6.65) and (6.66) contain only quasi-particle creation operators, their diagrammatic representation do not have any directed lines beneath the interaction line.

Diagrams Representing Matrix Elements

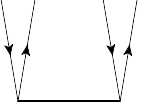
We will now consider the third representation where diagrams are interpreted as matrix elements of operators between Slater determinants. We present this representation by showing some examples.

Example 1

$$\text{Diagram 12} = \langle \Phi_i^a | \hat{T}_1 | \Phi_0 \rangle \tag{6.127}$$

Consider the diagrammatic form of \widehat{T}_1 . Since $|\Phi_0\rangle$ and $|\Phi_i^a\rangle$ are represented by empty space and a pair particle-hole lines, respectively, the diagram in Eq. (6.127) may be interpreted from bottom to top as the matrix element of \widehat{T}_1 between the reference determinant $|\Phi_0\rangle$ (on its right) and the one-particle one-hole (1p1h) excited determinant $\langle\Phi_i^a|$ (on its left).

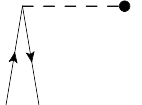
Example 2



$$= \langle\Phi_{ij}^{ab}|\widehat{T}_2|\Phi_0\rangle \quad (6.128)$$

Consider the diagrammatic form of \widehat{T}_2 . Since $|\Phi_0\rangle$ and $|\Phi_{ij}^{ab}\rangle$ are represented by empty space and two pairs of particle-hole lines, respectively, the diagram in Eq. (6.128) may be interpreted from bottom to top as the matrix element of \widehat{T}_2 between the reference determinant $|\Phi_0\rangle$ (on its right) and the two-particle two-hole (2p2h) excited determinant $\langle\Phi_{ij}^{ab}|$ (on its left).

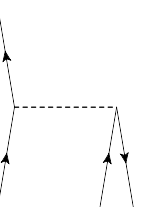
Example 3



$$= \langle\Phi_0|\widehat{F}_N|\Phi_i^a\rangle \quad (6.129)$$

Consider the fourth diagram of \widehat{F}_N in Eq. (6.123). Since $|\Phi_0\rangle$ and $|\Phi_i^a\rangle$ are represented by empty space and a pair of particle-hole lines, respectively, the diagram in Eq. (6.129) may be interpreted from bottom to top as the matrix element of \widehat{F}_N between the reference determinant $|\Phi_0\rangle$ (on its right) and the one-particle one-hole (1p1h) excited determinant $\langle\Phi_i^a|$ (on its left).

Example 4



$$= \langle\Phi^c|\widehat{V}_N|\Phi_i^{ab}\rangle \quad (6.130)$$

Consider the fourth diagram of \widehat{V}_N in Eq. (6.124). Since $|\Phi_i^{ab}\rangle$ is represented by two particle lines and one hole line, and $|\Phi^c\rangle$ is represented by one particle line, the diagram in Eq. (6.130) may be interpreted from bottom to top as the matrix element of \widehat{V}_N between the determinant $|\Phi_i^{ab}\rangle$ (on its right) and the determinant $\langle\Phi^c|$ (on its left).

We have now considered four examples that illustrate the matrix element representation of diagrams. This representation able us to find the diagrams that contribute to the CC equations in a very practical and convenient way. Before we present how this is done i practice, the concept of excitation level must be introduced. The excitation level ξ of a diagram is defined as

$$\xi = \frac{n_c - n_a}{2}, \quad (6.131)$$

where n_c is the number of quasi-particle creation lines, and n_a is the number of quasi-particle annihilation lines. Denoting $\xi_{X,i}$ as the excitation level of the i -th diagram of \widehat{X} , we obtain the

following excitation levels of \hat{F}_N , \hat{V}_N , \hat{T}_1 and \hat{T}_2 :

$$\begin{array}{ll}
 \xi_{F_N,1} = 0 & \xi_{V_N,1} = 0 \\
 \xi_{F_N,2} = 0 & \xi_{V_N,2} = 0 \\
 \xi_{F_N,3} = -1 & \xi_{V_N,3} = 0 \\
 \xi_{F_N,4} = +1 & \xi_{V_N,4} = -1 \\
 \xi_{T_1} = +1 & \xi_{V_N,5} = -1 \\
 \xi_{T_2} = +2 & \xi_{V_N,6} = +1 \\
 & \xi_{V_N,7} = +1 \\
 & \xi_{V_N,8} = +2 \\
 & \xi_{V_N,9} = -2
 \end{array}$$

For example, in the third diagram of \hat{V}_N (see Eq. 6.124), we have one “incoming” 1p1h excited determinant and one “outgoing” 1p1h excited determinant. Thus no additional excitations are produced, leading to $\xi_{V_N,3} = 0$. In the eighth diagram of \hat{V}_N , however, we have one “incoming” reference determinant and one “outgoing” 2p2h excited determinant, leading to $\xi_{V_N,8} = +2$.

6.4.5 Energy Equation on Diagrammatic Form

We will in this section present how the matrix representation of diagrams can be used in order to determine the nonzero contributions to the energy equation. Our task is to translate the equation into diagrammatic form by considering each term in

$$E_{CC} = \langle \Phi_0 | (\hat{H}_N + \hat{H}_N \hat{T} + \frac{1}{2!} \hat{H}_N \hat{T}^2 + \frac{1}{3!} \hat{H}_N \hat{T}^3 + \frac{1}{4!} \hat{H}_N \hat{T}^4 + \dots)_c | \Phi_0 \rangle, \quad (6.132)$$

where $\hat{T} = \hat{T}_1 + \hat{T}_2$, and the c -subscript denotes that \hat{H}_N must have at least one contraction with every excitation operator. The normal-ordered form of the two-body Hamiltonian is given in Eq. (6.75). The diagrammatic representations of \hat{T}_1 , \hat{T}_2 , \hat{F}_N and \hat{V}_N are given in Eqs. (6.125), (6.126), (6.123) and (6.124), respectively. We first observe that each matrix element in Eq. (6.132) has one incoming reference determinant (on its right) and one outgoing reference determinant (on its left). Thus, diagrams associated with the energy equation cannot contain directed lines (external lines) that extend above or below the diagram. A diagram contributing to the equation must therefore have *total* excitation level zero, and contain the reference determinant both at the bottom and top of the diagram. Furthermore, Eq. (6.132) contain nested commutators of \hat{H}_N , \hat{T}_1 and \hat{T}_2 , producing operator products. In the diagrammatic representation of an operator product, the rightmost operator has its interaction line at the bottom of the diagram, and the leftmost operator has its interaction line at the top. First we observe that the diagrams representing \hat{T}_1 and \hat{T}_2 have no external lines. In Eq. (6.132), \hat{H}_N must have at least one contraction with every excitation operator. When a quasi-particle creation line from one diagram is merged with a quasi-particle annihilation line from another diagram, the diagrams are said to be connected. This is analogous to contractions in Wick’s theorem. Since the total excitation level of diagrams associated with the energy equation must be zero, and the lowest excitation level of \hat{H}_N is -2 , \hat{H}_N cannot produce a total excitation level of zero. If we were to include $\hat{T}_3 \dots \hat{T}_N$, diagrams including terms with these excitations operators would not contribute to the energy. Furthermore, all terms with \hat{T}^n ($n \geq 3$) produce excitation level $\xi \geq 3$, meaning that \hat{H}_N (with minimum excitation level -2) cannot produce a total excitation level of zero. Moreover, when $n = 2$, \hat{T}_2^2 produces the excitation level $+4$. Thus Eq. (6.132) simplifies to

$$E_{CC} = \langle \Phi_0 | (\hat{H}_N \hat{T}_1 + \hat{H}_N \hat{T}_2 + \frac{1}{2} \hat{H}_N \hat{T}_1)_c | \Phi_0 \rangle, \quad (6.133)$$

where we have only included those terms with total excitation level of zero. This is the same expression as we obtained by using Wick’s theorem. We will in the following transform each term in Eq. (6.132) to a diagrammatic form.

1. Consider $\langle \Phi_0 | (\hat{H}_N \hat{T}_1)_c | \Phi_0 \rangle$. The diagrammatic representation of \hat{T}_1 is given in Eq. (6.125) with excitation level +1. We require the diagrams of \hat{F}_N in Eq. (6.123) and \hat{V}_N in Eq. (6.124) with excitation level -1 and the reference determinant at the top of the diagram. The third diagram of \hat{F}_N is the only diagram that satisfies these criterions. In order to obtain a total excitation level of zero, \hat{F}_N and \hat{T}_1 must be fully connected, viz.

$$(6.134)$$

2. Consider $\langle \Phi_0 | (\hat{H}_N \hat{T}_2)_c | \Phi_0 \rangle$. The diagrammatic representation of \hat{T}_2 is given in Eq. (6.126) with excitation level +2. We require the diagrams of \hat{H}_N with excitation level -2 and the reference determinant at top of the diagram. Obviously, \hat{F}_N cannot connect to \hat{T}_2 producing a total excitation level of zero. The ninth diagram of \hat{V}_N in Eq. (6.124) satisfy the criterions. We then fully connect the diagrams, viz.

$$(6.135)$$

3. Consider $\langle \Phi_0 | (\hat{H}_N \hat{T}_1^2)_c | \Phi_0 \rangle$. Since \hat{T}_1 commute with itself, their vertical ordering in the diagram is not important. The diagrammatic form of the operator product \hat{T}_1^2 is given as

$$\hat{T}_1^2 = \begin{array}{c} \text{two vertical lines with arrows pointing down} \\ \text{connected by a solid horizontal line with a dot at each end} \end{array}, \quad (6.136)$$

with excitation level +2. The only diagram of \hat{H}_N with excitation level -2 and no external lines at the top, is the ninth fragment of \hat{V}_N in Eq. (6.124). We then fully connect the diagrams, yielding

$$(6.137)$$

The diagrammatic form of the energy equation finally reads

$$E_{CC} = \begin{array}{c} \text{one vertical line with an arrow pointing down} \\ \text{connected by a dashed horizontal line with a dot at each end} \end{array} + \begin{array}{c} \text{two pairs of vertical lines with arrows pointing down} \\ \text{connected by dashed horizontal lines with dots at each end} \end{array} + \begin{array}{c} \text{two pairs of vertical lines with arrows pointing down} \\ \text{connected by solid horizontal lines with dots at each end} \end{array}. \quad (6.138)$$

These diagrams can be transformed to algebraic expression by using the so-called diagram rules. Before we present these, we transform the amplitude equations to diagrammatic form.

6.4.6 Amplitude Equations on Diagrammatic Form

We will in this section transform the amplitude equations into diagrammatic forms. The amplitude equations are given as

$$\langle \Phi_i^a | e^{-\hat{T}} \hat{H}_N e^{\hat{T}} | \Phi_0 \rangle = 0 \quad (6.139)$$

$$\langle \Phi_{ij}^{ab} | e^{-\hat{T}} \hat{H}_N e^{\hat{T}} | \Phi_0 \rangle = 0. \quad (6.140)$$

\hat{T}_1 Amplitude Equation

We will now transform the \hat{T}_1 equation into a diagrammatic form. Inserting Eq. (6.111) into Eq. (6.139), yields

$$\langle \Phi_i^a | (\hat{H}_N + \hat{H}_N \hat{T} + \frac{1}{2!} \hat{H}_N \hat{T}^2 + \frac{1}{3!} \hat{H}_N \hat{T}^3 + \frac{1}{4!} \hat{H}_N \hat{T}^4 + \dots)_c | \Phi_0 \rangle = 0, \quad (6.141)$$

where $\hat{T} = \hat{T}_1 + \hat{T}_2$, and the c -subscript denote that \hat{H}_N must connect with every excitation operator. Each matrix element has the reference determinant on its right and the one-particle one-hole (1p1h) excited determinant on its left. Diagrams that contribute to the equation must therefore satisfy the following three criterion:

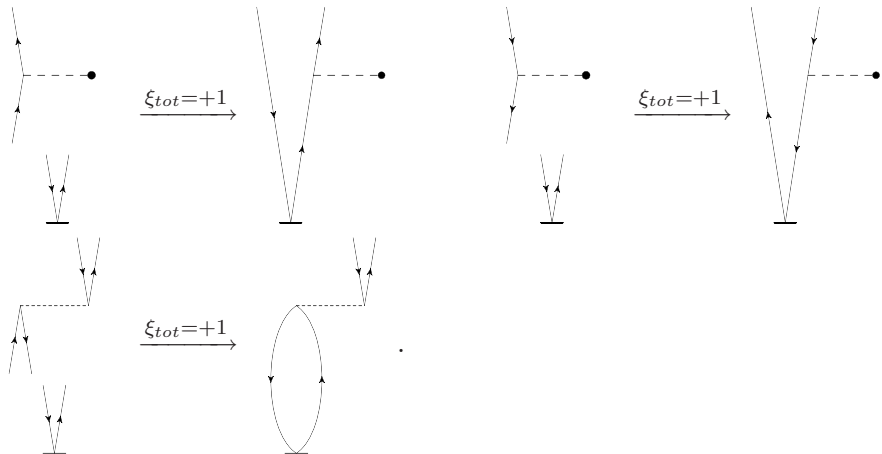
1. Total excitation level +1.
2. The reference determinant at the bottom of the diagram.
3. The 1p1h excited determinant at the top of the diagram.

Since \hat{H}_N has minimum excitation level of -2 , and \hat{T}^n ($n \geq 4$) have excitation level $\xi \geq 4$, none of the diagrams representing $(\hat{H}_N \hat{T}^n)_c$ ($n \geq 4$) fulfill these criterions. Moreover, since \hat{T}_2^2 and \hat{T}_2^3 have excitation level +4 and +6, respectively, none of the diagrams representing $\hat{H}_N \hat{T}_2^2$ and $\hat{H}_N \hat{T}_2^3$ contribute. The \hat{T}_1 amplitude equation thus reads

$$\langle \Phi_i^a | (\hat{H}_N + \hat{H}_N \hat{T}_1 + \hat{H}_N \hat{T}_2 + \frac{1}{2} \hat{H}_N \hat{T}_1^2 + \hat{H}_N \hat{T}_1 \hat{T}_2 + \frac{1}{6} \hat{H}_N \hat{T}_1^3)_c | \Phi_0 \rangle = 0. \quad (6.142)$$

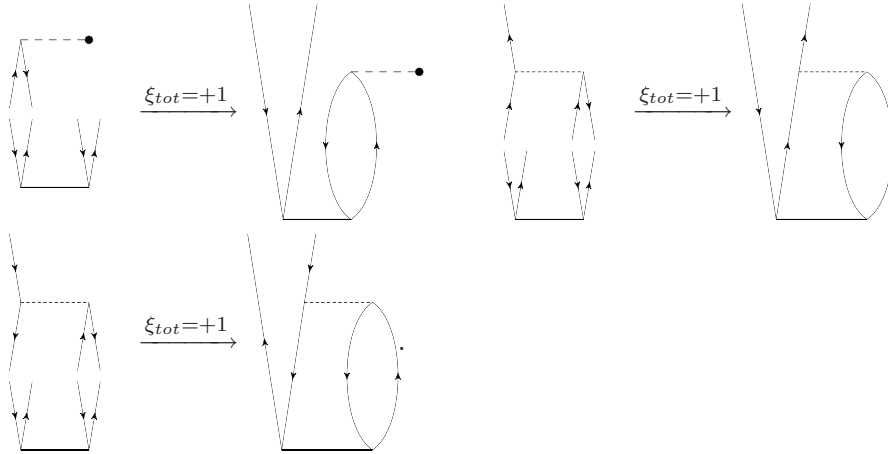
We will in the following consider the diagrams of \hat{T}_1 , \hat{T}_2 , \hat{F}_N and \hat{V}_N in Eq. (6.125), (6.126), (6.123) and (6.124), respectively, and transform each term into a diagrammatic form.

1. Consider $\langle \Phi_i^a | \hat{H}_N | \Phi_0 \rangle$. The diagrams of \hat{V}_N do not contribute to the equation since none of them satisfy our criterions. This is a consequence of the fact that \hat{V}_N is a two-body operator. The fourth fragment of \hat{F}_N , however, contribute.
2. Consider $\langle \Phi_i^a | (\hat{H}_N \hat{T}_1)_c | \Phi_0 \rangle$. Obviously, \hat{T}_1 has excitation level +1. Thus we require the diagrams of \hat{H}_N with an excitation level of zero that can connect to \hat{T}_1 satisfying the criterions above. We observe that the first and second diagram of \hat{F}_N , and the third fragment of \hat{V}_N , can connect to \hat{T}_1 in this way. We obtain the following three contributions:

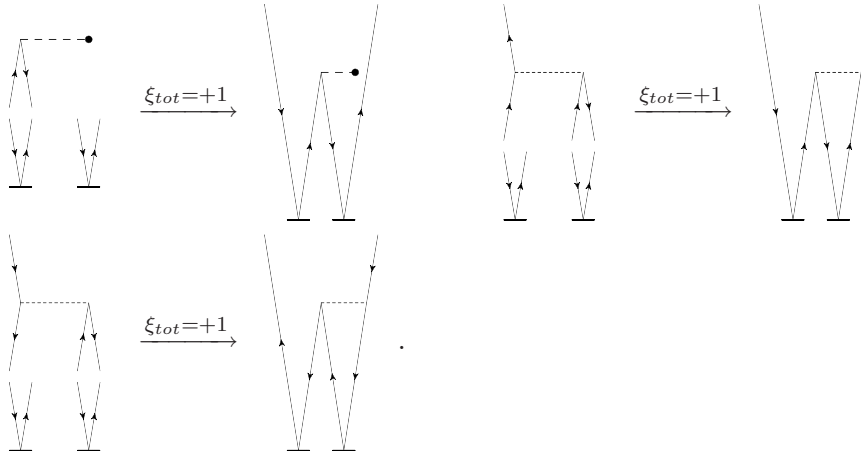


3. Consider $\langle \Phi_i^a | (\hat{H}_N \hat{T}_2)_c | \Phi_0 \rangle$. Obviously, \hat{T}_2 has excitation level +2. Thus we require the diagrams of \hat{H}_N with excitation level -1 that can connect to \hat{T}_2 satisfying our criterions.

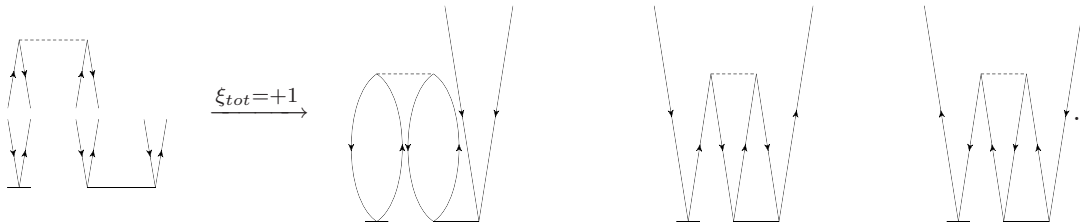
The third fragment of \hat{F}_N , and the fourth and fifth fragment of \hat{V}_N , give contributions to the equation. By connecting the diagrams, we obtain the following contributions:



4. Consider $\langle \Phi_i^a | (\frac{1}{2} \hat{H}_N \hat{T}_1^2)_c | \Phi_0 \rangle$. Obviously, \hat{T}_1^2 has excitation level +2. As for the previous term, we require the third diagram of \hat{F}_N , and the fourth and fifth diagram of \hat{V}_N . These diagrams have excitation level +1 and can connect to \hat{T}_1^2 satisfying our criterions. We obtain the following contributions:

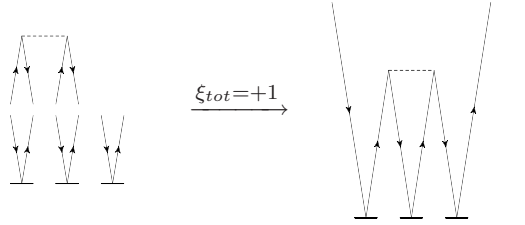


5. Consider $\langle \Phi_i^a | (\hat{H}_N \hat{T}_1 \hat{T}_2)_c | \Phi_0 \rangle$. We first observe that $\hat{T}_1 \hat{T}_2$ has excitation level +3. In order to obtain at total excitation level of +1, $\hat{T}_1 \hat{T}_2$ must connect to a diagram with excitation level -2, i.e. the ninth diagram of \hat{V}_N . This diagram may be connected to $\hat{T}_1 \hat{T}_2$ in three different ways. We obtain the following contributions to the equation:

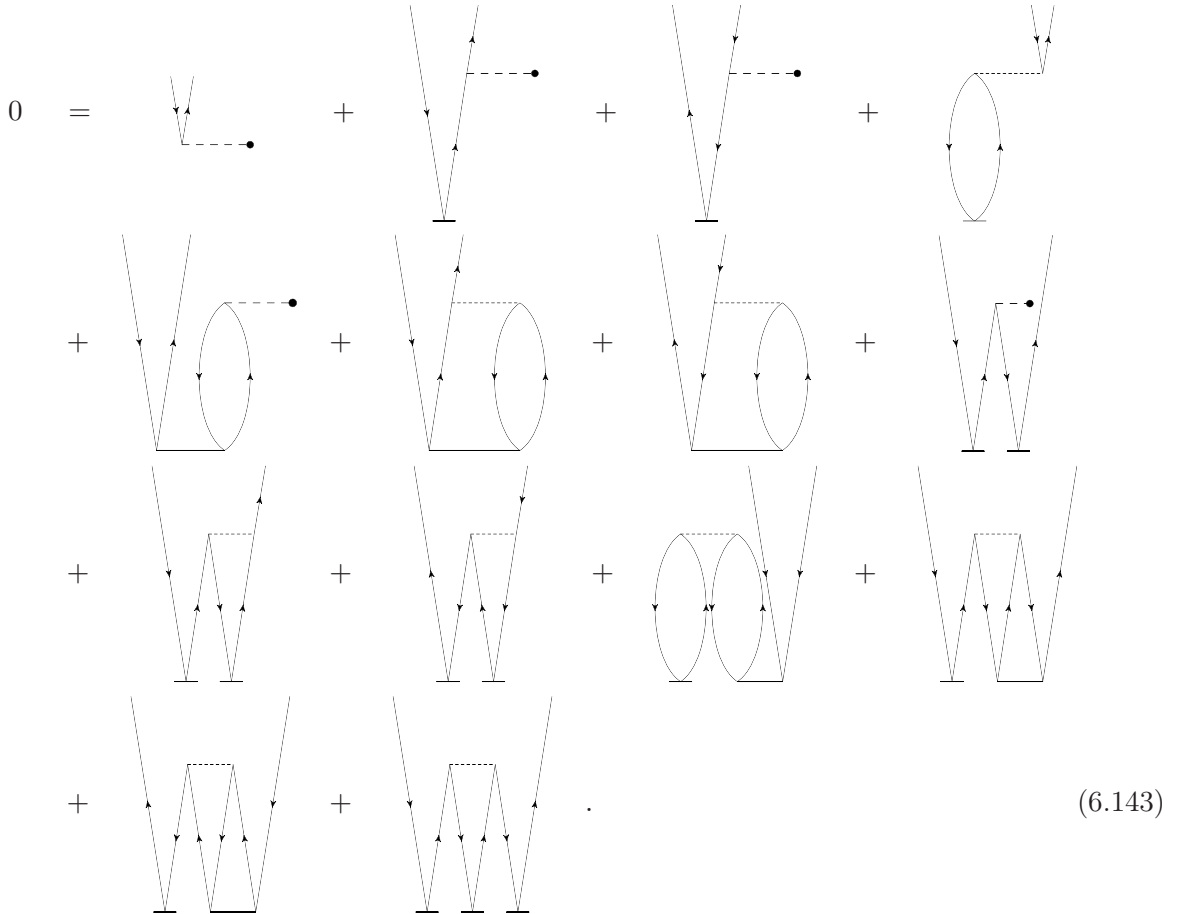


6. Consider $\langle \Phi_i^a | (\frac{1}{6} \hat{H}_N \hat{T}_1^3)_c | \Phi_0 \rangle$. Since \hat{T}_1^3 has excitation level +3, we require the ninth

diagram fragment of \hat{V}_N with excitation level -2 , yielding the following contribution



We finally obtain the diagrammatic representation of the \hat{T}_1 amplitude equation,



\hat{T}_2 Amplitude Equation

We will now transform the \widehat{T}_2 equation into a diagrammatic form. Inserting Eq. (6.111) into Eq. (6.140), yields

$$\langle \Phi_{ij}^{ab} | (\hat{H}_N + \hat{H}_N \hat{T} + \frac{1}{2!} \hat{H}_N \hat{T}^2 + \frac{1}{3!} \hat{H}_N \hat{T}^3 + \frac{1}{4!} \hat{H}_N \hat{T}^4 + \dots)_c | \Phi_0 \rangle = 0, \quad (6.144)$$

where $\widehat{T} = \widehat{T}_1 + \widehat{T}_2$, and the c -subscript denotes that \widehat{H}_N must have at least one contraction with every excitation operator. Each matrix element in the equation has the reference determinant on its right and the two-particle two-hole (2p2h) excited determinant on its left. Diagrams that contribute to the equation must therefore satisfy the following three criterion:

1. Total excitation level +2.
 2. The reference determinant at the bottom of the diagram.
 3. The 2p2h excited determinant at the top of the diagram.

Since \hat{H}_N has minimum excitation level -2 , and \hat{T}^n ($n \geq 5$) have excitation level $\xi \geq 5$, diagrams representing $(\hat{H}_N \hat{T}^n)_c$ ($n \geq 5$) do not satisfy our criterions. Moreover, since \hat{T}_2^3 and \hat{T}_2^4 have excitation level $+6$ and $+8$, respectively, $(\hat{H}_N \hat{T}_2^3)_c$ and $(\hat{H}_N \hat{T}_2^4)_c$ do not contribute to the equation. Thus the \hat{T}_2 equation reduces to

$$0 = \langle \Phi_{ij}^{ab} | (\hat{H}_N + \hat{H}_N \hat{T}_1 + \hat{H}_N \hat{T}_2 + \frac{1}{2} \hat{H}_N \hat{T}_1^2 + \frac{1}{2} \hat{H}_N \hat{T}_2^2 + \hat{H}_N \hat{T}_1 \hat{T}_2 + \frac{1}{6} \hat{H}_N \hat{T}_1^3 + \frac{1}{2} \hat{T}_1^2 \hat{T}_2)_c | \Phi_0 \rangle.$$

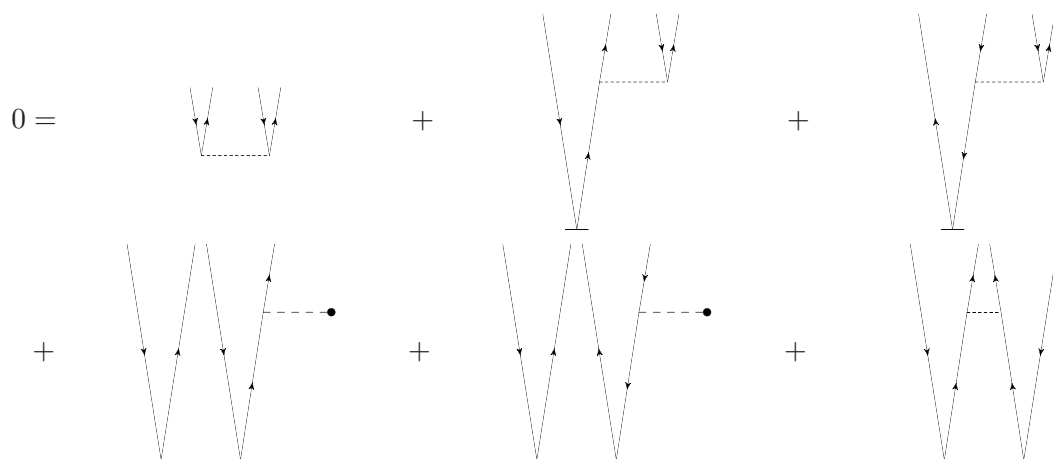
In order to transform each term into a diagrammatic expression, we use the same procedure as we did for the \hat{T}_1 equation. For each term $\langle \Phi_{ij}^{ab} | \hat{H}_N \hat{X} | \Phi_0 \rangle$, where \hat{X} has excitation level ξ_X , the following procedure is used to obtain the diagrammatic expression:

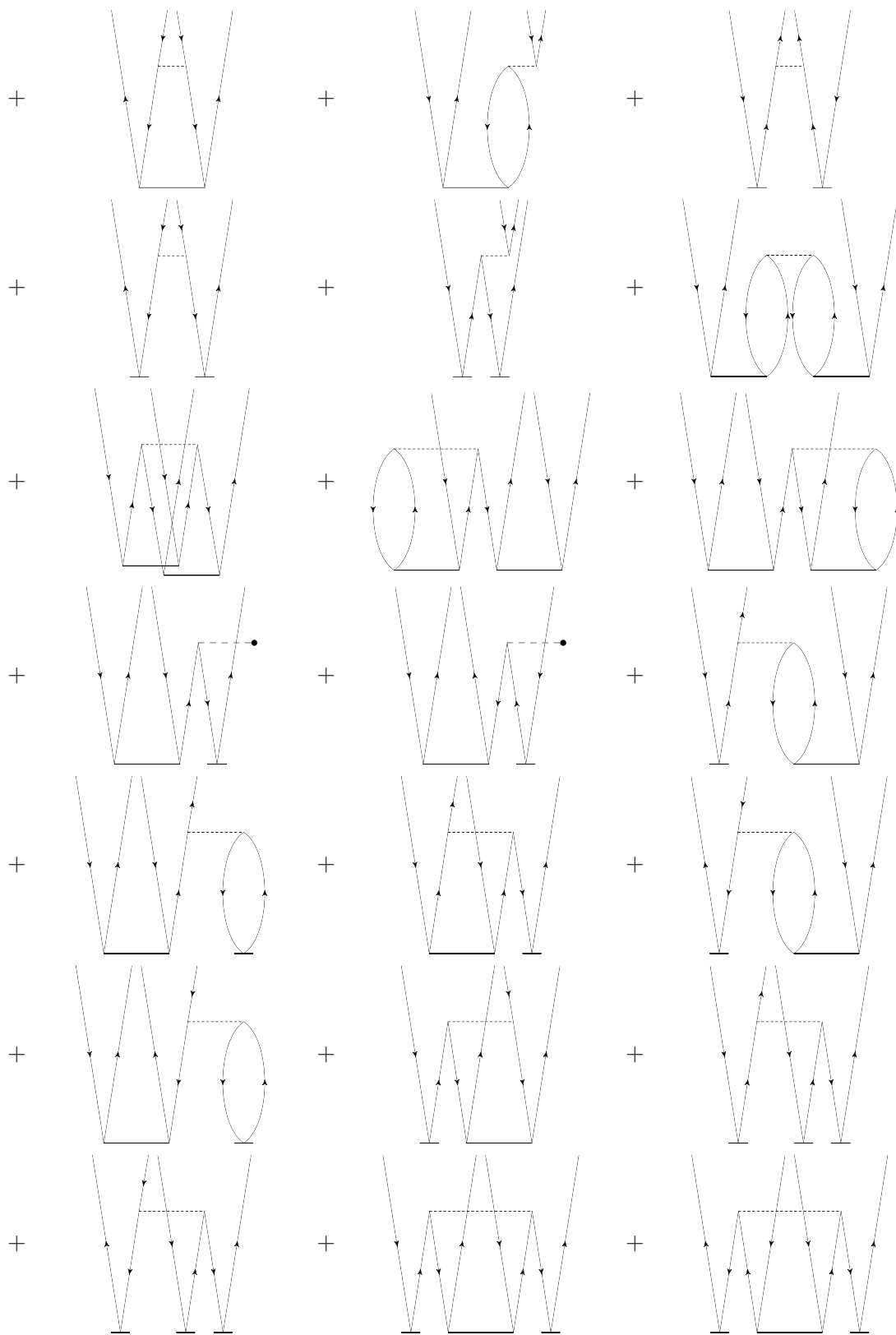
1. Identify the diagrams of \hat{H}_N with the 2p2h excited determinant of the top of the diagram, and excitation level ξ that satisfies

$$\xi + \xi_X = 2. \quad (6.145)$$

2. For each diagram that satisfies 1., connect this diagram to \hat{X} in accordance with the three criterions listed above.

We will not show the derivation of the diagrammatic forms as we did for the \hat{T}_1 . The final form of \hat{T}_2 reads:





$$+ \begin{array}{c} | \\ \searrow \nearrow \\ | \\ \searrow \nearrow \\ | \end{array} \text{---} \begin{array}{c} | \\ \searrow \nearrow \\ | \\ \searrow \nearrow \\ | \end{array} + \begin{array}{c} | \\ \searrow \nearrow \\ | \\ \searrow \nearrow \\ | \end{array} \text{---} \begin{array}{c} | \\ \searrow \nearrow \\ | \\ \searrow \nearrow \\ | \end{array} + \begin{array}{c} | \\ \searrow \nearrow \\ | \\ \searrow \nearrow \\ | \end{array} \text{---} \begin{array}{c} | \\ \searrow \nearrow \\ | \\ \searrow \nearrow \\ | \end{array} + \begin{array}{c} | \\ \searrow \nearrow \\ | \\ \searrow \nearrow \\ | \end{array} \text{---} \begin{array}{c} | \\ \searrow \nearrow \\ | \\ \searrow \nearrow \\ | \end{array} \quad (6.146)$$

Diagram Rules

The diagrammatic form of the energy and amplitude equations in (6.138), (6.143) and (6.146) can be transformed into algebraic expressions by so-called diagram rules. In the following, the rules are listed.

1. Label all directed lines with indices $ijk\dots$ (hole lines) and $abc\dots$ (particle lines).
2. Each operator line contributes with an integral or amplitude.

$$\begin{aligned}\hat{T}_1 &\rightarrow t_i^a \\ \hat{T}_2 &\rightarrow t_{ij}^{ab} \\ \hat{F}_N &\rightarrow f_{\text{in}}^{\text{out}} \\ \hat{V}_N &\rightarrow \langle \text{left-out right-out} | v | \text{left-in right-in} \rangle\end{aligned}$$

3. Summation over all internal indices, viz. all indices that label lines that begin and end at an operator line.
4. A prefactor of $(-1)^{n_h+n_l}$ is included in the algebraic expression, where n_h denotes the number of hole lines, and n_l denotes the number of loops. A loop is defined as either a route of directed lines that returns to its beginning, or a route that begins and ends at an external line.
5. For each pair of equivalent lines, i.e. lines that begin and end at the same operator line, a prefactor of $\frac{1}{2}$ is included.
6. For each pair of equivalent vertices, i.e. two \hat{T}_n operator lines that connect to a fragment of \hat{H}_N in exactly the same manner, a prefactor of $\frac{1}{2}$ is included.
7. For each pair of unique external hole or particle lines, a permutation function $P(pq)$ is included. $P(pq)$ acting on a function $f(pq)$ yields

$$P(pq)f(p,q) \equiv f(p,q) - f(q,p),$$

The permutation function is included in order to ensure antisymmetry of the final expression.

6.4.7 Amplitude Equations on Algebraic Form

We will in this section utilize the diagram rules in order to transform the amplitude equations into algebraic expressions. We will use Einstein's summation convention, viz.

$$f_a^i t_i^a \equiv \sum_{ia} f_a^i t_i^a. \quad (6.147)$$

Thus, identical quantum numbers in an expression implies a summation.

\hat{T}_1 Amplitude Equation

We will in the following transform each diagram of Eq. (6.143) into an algebraic expression.

$$= f_i^a \quad (6.148)$$

$$= -f_i^j t_j^a \quad (6.149)$$

$$= f_a^i t_j^{ba} \quad (6.150)$$

$$= -\frac{1}{2} \langle ij|v|ka \rangle t_{ij}^{ba} \quad (6.151)$$

$$= -\langle ia|v|bc \rangle t_j^b t_i^c \quad (6.152)$$

$$= \langle ij|v|ab \rangle t_i^a t_{jk}^{bc} \quad (6.153)$$

$$= \frac{1}{2} \langle ij|v|ab \rangle t_i^c t_{jk}^{ab} \quad (6.154)$$

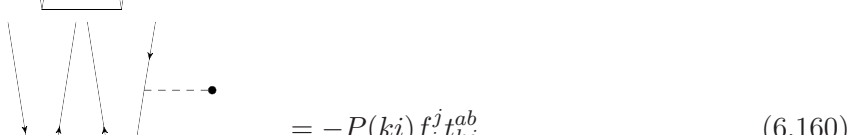
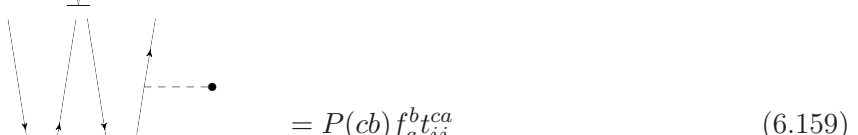
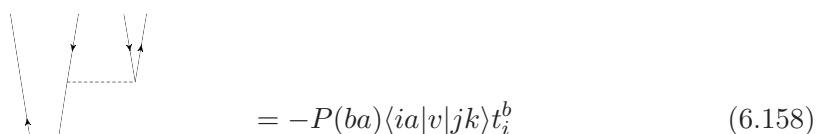
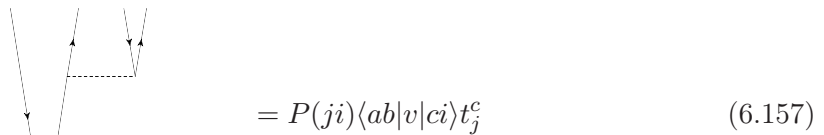
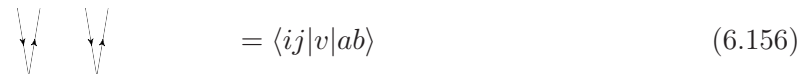
$$= \langle ij|v|ab \rangle t_k^a t_i^b t_j^c \quad (6.154)$$

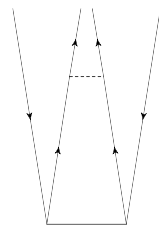
The final algebraic expression of the \hat{T}_1 equation reads,

$$0 = f_i^a + f_a^b t_i^a - f_i^j t_j^a + \langle ia|v|bj\rangle t_i^b + f_a^i t_{ji}^{ba} + \frac{1}{2} \langle ai|v|bc\rangle t_{ji}^{bc} - \frac{1}{2} \langle ij|v|ka\rangle t_{ij}^{ba} \\ - f_a^i t_j^a t_i^b - \langle ia|v|bc\rangle t_j^b t_i^c + \langle ij|v|ak\rangle t_i^b t_j^a + \langle ij|v|ab\rangle t_i^a t_{jk}^{bc} + \frac{1}{2} \langle ij|v|ab\rangle t_k^a t_{ij}^{bc} \\ + \frac{1}{2} \langle ij|v|ab\rangle t_i^c t_{jk}^{ab} + \langle ij|v|ab\rangle t_k^a t_i^b t_j^c. \quad (6.155)$$

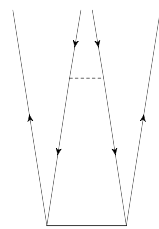
\hat{T}_2 Amplitude Equation

We will in the following transform each diagram of Eq. (6.146) into an algebraic expression.

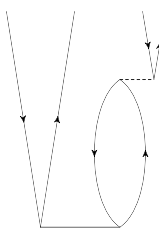




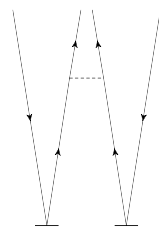
$$= \frac{1}{2} \langle ab|v|cd\rangle t_{ij}^{cd} \quad (6.161)$$



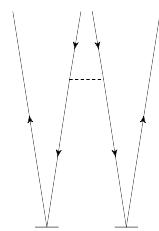
$$= \frac{1}{2} \langle ij|v|kl\rangle t_{ij}^{ab} \quad (6.162)$$



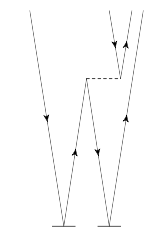
$$= P(kj)P(ca)\langle ia|v|bj\rangle t_{ki}^{cb} \quad (6.163)$$



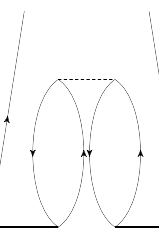
$$= \frac{1}{2} P(ij) \langle ab|v|cd\rangle t_i^c t_j^d \quad (6.164)$$



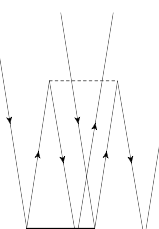
$$= \frac{1}{2} P(ab) \langle ij|v|kl\rangle t_i^a t_j^b \quad (6.165)$$



$$= P(kj)P(ac)\langle ia|v|bj\rangle t_k^b t_i^c \quad (6.166)$$



$$= \frac{1}{2} P(kl)P(cd)\langle ij|v|ab\rangle t_{ki}^{ca} t_{jl}^{bd} \quad (6.167)$$



$$= \frac{1}{4} \langle ij|v|ab\rangle t_{kl}^{ab} t_{ij}^{cd} \quad (6.168)$$

$$= -\frac{1}{2}P(kl)\langle ij|v|ab\rangle t_{ik}^{ab}t_{jl}^{cd} \quad (6.169)$$

$$= -\frac{1}{2}P(cd)\langle ij|v|ab\rangle t_{kl}^{ca}t_{ij}^{db} \quad (6.170)$$

$$= -P(bc)f_a^i t_{jk}^{ba}t_i^c \quad (6.171)$$

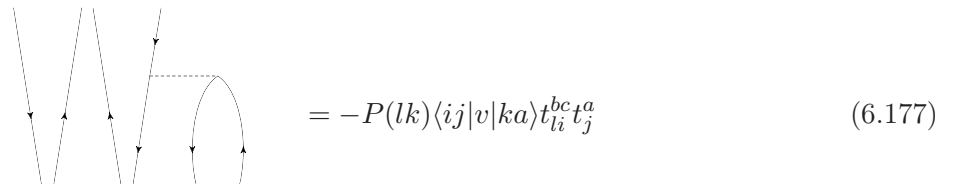
$$= -P(jk)f_a^i t_{ji}^{bc}t_k^a \quad (6.172)$$

$$= P(jk)P(ad)\langle ai|v|bc\rangle t_j^b t_{ik}^{cd} \quad (6.173)$$

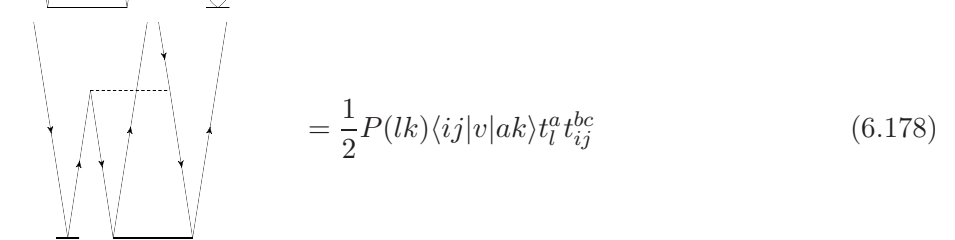
$$= P(da)\langle ai|v|bc\rangle t_{jk}^{db}t_i^c \quad (6.174)$$

$$= -\frac{1}{2}P(ad)\langle ai|v|bc\rangle t_{jk}^{bc}t_i^d \quad (6.175)$$

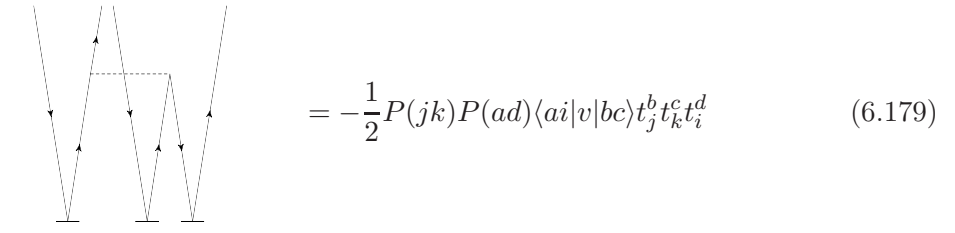
$$= -P(bc)P(kl)\langle ij|v|ka\rangle t_i^b t_{jl}^{ac} \quad (6.176)$$



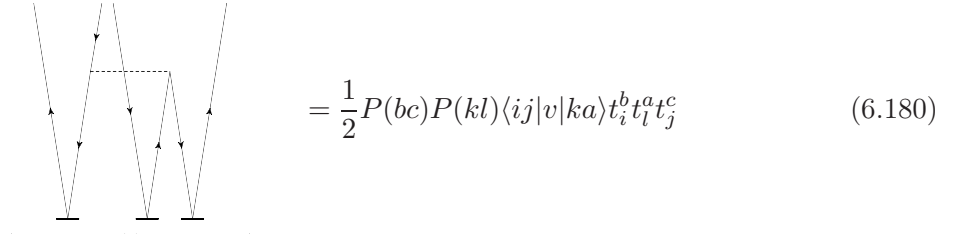
$$= -P(lk)\langle ij|v|ka\rangle t_{li}^{bc}t_j^a \quad (6.177)$$



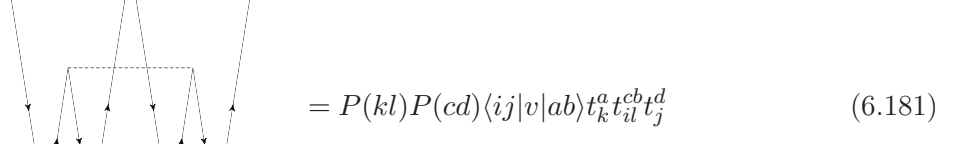
$$= \frac{1}{2}P(lk)\langle ij|v|ak\rangle t_l^a t_{ij}^{bc} \quad (6.178)$$



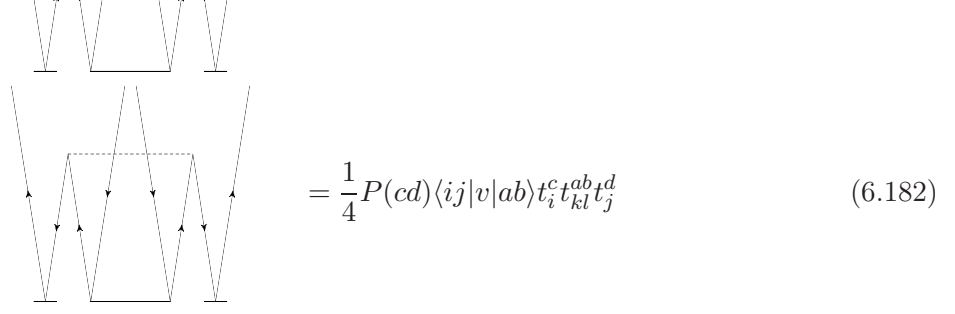
$$= -\frac{1}{2}P(jk)P(ad)\langle ai|v|bc\rangle t_j^b t_k^c t_i^d \quad (6.179)$$



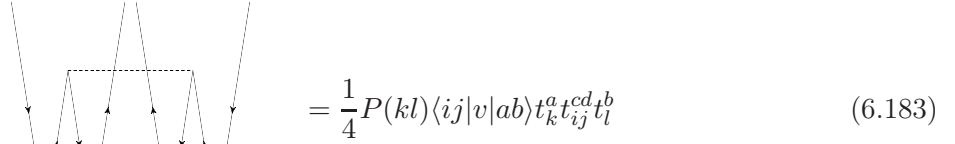
$$= \frac{1}{2}P(bc)P(kl)\langle ij|v|ka\rangle t_i^b t_l^a t_j^c \quad (6.180)$$



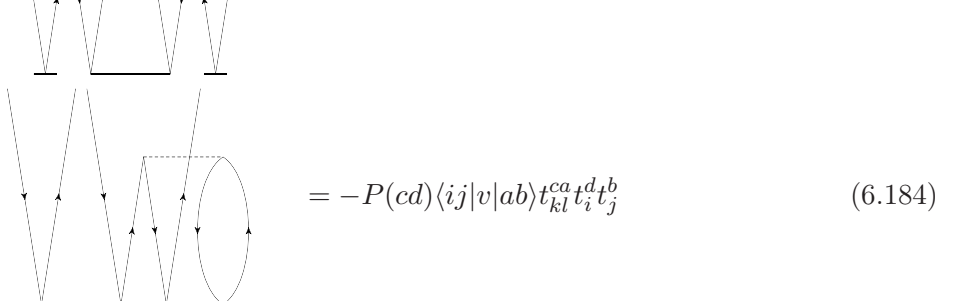
$$= P(kl)P(cd)\langle ij|v|ab\rangle t_k^a t_{il}^{cb} t_j^d \quad (6.181)$$



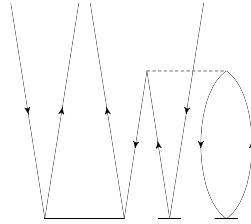
$$= \frac{1}{4}P(cd)\langle ij|v|ab\rangle t_i^c t_{kl}^{ab} t_j^d \quad (6.182)$$



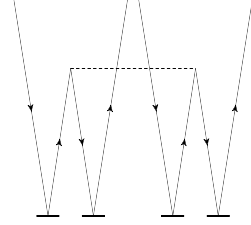
$$= \frac{1}{4}P(kl)\langle ij|v|ab\rangle t_k^a t_{ij}^{cd} t_l^b \quad (6.183)$$



$$= -P(cd)\langle ij|v|ab\rangle t_{kl}^{ca} t_i^d t_j^b \quad (6.184)$$



$$= -P(kl)\langle ij|v|ab\rangle t_{ki}^{cd}t_l^a t_j^b \quad (6.185)$$



$$= \frac{1}{4}P(kl)P(cd)\langle ij|v|ab\rangle t_k^a t_i^c t_l^b t_j^d \quad (6.186)$$

Collecting all terms, we finally obtain the algebraic expression of the \widehat{T}_2 equation,

$$\begin{aligned} 0 = & \langle ij|v|ab\rangle + P(ji)\langle ab|v|ci\rangle t_j^c - P(ba)\langle ia|v|jk\rangle t_i^b + P(cb)f_a^b t_{ij}^{ca} - P(ki)f_i^j t_{kj}^{ab} \\ & + \frac{1}{2}\langle ab|v|cd\rangle t_{ij}^{cd} + \frac{1}{2}\langle ij|v|kl\rangle t_{ij}^{ab} + P(kj)P(ca)\langle ia|v|bj\rangle t_{ki}^{cb} + \frac{1}{2}P(ij)\langle ab|v|cd\rangle t_i^c t_j^d \\ & + \frac{1}{2}P(ab)\langle ij|v|kl\rangle t_i^a t_j^b + P(kj)P(ac)\langle ia|v|bj\rangle t_k^b t_i^c + \frac{1}{2}P(kl)P(cd)\langle ij|v|ab\rangle t_{ki}^{ca} t_{jl}^{bd} \\ & + \frac{1}{4}\langle ij|v|ab\rangle t_{kl}^{ab} t_{ij}^{cd} - \frac{1}{2}P(kl)\langle ij|v|ab\rangle t_{ik}^{ab} t_{jl}^{cd} - \frac{1}{2}P(cd)\langle ij|v|ab\rangle t_{kl}^{ca} t_{ij}^{db} - P(bc)f_a^i t_{jk}^{ba} t_i^c \\ & - P(jk)f_a^i t_{ji}^{bc} t_k^a + P(jk)P(ad)\langle ai|v|bc\rangle t_j^b t_{ik}^{cd} + P(da)\langle ai|v|bc\rangle t_{jk}^{db} t_i^c - \frac{1}{2}P(ad)\langle ai|v|bc\rangle t_{jk}^{bc} t_i^d \\ & - P(bc)P(kl)\langle ij|v|ka\rangle t_i^b t_{jl}^{ac} - P(lk)\langle ij|v|ka\rangle t_{li}^{bc} t_j^a + \frac{1}{2}P(lk)\langle ij|v|ak\rangle t_l^a t_{ij}^{bc} \\ & - \frac{1}{2}P(jk)P(ad)\langle ai|v|bc\rangle t_j^b t_k^c t_i^d + \frac{1}{2}P(bc)P(kl)\langle ij|v|ka\rangle t_i^b t_l^a t_j^c + P(kl)P(cd)\langle ij|v|ab\rangle t_k^a t_{il}^{cb} t_j^d \\ & + \frac{1}{4}P(cd)\langle ij|v|ab\rangle t_i^c t_{kl}^{ab} t_j^d + \frac{1}{4}P(kl)\langle ij|v|ab\rangle t_k^a t_{ij}^{cd} t_l^b - P(cd)\langle ij|v|ab\rangle t_{kl}^{ca} t_i^d t_j^b \\ & - P(kl)\langle ij|v|ab\rangle t_{ki}^{cd} t_l^a t_j^b + \frac{1}{4}P(kl)P(cd)\langle ij|v|ab\rangle t_k^a t_i^c t_l^b t_j^d. \end{aligned} \quad (6.187)$$

The amplitude equations are coupled and non-linear in the amplitudes t_i^a and t_{ij}^{ab} . Therefore, they must be solved iteratively. At this point we will not go further into how this is done in a practical computer program. We will in Chapter 7 present the implementation of the equations in detail.

Part III

IMPLEMENTATIONS AND RESULTS

Chapter 7

Implementation

In this chapter we present the implementation of the Hartree-Fock (HF) method and the Coupled-Cluster Singles and Doubles (CCSD) method. We also present the code-structures and the implementation of classes. The focus will be on the CCSD code and its structure. We will present the implementation of the algorithm, the energy equation and the amplitude equations in detail. Implementation of important analytical expressions will be shown with pseudo-codes. We will also present how to run the codes.

Both programs are object-oriented. When designing numerical software in computational science, it is often common to specialize it to the problem that is examined. It is often timesaving (in the sense that one obtain results for a specific problem) to start programming without considering generalizations, class implementations, and so forth. In many-body methods, such as for example Variational Monte Carlo (see [25]), only small changes are often required when considering other systems. A specialized code scatters the parts which needs modifications around. An object-oriented programming style offers an amazing opportunity to structure the code into parts that are “independent”. Such a programming style also able us to generalize parts of the code that are identical for many systems. Moreover, when the original system changes, the class structure often require modifications at welldefined places.

The middle-level C++ language [41] has been chosen for its efficiency and its opportunity for object-orientation. One of its competitors, Python [42], which is a general-purpose high-level programming language, has a simpler syntax and offers the opportunity object-orientation. However, it cannot compete with the efficiency of C++. Furthermore, we have used the BLITZ++ library for handling arrays, and LPP/LAPACK libraries providing routines for linear algebra.

7.1 Implementation of the Hartree-Fock Method

We will in this section present the implementation of the Restricted Hartree-Fock method (RHF) for a 2-dimensional closed-shell parabolic quantum dot. The program is structured into classes, with base classes and derived classes. By relatively small changes, the code can handle other electronic systems such as atoms. The current version of the program only considers the closed-shell system where the orbitals within a shell are all occupied. An extension of the code would obviously be to handle open-shell systems. This would require a linear combination of Slater determinants in the ansatz.

We have implemented the Hartree-Fock scheme presented in Chapter 5. The Hartree-Fock orbitals in Eq. (5.2) are expanded in single-particle basis functions, and the expansion coefficients are varied in order to minimize the energy expectation value in Eq. (5.4). The minimization is done through solving the Hartree-Fock equations in (5.14) iteratively. The program calculates an approximation of the ground state energy, and computes the Hartree-Fock orbitals (expansion coefficients) that minimize the energy.

7.1.1 Overview

The HF scheme presented in Chapter 5 considers the case of a two-body Hamiltonian. The central equations are given in Eqs. (5.2), (5.5) and (5.14). The system under consideration is defined through

1. the single-particle matrix elements $\langle\alpha|h|\beta\rangle$, and
2. the two-particle interaction matrix elements $\langle\alpha\beta|v|\gamma\delta\rangle$,

where \hat{h} is the single-particle Hamiltonian and \hat{v} is the interaction operator. In the parabolic quantum dot case, \hat{h} is given in Eq. (4.93), and \hat{v} is the Coulomb interaction in Eq. (4.94). Moreover, the matrix elements also define the basis set, i.e. the single-particle functions that we expand the HF orbitals in. By small changes in the code, the program can handle other functions as well. In order to run the program, two data-files must be provided:

1. One file containing single-particle matrix elements $\langle\alpha|h|\beta\rangle$, with setup

$$\alpha \quad \beta \quad \langle\alpha|h|\beta\rangle$$

2. One file containing interaction elements $\langle\alpha\beta|v|\gamma\delta\rangle$, with setup

$$\alpha \quad \beta \quad \gamma \quad \delta \quad \langle\alpha\beta|v|\gamma\delta\rangle$$

The configuration parameters is written in `parameters.inp`. An example is shown in Table 7.1.1.

```
#####
# CONFIGURATION FILE
# System: 2-dimensional Parabolic Quantum Dot
# Method: Hartree-Fock
#####

# --- Model space parameters
N = 2          # number of electrons (closed-shell, i.e. 2,6,12,20,30,...)
R = 10         # number of shells in the basis
dim = 2        # dimensions
Rf = 1         # fermi-shell

# --- Interaction parameters
omega = 1.0    # oscillator strength

# --- Computational parameters
tol = 1e-10      # self-consistency tolerance
max_iter = 500   # maximum number of iterations
sp_energy_file = spEnergy.dat  # <p|h|q>-file
tp_energy_file = interaction.dat # <pq|v|rs>-file

# --- Storing parameters
int_type      = standard       # type of interaction
```

Table 7.1: `parameters.inp`: HF configuration parameters file for a 2-dimensional parabolic quantum dot.

7.1.2 Validation of the Code

The Hartree-Fock code should reproduce the solutions of the non-interacting system. For $N = 2, 6, 12$ and 20 , the non-interacting energy is $2\hbar\omega$, $10\hbar\omega$, $28\hbar\omega$ and $60\hbar\omega$, respectively. The code reproduced these results. However, a complete validation requires that we reproduce other HF results for the interacting system. Our program reproduces the HF results of Ref. [43].

7.1.3 Code Structure and Class Implementation

The program is structured into classes, with base classes and derived classes. This offers the opportunity to divide parts of the code that are specified by the system, and the parts that are identical for every system, into different fragments. Thus in order to handle other systems, we can modify the code in well-defined parts of the program. This is the beauty of object-oriented numeric computing. See [41] for an introduction. The code is divided into four base classes, viz. `HfAlgo`, `quantumNumber`, `singleParticleElement` and `interactionElement`. These classes include members (i.e. variables and functions) that are universal in the sense that they are common for all system. Each base class has a derived class associated with it. They are named `algo1`, `qdotQuantumNumber`, `sp1` and `coulombElement`, respectively.

The code is tuned to deal with the harmonic oscillator basis (see Eq. 4.65). Since we are dealing with closed-shell systems only, we only include full shells in the basis. Thus the size of the basis is determined by the number of shells. This number defines the orbitals that are included. The objective of `qdotQuantumNumber` is to handle the single-particle orbitals. It establish the mapping

$$|\alpha\rangle \rightarrow |n\ m\ m_s\rangle, \quad (7.1)$$

shown in Table 8.1. It also establish a mapping scheme for each orbital-couple $|\alpha\beta\rangle$, i.e.

$$|p\rangle \rightarrow |\alpha\beta\rangle. \quad (7.2)$$

For each couple it calculates the total angular momentum

$$M = m_\alpha + m_\beta, \quad (7.3)$$

and total spin

$$M_s = m_{s_\alpha} + m_{s_\beta}, \quad (7.4)$$

and tabulates couples with equal M and M_s . Furthermore, the aim of `singleParticleElement` is to read $\langle\alpha|h|\beta\rangle$ from file and store the elements. Since we are using the harmonic oscillator functions as basis functions, the single-particle matrix is diagonal, i.e.

$$\langle\alpha\beta|h|\gamma\delta\rangle = \varepsilon_\alpha \delta_{\alpha\beta}, \quad (7.5)$$

where ε_α is given in Eq. (8.16). For each M and M_s , called a channel, the program declares an object of `interactionElement` which stores all matrix elements

$$\langle p|v|q\rangle \equiv \langle\alpha\beta|v|\gamma\delta\rangle \quad (7.6)$$

in a two-dimensional array. This can be done since

$$\langle MM_s|v|\tilde{M}\tilde{M}_s\rangle = 0, \quad (7.7)$$

when $M \neq \tilde{M}$ or/and $M_s \neq \tilde{M}_s$. Thus we only store nonzero matrix elements, and avoid a four-dimensional array.

The `HfAlgo` class is an abstract base class constructed for the Hartree-Fock algorithm. We have chosen to implement the specific HF scheme (presented in Chapter 5) in the derived class `algo1`. The header file of `HfAlgo` is shown below. All members are defined in `algo1`.

```
class HfAlgo {
protected:
    int N;                                // number of particles
    int nbBasis;                            // number of basis functions
    double energyDiff;                      // energy difference
    double oldEnergy, newEnergy;            // hartree-fock energy for (i-1)'th and i'th iteration
```

```

double** HF_matrix;           // Hartree-Fock matrix
double* eigenvalues;          // eigenvalues
singleParticleElement* spMatrixElement; // sp matrix elements <a/h/b>
interactionElement** tpMatrixElement; // tp matrix elements <ab/v/cd>
quantumNumber* QN;            // quantum number object
double* off_diag;             // to be used in Householder's method
char* spEnergy_file;
char* interaction_file;
public:
    double** eigenvectors;      // eigenvectors
    double hfEnergy;             // hartree-fock energy
    int iter;                   // number of iterations in self-consistency procedure
    int maxIter;                // maximum iteration value
    double tol;                  // self-consistency tolerance
    ofstream file;
/*
 * allocate and set up single-particle matrix element object
 */
virtual void setUp_spMatrixElement() = 0;
/*
 * allocate and calculate two-particle (interaction) matrix elements
 */
virtual void setUp_tpMatrixElement() = 0;
/*
 * virtual run-algo function
 */
virtual void runAlgo() = 0;
/*
 * write HF-coeff to file
 */
virtual void write_hf_coeff_to_file() = 0;
/*
 * generates the hartree-fock matrix
 */
virtual void getHFmatrix() = 0;
/*
 * function that re-arrange the eigenvalues (with corresponding eigenvectors)
 * from the minimum value to the maximum value
 */
virtual void reArrangeEig() = 0;
/*
 * function that returns the hartree-fock energy from given single-particle HF energies
 */
virtual double getHFenergy() = 0;
/*
 *
 */
virtual void eigSolver(double**, double*, int) = 0;
/*
 * virtual destructor
 */
virtual ~HfAlgo(){
    delete[] HF_matrix;
    delete[] eigenvectors;
    delete[] eigenvalues;
    delete spMatrixElement;
    delete[] tpMatrixElement;
    delete[] off_diag;
}
};


```

Consider the Hartree-Fock equations in Eq. (5.14). We define the Hartree-Fock matrix

(HF_matrix) as

$$h^{\text{HF}} \equiv \begin{pmatrix} \tilde{h}_{11} & \tilde{h}_{12} & \tilde{h}_{13} & \tilde{h}_{14} & \cdots & \tilde{h}_{1n} \\ \tilde{h}_{21} & \tilde{h}_{22} & \tilde{h}_{23} & \tilde{h}_{24} & \cdots & \tilde{h}_{2n} \\ \tilde{h}_{31} & \tilde{h}_{32} & \tilde{h}_{33} & \tilde{h}_{34} & \cdots & \tilde{h}_{3n} \\ \tilde{h}_{41} & \tilde{h}_{42} & \tilde{h}_{43} & \tilde{h}_{44} & \cdots & \tilde{h}_{4n} \\ \vdots & \vdots & \vdots & \vdots & \ddots & \vdots \\ \tilde{h}_{n1} & \tilde{h}_{n2} & \tilde{h}_{n3} & \tilde{h}_{n4} & \cdots & \tilde{h}_{nn} \end{pmatrix}, \quad (7.8)$$

where $\tilde{h}_{\alpha\beta} \equiv h_{\alpha\beta}^{\text{HF}}$ (see Eq. 5.13), and n is the number of basis functions. Furthermore, we define the coefficient vector (**eigenvectors**) as

$$\mathbf{C}_k \equiv \begin{pmatrix} C_{k1} \\ C_{k2} \\ C_{k3} \\ C_{k4} \\ \vdots \\ C_{kn} \end{pmatrix}, \quad (7.9)$$

which contains the expansion coefficients of HF orbital k (see Eq. 5.2). The HF equation for orbital k can thus be written as the following matrix eigenvalue equation,

$$h^{\text{HF}} \mathbf{C}_k = \vartheta_k \mathbf{C}_k, \quad (7.10)$$

where ϑ_k is the eigenvalue of \mathbf{C}_k . Since the HF matrix depends on all the other coefficient vectors ($\mathbf{C}_1, \mathbf{C}_2, \dots, \mathbf{C}_n$), the equation is non-linear and must be solved iteratively. We end up with the following HF algorithm.

Hartree-Fock Algorithm

1. Calculate $\langle \alpha | h | \beta \rangle$ and $\langle \alpha \beta | v | \gamma \delta \rangle$.
2. Initialize coefficient vectors $\mathbf{C}_1, \mathbf{C}_2, \dots, \mathbf{C}_N$.
3. While not converged:
 - a. Calculate the HF matrix.
 - b. Calculate the eigenvectors and eigenvalues of the HF matrix.
 - c. Determine the eigenvectors with the N lowest eigenvalues, where N is the number of particles in the system.
 - d. Calculate new HF energy.
 - e. Calculate the difference between the new HF energy and the energy from the previous iteration.

Results: HF energy and expansion coefficients.

The single-particle elements $\langle \alpha | h | \beta \rangle$ and interaction elements $\langle \alpha \beta | v | \gamma \delta \rangle$ are read from file in `algo1::setUp_spMatrixElement()` and `algo1::setUp_tpMatrixElement()`, respectively. The **eigenvector** matrix is defined as

$$\mathbf{C} \equiv (\mathbf{C}_1 \quad \mathbf{C}_2 \quad \cdots \quad \mathbf{C}_n), \quad (7.11)$$

where n is the number of basis functions. It is initialized to

$$\mathbf{C} = \mathbf{I}, \quad (7.12)$$

i.e. the identity matrix, in `algo1::algo1(..)`. The initial HF ansatz is thus equal to the non-interacting ground state. The iteration procedure is implemented in `algo1::runAlgo()`. A pseudo-code is shown below.

```
void algo1::runAlgo(){
    ...
    while(abs(energyDiff)>tol && (iter+1)<maxIter){
        // update iteration variable
        iter += 1;
        // calculate the hartree-fock matrix
        getHFmatrix();
        // calculate new eigenvalues and eigenvectors by Householders method
        eigSolver(HF_matrix, eigenvalues, nbBasis);
        // determine the smallest energy eigenvalues with corresponding eigenvectors
        reArrangeEig();
        // get new hartree-fock energy
        newEnergy = getHFenergy();
        // difference between new and old hartree-fock energy
        energyDiff = newEnergy - oldEnergy;
        // prepare for next iteration
        oldEnergy = newEnergy;
        ...
    } // end self-consistency loop
    // update hartree-fock energy variable
    hfEnergy = oldEnergy;
    ...
}
```

The HF energy is calculated by the formula [25]

$$E_{\text{HF}} = \frac{1}{2} \sum_{k=1}^N (\vartheta_k + \langle \varphi_k | h | \varphi_k \rangle), \quad (7.13)$$

where

$$\langle \varphi_k | h | \varphi_k \rangle = \sum_{\alpha\beta} C_{k\alpha}^* C_{k\beta} \langle \alpha | h | \beta \rangle \quad (7.14)$$

is the HF orbital in Eq. (5.2). It can be shown that this expression is equal to Eq. (5.5).

7.2 Implementation of the Coupled-Cluster method

In this section we present the implementation of the Coupled-Cluster Singles and Doubles method (CCSD). The program can in principle handle other electronic systems such as the 3-dimensional parabolic quantum dot, quantum dots with other confinement potentials, atoms, molecules, and so forth, *without* modifying the code. One of the main disadvantages of a generalized-code requirement is that the code becomes less numerical efficient. Nevertheless, in the case of a parabolic quantum dot in 2 dimensions, the program is able to handle 20 electron with 110 basis functions (10 shells) in approximately 2 days. In this thesis we have chosen to develop a generalized m -scheme code that in principle is able to handle all electronic systems. The current version of the program can only handle closed-shell systems. Thus for the parabolic quantum dot in 2 dimensions, CCSD calculations can only be done for 2, 6, 12, 20, 30, 42, etc. electrons. The reason is that in the CC wavefunction, the exponentiated cluster operator \hat{T} acts on the ground state of the non-interacting system. The non-interacting ground state of an open-shell

system cannot be written as one Slater determinant, but as a linear combination of determinants. Thus in order to handle open-shell systems, a linear combination of Slater determinants must be included in the reference state.

The program calculates an approximation to the ground state energy of the closed-shell. Moreover, it determines the excitation amplitudes t_i^a and t_{ij}^{ab} that define the CC wavefunction. We will in this section present our implementation of the CCSD method, and the structure of the computer program. We will also present the validation of the code.

7.2.1 Overview

The many-body system under study is specified through

1. the single-particle matrix elements $\langle \alpha | h | \beta \rangle$, and
2. the two-particle matrix elements $\langle \alpha \beta | v | \gamma \delta \rangle_{AS}$,

where \hat{h} is the one-particle Hamiltonian, and \hat{v} is the two-body interaction. The “AS” subscript denotes that the elements are antisymmetrized, i.e.

$$\langle \alpha \beta | v | \gamma \delta \rangle_{AS} = \langle \alpha \beta | v | \gamma \delta \rangle - \langle \alpha \beta | v | \gamma \delta \rangle.$$

The single-particle basis, and thus the N -particle model space, is defined through the matrix elements. The matrix elements can sometimes be difficult, or perhaps impossible, to calculate analytically. In these cases, numerical integration is necessary. Two data files must be provided in order to run the CCSD program; one containing the single-particle elements $\langle \alpha | h | \beta \rangle$ and one containing $\langle \alpha \beta | v | \gamma \delta \rangle$. These files must have the following structures:

- | | | | | | |
|----|----------|---------|--------------------------------------|----------|--|
| 1. | α | β | $\langle \alpha h \beta \rangle$ | | |
| 2. | α | β | γ | δ | $\langle \alpha \beta v \gamma \delta \rangle$ |

Before this can be done, the model space must be determined with a proper mapping of single-particle states. Each basis function must be labeled with an integer between 0 and $n_b - 1$, where n_b is the number of basis functions. Functions that are in the occupied space must be labeled with integers from 0 up to $n_h - 1$, where n_h is the number of hole states (i.e. number of particles in the system). Basis functions that are in the unoccupied space must be labeled with integers from n_h up to $n_b - 1$. When a proper mapping is determined and the matrix elements are calculated and stored in two separate files, the CCSD calculation can in principle start. The main-file, `main.cpp`, requires 6 arguments:

1. `nh`: Number of hole states, i.e. occupied single-particle orbitals
2. `np`: Number of particle states, i.e. unoccupied single-particle orbitals
3. `tol`: Self-consistency tolerance
4. `max_Iter`: Maximum number of iterations
5. `sp_energy_file`: $\langle \alpha | h | \beta \rangle$ -filename
6. `tp_energy_file`: $\langle \alpha \beta | v | \gamma \delta \rangle$ -filename

We have written a PYTHON script (`ccsd.py`) for the 2-dimensional parabolic quantum dot. It reads configuration parameters from `parameters.inp` (shown below), starts the CCSD calculation, and organizes the results into folders. If we were to consider another electron system, a new configuration script must be provided. Alternatively, the arguments above can be typed in manually.

```
#####
# CONFIGURATION FILE
# System: 2-dimensional Parabolic Quantum Dot
# Method: Coupled-Cluster Singles and Doubles
#####

# --- Model space parameters
N = 2          # number of electrons (closed-shell, i.e. 2,6,12,20,30,...)
Rb = 2         # number of shells (1,2,3,4,5,...)

# --- Interaction parameters
omega = 1.0    # oscillator strength

# --- Computational parameters
tol = 1e-7      # self-consistency tolerance
max_iter = 500   # maximum number of iterations
sp_energy_file = spEnergy.dat # <p/h/q>-file
tp_energy_file = interaction.dat # <pq/v/rs>-file

# -- Storing parameters
int_type = standard # type of interaction
```

Table 7.2: `parameters.inp`: CCSD configuration parameters file for a 2-dimensional parabolic quantum dot.

7.2.2 Validation of the Code

When a method has been implemented in a computer program, the code must be checked for errors. The first check is often to run the program for the non-interacting case, where analytical expressions often can be obtained. The program should obviously reproduce these analytical results. However, although the program reproduces the non-interacting energies, the whole code is still not validated. The CCSD code can be validated through exact diagonalization of the Hamiltonian for the 2-particle case. In the literature, exact diagonalization is commonly called Full Configuration Interaction method (FCI). We will now give a very shallow presentation of the basic concepts of FCI. We refer to [38] for a more profound introduction.

We define the Hamiltonian of the N -electron system as

$$\hat{H} = \hat{H}_0 + \hat{V},$$

where

$$\hat{H}_0 = \sum_{i=1}^N \hat{h}_i \tag{7.15}$$

is the Hamiltonian of the non-interacting system, and

$$\hat{V} = \sum_{i=1 < j}^N \hat{v}_{ij} \tag{7.16}$$

is the interaction. Furthermore, we define

$$\mathcal{B}_1 \equiv \{|\alpha_i\rangle\}_{i=1}^{d_m} \tag{7.17}$$

to be an arbitrary basis set of the model space with dimensionality d_m . In the matrix formulation of quantum mechanics [1], the time-independent Schrödinger equation reads

$$\mathbf{H}\mathbf{c} = E\mathbf{c}, \tag{7.18}$$

where the Hamiltonian matrix is defined by its elements $H_{mn} = \langle \Phi_m | \hat{H} | \Phi_n \rangle$, $|\Phi_m\rangle$ is a Slater determinant (build up of orbitals contained in \mathcal{B}), and

$$\mathbf{c} = \begin{pmatrix} c_1 \\ c_2 \\ c_3 \\ \vdots \\ c_{N_B} \end{pmatrix}.$$

When $d_m \rightarrow \infty$, the energy eigenvalue equation in (7.18) yields exact eigenvalues and eigenvectors. However, the Hilbert space must be truncated, and the solution of Eq. (7.18) within a truncated Hilbert space of dimensionality d_m gives an approximation to the eigenfunctions and eigenvalues. For a given value of d_m , the eigenfunctions is given as

$$|\Psi_\lambda\rangle = \sum_{i=1}^{d_m} c_{\lambda i} |\Phi_i\rangle. \quad (7.19)$$

By writing the Hamiltonian in second quantized form, i.e.

$$\hat{H} = \sum_{\alpha\beta} \langle \alpha | h | \beta \rangle a_\alpha^\dagger a_\beta + \frac{1}{4} \sum_{\alpha\beta\gamma\delta} \langle \alpha\beta | v | \gamma\delta \rangle a_\alpha^\dagger a_\beta^\dagger a_\delta a_\gamma,$$

we conclude that, due to Wick's theorem, the matrix element $H_{mn} = \langle \Phi_m | \hat{H} | \Phi_n \rangle$ can be written in terms of $\langle \alpha | h | \beta \rangle$ and $\langle \alpha\beta | v | \gamma\delta \rangle$.

We now choose the harmonic oscillator functions as basis functions. Analytical expressions can be obtained for $\langle \alpha\beta | v | \gamma\delta \rangle$ (see [44]). Thus for a given size of the model space, the Hamiltonian matrix can be computed, and approximate eigenvalues and eigenfunctions can be found by diagonalization. Exact diagonalization (FCI) results can be used to validate CCSD results, and in principle all CC schemes (CCSDT, CCSDTQ, and so forth). For a given model space, the CCSDT..N energy (N is the number of electrons) is equal to the energy obtained by exact diagonalization [38]. We have validated the CCSD by considering the 2-electron parabolic quantum dot in 2 shells, i.e. 6 basis functions. We have used the following mapping:

$$\begin{aligned} |0\rangle &\rightarrow |n=0, m=0, m_s=-1/2\rangle \\ |1\rangle &\rightarrow |n=0, m=0, m_s=+1/2\rangle \\ |2\rangle &\rightarrow |n=0, m=-1, m_s=-1/2\rangle \\ |3\rangle &\rightarrow |n=0, m=-1, m_s=+1/2\rangle \\ |4\rangle &\rightarrow |n=0, m=+1, m_s=-1/2\rangle \\ |5\rangle &\rightarrow |n=0, m=+1, m_s=+1/2\rangle \end{aligned} \quad (7.20)$$

Since the Coulomb interaction is spherically symmetric and does not depend on the spin, the only nonzero interaction elements are

$$\langle M, M_s | v | M, M_s \rangle,$$

where

$$\begin{aligned} M &= m_\alpha + m_\beta = m_\gamma + m_\delta = 0 \\ M_s &= m_{s_\alpha} + m_{s_\beta} = m_{s_\gamma} + m_{s_\delta} = 0. \end{aligned}$$

We observe that $|01\rangle$, $|25\rangle$ and $|34\rangle$ have $M = 0$ and $M_s = 0$, and the dimensionality \mathbf{H} reduces to 3. The Hamiltonian reads

$$\mathbf{H} = \begin{pmatrix} \langle \Phi_{01} | H_0 | \Phi_{01} \rangle + \langle \Phi_{01} | V | \Phi_{01} \rangle & \langle \Phi_{01} | H_0 | \Phi_{25} \rangle + \langle \Phi_{01} | V | \Phi_{25} \rangle & \langle \Phi_{01} | H_0 | \Phi_{34} \rangle + \langle \Phi_{01} | V | \Phi_{34} \rangle \\ \langle \Phi_{25} | H_0 | \Phi_{01} \rangle + \langle \Phi_{25} | V | \Phi_{01} \rangle & \langle \Phi_{25} | H_0 | \Phi_{25} \rangle + \langle \Phi_{25} | V | \Phi_{25} \rangle & \langle \Phi_{25} | H_0 | \Phi_{34} \rangle + \langle \Phi_{25} | V | \Phi_{34} \rangle \\ \langle \Phi_{34} | H_0 | \Phi_{01} \rangle + \langle \Phi_{34} | V | \Phi_{01} \rangle & \langle \Phi_{34} | H_0 | \Phi_{25} \rangle + \langle \Phi_{34} | V | \Phi_{25} \rangle & \langle \Phi_{34} | H_0 | \Phi_{34} \rangle + \langle \Phi_{34} | V | \Phi_{34} \rangle \end{pmatrix},$$

where the Slater determinant is defined as

$$|\Phi_{\alpha\beta}\rangle = \frac{1}{\sqrt{2}}(|\alpha\beta\rangle - |\beta\alpha\rangle). \quad (7.21)$$

We then obtain

$$\begin{aligned} \mathbf{H} &= \begin{pmatrix} 2 + \langle 01|v|01\rangle_{AS} & \langle 01|v|25\rangle_{AS} & \langle 01|v|34\rangle_{AS} \\ \langle 25|v|01\rangle_{AS} & 4 + \langle 25|v|25\rangle_{AS} & \langle 25|v|34\rangle_{AS} \\ \langle 34|v|01\rangle_{AS} & \langle 34|v|25\rangle_{AS} & 4 + \langle 34|v|34\rangle_{AS} \end{pmatrix} \\ &= \begin{pmatrix} 3.2533141373154997 & 0.3133285343288749 & -0.3133285343288749 \\ 0.3133285343288749 & 4.8616534694044069 & -0.2349964007466563 \\ -0.3133285343288749 & -0.2349964007466563 & 4.8616534694044069 \end{pmatrix}, \end{aligned}$$

by using the formula in Eq. (8.16) and the analytical expressions in [44]. MATLAB yields the following diagonalization result,

$$E_0 = 3.152328007096850.$$

Our CCSD program reproduces this result.

7.2.3 Code Structure and Class Implementation

The code is structured into four *abstract* base classes:

- **CCalgo**: CCSD algorithm class.
- **Amplitudes**: Class for handling the CCSD amplitudes t_i^a and t_{ij}^{ab} .
- **Fmatrix**: Class for handling the F-matrix in Eq. (6.72).
- **Interaction**: Class for handling the interaction elements $\langle\alpha\beta|v|\gamma\delta\rangle$.

The following derived classes have been constructed:

- **ccsd1**: Implementation of the CCSD algorithm.
- **amp1**: Implementation of the amplitude equations, structuring of amplitudes, and calculations of intermediates.
- **Fmatrix**: Structuring of $\langle\alpha|h|\beta\rangle$, calculation and structuring of F-matrix.
- **Interaction**: Structuring of $\langle\alpha\beta|v|\gamma\delta\rangle$.

Figure 7.2.3 shows the class diagrams of our CCSD program. We will in the following sections present each class, its structure and functionality. The focus will be on the implementations of the CCSD algorithm, the energy equation and the amplitude equations.



Figure 7.1: Class diagrams of our CCSD program.

7.2.4 Implementation of the CCSD Algorithm

The CCSD algorithm is implemented in `ccsd1`. The derived class inherits all members of `CCalgo` and defines these. The header file `CCalgo.hpp` is shown below.

```
//// CCalgo.hpp /**
class CCalgo {
public:
    // number of hole states
    int nh;
    // number of particle states;
    int np;
    // f-matrix object
    Fmatrix* F;
    // interaction object
    Interaction* V;
    // amplitude object
    Amplitudes* T;
    // reference energy <Phi_0|H|Phi_0>
    double E_ref;
    // new ground state energy
    double E_new;
    // old ground state energy
    double E_old;
    // self-consistency tolerance
    double tol;
    // maximum number of iterations
    int max_iter;
    // iteration variable
    int iter;
    // output file
    ofstream file;
    // <p|h|q>-file
    char* sp_energy_file;
    // <pq|v|rs>-file
    char* tp_energy_file;
/*
 * constructor
 */
CCalgo();
/*
 * destructor
 */
virtual ~CCalgo();
/*
 * start ccsd calculation
 */
virtual void start_calculation() = 0;
/*
 * self-consistent iteration procedure
 */
virtual void start_iteration_procedure() = 0;
/*
 * set up reference energy <Phi_0|H|Phi_0>
 */
virtual void calculate_ref_energy() = 0;
/*
 * calculate coupled-cluster energy
 */
virtual void calculate_energy() = 0;
};
```

The aim of constructing an abstract base class `CCalgo` is that other algorithm schemes can be implemented in derived classes. The members shown in the header file are universal in the sense that they are needed in most schemes. Moreover, additional variables and functions can of course

be included in derived classes. We have in this thesis implemented the following CCSD algorithm in `ccsd1`.

Coupled-Cluster Algorithm

1. Set up model space
2. Calculate f_p^q and $\langle pq|v|rs \rangle$
3. Set up reference energy $E_{\text{ref}} = \langle \Phi_0 | \hat{H} | \Phi_0 \rangle$
4. Initialize amplitudes t_i^a and t_{ij}^{ab} , and energy variables E_{new} and E_{old}
5. While not converged ($\text{diff} > \epsilon$)
 - a. Calculate intermediates
 - b. Calculate new 1p1h excitation amplitudes t_i^a
 - c. Calculate new 2p2h excitation amplitudes t_{ij}^{ab}
 - d. Calculate new energy E_{new}
 - e. Calculate $\text{diff} = E_{\text{new}} - E_{\text{old}}$
 - f. Set $E_{\text{old}} = E_{\text{new}}$

Results: Ground state energy E_{new} , and excitation amplitudes t_i^a and t_{ij}^{ab} .

The number of basis functions, i.e. the dimension of the single-particle model space, is given as

$$n_b = n_h + n_p, \quad (7.22)$$

where n_h and n_p are given in the arguments of `main.cpp`. However, the basis in itself is determined by the single-particle matrix elements $\langle \alpha|h|\beta \rangle$ or interaction elements $\langle \alpha\beta|v|\gamma\delta \rangle$. Thus the model space is determined by the matrix elements. The f_p^q -elements are calculated in `f1`. We will present `f1` and `int1` in the next two sections. Items 1-5 are carried out in `ccsd1::start_calculation()`. The code is shown below.

```
void ccsd1::start_calculation(){
    // read interaction energy elements
    V->read_interaction();
    // read <p/h/q>-elements from file
    F->read_sp_energy();
    // set up f-matrix
    F->set_up_fmatrix();
    // set up reference energy E_ref = <phi_0|H|phi_0>
    calculate_ref_energy();
    // initialize t1 amplitudes
    T->init_t1();
    // initialize t2 amplitudes
    T->init_t2();
    ...
    // initialize energy
    E_new = E_ref;
    E_old = 0;
    // start self-consistency procedure
    start_iteration_procedure();
} // end start_calculation
```

Items 5a-f are implemented in `ccsd1::start_iteration_procedure()`. The code is shown below.

```
void ccsd1::start_iteration_procedure(){
    ...
    // self-consistent iteration procedure
    while(abs(diff)>tol && iter<max_iter){
        // update iteration variable
        iter = iter + 1;
        // calculate t1 amplitudes
        T->calc_t1();
        // calculate t2 amplitude
        T->calc_t2();
        // calculate energy
        calculate_energy();
        // energy difference
        diff = E_new - E_old;
        // update amplitudes
        T->t1_old = T->t1;
        T->t2_old = T->t2;
        // update old energy variable
        E_old = E_new;
    }
    // save data
    ...
} // end start_iteration_procedure
```

We start out with initial amplitudes t_i^a and t_{ij}^{ab} . These are inserted into the amplitude equations yielding new amplitudes. Then we calculate the new CC energy, and determine whether the energy is converged or not. If not, the procedure starts over again, till convergence is obtained.

In order to calculate the ground state energy, the reference energy is needed (see Eq. 6.84). The expression reads

$$E_{\text{ref}} = \langle \Phi_0 | \hat{H} | \Phi_0 \rangle = \sum_i \langle i | h | i \rangle + \frac{1}{2} \sum_{ij} \langle ij | v | ij \rangle,$$

and is implemented in `void ccsd1::calculate_ref_energy()`.

```
void ccsd1::calculate_ref_energy(){
    ...
    // E_ref = <phi_0|H|phi_0> = SUM_i <i|h_0|i> + 0.5*SUM_ij <i j|v|i j>
    E_ref = 0.0;
    for(i=0; i<nh; i++){
        E_ref += F->s_hh(i,i);
        for(j=0; j<nh; j++){
            E_ref += 0.5*V->hhhh(i,j,i,j);
        }
    }
} // end calculate_ref_energy
```

For each iteration in the self-consistency procedure, the new CC energy is calculated for given values of t_i^a and t_{ij}^{ab} . The energy equation

$$E_{\text{CC}} = \sum_{ia} f_a^i t_i^a + \frac{1}{2} \sum_{ijab} \langle ij | v | ab \rangle t_i^a t_j^b + \frac{1}{4} \sum_{ijab} \langle ij | v | ab \rangle t_{ij}^{ab}$$

is implemented in `void ccsd1::calculate_energy()`.

```
void ccsd1::calculate_energy(){
    ...
    // <Phi_0|HT1|Phi_0>
    p1 = 0.0;
    for(i=0; i<nh; i++) {
```

```

        for(a=0; a<np; a++){
            p1 = p1 + F->f_hp(i,a)*T->t1(a,i);
        }
    }
    // <Phi_0|HT1T1|Phi_0>
    p2 = 0.0;
    for(j=0; j<nh; j++){
        for(i=0; i<nh; i++){
            for(b=0; b<np; b++){
                for(a=0; a<np; a++){
                    p2 = p2 + V->pphh(a,b,i,j)*T->t1(a,i)*T->t1(b,j);
                }
            }
        }
    }
    p2 = p2*0.5;
    // <Phi_0|HT2|Phi_0>
    p3 = 0.0;
    for(j=0; j<nh; j++){
        for(i=0; i<nh; i++){
            for(b=0; b<np; b++){
                for(a=0; a<np; a++){
                    p3 = p3 + V->pphh(a,b,i,j)*T->t2(a,b,i,j);
                }
            }
        }
    }
    p3 = p3*0.25;
    // total coupled-cluster energy
    p = p1 + p2 + p3;
    // total ground state energy
    E_new = p + E_ref;
    ...
} // end calculate_energy

```

The rest of the functions in `ccsd1::start_calculation` and `ccsd1::start_iteration_procedure()` will be described soon.

7.2.5 F-matrix and Interaction Elements

The F-matrix is defined in Eq. (6.71). We have chosen to construct an abstract `Fmatrix` class, and a derived class `f1` that defines its members. The header file `Fmatrix.hpp` is shown below.

```

/// Fmatrix.hpp /**
class Fmatrix {
public:
    // f-matrices
    Array<double,2> f_hh;
    Array<double,2> f_hp;
    Array<double,2> f_ph;
    Array<double,2> f_pp;
    // sp-energy matrices
    Array<double,2> s_hh;
    Array<double,2> s_hp;
    Array<double,2> s_ph;
    Array<double,2> s_pp;
    // <p/h/q>-file
    char* sp_energy_file;
    // Interaction* object
    Interaction* V;
    /*
     * constructor
     */
    Fmatrix();
}

```

```

/*
 * read single-particle energies from file
 */
virtual void read_sp_energy() = 0;
/*
 * set up f-matrix
 */
virtual void set_up_fmatrix() = 0;
/*
 * destructor
 */
virtual ~Fmatrix();
};

```

The function `f1::read_sp_energy()` reads the single-particle elements $\langle \alpha|h|\beta \rangle$ from file, and structure the data into four arrays `s_hh`, `s_hp`, `s_ph` and `s_pp`. The `h` denotes a hole state i , while `p` denotes a particle state a . The position of `h/p` reflects the position of the states in the matrix elements, viz.

$$\begin{aligned}s_{hh} &= \langle i|h|i \rangle \\ s_{hp} &= \langle i|h|a \rangle \\ s_{ph} &= \langle a|h|i \rangle \\ s_{pp} &= \langle a|h|b \rangle.\end{aligned}$$

Furthermore, the elements of the F-matrix are defined as

$$f_p^q = \langle p|h|q \rangle + \sum_i \langle pi|v|qi \rangle, \quad (7.23)$$

where the interaction elements are antisymmetrized, and $pqr..$ denote both hole and particle states. The elements are structured into four arrays,

$$\begin{aligned}f_{hh} &= f_i^j \\ f_{hp} &= f_i^a \\ f_{ph} &= f_a^i \\ f_{pp} &= f_a^b.\end{aligned}$$

The function `f1::set_up_fmatrix()` calculates and structures the F-matrix. The code is shown below.

```

void f1::set_up_fmatrix(){
    ...
    // set up f_hh = <i/h_0/j> + SUM_k <i k//j k>
    for(i=0; i<nh; i++){
        for(j=0; j<nh; j++){
            f_hh(i,j) = s_hh(i,j);
            for(k=0; k<nh; k++){
                f_hh(i,j) += V->hhhh(i,k,j,k);
            }
        }
    }
    // set up f_hp = <i/h_0/a> + SUM_k <i k//a k>
    // <h h//p h> = <p h//h h>
    for(i=0; i<nh; i++){
        for(a=0; a<np; a++){
            f_hp(i,a) = s_hp(i,a);
            for(k=0; k<nh; k++){
                f_hp(i,a) += V->phhh(a,k,i,k);
            }
        }
    }
}

```

```

}
// set up f_ph = <a|h_0|i> + SUM_k <a k||i k>
for(a=0; a<np; a++){
    for(i=0; i<nh; i++){
        f_ph(a,i) = s_ph(a,i);
        for(k=0; k<nh; k++){
            f_ph(a,i) += V->phhh(a,k,i,k);
        }
    }
}
// set up f_pp = <a|h_0|b> + SUM_k <a k||b k>
for(a=0; a<np; a++){
    for(b=0; b<np; b++){
        f_pp(a,b) = s_pp(a,b);
        for(k=0; k<nh; k++){
            f_pp(a,b) += V->phpb(a,k,b,k);
        }
    }
}
} // end set_up_fmatrix

```

The abstract base class `Interaction`, with derived class `int1`, is constructed to handle the interaction elements $\langle pq|v|rs \rangle$. The header file `Interaction.hpp` is shown below.

```

/// Interaction.hpp /**
class Interaction {
public:
    // number of hole states
    int nh;
    // number of particle states
    int np;
    // interaction matrices
    Array<double,4> hhhh;      // <hh||hh>
    Array<double,4> phhh;      // <ph||hh>
    Array<double,4> pphh;      // <pp||hh>
    Array<double,4> phph;      // <ph||ph>
    Array<double,4> ppph;      // <pp||ph>
    Array<double,4> pppp;      // <pp||pp>
    // <pq|v|rs>-file
    char* tp_energy_file;
/*
 * constructor
 */
Interaction();
/*
 * read interaction elements <p q||r s> from file
 */
virtual void read_interaction() = 0;
/*
 * destructor
 */
virtual ~Interaction();
};

```

The aim of the class is to read $\langle pq|v|rs \rangle$ from file, and structure the data into six arrays: `hhhh`, `phhh`, `pphh`, `phph`, `ppph` and `pppp`. The position of `h/p` reflects the position of the corresponding

state in the interaction element, viz.

$$\begin{aligned} \text{hhhh} &= \langle ij|v|kl \rangle \\ \text{phhh} &= \langle aj|v|kl \rangle \\ \text{pphh} &= \langle ab|v|kl \rangle \\ \text{phph} &= \langle aj|v|bl \rangle \\ \text{ppph} &= \langle ab|v|cl \rangle \\ \text{pppp} &= \langle ab|v|cd \rangle, \end{aligned}$$

where $ijkl..$ denote hole states, and $abcd..$ denote particle states. If we were to store $\langle pq|v|rs \rangle$ in a four-dimensional array, we would use unnecessary amount of memory. The matrix would actually increase exponentially with respect to the size of the basis. Furthermore, since $\langle \alpha\beta|v|\gamma\delta \rangle$ is antisymmetrized, i.e.

$$\langle pq|v|rs \rangle = \langle rs|v|pq \rangle = \langle qp|v|sr \rangle = -\langle pq|v|sr \rangle = -\langle qp|v|rs \rangle,$$

we obtain the following matrix relations,

$$\begin{aligned} \text{phhh} &= -\text{hphh} = \text{hhph} = -\text{hhhp} \\ \text{pphh} &= \text{hhpp} \\ \text{phph} &= \text{hphp} = -\text{hpph} = -\text{phhp} \\ \text{ppph} &= \text{phpp} = -\text{pphp} = -\text{hppp}. \end{aligned}$$

All possible combinations are covered. Thus it is sufficient to only store $\langle pq|v|rs \rangle$ with p, q, r and s matching one of the six arrays. The function `int1::read_interaction()` reads $\langle pq|v|rs \rangle$ from file and structures the elements. For a given array-name (`hhhh`, `phhh`, and so forth), we know the orbital subspace of each single-particle state in the elements. Thus we number each element from 0 up to number of hole/particle states. For example, assume we have 6 basis functions with the mapping given in Eq. (7.20). We also assume that we have 2 hole states, i.e. $|0\rangle$ and $|1\rangle$. Thus we have 4 particle states: $|2\rangle$, $|3\rangle$, $|4\rangle$ and $|5\rangle$. Let $nh = 2$ (number of hole states) and $np = 4$ (number of particle states). The following examples illustrate the convention used to store the interaction elements.

$$\begin{aligned} \text{phph}(1,1,2,0) &= \langle (nh+1)1|v|(nh+2)2 \rangle = \langle 31|v|40 \rangle \\ \text{pphh}(1,3,0,1) &= \langle (nh+1)(nh+3)|v|01 \rangle = \langle 35|v|01 \rangle \\ \text{ppph}(0,1,2,1) &= \langle (nh)(nh+1)|v|(nh+2)1 \rangle = \langle 23|v|41 \rangle \end{aligned}$$

7.2.6 Implementation of the Amplitude Equations

We will in this section present our implementation of the CCSD amplitude equations in detail. We have constructed the abstract base class `Amplitudes`, and the derived class `amp1` with the implementation. The objective of the class is to calculate new amplitudes from old (previous iteration) amplitudes. See CCSD algorithm in Sec. 7.2.4. The header file `Amplitudes.hpp` is shown below.

```
class Amplitudes {
public:
    // number of hole states
    int nh;
    // number of particle states
    int np;
    // T1 amplitude arrays
    Array<double,2> t1;
    Array<double,2> t1_old;
    // T2 amplitude array
```

```

Array<double,4> t2;
Array<double,4> t2_old;
// Fmatrix object
Fmatrix* F;
// Interaction object
Interaction* V;
// output files
ofstream file;
ofstream file2;
/*
 * intermediate arrays
 */
Array<double,2> I1;
Array<double,2> I2;
Array<double,2> I3;
Array<double,4> I4;
Array<double,4> I5;
Array<double,4> I6;
Array<double,4> I7;
Array<double,2> I8;
Array<double,4> I9;
Array<double,4> I10;
Array<double,4> I11;
/*
 * intermediates calculation
 */
virtual void calc_I1() = 0;
virtual void calc_I2() = 0;
virtual void calc_I3() = 0;
virtual void calc_I4() = 0;
virtual void calc_I5() = 0;
virtual void calc_I6() = 0;
virtual void calc_I7() = 0;
virtual void calc_I8() = 0;
virtual void calc_I9() = 0;
virtual void calc_I10() = 0;
virtual void calc_I11() = 0;
/*
 * T1 functions
 */
virtual void init_t1() = 0;
virtual void calc_t1() = 0;
virtual void calc_t1_intermediates() = 0;
virtual void calc_t1_term2(Array<double,2>) = 0;
virtual void calc_t1_term3(Array<double,2>) = 0;
virtual void calc_t1_term4(Array<double,2>) = 0;
virtual void calc_t1_term5(Array<double,2>) = 0;
virtual void calc_t1_term6(Array<double,2>) = 0;
virtual void calc_t1_term7(Array<double,2>) = 0;
virtual void calc_t1_d(Array<double,2>) = 0;
/*
 * T2 functions
 */
virtual void init_t2() = 0;
virtual void calc_t2() = 0;
virtual void calc_t2_intermediates() = 0;
virtual void calc_t2_term2(Array<double,4>) = 0;
virtual void calc_t2_term3(Array<double,4>) = 0;
virtual void calc_t2_term4(Array<double,4>) = 0;
virtual void calc_t2_term5(Array<double,4>) = 0;
virtual void calc_t2_term6(Array<double,4>) = 0;
virtual void calc_t2_term7(Array<double,4>) = 0;
virtual void calc_t2_term8(Array<double,4>) = 0;
virtual void calc_t2_d(Array<double,4>) = 0;
/*

```

```

    * constructor
    */
Amplitudes();
/*
 * destructor
 */
~Amplitudes();
/*
 * write converged amplitudes to file
 */
virtual void write_amplitudes_to_file() = 0;
};

```

We now turn to the implementation of the amplitude equations. The formal expressions are given in Eqs. (6.139) and (6.140), and the diagrammatic representations in Eqs. (??) and (??). The algebraic expressions are given in Eqs. (6.155) and (6.187). Before we turn to the implementation of the amplitude equations, manipulations of the algebraic expressions are needed.

Consider the \hat{T}_1 equation in Eq. (6.155). We first rearrange the equation into

$$\begin{aligned} 0 = f_i^a + \langle ia|v|bj\rangle t_i^b + \frac{1}{2}\langle ai|v|bc\rangle t_{ji}^{bc} + & \left(f_a^b t_i^a - \langle ia|v|bc\rangle t_j^b t_i^c \right) \\ & + \left(-f_i^j t_j^a - f_a^i t_j^a t_i^b + \langle ij|v|ak\rangle t_i^b t_j^a + \langle ij|v|ab\rangle t_k^a t_i^b t_j^c + \frac{1}{2}\langle ij|v|ab\rangle t_i^c t_{jk}^{ab} \right) \\ & + \left(-\frac{1}{2}\langle ij|v|ka\rangle t_{ij}^{ba} + \frac{1}{2}\langle ij|v|ab\rangle t_k^a t_{ij}^{bc} \right) + \left(f_a^i t_{ji}^{ba} + \langle ij|v|ab\rangle t_i^a t_{jk}^{bc} \right), \end{aligned}$$

leading to

$$\begin{aligned} 0 = f_i^a + \langle ia|v|bj\rangle t_i^b + \frac{1}{2}\langle ai|v|bc\rangle t_{ji}^{bc} + & \left(f_a^b t_i^a + \langle ai|v|bc\rangle t_j^b t_i^c \right) \\ & - \left(f_i^j t_j^a + f_a^i t_j^a t_i^b + \langle ij|v|ka\rangle t_i^b t_j^a + \langle ji|v|ab\rangle t_k^a t_i^b t_j^c + \frac{1}{2}\langle ji|v|ab\rangle t_i^c t_{jk}^{ab} \right) \\ & + \frac{1}{2} \left(\langle ij|v|ka\rangle t_{ij}^{ab} + \langle ij|v|ab\rangle t_k^a t_{ij}^{bc} \right) + \left(f_a^i t_{ji}^{ba} + \langle ij|v|ab\rangle t_i^a t_{jk}^{bc} \right). \end{aligned}$$

Relabeling some of the dummy-indices and moving amplitudes outside the parenthesis, yields

$$\begin{aligned} 0 = f_i^a + \langle ma|v|ei\rangle t_m^e + \frac{1}{2}\langle am|v|ef\rangle t_{im}^{ef} + & \left(f_e^a + \langle am|v|ef\rangle t_m^f \right) t_i^e \\ & - \left(f_i^m + f_e^m t_i^e + \langle mn|v|ie\rangle t_n^e + \langle mn|v|ef\rangle t_i^e t_n^f + \frac{1}{2}\langle mn|v|ef\rangle t_{in}^{ef} \right) t_m^a \\ & + \frac{1}{2} \left(\langle mn|v|ie\rangle + \langle mn|v|fe\rangle t_i^f \right) t_{mn}^{ea} + \left(f_e^m + \langle mn|v|ef\rangle t_n^f \right) t_{im}^{ae}. \end{aligned}$$

We define the following *intermediates*,

$$\begin{aligned} [I1]_e^a & \equiv f_e^a + \langle am|v|ef\rangle t_m^f \\ & = f_e^a + \langle ef|v|am\rangle t_m^f \end{aligned} \tag{7.24}$$

$$\begin{aligned} [I2]_e^m & \equiv f_e^m + \langle mn|v|ef\rangle t_n^f \\ & = f_e^m + \langle ef|v|mn\rangle t_n^f \end{aligned} \tag{7.25}$$

$$\begin{aligned} [I3]_i^m & \equiv f_i^m + f_e^m t_i^e + \langle mn|v|ie\rangle t_n^e + \langle mn|v|ef\rangle t_i^e t_n^f + \frac{1}{2}\langle mn|v|ef\rangle t_{in}^{ef} \\ & = f_i^m + \langle mn|v|ie\rangle t_n^e + \frac{1}{2}\langle mn|v|ef\rangle t_{in}^{ef} + \left(f_e^m + \langle mn|v|ef\rangle t_n^f \right) t_i^e \\ & = f_i^m - \langle ei|v|mn\rangle t_n^e + \frac{1}{2}\langle ef|v|mn\rangle t_{in}^{ef} + \left(f_e^m + \langle ef|v|mn\rangle t_n^f \right) t_i^e \\ & = f_i^m - \langle ei|v|mn\rangle t_n^e + \frac{1}{2}\langle ef|v|mn\rangle t_{in}^{ef} + [I2]_e^m t_i^e \end{aligned} \tag{7.26}$$

$$\begin{aligned}
 [I4]_{ie}^{mn} &\equiv \langle mn|v|ie\rangle + \langle fe|v|mn\rangle t_i^f \\
 &= -\langle ei|v|mn\rangle + \frac{1}{2}\langle fe|v|mn\rangle t_i^f + \frac{1}{2}\langle fe|v|mn\rangle t_i^f \\
 &= [I5]_{ie}^{mn} + \frac{1}{2}\langle fe|v|mn\rangle t_i^f
 \end{aligned} \tag{7.27}$$

$$[I5]_{ie}^{mn} \equiv -\langle ei|v|mn\rangle + \frac{1}{2}\langle fe|v|mn\rangle t_i^f \tag{7.28}$$

Using these definitions, the \hat{T}_1 amplitude equation reads

$$\begin{aligned}
 0 &= f_i^a + \langle ma|v|ei\rangle t_m^e + \frac{1}{2}\langle am|v|ef\rangle t_{im}^{ef} + [I1]_e^a t_i^e - [I3]_i^m t_m^a \\
 &\quad + \frac{1}{2}[I4]_{ie}^{mn} t_{mn}^{ea} + [I2]_e^m t_{im}^{ae}.
 \end{aligned}$$

We want to obtain an equation for t_i^a . Rewriting the equation into

$$\begin{aligned}
 0 &= f_i^a + \langle ia|v|ai\rangle t_i^a + (1 - \delta_{ea}\delta_{mi})\langle ma|v|ei\rangle t_m^e + \frac{1}{2}\langle am|v|ef\rangle t_{im}^{ef} \\
 &\quad + [I1]_a^a t_i^a + (1 - \delta_{ea})[I1]_e^a t_i^e - [I3]_i^i t_i^a - (1 - \delta_{mi})[I3]_i^m t_m^a \\
 &\quad + \frac{1}{2}[I4]_{ie}^{mn} t_{mn}^{ea} + [I2]_e^m t_{im}^{ae},
 \end{aligned}$$

and collecting all t_i^a -terms, yields

$$\begin{aligned}
 0 &= f_i^a + \left(\langle ia|v|ai\rangle + [I1]_a^a - [I3]_i^i \right) t_i^a + \frac{1}{2}\langle am|v|ef\rangle t_{im}^{ef} \\
 &\quad + (1 - \delta_{ea}\delta_{mi})\langle ma|v|ei\rangle t_m^e + (1 - \delta_{ea})[I1]_e^a t_i^e - (1 - \delta_{mi})[I3]_i^m t_m^a \\
 &\quad + \frac{1}{2}[I4]_{ie}^{mn} t_{mn}^{ea} + [I2]_e^m t_{im}^{ae}.
 \end{aligned}$$

We now define

$$d_i^a \equiv -\langle ia|v|ai\rangle - [I1]_a^a + [I3]_i^i, \tag{7.29}$$

leading to the following equation for t_i^a ,

$$\begin{aligned}
 d_i^a t_i^a &= f_i^a + \frac{1}{2}\langle ef|v|am\rangle t_{im}^{ef} - (1 - \delta_{ea}\delta_{mi})\langle am|v|ei\rangle t_m^e + (1 - \delta_{ea})[I1]_e^a t_i^e \\
 &\quad - (1 - \delta_{mi})[I3]_i^m t_m^a + \frac{1}{2}[I4]_{ie}^{mn} t_{mn}^{ea} + [I2]_e^m t_{im}^{ae}.
 \end{aligned} \tag{7.30}$$

This equation is implemented in `amp1::calc_t1()`. In the following we also show the implementation of each term in Eq. (7.30). The implementation of the intermediates will be shown after the \hat{T}_2 equation is modified.

```

void amp1::calc_t1(){
    ...
    // calculate intermediates I1, I2, I3, I4 and I5
    calc_t1_intermediates();
    ...
    // f_i^a
    t1 = F->f_ph;
    // 0.5<ef|v|am>t_(im)^^(ef)
    calc_t1_term2(temp);
    t1 = t1 + temp;
    // -(1 - \delta_(ea)\delta_(mi))<am|v|ei>t_m^e
    calc_t1_term3(temp);
    t1 = t1 + temp;
    // (1 - \delta_(ea))[I1]_e^at_i^a
    calc_t1_term4(temp);
}

```

```

t1 = t1 + temp;
// -(1 - \delta_{ea}(mi)) [I3]_i^m t_m^a
calc_t1_term5(temp);
t1 = t1 + temp;
// 0.5[I4]_(ie)^{(mn)} t_(mn)^{(ea)}
calc_t1_term6(temp);
t1 = t1 + temp;
// [I2]_e^m t_(im)^{(ae)}
calc_t1_term7(temp);
t1 = t1 + temp;
// calculate denominator d_i^a
calc_t1_d(temp);

// calculate final t1 amplitudes
t1 = t1/temp;
...
} //end calc_t1
    
```

$$d_i^a t_i^a \leftarrow \frac{1}{2} \langle ef | v | am \rangle t_{im}^{ef}$$

```

void amp1::calc_t1_term2(Array<double,2> ans){
    ...
    for(i=0; i<nh; i++){
        for(a=0; a<np; a++){
            temp = 0.0;
            for(m=0; m<nh; m++){
                for(f=0; f<np; f++){
                    for(e=0; e<np; e++){
                        temp = temp + V->ppph(e,f,a,m)*t2_old(e,f,i,m);
                    }
                }
            }
            ans(a,i) = ans(a,i) + 0.5*temp;
        }
    }
} // end calc_t1_term2
    
```

$$d_i^a t_i^a \leftarrow -(1 - \delta_{ea}\delta_{mi}) \langle am | v | ei \rangle t_m^e$$

```

void amp1::calc_t1_term3(Array<double,2> ans){
    ...
    for(i=0; i<nh; i++){
        for(a=0; a<np; a++){
            temp = 0.0;
            for(m=0; m<nh; m++){
                for(e=0; e<np; e++){
                    if(m!=i || e!=a){
                        temp = temp + V->phph(a,m,e,i)*t1_old(e,m);
                    }
                }
            }
            ans(a,i) = ans(a,i) - temp;
        }
    }
} // end calc_t1_term3
    
```

$$d_i^a t_i^a \leftarrow (1 - \delta_{ea}) [I1]_e^a t_i^e$$

```

void amp1::calc_t1_term4(Array<double,2> ans){
    ...
    for(i=0; i<nh; i++){
        for(a=0; a<np; a++){
            temp = 0.0;
            for(e=0; e<np; e++){
                if(e!=a){
                    temp = temp + I1(a,e)*t1_old(e,i);
                }
            }
            ans(a,i) = ans(a,i) + temp;
        }
    }
} // end calc_t1_term4
    
```

$$d_i^a t_i^a \leftarrow -(1 - \delta_{mi}) [I3]_i^m t_m^a$$

```

void amp1::calc_t1_term5(Array<double,2> ans){
    ...
    for(i=0; i<nh; i++){
        for(a=0; a<np; a++){
            temp = 0.0;
            for(m=0; m<nh; m++){
                if(m!=i){
                    temp = temp + I3(m,i)*t1_old(a,m);
                }
            }
            ans(a,i) = ans(a,i) - temp;
        }
    }
} // end calc_t1_term5
    
```

$$d_i^a t_i^a \leftarrow \frac{1}{2} [I4]_{ie}^{mn} t_{mn}^{ea}$$

```

void amp1::calc_t1_term6(Array<double,2> ans){
    ...
    for(i=0; i<nh; i++){
        for(a=0; a<np; a++){
            temp = 0.0;
            for(n=0; n<nh; n++){
                for(m=0; m<nh; m++){
                    for(e=0; e<np; e++){
                        temp = temp + I4(m,n,i,e)*t2_old(e,a,m,n);
                    }
                }
            }
            ans(a,i) = ans(a,i) + 0.5*temp;
        }
    }
} // end calc_t1_term6
    
```

$$d_i^a t_i^a \leftarrow [I2]_e^m t_{im}^{ae}$$

```

void amp1::calc_t1_term7(Array<double,2> ans){
    ...
    for(i=0; i<nh; i++){
        for(a=0; a<np; a++){
            temp = 0.0;
            for(m=0; m<nh; m++){
        
```

```

        for(e=0; e<np; e++){
            temp = temp + I2(m,e)*t2_old(a,e,i,m);
        }
        ans(a,i) = ans(a,i) + temp;
    }
}

} // end calc_t1_term7
    
```

$$d_i^a \equiv -\langle ia|v|ai\rangle - [I1]_a^a + [I3]_i^i = \langle ai|v|ai\rangle - [I1]_a^a + [I3]_i^i,$$

```

void amp1::calc_t1_d(Array<double,2> ans){
    ...
    for(i=0; i<nh; i++){
        for(a=0; a<np; a++){
            ans(a,i) = V->phph(a,i,a,i) - I1(a,a) + I3(i,i);
        }
    }
}

} // end calc_t1_d
    
```

Consider the \widehat{T}_2 equation in Eq. (6.187). We first rearrange the equation into

$$\begin{aligned}
 0 &= \langle ij|v|ab\rangle + \frac{1}{2}\langle ab|v|cd\rangle t_{ij}^{cd} \\
 &+ \left(P(ki)f_i^j t_{kj}^{ab} + P(jk)f_a^i t_{ji}^{bc} t_k^a + P(lk)\langle ij|v|ka\rangle t_{li}^{bc} t_j^a + P(kl)\langle ij|v|ab\rangle t_{ki}^{cd} t_l^a t_j^b \right. \\
 &\quad \left. + \frac{1}{2}P(kl)\langle ij|v|ab\rangle t_{ik}^{ab} t_{jl}^{cd} \right) \\
 &+ \frac{1}{2} \left(\langle ij|v|kl\rangle t_{ij}^{ab} + P(lk)\langle ij|v|ak\rangle t_l^a t_{ij}^{bc} + \frac{1}{2}\langle ij|v|ab\rangle t_{kl}^{ab} t_{ij}^{cd} + \frac{1}{4}P(kl)\langle ij|v|ab\rangle t_k^a t_{ij}^{cd} t_l^b \right) \\
 &+ \left(P(cb)f_a^b t_{ij}^{ca} - P(bc)f_a^i t_{jk}^{ba} t_k^c + P(da)\langle ai|v|bc\rangle t_{jk}^{db} t_i^c - P(cd)\langle ij|v|ab\rangle t_{kl}^{ca} t_i^d t_j^b \right. \\
 &\quad \left. - \frac{1}{2}P(cd)\langle ij|v|ab\rangle t_{kl}^{ca} t_{ij}^{db} \right) \\
 &+ \left(P(kj)P(ca)\langle ia|v|bj\rangle t_{ki}^{cb} + P(jk)P(ad)\langle ai|v|bc\rangle t_j^b t_{ik}^{cd} - P(bc)P(kl)\langle ij|v|ka\rangle t_i^b t_{jl}^{ac} \right. \\
 &\quad \left. + P(kl)P(cd)\langle ij|v|ab\rangle t_k^a t_{il}^{cb} t_j^d + \frac{1}{2}P(kl)P(cd)\langle ij|v|ab\rangle t_{ki}^{ca} t_{jl}^{bd} \right) \\
 &+ \left(-P(ba)\langle ia|v|jk\rangle t_i^b - \frac{1}{2}P(ad)\langle ai|v|bc\rangle t_{jk}^{bc} t_i^d + P(kj)P(ac)\langle ia|v|bj\rangle t_k^b t_i^c \right. \\
 &\quad \left. - \frac{1}{2}P(jk)P(ad)\langle ai|v|bc\rangle t_j^b t_k^c t_i^d + \frac{1}{2}P(ab)\langle ij|v|kl\rangle t_i^a t_j^b + \frac{1}{4}P(cd)\langle ij|v|ab\rangle t_i^c t_{kl}^{ab} t_j^d \right. \\
 &\quad \left. + \frac{1}{2}P(bc)P(kl)\langle ij|v|ka\rangle t_i^b t_l^a t_j^c + \frac{1}{4}P(kl)P(cd)\langle ij|v|ab\rangle t_k^a t_i^c t_l^b t_j^d \right) \\
 &+ \left(P(ji)\langle ab|v|ci\rangle t_j^c + \frac{1}{2}P(ij)\langle ab|v|cd\rangle t_i^c t_j^d \right)
 \end{aligned} \tag{7.31}$$

Relabeling some of the dummy-indices, and moving amplitudes and P -functions outside the parenthesis, yields

$$\begin{aligned}
 &= \langle ab|v|ij\rangle + \frac{1}{2}\langle ab|v|ef\rangle t_{ij}^{ef} \\
 &- P(ij) \left(f_j^m + f_e^m t_j^e + \langle mn|v|je\rangle t_n^e + \langle mn|v|ef\rangle t_j^e t_n^f + \frac{1}{2}P(kl)\langle mn|v|ef\rangle t_{jn}^{ef} \right) t_{im}^{ab} \\
 &+ \frac{1}{2} \left(\langle mn|v|ij\rangle + P(ij)\langle mn|v|ie\rangle t_j^e + \frac{1}{2}\langle mn|v|ef\rangle t_{ij}^{ef} + \frac{1}{2}P(ij)\langle mn|v|ef\rangle t_i^e t_j^f \right) t_{mn}^{ab} \\
 &+ P(ab) \left(f_e^b - f_e^m t_m^b + \langle bm|v|ef\rangle t_m^f - \langle mn|v|ef\rangle t_m^b t_n^f - \frac{1}{2}\langle mn|v|ef\rangle t_{mn}^{bf} \right) t_{ij}^{ae} \\
 &+ P(ij)P(ab) \left(\langle mb|v|ej\rangle + \langle bm|v|fe\rangle t_j^f - \langle nm|v|je\rangle t_n^b - \langle nm|v|fe\rangle t_n^b t_j^f + \frac{1}{2}\langle nm|v|fe\rangle t_{jn}^{bf} \right) t_{im}^{ae} \\
 &- P(ab) \left(\langle mb|v|ij\rangle + \frac{1}{2}\langle mb|v|ef\rangle t_{ij}^{ef} + P(jk)\langle mb|v|ej\rangle t_i^e + \frac{1}{2}P(jk)\langle bm|v|fe\rangle t_i^e t_j^f \right. \\
 &\quad \left. - \frac{1}{2}\langle mn|v|ij\rangle t_n^b - \frac{1}{4}\langle mn|v|ef\rangle t_n^b t_{ij}^{ef} - \frac{1}{2}P(jk)\langle mn|v|ie\rangle t_n^b t_j^e - \frac{1}{4}P(jk)\langle mn|v|fe\rangle t_n^b t_j^e t_i^f \right) t_m^a \\
 &+ P(ij) \left(\langle ab|v|ej\rangle + \frac{1}{2}\langle ab|v|ef\rangle t_j^f \right) t_i^e. \tag{7.32}
 \end{aligned}$$

In order to simplify the equation, we first define

$$[I6]_{ej}^{mb} \equiv -\langle bm|v|ej\rangle + \frac{1}{2}\langle fe|v|bm\rangle t_j^f.$$

We now consider each expression in parenthesis in Eq. (7.32). We define the following intermediates:

$$\begin{aligned}
 [I7]_{ij}^{mn} &\equiv \langle mn|v|ij\rangle + P(ij)\langle mn|v|ie\rangle t_j^e + \frac{1}{2}\langle mn|v|ef\rangle t_{ij}^{ef} + \frac{1}{2}P(ij)\langle mn|v|ef\rangle t_i^e t_j^f \\
 &= \langle mn|v|ij\rangle + \frac{1}{2}\langle mn|v|ef\rangle t_{ij}^{ef} + P(ij) \left(\langle mn|v|ie\rangle + \frac{1}{2}\langle mn|v|fe\rangle t_i^f \right) t_j^e \\
 &= \langle mn|v|ij\rangle + \frac{1}{2}\langle ef|v|mn\rangle t_{ij}^{ef} + P(ij) \left(-\langle ei|v|mn\rangle + \frac{1}{2}\langle fe|v|mn\rangle t_i^f \right) t_j^e \\
 &= \langle mn|v|ij\rangle + \frac{1}{2}\langle ef|v|mn\rangle t_{ij}^{ef} + P(ij) [I5]_{ie}^{mn} t_j^e \tag{7.33}
 \end{aligned}$$

$$\begin{aligned}
 [I8]_e^b &\equiv f_e^b - f_e^m t_m^b + \langle bm|v|ef\rangle t_m^f - \langle mn|v|ef\rangle t_m^b t_n^f - \frac{1}{2}\langle mn|v|ef\rangle t_{mn}^{bf} \\
 &= \left(f_e^b + \langle bm|v|ef\rangle t_m^f \right) - \frac{1}{2}\langle mn|v|ef\rangle t_{mn}^{bf} - \left(f_e^m + \langle mn|v|ef\rangle t_n^f \right) t_m^b \\
 &= \left(f_e^b + \langle ef|v|bm\rangle t_m^f \right) - \frac{1}{2}\langle ef|v|mn\rangle t_{mn}^{bf} - \left(f_e^m + \langle ef|v|mn\rangle t_n^f \right) t_m^b \\
 &= [I1]_e^b - \frac{1}{2}\langle mn|v|ef\rangle t_{mn}^{bf} - [I2]_e^m t_m^b \tag{7.34}
 \end{aligned}$$

$$\begin{aligned}
 [I9]_{ej}^{mb} &\equiv \langle mb|v|ej\rangle + \langle bm|v|fe\rangle t_j^f - \langle nm|v|je\rangle t_n^b - \langle nm|v|fe\rangle t_n^b t_j^f + \frac{1}{2} \langle nm|v|fe\rangle t_{jn}^{bf} \\
 &= \left(\langle mb|v|ej\rangle + \frac{1}{2} \langle bm|v|fe\rangle t_j^f \right) + \frac{1}{2} \langle bm|v|fe\rangle t_j^f - \left(\langle nm|v|je\rangle + \langle nm|v|fe\rangle t_j^f \right) t_n^b \\
 &\quad + \frac{1}{2} \langle nm|v|fe\rangle t_{jn}^{bf} \\
 &= \left(-\langle bm|v|ej\rangle + \frac{1}{2} \langle fe|v|bm\rangle t_j^f \right) + \frac{1}{2} \langle fe|v|bm\rangle t_j^f \\
 &\quad - \left(-\langle ej|v|nm\rangle + \frac{1}{2} \langle fe|v|nm\rangle t_j^f + \frac{1}{2} \langle fe|v|nm\rangle t_j^f \right) t_n^b + \frac{1}{2} \langle fe|v|nm\rangle t_{jn}^{bf} \\
 &= [I6]_{ej}^{mb} + \frac{1}{2} \langle fe|v|bm\rangle t_j^f - [I4]_{je}^{nm} t_n^b + \frac{1}{2} \langle fe|v|nm\rangle t_{jn}^{bf} \tag{7.35}
 \end{aligned}$$

$$\begin{aligned}
 [I10]_{ij}^{mb} &\equiv \langle mb|v|ij\rangle + \frac{1}{2} \langle mb|v|ef\rangle t_{ij}^{ef} + P(ij) \langle mb|v|ej\rangle t_i^e + \frac{1}{2} P(ij) \langle bm|v|fe\rangle t_i^e t_j^f \\
 &\quad - \frac{1}{2} \langle mn|v|ij\rangle t_n^b - \frac{1}{4} \langle mn|v|ef\rangle t_n^b t_{ij}^{ef} - \frac{1}{2} P(ij) \langle mn|v|ie\rangle t_n^b t_i^e \\
 &\quad - \frac{1}{4} P(ij) \langle mn|v|fe\rangle t_n^b t_i^e t_j^f \\
 &= \langle mb|v|ij\rangle + \frac{1}{2} \langle mb|v|ef\rangle t_{ij}^{ef} + P(ij) \left(\langle mb|v|ej\rangle + \frac{1}{2} \langle bm|v|fe\rangle t_j^f \right) t_i^e \\
 &\quad - \frac{1}{2} \left(\langle mn|v|ij\rangle + \frac{1}{2} \langle mn|v|ef\rangle t_{ij}^{ef} + P(ij) \left(\langle mn|v|ie\rangle + \frac{1}{2} \langle mn|v|fe\rangle t_i^f \right) t_j^e \right) t_n^b \\
 &= -\langle bm|v|ij\rangle - \frac{1}{2} \langle ef|v|bm\rangle t_{ij}^{ef} + P(ij) \left(-\langle bm|v|ej\rangle + \frac{1}{2} \langle fe|v|bm\rangle t_j^f \right) t_i^e \\
 &\quad - \frac{1}{2} \left(\langle mn|v|ij\rangle + \frac{1}{2} \langle ef|v|mn\rangle t_{ij}^{ef} + P(ij) \left(-\langle ei|v|mn\rangle + \frac{1}{2} \langle fe|v|mn\rangle t_i^f \right) t_j^e \right) t_n^b \\
 &= -\langle bm|v|ij\rangle - \frac{1}{2} \langle ef|v|bm\rangle t_{ij}^{ef} + P(ij) [I6]_{ej}^{mb} t_i^e - \frac{1}{2} [I7]_{ij}^{mn} t_n^b \tag{7.36}
 \end{aligned}$$

$$[I11]_{ej}^{ab} \equiv \langle ab|v|ej\rangle + \frac{1}{2} \langle ab|v|ef\rangle t_j^f \tag{7.37}$$

The \widehat{T}_2 equation can now be written as

$$\begin{aligned}
 0 &= \langle ab|v|ij\rangle + \frac{1}{2} \langle ab|v|ef\rangle t_{ij}^{ef} - P(ij) [I3]_j^m t_{im}^{ab} + \frac{1}{2} [I7]_{ij}^{mn} t_{mn}^{ab} + P(ab) [I8]_e^b t_{ij}^{ae} \\
 &\quad + P(ij)P(ab) [I9]_{ej}^{mb} t_{im}^{ae} - P(ab) [I10]_{ij}^{mb} t_m^a + P(ij) [I11]_{ej}^{ab} t_i^e. \tag{7.38}
 \end{aligned}$$

We want to obtain an equation for t_{ij}^{ab} . Rewriting the equation into

$$\begin{aligned}
 0 &= \langle ab|v|ij\rangle + \frac{1}{2} \langle ab|v|ab\rangle t_{ij}^{ab} + \frac{1}{2} (1 - \delta_{ea} \delta_{fb}) \langle ab|v|ef\rangle t_{ij}^{ef} - P(ij) [I3]_j^j t_{ij}^{ab} \\
 &\quad - P(ij) (1 - \delta_{mj}) [I3]_j^m t_{im}^{ab} + \frac{1}{2} [I7]_{ij}^{ij} t_{ij}^{ab} + \frac{1}{2} (1 - \delta_{mi} \delta_{nj}) [I7]_{ij}^{mn} t_{mn}^{ab} \\
 &\quad + P(ab) [I8]_b^b t_{ij}^{ab} + P(ab) (1 - \delta_{eb}) [I8]_e^b t_{ij}^{ae} + P(ij)P(ab) [I9]_{ej}^{mb} t_{im}^{ae} \\
 &\quad - P(ab) [I10]_{ij}^{mb} t_m^a + P(ij) [I11]_{ej}^{ab} t_i^e. \tag{7.39}
 \end{aligned}$$

and collecting all t_{ij}^{ab} -terms, yields

$$\begin{aligned}
 0 = & \langle ab|v|ij\rangle + \left(\frac{1}{2}\langle ab|v|ab\rangle - P(ij)[I3]_j^j + \frac{1}{2}[I7]_{ij}^{ij} + P(ab)[I8]_b^b \right) t_{ij}^{ab} \\
 & + \frac{1}{2}(1 - \delta_{ea}\delta_{fb})\langle ab|v|ef\rangle t_{ij}^{ef} - P(ij)(1 - \delta_{mj})[I3]_j^m t_{im}^{ab} \\
 & + \frac{1}{2}(1 - \delta_{mi}\delta_{nj})[I7]_{ij}^{mn} t_{mn}^{ab} + P(ab)(1 - \delta_{eb})[I8]_e^b t_{ij}^{ae} \\
 & + P(ij)P(ab)[I9]_{ej}^{mb} t_{im}^{ae} - P(ab)[I10]_{ij}^{mb} t_m^a + P(ij)[I11]_{ej}^{ab} t_i^e.
 \end{aligned} \tag{7.40}$$

By defining

$$d_{ij}^{ab} \equiv -\frac{1}{2}\langle ab|v|ab\rangle + P(ij)[I3]_j^j - \frac{1}{2}[I7]_{ij}^{ij} - P(ab)[I8]_b^b, \tag{7.41}$$

we obtain the following \widehat{T}_2 amplitude equation,

$$\begin{aligned}
 d_{ij}^{ab} t_{ij}^{ab} = & \langle ab|v|ij\rangle + \frac{1}{2}(1 - \delta_{ea}\delta_{fb})\langle ab|v|ef\rangle t_{ij}^{ef} - P(ij)(1 - \delta_{mj})[I3]_j^m t_{im}^{ab} \\
 & + \frac{1}{2}(1 - \delta_{mi}\delta_{nj})[I7]_{ij}^{mn} t_{mn}^{ab} + P(ab)(1 - \delta_{eb})[I8]_e^b t_{ij}^{ae} \\
 & + P(ij)P(ab)[I9]_{ej}^{mb} t_{im}^{ae} - P(ab)[I10]_{ij}^{mb} t_m^a + P(ij)[I11]_{ej}^{ab} t_i^e.
 \end{aligned} \tag{7.42}$$

This equation is implemented in `amp1::calc_t2()`, which is shown below. We will in the following also show the implementation of each term in Eq. (7.42).

```

void amp1::calc_t2(){
    ...
    // calculate intermediates I6, I7, I8, I9, I10 and I11
    calc_t2_intermediates();
    ...
    // <ab/v/ij>
    t2 = V->pphh;
    // 0.5(1 - \delta_{ea}\delta_{fb})<ab/v/ef>t_(ij)^^(ef)
    calc_t2_term2(temp);
    t2 = t2 + temp;
    // - P(ij)(1 - \delta_{mj})[I3]_j^m t_(im)^^(ab)
    calc_t2_term3(temp);
    t2 = t2 + temp;
    // 0.5(1 - \delta_{mi}\delta_{nj})[I7]_(ij)^^(mn)t_(mn)^^(ab)
    calc_t2_term4(temp);
    t2 = t2 + temp;
    // P(ab)(1 - \delta_{eb})[I8]_e^bt_(ij)^^(ae)
    calc_t2_term5(temp);
    t2 = t2 + temp;
    // P(ij)P(ab)[I9]_(ej)^^(mb)t_(im)^^(ae)
    calc_t2_term6(temp);
    t2 = t2 + temp;
    // -P(ab)[I10]_(ij)^^(mb)t_m^a
    calc_t2_term7(temp);
    t2 = t2 + temp;
    // P(ij)[I11]_(ej)^^(ab)t_i^e
    calc_t2_term8(temp);
    t2 = t2 + temp;
    // calculating denominator d_(ij)^^(ab)
    calc_t2_d(temp);

    // calculating final t2 amplitudes
    t2 = t2/temp;
    ...
} // end t2_calc

```

$$d_{ij}^{ab} \leftarrow \frac{1}{2}(1 - \delta_{ea}\delta_{fb})\langle ab|v|ef\rangle t_{ij}^{ef}$$

```

void amp1::calc_t2_term2(Array<double,4> ans){
    ...
    for(j=0; j<nh; j++){
        for(i=0; i<nh; i++){
            for(b=0; b<np; b++){
                for(a=0; a<np; a++){
                    temp = 0.0;
                    for(f=0; f<np; f++){
                        for(e=0; e<np; e++){
                            if(a!=e || b!=f){
                                temp = temp + V->pppp(a,b,e,f)*t2_old(e,f,i,j);
                            }
                        }
                    }
                    ans(a,b,i,j) = 0.5*temp;
                }
            }
        }
    }
} // end calc_t2_term2

```

$$d_{ij}^{ab} \leftarrow -P(ij)(1 - \delta_{mj}) [I3]_j^m t_{im}^{ab}$$

```

void amp1::calc_t2_term3(Array<double,4> ans){
    ...
    for(j=0; j<nh; j++){
        for(i=0; i<nh; i++){
            for(b=0; b<np; b++){
                for(a=0; a<np; a++){
                    temp = 0.0;
                    for(m=0; m<nh; m++){
                        temp1 = 0.0;
                        temp2 = 0.0;
                        if(j!=m){
                            temp1 = I3(m,j)*t2_old(a,b,i,m);
                        }
                        if(i!=m){
                            temp2 = I3(m,i)*t2_old(a,b,j,m);
                        }
                        temp = temp + (temp1 - temp2);
                    }
                    ans(a,b,i,j) = -temp;
                }
            }
        }
    }
} // end calc_t2_term3

```

$$d_{ij}^{ab} \leftarrow \frac{1}{2}(1 - \delta_{mi}\delta_{nj}) [I7]_{ij}^{mn} t_{mn}^{ab}$$

```

void amp1::calc_t2_term4(Array<double,4> ans){
    ...
    for(j=0; j<nh; j++){
        for(i=0; i<nh; i++){
            for(b=0; b<np; b++){
                for(a=0; a<np; a++){
                    temp = 0.0;
                    for(n=0; n<nh; n++){
                        for(m=0; m<nh; m++){

```

```

        if(i!=m || j!=n){
            temp = temp + I7(m,n,i,j)*t2_old(a,b,m,n);
        }
    }
}
ans(a,b,i,j) = 0.5*temp;
}
}
}

} // end calc_t2_term4

```

$$d_{ij}^{ab} \leftarrow P(ab)(1 - \delta_{eb}) [I8]_e^b t_{ij}^{ae}$$

```

void amp1::calc_t2_term5(Array<double,4> ans){
    ...
    for(j=0; j<nh; j++){
        for(i=0; i<nh; i++){
            for(b=0; b<np; b++){
                for(a=0; a<np; a++){
                    temp = 0.0;
                    for(e=0; e<np; e++){
                        temp1 = 0.0;
                        temp2 = 0.0;
                        if(b!=e){
                            temp1 = I8(b,e)*t2_old(a,e,i,j);
                        }
                        if(a!=e){
                            temp2 = I8(a,e)*t2_old(b,e,i,j);
                        }
                        temp = temp + (temp1 - temp2);
                    }
                    ans(a,b,i,j) = temp;
                }
            }
        }
    }
} // end calc_t2_term5

```

$$d_{ij}^{ab} \leftarrow P(ij)P(ab) [I9]_{ej}^{mb} t_{im}^{ae}$$

```

void amp1::calc_t2_term6(Array<double,4> ans){
    ...
    for(j=0; j<nh; j++){
        for(i=0; i<nh; i++){
            for(b=0; b<np; b++){
                for(a=0; a<np; a++){
                    temp = 0.0;
                    for(m=0; m<nh; m++){
                        for(e=0; e<np; e++){
                            temp = temp + ((I9(m,b,e,j)*t2_old(a,e,i,m) - I9(m,a,e,j)*t2_old(b,e,i,m)) -
                                (I9(m,b,e,i)*t2_old(a,e,j,m) - I9(m,a,e,i)*t2_old(b,e,j,m)));
                        }
                    }
                    ans(a,b,i,j) = temp;
                }
            }
        }
    }
} // end calc_t2_term6

```

$$d_{ij}^{ab} \leftarrow -P(ab) [I10]_{ij}^{mb} t_m^a$$

```
void amp1::calc_t2_term7(Array<double,4> ans){
    ...
    /*
     * t1 used instead if t1_old for a quicker convergence
     */
    for(j=0; j<nh; j++){
        for(i=0; i<nh; i++){
            for(b=0; b<np; b++){
                for(a=0; a<np; a++){
                    temp = 0.0;
                    for(m=0; m<nh; m++){
                        temp = temp + (I10(m,b,i,j)*t1(a,m) - I10(m,a,i,j)*t1(b,m));
                    }
                    ans(a,b,i,j) = -temp;
                }
            }
        }
    }
} // end calc_t2_term7
```

$$d_{ij}^{ab} \leftarrow P(ij) [I11]_{ej}^{ab} t_i^e$$

```
void amp1::calc_t2_term8(Array<double,4> ans){
    ...
    /*
     * t1 used instead if t1_old for a quicker convergence
     */
    for(j=0; j<nh; j++){
        for(i=0; i<nh; i++){
            for(b=0; b<np; b++){
                for(a=0; a<np; a++){
                    temp = 0.0;
                    for(e=0; e<np; e++){
                        temp = temp + (I11(a,b,e,j)*t1(e,i) - I11(a,b,e,i)*t1(e,j));
                    }
                    ans(a,b,i,j) = temp;
                }
            }
        }
    }
} // end calc_t2_term8
```

$$d_{ij}^{ab} \equiv P(ij) [I3]_j^j - P(ab) [I8]_b^b - \frac{1}{2} [I7]_{ij}^{ij} - \frac{1}{2} \langle ab|v|ab\rangle$$

```
void amp1::calc_t2_d(Array<double,4> ans){
    ...
    for(j=0; j<nh; j++){
        for(i=0; i<nh; i++){
            for(b=0; b<np; b++){
                for(a=0; a<np; a++){
                    ans(a,b,i,j) = I3(i,i) + I3(j,j) - I8(a,a) - I8(b,b) - 0.5*I7(i,j,i,j) -
                        0.5*V->pppp(a,b,a,b);
                }
            }
        }
    }
} // end calc_t2_d
```

We will in the following show the implementation of the intermediates.

$$[I1]_e^a = f_e^a + \langle ef|v|am\rangle t_m^f$$

```
void amp1::calc_I1(){
    ...
    I1 = F->f_pp;
    for(e=0; e<np; e++){
        for(a=0; a<np; a++){
            for(m=0; m<nh; m++){
                for(f=0; f<np; f++){
                    I1(a,e) = I1(a,e) + V->ppph(e,f,a,m)*t1(f,m);
                }
            }
        }
    }
} // end calc_I1
```

$$[I2]_e^m = f_e^m + \langle ef|v|mn\rangle t_n^f$$

```
void amp1::calc_I2(){
    ...
    I2 = F->f_hp;
    for(e=0; e<np; e++){
        for(m=0; m<nh; m++){
            for(n=0; n<nh; n++){
                for(f=0; f<np; f++){
                    I2(m,e) = I2(m,e) + V->pphh(e,f,m,n)*t1(f,n);
                }
            }
        }
    }
} // end calc_I2
```

$$[I3]_i^m = f_i^m - \langle ei|v|mn\rangle t_n^e + \frac{1}{2} \langle ef|v|mn\rangle t_{in}^{ef} + [I2]_e^m t_i^e$$

```
void amp1::calc_I3(){
    ...
    I3 = F->f_hh;
    for(i=0; i<nh; i++){
        for(m=0; m<nh; m++){
            for(n=0; n<nh; n++){
                for(e=0; e<np; e++){
                    I3(m,i) = I3(m,i) - V->phhh(e,i,m,n)*t1(e,n);
                }
            }
        }
        for(i=0; i<nh; i++){
            for(m=0; m<nh; m++){
                for(n=0; n<nh; n++){
                    for(f=0; f<np; f++){
                        for(e=0; e<np; e++){
                            I3(m,i) = I3(m,i) + 0.5*V->pphh(e,f,m,n)*t2(e,f,i,n);
                        }
                    }
                }
            }
        }
    }
}
```

```

        for(e=0; e<np; e++){
            I3(m,i) = I3(m,i) + I2(m,e)*t1(e,i);
        }
    }
}

} // end calc_I3
    
```

$$[I4]_{ie}^{mn} = [I5]_{ie}^{mn} + \frac{1}{2} \langle fe|v|mn\rangle t_i^f$$

```

void amp1::calc_I4(){
    ...
    I4 = I5;
    for(e=0; e<np; e++){
        for(i=0; i<nh; i++){
            for(n=0; n<nh; n++){
                for(m=0; m<nh; m++){
                    for(f=0; f<np; f++){
                        I4(m,n,i,e) = I4(m,n,i,e) + 0.5 * V->pphh(f,e,m,n)*t1(f,i);
                    }
                }
            }
        }
    }
}

} // end calc_I4
    
```

$$[I5]_{ie}^{mn} = -\langle ei|v|mn\rangle + \frac{1}{2} \langle fe|v|mn\rangle t_i^f$$

```

void amp1::calc_I5(){
    ...
    I5 = 0.0;
    for(e=0; e<np; e++){
        for(i=0; i<nh; i++){
            for(n=0; n<nh; n++){
                for(m=0; m<nh; m++){
                    I5(m,n,i,e) = -V->phhh(e, i, m, n);
                    for(f=0; f<np; f++){
                        I5(m,n,i,e) = I5(m,n,i,e) + 0.5 * V->pphh(f,e,m,n)*t1(f,i);
                    }
                }
            }
        }
    }
}

} // end calc_I5
    
```

$$[I6]_{ej}^{mb} = -\langle bm|v|ej\rangle + \frac{1}{2} \langle fe|v|bm\rangle t_j^f$$

```

void amp1::calc_I6(){
    ...
    I6 = 0.0;
    for(j=0; j<nh; j++){
        for(e=0; e<np; e++){
            for(m=0; m<nh; m++){
                for(b=0; b<np; b++){
                    I6(m,b,e,j) = -V->pphh(b,m,e,j);
                }
            }
        }
    }
}

} // end calc_I6
    
```

```

        for(b=0; b<np; b++){
            for(e=0; e<np; e++){
                for(j=0; j<nh; j++){
                    for(f=0; f<np; f++){
                        I6(m,b,e,j) = I6(m,b,e,j) + 0.5 * V->ppph(f,e,b,m)*t1(f,j);
                    }
                }
            }
        }
    } // end calc_I6
}

```

$$[I7]_{ij}^{mn} = \langle mn|v|ij\rangle + \frac{1}{2}\langle ef|v|mn\rangle t_{ij}^{ef} + P(ij) [I5]_{ie}^{mn} t_j^e$$

```

void amp1::calc_I7(){
    ...
    double temp = 0.0;
    I7 = V->hhhh;
    for(j=0; j<nh; j++){
        for(i=0; i<nh; i++){
            for(n=0; n<nh; n++){
                for(m=0; m<nh; m++){
                    temp = 0.0;
                    for(f=0; f<np; f++){
                        for(e=0; e<np; e++){
                            temp = temp + V->pphh(e,f,m,n)*t2(e,f,i,j);
                        }
                    }
                    I7(m,n,i,j) = I7(m,n,i,j) + 0.5*temp;
                }
            }
        }
    }
    for(j=0; j<nh; j++){
        for(i=0; i<nh; i++){
            for(n=0; n<nh; n++){
                for(m=0; m<nh; m++){
                    temp = 0.0;
                    for(e=0; e<np; e++){
                        temp = temp + (I5(m,n,i,e)*t1(e,j) - I5(m,n,j,e)*t1(e,i));
                    }
                    I7(m,n,i,j) = I7(m,n,i,j) + temp;
                }
            }
        }
    }
} // end calc_I7
}

```

$$[I8]_e^b = [I1]_e^b - \frac{1}{2}\langle mn|v|ef\rangle t_{mn}^{bf} - [I2]_e^m t_m^b$$

```

void amp1::calc_I8(){
    ...
    I8 = I1;
    for(e=0; e<np; e++){
        for(b=0; b<np; b++){
            for(m=0; m<nh; m++){
                for(n=0; n<nh; n++){
                    for(f=0; f<np; f++){
                        I8(b,e) = I8(b,e) - 0.5*V->pphh(e,f,m,n)*t2(b,f,m,n);
                    }
                }
            }
        }
    }
}

```

```

        }
    }

    for(e=0; e<np; e++){
        for(b=0; b<np; b++){
            for(m=0; m<nh; m++){
                I8(b,e) = I8(b,e) - I2(m,e) * t1(b,m);
            }
        }
    }
} // end calc_I8

```

$$[I9]_{ej}^{mb} = [I6]_{ej}^{mb} + \frac{1}{2} \langle fe|v|bm\rangle t_j^f - [I4]_{je}^{nm} t_n^b + \frac{1}{2} \langle fe|v|nm\rangle t_{jn}^{bf}$$

```

void amp1::calc_I9(){
    ...
    I9 = I6;
    for(m=0; m<nh; m++){
        for(b=0; b<np; b++){
            for(e=0; e<np; e++){
                for(j=0; j<nh; j++){
                    for(f=0; f<np; f++){
                        I9(m,b,e,j) = I9(m,b,e,j) + 0.5 * V->ppph(f,e,b,m)*t1(f,j);
                    }
                }
            }
        }
    }
    for(m=0; m<nh; m++){
        for(b=0; b<np; b++){
            for(e=0; e<np; e++){
                for(j=0; j<nh; j++){
                    for(n=0; n<nh; n++){
                        I9(m,b,e,j) = I9(m,b,e,j) - I4(n,m,j,e)*t1(b,n);
                    }
                }
            }
        }
    }
    for(m=0; m<nh; m++){
        for(b=0; b<np; b++){
            for(e=0; e<np; e++){
                for(j=0; j<nh; j++){
                    for(n=0; n<nh; n++){
                        for(f=0; f<np; f++){
                            I9(m,b,e,j) = I9(m,b,e,j) + 0.5*V->pphh(f,e,n,m)*t2(b,f,j,n);
                        }
                    }
                }
            }
        }
    }
} // end calc_I9

```

$$[I10]_{ij}^{mb} = -\langle bm|v|ij\rangle - \frac{1}{2} \langle ef|v|bm\rangle t_{ij}^{ef} + P(ij) [I6]_{ej}^{mb} t_i^e - \frac{1}{2} [I7]_{ij}^{mn} t_n^b$$

```

void amp1::calc_I10(){
    ...
    double temp = 0.0;
    I10 = 0.0;
    for(j=0; j<nh; j++){

```

```

    for(i=0; i<nh; i++){
        for(m=0; m<nh; m++){
            for(b=0; b<np; b++){
                I10(m,b,i,j) = -V->phhh(b,m,i,j);
            }
        }
    }

    for(j=0; j<nh; j++){
        for(i=0; i<nh; i++){
            for(b=0; b<np; b++){
                for(m=0; m<nh; m++){
                    temp = 0.0;
                    for(f=0; f<np; f++){
                        for(e=0; e<np; e++){
                            temp = temp - V->ppph(e,f,b,m)*t2(e,f,i,j);
                        }
                    }
                    I10(m,b,i,j) = I10(m,b,i,j) + 0.5*temp;
                }
            }
        }
    }

    for(j=0; j<nh; j++){
        for(i=0; i<nh; i++){
            for(b=0; b<np; b++){
                for(m=0; m<nh; m++){
                    temp = 0.0;
                    for(e=0; e<np; e++){
                        temp = temp + (I6(m,b,e,j)*t1(e,i) - I6(m,b,e,i)*t1(e,j));
                    }
                    I10(m,b,i,j) = I10(m,b,i,j) + temp;
                }
            }
        }
    }

    for(j=0; j<nh; j++){
        for(i=0; i<nh; i++){
            for(b=0; b<np; b++){
                for(m=0; m<nh; m++){
                    temp = 0.0;
                    for(n=0; n<nh; n++){
                        temp = temp + I7(m,n,i,j)*t1(b,n);
                    }
                    I10(m,b,i,j) = I10(m,b,i,j) - 0.5*temp;
                }
            }
        }
    }
}

// end calc_I10

```

$$[I11]_{ej}^{ab} = \langle ab|v|ej\rangle + \frac{1}{2}\langle ab|v|ef\rangle t_j^f.$$

```

void ampi::calc_I11(){
    ...
    double temp = 0.0;
    I11 = V->ppph;
    for(j=0; j<nh; j++){
        for(e=0; e<np; e++){
            for(b=0; b<np; b++){
                for(a=0; a<np; a++){
                    temp = 0.0;
                    for(f=0; f<np; f++){

```

```
    temp = temp + V->pppp(a,b,e,f)*t1(f,j);
}
I11(a,b,e,j) = I11(a,b,e,j) + 0.5*temp;
}
}
}

} // end calc_I11
```

Chapter 8

Numerical Results and Analysis

8.1 Standard interaction

In this section we present the Hartree-Fock (HF) and Coupled-Cluster Singles and Doubles (CCSD) results for a 2-dimensional parabolic quantum dot. The model Hamiltonian reads

$$\hat{H} = -\frac{\hbar^2}{2m^*} \sum_{i=1}^N \nabla_i^2 + \frac{1}{2} m^* \omega^2 \sum_{i=1}^N r_i^2 + \frac{e^2}{4\pi\epsilon_0\epsilon_r} \sum_{i=1 < j}^N \frac{1}{r_{ij}}. \quad (8.1)$$

See Sec. 4.4 for a discussion. In Sec. 4.5 we scaled the Hamiltonian into the following dimensionless form,

$$\hat{H}' = -\frac{\omega'}{2} \sum_{i=1}^N \nabla_i'^2 + \frac{1}{2} \omega' \sum_{i=1}^N r_i'^2 + \sqrt{\omega'} \sum_{i=1 < j}^N \frac{1}{r_{ij}'}, \quad (8.2)$$

where

$$\omega' = \frac{\hbar\kappa^2}{m^*} \omega \quad (8.3)$$

$$\kappa = \frac{4\pi\epsilon_0\epsilon_r\hbar}{e^2} \quad (8.4)$$

$$r_i' = l_0 r_i \quad (8.5)$$

$$r_{ij}' = l_0 r_{ij} \quad (8.6)$$

$$\nabla_i'^2 = \frac{1}{l_0^2} \nabla_i^2 \quad (8.7)$$

$$l_0 = \frac{\hbar\kappa}{m^*}. \quad (8.8)$$

We refer to Sec. 4.5 for a full derivation. Length is now measured in units of l_0 , ω' in units of ω_k and energy in units of effective Hartrees E_H^* , defined as

$$E_H^* \equiv \frac{m^*}{\kappa^2}. \quad (8.9)$$

We observe from Eq. (8.2) that the frequency constitutes an important parameter in the system. A change in the frequency will influence all parts that contribute to the total energy, and thus change the energy spectrum. Qualitatively, this is what we expect. For example, when ω increases, the harmonic oscillator potential pushes the electrons harder together. This would obviously affect the contributions from both the electron-electron repulsion, and the kinetic energy. From an experimental point of view, the frequency is a controllable quantity. It is therefore interesting to analyze numerical calculations for different frequencies in order to gain

important information of the system, such as correlation energies. In addition, the reliability of numerical methods can be studied by such an analysis.

All numerical calculations have been done with the dimensionless Hamiltonian in Eq. (8.2), and the results are presented in this scaling. Therefore, we will from now on drop the ' \prime -subscript. In this section we present the HF and CCSD results obtained with standard interaction, i.e. Coulomb interaction. Both HF and CCSD require a single-particle basis set, and we have in these calculations chosen the eigenfunctions of

$$\left(-\frac{\omega}{2} \sum_{i=1}^N \nabla_i^2 + \frac{1}{2} \omega \sum_{i=1}^N r_i^2 \right) \psi_\alpha(\mathbf{r}) = \varepsilon_\alpha \psi_\alpha(\mathbf{r}) \quad (8.10)$$

as basis functions, where α denote a set of three quantum numbers (n, m, m_s) . We identify this equation as the time-independent Schrödinger equation for the single-electron parabolic quantum (see Sec. 4.3), in our dimensionless scaling. Multiplying the Hamiltonian in Eq. (8.10) by E_H^* yields back the expression in Eq. (4.28). Furthermore, the total wavefunction $\psi_\alpha(\mathbf{r})$ is given as (see Sec. 2.2.3)

$$\psi_\alpha(\mathbf{r}) = \phi_{nm}(x, y) \otimes |\chi_{m_s}\rangle, \quad (8.11)$$

where $\phi_{nm}(x, y)$ is the spatial part, and $|\chi_{m_s}\rangle$ is the spin part. The quantum number m_s is associated with the z-projection of the spin, and is given as

$$m_s = \pm \frac{1}{2}, \quad (8.12)$$

with corresponding eigenvectors

$$\begin{vmatrix} 1 \\ 2 \end{vmatrix} \equiv |+\rangle \quad (8.13)$$

$$\begin{vmatrix} -1 \\ 2 \end{vmatrix} \equiv |-\rangle, \quad (8.14)$$

which is often referred to as spin up and spin down, respectively. See Sec. (2.2.2). The spatial part of the wavefunction satisfy

$$\left(-\frac{\omega}{2} \sum_{i=1}^N \nabla_i^2 + \frac{1}{2} \omega \sum_{i=1}^N r_i^2 \right) \phi_{nm}(x, y) = \varepsilon_{nm} \phi_{nm}(x, y), \quad (8.15)$$

where n and m are quantum numbers, and ε_{nm} is the energy eigenvalue. Since the Hamiltonian in Eq. (8.15) is “linear” in ω , the eigenfunctions do not depend on the frequency. However, the energy eigenvalue ε_{nm} depends on ω , and is given as (see Eq. 4.66)

$$\varepsilon_{nm} = (1 + 2n + |m|)\omega. \quad (8.16)$$

The eigenfunctions of Eq. (8.15) is given in Eq. (4.58) with $m^* = \hbar = 1$. We will refer to the total wavefunctions in Eq. (8.11) as harmonic oscillator functions. We will in the following use the bra-ket notation $|\alpha\rangle$ referring to the harmonic oscillator function in Eq. (8.11).

Since \hat{h} is the single-electron Hamiltonian in Eq. (8.15), our choice of basis leads to a diagonal single-particle matrix,

$$\langle \alpha | h | \beta \rangle = \delta_{\alpha\beta} \varepsilon_\alpha, \quad (8.17)$$

where $\alpha = (n, m, m_s)$ and $\varepsilon_\alpha = \varepsilon_{nm}$. As pointed out in the previous chapter, both programs read $\langle \alpha | h | \beta \rangle$ and $\langle \alpha \beta | v | \gamma \delta \rangle$ from file. The required file structure is shown in Secs. (7.1) and (7.2). We established the mapping $\alpha \rightarrow (n, m, m_s)$ shown in Table 8.1. Table 8.2 shows the shell

α	n	m	s																				
0	0	0	-1	20	0	-4	-1	40	2	1	-1	60	1	-5	-1	80	2	-4	-1	100	2	5	-1
1	0	0	1	21	0	-4	1	41	2	1	1	61	1	-5	1	81	2	-4	1	101	2	5	1
2	0	-1	-1	22	0	4	-1	42	0	-6	-1	62	1	5	-1	82	2	4	-1	102	3	-3	-1
3	0	-1	1	23	0	4	1	43	0	-6	1	63	1	5	1	83	2	4	1	103	3	-3	1
4	0	1	-1	24	1	-2	-1	44	0	6	-1	64	2	-3	-1	84	3	-2	-1	104	3	3	-1
5	0	1	1	25	1	-2	1	45	0	6	1	65	2	-3	1	85	3	-2	1	105	3	3	1
6	0	-2	-1	26	1	2	-1	46	1	-4	-1	66	2	3	-1	86	3	2	-1	106	4	-1	-1
7	0	-2	1	27	1	2	1	47	1	-4	1	67	2	3	1	87	3	2	1	107	4	-1	1
8	0	2	-1	28	2	0	-1	48	1	4	-1	68	3	-1	-1	88	4	0	-1	108	4	1	-1
9	0	2	1	29	2	0	1	49	1	4	1	69	3	-1	1	89	4	0	1	109	4	1	1
10	1	0	-1	30	0	-5	-1	50	2	-2	-1	70	3	1	-1	90	0	-9	-1				
11	1	0	1	31	0	-5	1	51	2	-2	1	71	3	1	1	91	0	-9	1				
12	0	-3	-1	32	0	5	-1	52	2	2	-1	72	0	-8	-1	92	0	9	-1				
13	0	-3	1	33	0	5	1	53	2	2	1	73	0	-8	1	93	0	9	1				
14	0	3	-1	34	1	-3	-1	54	3	0	-1	74	0	8	-1	94	1	-7	-1				
15	0	3	1	35	1	-3	1	55	3	0	1	75	0	8	1	95	1	-7	1				
16	1	-1	-1	36	1	3	-1	56	0	-7	-1	76	1	-6	-1	96	1	7	-1				
17	1	-1	1	37	1	3	1	57	0	-7	1	77	1	-6	1	97	1	7	1				
18	1	1	-1	38	2	-1	-1	58	0	7	-1	78	1	6	-1	98	2	-5	-1				
19	1	1	1	39	2	-1	1	59	0	7	1	79	1	6	1	99	2	-5	1				

Table 8.1: Mapping scheme for harmonic oscillator functions. The functions are given by three quantum numbers: n , m and m_s . The first two quantum numbers, n and m , emerge when solving Eq. (8.15). See Sec. 4.3. The allowed values are $n = 0, 2, 3, \dots$ and $m = 0, \pm 1, \pm 2, \pm 3, \dots$ The third quantum number, m_s , is associated with the z-projection of the spin, with allowed values $m_s = \pm 1/2$ (spin up/down). We have in our implementation chosen to represent $m_s = 1/2$ with 1, and $m_s = -1/2$ with -1.

R	$ \alpha\rangle$
1	0-1
2	2-5
3	6-11
4	12-19
5	20-29
6	30-41
7	42-55
8	56-71
9	72-89
10	90-109

Table 8.2: Shell structure of the parabolic quantum dot in 2 dimensions. The shell number is denoted by R , and the harmonic oscillator functions are denoted by $|\alpha\rangle$. The mapping scheme $\alpha \rightarrow (n, m, s)$ is given in Table 8.1.

structure in the α -labeling of harmonic oscillator functions. Furthermore, in order to calculate the antisymmetrized interaction elements

$$\langle \alpha\beta|v|\gamma\delta \rangle, \quad (8.18)$$

where v is the Coulomb interaction (standard interaction), we have used the analytical expressions derived in [44]. Some of the elements are tabulated in Table 8.4.

8.1.1 Tables of Numerical Results

The HF and CCSD results are tabulated in Tables 8.5-8.9. We have done calculations for 2, 6, 12 and 20 electrons, and oscillator frequencies ranging from 0.2 up to 50. In the 2-electron case, the CCSD energy converges for all values of ω . However, for systems containing 6, 12 and 20 electrons, the energy does not converge for $\omega = 0.2$, $\omega = 0.2 - 0.8$, and $\omega = 0.2 - 1.0$, respectively. In Tables 8.5-8.8 we present our HF and CCSD results for different size of the model space, denoted by R^b . This quantity is the number of shells included in the basis. Since we are

α	ϵ_α										
0	1	20	5	40	6	60	8	80	9	100	10
1	1	21	5	41	6	61	8	81	9	101	10
2	2	22	5	42	7	62	8	82	9	102	10
3	2	23	5	43	7	63	8	83	9	103	10
4	2	24	5	44	7	64	8	84	9	104	10
5	2	25	5	45	7	65	8	85	9	105	10
6	3	26	5	46	7	66	8	86	9	106	10
7	3	27	5	47	7	67	8	87	9	107	10
8	3	28	5	48	7	68	8	88	9	108	10
9	3	29	5	49	7	69	8	89	9	109	10
10	3	30	6	50	7	70	8	90	10		
11	3	31	6	51	7	71	8	91	10		
12	4	32	6	52	7	72	9	92	10		
13	4	33	6	53	7	73	9	93	10		
14	4	34	6	54	7	74	9	94	10		
15	4	35	6	55	7	75	9	95	10		
16	4	36	6	56	8	76	9	96	10		
17	4	37	6	57	8	77	9	97	10		
18	4	38	6	58	8	78	9	98	10		
19	4	39	6	59	8	79	9	99	10		

Table 8.3: Single-particle energies $\epsilon_\alpha/\omega = \epsilon_{nm}/\omega = (1 + |m| + 2n)$. The harmonic oscillator functions are defined by α . The mapping between α and (n, m, s) is given in Table 8.1.

dealing with closed-shell systems, the basis will only contain functions belonging to filled shells. Thus according to Table 8.2, the single-particle basis is given as

$$\mathcal{B} = \{|\alpha\rangle\}_{\alpha=0}^{\alpha_{max}}, \quad (8.19)$$

where α_{max} is equal to 1, 5, 11, 19, 29, 41, 55, 71, 89 or 109. The size of the basis can therefore be characterized by the number of shells in the basis, R^b . For example, when $R^b = 4$, the single-particle basis is given by Eq. (8.19) with $\alpha_{max} = 19$. We have in the Table 8.5-8.8 presented the numerical results from $R^b = R^f$ up to $R^b = 10$, where R^f is the Fermi-shell of the systems.

α	β	γ	δ	$\langle \alpha\beta v \gamma\delta \rangle$
0	1	0	1	1.2533141373154997
0	1	0	11	-0.3133285343288749
0	1	1	0	-1.2533141373154997
0	1	2	5	0.3133285343288749
0	1	3	4	-0.3133285343288749
0	5	4	1	0.3133285343288750
0	5	5	0	-0.9399856029866251
0	6	0	6	0.6266570686577521
0	6	6	0	-0.6266570686577521
0	7	0	7	0.7441552690310801
0	7	1	6	-0.1174982003733280
0	7	2	3	0.2769459142039872
0	7	3	2	-0.2769459142039872
0	7	6	1	0.1174982003733280
0	11	0	11	0.8616534694044069
0	11	1	0	0.3133285343288749
0	11	5	2	-0.0783321335822187
0	11	10	1	0.2349964007466563
0	11	11	0	-0.8616534694044069
1	0	0	1	-1.2533141373154997
2	3	3	2	-0.8616534694044082
2	3	6	1	0.2769459142039873
2	5	0	1	0.3133285343288749
2	5	0	11	0.0783321335822187
2	5	1	0	-0.3133285343288749
2	5	1	10	-0.0783321335822187
2	5	2	5	0.8616534694044069
2	5	3	4	-0.2349964007466563
2	5	4	3	0.2349964007466563
2	5	5	2	-0.8616534694044069
2	5	10	1	0.0783321335822187
3	4	0	1	-0.3133285343288749
3	4	2	5	-0.2349964007466563
3	4	3	4	0.8616534694044069
5	2	4	3	-0.2349964007466563
5	2	5	2	0.8616534694044069
5	2	10	1	-0.0783321335822187
5	2	11	0	0.0783321335822187
5	3	3	5	-0.6266570686577506
5	3	5	3	0.6266570686577506

Table 8.4: Interaction elements $\langle \alpha\beta|v|\gamma\delta \rangle$, where α, β, γ and δ are harmonic oscillator functions, and v is the Coulomb interaction.

ω	R^b	$N = 2$				$N = 6$			
		Standard interaction		Effective interaction		Standard interaction		Effective interaction	
		HF	CCSD	HF	CCSD	HF	CCSD	HF	CCSD
0.2	1	0.960499	0.960499	0.773971	0.773971	-	x	x	x
	2	0.960499	0.867622	0.773971	0.773971	7.464866	7.464866	4.639008	4.639008
	3	0.882576	0.780532	0.815443	0.773971	6.957617	x	x	6.377223
	4	0.882576	0.778312	0.815443	0.773971	6.431804	x	x	x
	5	0.882333	0.777003	0.837032	0.773971	6.382348	x	x	x
	6	0.882333	0.776314	0.837032	0.773971	6.299371	x	x	x
	7	0.882297	0.775861	0.847805	0.773971	6.296476	x	x	x
	8	0.882297	0.775550	0.847805	0.773971	6.293557	x	6.104401	x
	9	0.882293	0.775323	0.854431	0.773971	6.293557	x	6.138031	x
	10	0.882293	0.775150	0.854431	0.773971	6.293542	x	6.155791	x
0.4	1	1.592665	1.592665	1.375594	1.375594	-	-	-	-
	2	1.592665	1.494392	1.375594	1.375594	11.728488	11.728488	7.931966	7.931966
	3	1.508042	1.392856	1.427126	1.375594	11.156151	11.005419	x	x
	4	1.508042	1.386722	1.427126	1.375594	10.504554	10.208494	x	x
	5	1.508024	1.383259	1.453967	1.375594	10.467626	10.064250	x	x
	6	1.508024	1.381489	1.453967	1.375594	10.405715	9.987983	10.045408	9.890108
	7	1.508015	1.380338	1.467257	1.375594	10.405292	9.977274	10.173956	9.944735
	8	1.508015	1.379554	1.467257	1.375594	10.405222	9.970650	10.196753	9.942164
	9	1.508011	1.378983	1.475288	1.375594	10.405195	9.966218	10.227403	9.939521
	10	1.508011	1.378551	1.475288	1.375594	10.405166	9.963027	10.245645	9.940905
0.6	1	2.170813	2.170813	1.936931	1.936931	-	-	-	-
	2	2.170813	2.070856	1.936931	1.936931	15.465426	15.465426	10.946441	10.946441
	3	2.083158	1.962891	1.994233	1.936931	14.864332	14.703670	x	x
	4	2.083158	1.953712	1.994233	1.936931	14.135156	13.814684	x	x
	5	2.082926	1.948533	2.024000	1.936931	14.106585	13.690123	x	13.432229
	6	2.082926	1.945869	2.024000	1.936931	14.059885	13.621142	13.683596	13.505043
	7	2.082926	1.944135	2.038722	1.936931	14.059867	13.604622	13.811551	13.556509
	8	2.082926	1.942953	2.038722	1.936931	14.059716	13.594539	13.836037	13.552735
	9	2.082924	1.942090	2.047546	1.936931	14.059698	13.587834	13.868257	13.549756
	10	2.082924	1.941436	2.047546	1.936931	14.059697	13.583037	13.887058	13.550906
0.8	1	2.720998	2.720998	2.475905	2.475905	-	-	-	-
	2	2.720998	2.620341	2.475905	2.475905	18.929733	18.929733	13.811468	13.811468
	3	2.631563	2.508827	2.537139	2.475905	18.312821	18.144988	x	x
	4	2.631563	2.497304	2.537139	2.475905	17.528556	17.193050	x	x
	5	2.631058	2.490771	2.568856	2.475905	17.505795	17.081893	16.933000	16.809860
	6	2.631058	2.487386	2.568856	2.475905	17.469841	17.018754	17.075290	16.880900
	7	2.631055	2.485175	2.584547	2.475905	17.469813	16.997854	17.207361	16.935520
	8	2.631055	2.483665	2.584547	2.475905	17.469269	16.985003	17.233916	16.931715
	9	2.631054	2.482560	2.593908	2.475905	17.469263	16.976408	17.268048	16.929259
	10	2.631054	2.481724	2.593908	2.475905	17.469257	16.970279	17.287339	16.930135
1.0	1	3.253314	3.253314	3.000000	3.000000	-	-	-	-
	2	3.253314	3.152329	3.000000	3.000000	22.219813	22.219813	16.578993	16.578993
	3	3.162691	3.038605	3.064154	3.000000	21.593198	21.419889	x	x
	4	3.162691	3.025232	3.064154	3.000000	20.766919	20.421325	x	x
	5	3.161921	3.017607	3.097299	3.000000	20.748402	20.319716	20.166941	20.033306
	6	3.161921	3.013627	3.097299	3.000000	20.720257	20.260893	20.310117	20.104242
	7	3.161909	3.011021	3.113707	3.000000	20.720132	20.236760	20.446045	20.162126
	8	3.161909	3.009237	3.113707	3.000000	20.719248	20.221750	20.474497	20.158637
	9	3.161909	3.007931	3.123465	3.000000	20.719248	20.211590	20.510432	20.156905
	10	3.161909	3.006938	3.123465	3.000000	20.719217	20.204345	20.530161	20.157541
2.0	1	5.772454	5.772454	5.496523	5.496523	-	-	-	-
	2	5.772454	5.671234	5.496523	5.496523	37.281425	37.281425	29.621623	29.621623
	3	5.679048	5.553152	5.568856	5.496523	36.637217	36.448558	x	x
	4	5.679048	5.534274	5.568856	5.496523	35.689555	35.322283	34.940481	34.895937
	5	5.677282	5.523274	5.605893	5.496523	35.681728	35.242971	35.067346	34.904897
	6	5.677282	5.517386	5.605893	5.496523	35.672333	35.193258	35.213499	34.977420
	7	5.677206	5.513491	5.624295	5.496523	35.671851	35.161115	35.360563	35.044569
	8	5.677206	5.510801	5.624295	5.496523	35.670358	35.140124	35.395567	35.043402
	9	5.677204	5.508822	5.635166	5.496523	35.670333	35.125055	35.438093	35.045024
	10	5.677204	5.507311	5.635166	5.496523	35.670144	35.114198	35.459520	35.045026

Table 8.5: Hartree-Fock and Coupled-Cluster Singles and Doubles results for a parabolic quantum dot with 2 and 6 electrons. All calculations are done with harmonic oscillator functions as basis functions. The size of the model space is given by the shell number R^b . For each oscillator frequency ω and R^b , calculated ground state energies are tabulated. Energy is measured in effective Hartrees E_H^* .

ω	R^b	$N = 2$				$N = 6$			
		Standard interaction		Effective interaction		Standard interaction		Effective interaction	
		HF	CCSD	HF	CCSD	HF	CCSD	HF	CCSD
3.0	1	8.170804	8.170804	7.883753	7.883753	-	-	-	-
	2	8.170804	8.069761	7.883753	7.883753	51.165337	51.165337	41.976374	41.976374
	3	8.076274	7.950410	7.960167	7.883753	50.517683	50.321752	x	x
	4	8.076274	7.928709	7.960167	7.883753	49.508478	49.135135	48.911412	48.888397
	5	8.073884	7.915891	7.999091	7.883753	49.504750	49.062885	48.870529	48.694263
	6	8.073884	7.908930	7.999091	7.883753	49.501573	49.014446	49.017179	48.767717
	7	8.073751	7.904296	8.018485	7.883753	49.501011	48.979127	49.168672	48.837661
	8	8.073751	7.901081	8.018485	7.883753	49.499580	48.955363	49.207459	48.838404
	9	8.073744	7.898706	8.029916	7.883753	49.499520	48.937698	49.254040	48.842291
	10	8.073744	7.896889	8.029916	7.883753	49.499237	48.924839	49.276642	48.842136
4.0	1	10.506628	10.506628	10.212604	10.212604	-	-	-	-
	2	10.506628	10.405775	10.212604	10.212604	64.439626	64.439626	53.969200	53.969200
	3	10.411470	10.285895	10.291594	10.212604	63.791597	63.591329	x	x
	4	10.411470	10.262419	10.291594	10.212604	62.743808	62.368661	62.222799	62.207046
	5	10.408646	10.248423	10.331687	10.212604	62.742006	62.298906	62.094434	61.909899
	6	10.408646	10.240751	10.331687	10.212604	62.741163	62.249606	62.240659	61.983603
	7	10.408469	10.235621	10.351708	10.212604	62.740611	62.212557	62.394121	62.054033
	8	10.408469	10.232050	10.351708	10.212604	62.739357	62.187127	62.435414	62.056216
	9	10.408456	10.229405	10.363494	10.212604	62.739276	62.167826	62.484777	62.061658
	10	10.408456	10.227378	10.363494	10.212604	62.738940	62.153663	62.508252	62.061505
5.0	1	12.802496	12.802496	12.503561	12.503561	-	-	-	-
	2	12.802496	12.701808	12.503561	12.503561	77.324332	77.324332	65.728844	65.728844
	3	12.706930	12.581669	12.584369	12.503561	76.676854	76.473661	x	x
	4	12.706930	12.556949	12.584369	12.503561	75.602124	75.226743	75.125654	75.113312
	5	12.703782	12.542112	12.625280	12.503561	75.601300	75.157693	74.943996	74.753920
	6	12.703782	12.533923	12.625280	12.503561	75.601221	75.106872	75.089461	74.827516
	7	12.703567	12.528429	12.645744	12.503561	75.600706	75.068703	75.243799	74.979503
	8	12.703567	12.524595	12.645744	12.503561	75.599630	75.042121	75.286899	74.900811
	9	12.703550	12.521751	12.657783	12.503561	75.599534	75.021677	75.338318	74.907377
	10	12.703550	12.519568	12.657783	12.503561	75.599173	75.006580	75.362476	74.907284
10.0	1	23.963327	23.963327	23.651663	23.651663	-	-	-	-
	2	23.963327	23.863173	23.651663	23.651663	138.642441	138.642441	122.653567	122.653567
	3	23.866830	23.742766	23.737201	23.651663	137.999396	137.789201	136.821655	136.817756
	4	23.866830	23.714877	23.737201	23.651663	136.856842	136.485196	136.468182	136.461845
	5	23.862773	23.697829	23.780202	23.651663	136.856753	136.413343	136.173391	135.970427
	6	23.862773	23.688243	23.780202	23.651663	136.854607	136.354504	136.314578	136.042076
	7	23.862443	23.681757	23.801822	23.651663	136.854284	136.313637	136.468590	136.107197
	8	23.862443	23.677199	23.801822	23.651663	136.853782	136.284071	136.516429	136.113676
	9	23.862411	23.673802	23.814526	23.651663	136.853661	136.260729	136.573456	136.123096
	10	23.862411	23.671183	23.814526	23.651663	136.853287	136.243183	136.599654	136.123432
20.0	1	45.604991	45.604991	45.283850	45.283850	-	-	-	-
	2	45.604991	45.505319	45.283850	45.283850	254.648664	254.648664	232.473626	232.473626
	3	45.507912	45.385045	45.372916	45.283850	254.011527	253.796720	252.813945	252.812952
	4	45.507912	45.354878	45.372916	45.283850	252.821683	252.457058	252.479052	252.475760
	5	45.503120	45.336174	45.417442	45.283850	252.820088	252.378355	252.117095	251.906240
	6	45.503120	45.325508	45.417442	45.283850	252.811954	252.309241	252.252367	251.974297
	7	45.502684	45.318241	45.439931	45.283850	252.811811	252.266330	252.402979	252.031493
	8	45.502684	45.313105	45.439931	45.283850	252.811687	252.234390	252.454257	252.040496
	9	45.502636	45.309263	45.453140	45.283850	252.811568	252.208972	252.515579	252.051740
	10	45.502636	45.306293	45.453140	45.283850	252.811247	252.189591	252.543550	252.052681
50.0	1	108.862269	108.862269	108.532386	108.532386	-	-	-	-
	2	108.862269	108.763094	108.532386	108.532386	586.407125	586.407125	551.989727	551.989727
	3	108.764735	108.643160	108.624706	108.532386	585.777168	585.558594	584.550992	584.550743
	4	108.764735	108.610971	108.624706	108.532386	584.547339	584.192313	584.236057	584.234700
	5	108.759222	108.590750	108.670612	108.532386	584.542520	584.103507	583.821763	583.605066
	6	108.759222	108.579064	108.670612	108.532386	584.524974	584.021400	583.949063	583.667717
	7	108.758672	108.571049	108.693908	108.532386	584.524954	583.976331	584.093494	583.713833
	8	108.758672	108.565356	108.693908	108.532386	584.524950	583.941913	584.147709	583.725123
	9	108.758604	108.561080	108.707593	108.532386	584.524852	583.914635	584.212909	583.737561
	10	108.758604	108.557765	108.707593	108.532386	584.524623	583.893560	584.242692	583.739292

Table 8.6: Hartree-Fock and Coupled-Cluster Singles and Doubles results for a parabolic quantum dot with 2 and 6 electrons. All calculations are done with harmonic oscillator functions as basis functions. The size of the model space is given by the shell number R^b . For each oscillator frequency ω and R^b , calculated ground state energies are tabulated. Energy is measured in effective Hartrees E_H^* .

ω	R^b	$N = 12$				$N = 20$			
		Standard interaction		Effective interaction		Standard interaction		Effective interaction	
		HF	CCSD	HF	CCSD	HF	CCSD	HF	CCSD
1.0	1	-	-	-	-	-	-	-	-
	2	-	-	-	-	-	-	-	-
	3	73.765549	73.765549	46.502552	46.502552	-	-	-	-
	4	70.673849	70.297531	42.000000	61.027715	-	-	-	-
	5	67.569930	66.989912	x	71.238897	-	-	-	-
	6	67.296869	66.452006	x	x	-	-	-	-
	7	66.934745	65.971686	x	x	-	-	-	-
	8	66.923094	65.889324	x	x	-	-	-	-
	9	66.912244	65.838932	66.175736	65.618539	-	-	-	-
	10	66.912035	65.806539	66.258111	65.634530	-	-	-	-
2.0	1	-	-	-	-	-	-	-	-
	2	-	-	-	-	-	-	-	-
	3	120.722260	120.722260	82.919042	82.919042	-	-	-	-
	4	117.339642	116.978642	x	103.906310	286.825295	286.825295	181.235783	181.235783
	5	113.660396	113.020282	x	x	276.898196	275.845577	x	220.636627
	6	113.484866	112.613571	x	x	267.269712	266.325997	x	259.240388
	7	113.247601	112.264166	111.434211	111.152591	266.213200	264.830000	x	286.808535
	8	113.246579	112.189996	112.058791	111.603983	264.933622	263.325189	x	
	9	113.246303	112.135551	112.495988	111.872020	264.874009	263.089951	x	
	10	113.245854	112.094025	112.562079	111.861880	264.809954	262.928937		260.714154
3.0	1	-	-	-	-	-	-	-	-
	2	-	-	-	-	-	-	-	-
	3	163.268256	163.268256	117.419306	117.419306	-	-	-	-
	4	159.769062	159.414625	x	143.421667	384.318425	384.318425	255.851700	255.851700
	5	155.762811	155.097118	x	x	373.776094	373.229501	255.473175	
	6	155.639179	154.762454	151.298879	x	363.162287	362.175933	x	
	7	155.475049	154.487959	153.647870	153.334781	362.323215	360.924104	x	
	8	155.475049	154.408521	154.257210	153.773520	361.277490	359.652011	x	
	9	155.474144	154.348106	154.686893	154.032341	361.254334	359.469820	x	
	10	155.473848	154.302641	154.759873	154.025320	361.233837	359.337510		358.202983
4.0	1	-	-	-	-	-	-	-	-
	2	-	-	-	-	-	-	-	-
	3	203.531098	203.531098	150.915215	150.915215	-	-	-	-
	4	199.971455	199.619694	x	x	475.926595	475.926595	328.200763	328.200763
	5	195.745462	195.066235	x	x	465.021258	464.483436	x	
	6	195.653702	194.776202	191.896341	x	453.717528	452.706359	x	
	7	195.535485	194.547735	193.671035	193.343218	453.029759	451.624943	x	
	8	195.535177	194.463255	194.278540	193.778488	452.163171	450.533964	x	
	9	195.532936	194.398503	194.713851	194.042575	452.154007	450.370119	447.620204	
	10	195.532772	194.350424	194.794571	194.040504	452.148052	450.245879	447.620204	
5.0	1	-	-	-	-	-	-	-	-
	2	-	-	-	-	-	-	-	-
	3	242.334879	242.334879	183.765318	183.765318	-	-	-	-
	4	238.739591	238.388819	x	x	563.773952	563.773952	399.094328	399.094328
	5	234.352741	233.665684	x	x	552.630093	552.098704	x	463.433094
	6	234.282331	233.405545	230.999630	230.911117	540.804720	539.777215	x	526.882127
	7	234.194820	233.207198	232.298553	231.961480	540.227793	538.821500	x	
	8	234.194059	233.118844	232.903979	232.393330	539.499326	537.871223	527.599736	x
	9	234.190797	233.051061	233.345264	232.663493	539.495941	537.713326	535.233890	534.738382
	10	234.190714	233.000991	233.432765	232.666033	539.494612	537.589832	536.834713	536.015305

Table 8.7: Hartree-Fock and Coupled-Cluster Singles and Doubles results for a parabolic quantum dot with 12 and 20 electrons. All calculations are done with harmonic oscillator functions as basis functions. The size of the model space is given by the shell number R^b . For each oscillator frequency ω and R^b , calculated ground state energies are tabulated. Energy is measured in effective Hartrees E_H^* .

ω	R^b	$N = 12$				$N = 20$			
		Standard interaction		Effective interaction		Standard interaction		Effective interaction	
		HF	CCSD	HF	CCSD	HF	CCSD	HF	CCSD
10.0	1	-	-	-	-	-	-	-	-
	2	-	-	-	-	-	-	-	-
	3	424.723373	424.723373	342.837272	342.837272	-	-	-	-
	4	421.066552	420.714412	387.852166	x	973.032700	973.032700	741.907454	741.907454
	5	416.245656	415.548025	x	x	961.371081	960.853435	x	x
	6	416.221892	415.352162	414.259253	414.204471	948.057077	946.995097	x	x
	7	416.198611	415.213229	414.221231	413.862491	947.765474	946.367418	x	x
	8	416.196677	415.115445	414.807209	414.274282	947.410305	945.798531	938.828011	938.708830
	9	416.191836	415.040983	415.261980	414.558155	947.409440	945.634643	943.208098	942.653517
	10	416.191833	414.985087	415.371069	414.576142	947.404930	945.499122	944.709187	943.856608
20.0	1	-	-	-	-	-	-	-	-
	2	-	-	-	-	-	-	-	-
	3	764.669757	764.669757	649.864219	649.864219	-	-	-	-
	4	760.999568	760.642727	717.086454	717.085698	1727.547904	1727.547904	1402.547504	1402.547504
	5	755.851177	755.158770	757.317038	757.286320	1715.636447	1715.121677	1528.572359	1528.568611
	6	755.847874	754.988910	754.752961	754.727375	1701.112340	1700.040683	1636.066502	1636.248392
	7	755.846430	754.864771	753.834848	753.463003	1701.000555	1699.622516	1695.229330	1695.426720
	8	755.844396	754.761753	754.381289	753.839129	1700.881357	1699.291198	1695.620663	1695.516615
	9	755.840282	754.683971	754.833236	754.118115	1700.876899	1699.113200	1696.546369	1695.980919
	10	755.840196	754.623201	754.960572	754.149732	1700.866177	1698.965611	1698.009292	1697.143442
50.0	1	-	-	-	-	-	-	-	-
	2	-	-	-	-	-	-	-	-
	3	1723.611301	1723.611301	1543.553745	1543.553745	-	-	-	-
	4	1719.954910	1719.591333	1651.443071	1651.443062	3834.126475	3834.126475	3322.973815	3322.973815
	5	1714.516506	1713.842082	1717.046895	1717.041097	3822.122324	3821.601747	3524.659120	3524.659055
	6	1714.514709	1713.670423	1714.072815	1714.062550	3806.466383	3805.411147	3709.512572	3709.510304
	7	1714.502278	1713.526638	1712.503731	1712.124312	3806.454602	3805.108329	3810.774973	3810.736980
	8	1714.500976	1713.420167	1712.983144	1712.440387	3806.448065	3804.882880	3804.309792	3804.269253
	9	1714.498844	1713.340085	1713.411514	1712.690503	3806.442304	3804.694261	3802.079664	3801.509670
	10	1714.498639	1713.274652	1713.555168	1712.734499	3806.431632	3804.541353	3803.408939	3802.545757

Table 8.8: Hartree-Fock and Coupled-Cluster Singles and Doubles results for a parabolic quantum dot with 12 and 20 electrons. All calculations are done with harmonic oscillator functions as basis functions. The size of the model space is given by the shell number R^b . For each oscillator frequency ω and R^b , calculated ground state energies are tabulated. Energy is measured in effective Hartrees E_H^* .

N	ω	$\langle \Phi_0 \hat{H}_0 \Phi_0 \rangle$	E_{HF}	E_{CCSD}	$E_{CCSD}-E_{HF}$	$\langle \Phi_0 \hat{H} \Phi_0 \rangle$	$\langle \Phi_0 \hat{H}_N \hat{T}_1 \Phi_0 \rangle$	$\langle \Phi_0 \hat{H}_N \hat{T}_1^2 \Phi_0 \rangle$	$\langle \Phi_0 \hat{H}_N \hat{T}_2 \Phi_0 \rangle$	$\langle \Phi_0 \hat{H}_N (\hat{T}_1 + \hat{T}_1^2 + \hat{T}_2) \Phi_0 \rangle$
2	0.2	0.4	0.882293	0.775150	-0.107143	0.960499	-0.079758	0.008869	-0.114460	-0.185349
	0.4	0.8	1.508011	1.378551	-0.129460	1.592665	-0.086879	0.007582	-0.134818	-0.214114
	0.6	1.2	2.082924	1.941436	-0.141488	2.170813	-0.090443	0.006770	-0.145703	-0.229377
	0.8	1.6	2.631054	2.481724	-0.149330	2.720998	-0.092663	0.006190	-0.152801	-0.239274
	1.0	2.0	3.161909	3.006938	-0.154971	3.253314	-0.094206	0.005745	-0.157915	-0.246376
	2.0	4.0	5.677204	5.507311	-0.169893	5.772454	-0.098061	0.004447	-0.171530	-0.265143
	3.0	6.0	8.073744	7.896889	-0.176855	8.170804	-0.099735	0.003774	-0.177955	-0.273915
	4.0	8.0	10.408456	10.227378	-0.181078	10.506628	-0.100707	0.003343	-0.181885	-0.279250
	5.0	10.0	12.703550	12.519568	-0.183982	12.802496	-0.101356	0.003035	-0.184606	-0.282928
	10.0	20.0	23.862411	23.671183	-0.191228	23.963327	-0.102895	0.002223	-0.191471	-0.292144
	20.0	40.0	45.502636	45.306293	-0.196343	45.604991	-0.103907	0.001609	-0.196400	-0.298698
	50.0	100.0	108.758604	108.557765	-0.200839	108.862269	-0.104739	0.001037	-0.200803	-0.304504
6	0.4	4.0	10.405166	9.963027	-0.442139	11.728488	-1.576346	0.257724	-0.446838	-1.765461
	0.6	6.0	14.059697	13.583037	-0.476660	15.465426	-1.634956	0.233265	-0.480698	-1.882389
	0.8	8.0	17.469257	16.970279	-0.498978	18.929733	-1.673066	0.215745	-0.502134	-1.959454
	1.0	10.0	20.719217	20.204345	-0.514872	22.219813	-1.700464	0.202215	-0.517218	-2.015468
	2.0	20.0	35.670144	35.114198	-0.555946	37.281425	-1.773149	0.161679	-0.555757	-2.167227
	3.0	30.0	49.499237	48.924839	-0.574398	51.165337	-1.807268	0.139802	-0.573032	-2.240498
	4.0	40.0	62.738940	62.153663	-0.585277	64.439626	-1.828063	0.125380	-0.583281	-2.285963
	5.0	50.0	75.599173	75.006580	-0.592593	77.324332	-1.842415	0.114887	-0.590225	-2.317752
	10.0	100.0	136.853287	136.243183	-0.610104	138.642441	-1.878444	0.086342	-0.607156	-2.399258
	20.0	200.0	252.811247	252.189591	-0.621656	254.648664	-1.904107	0.063785	-0.618751	-2.459073
	50.0	500.0	584.524623	583.893560	-0.631063	586.407125	-1.926850	0.041953	-0.628673	-2.513565
12	1.0	28.0	66.912035	65.806539	-1.105496	73.765549	-8.083917	1.180485	-1.055578	-7.959010
	2.0	56.0	113.245854	112.094025	-1.151829	120.722260	-8.483021	0.966841	-1.112054	-8.628235
	3.0	84.0	155.473848	154.302641	-1.171207	163.268256	-8.675835	0.846680	-1.136461	-8.965615
	4.0	112.0	195.532772	194.350424	-1.182348	203.531098	-8.795704	0.765705	-1.150674	-9.180674
	5.0	140.0	234.190714	233.000991	-1.189723	242.334879	-8.879606	0.705903	-1.160184	-9.333888
	10.0	280.0	416.191833	414.985087	-1.206746	424.723373	-9.094802	0.539378	-1.182862	-9.738286
	20.0	560.0	755.840196	754.623201	-1.216995	764.669757	-9.252451	0.403719	-1.197825	-10.046556
	50.0	1400.0	1714.498639	1713.274652	-1.223987	1723.611301	-9.395486	0.268914	-1.210076	-10.336649
	2.0	120.0	264.809954	262.928937	-1.881017	286.825295	-25.409371	3.303809	-1.790796	-23.896357
	3.0	180.0	361.233837	359.337510	-1.896327	384.318425	-26.104762	2.931583	-1.807734	-24.980915
	4.0	240.0	452.148052	450.245879	-1.902173	475.926595	-26.535690	2.672422	-1.817447	-25.680716
	5.0	300.0	539.494612	537.589832	-1.904780	563.773952	-26.837784	2.477431	-1.823767	-26.184120
	10.0	600.0	947.404930	945.499122	-1.905808	973.032700	-27.616252	1.920436	-1.837762	-27.533578
	20.0	1200.0	1700.866177	1698.965611	-1.900566	1727.547904	-28.189744	1.453073	-1.845622	-28.582293
	50.0	3000.0	3806.431632	3804.541353	-1.890279	3834.126475	-28.712212	0.977796	-1.850706	-29.585122

Table 8.9: Energy results for a parabolic quantum dot with 2, 6, 12 and 20 electrons in 2 dimensions. For each oscillator frequency ω , the following are tabulated: Non-interacting ground state energy $\langle \Phi_0 | \hat{H}_0 | \Phi_0 \rangle$, Hartree-Fock energy E_{HF} , Coupled-Cluster Singles and Doubles energy E_{CCSD} , difference between CCSD and HF energy ($E_{CCSD}-E_{HF}$), reference expectation energy $\langle \Phi_0 | \hat{H} | \Phi_0 \rangle$, and the three contributions to the correlation energy $\langle \Phi_0 | \hat{H}_N (\hat{T}_1 + \hat{T}_1^2 + \hat{T}_2) | \Phi_0 \rangle$ in Eq. (6.115). All calculations are done with model space $R^b = 10$. Energy is measured in effective Hartrees E_H^* .

8.1.2 General Analysis and Discussion

Consider the HF results for the 2-electron quantum dot ($N = 2$) in Tables 8.5 and 8.6. We observe that the HF energy does not change when the size of the basis increases from an odd to an even number by 1 shell. This behaviour occurs for all oscillator frequencies. For example, for $\omega = 1.0$, the HF energy remains 3.253314 when the basis is increased from $R^b = 1$ to $R^b = 2$. This can be understood by the following argument. The HF ansatz for $N = 2$ reads

$$\Phi_{\text{HF}}(\mathbf{r}_1, \mathbf{r}_2) = \begin{pmatrix} \varphi_a(\mathbf{r}_1) & \varphi_a(\mathbf{r}_2) \\ \varphi_b(\mathbf{r}_1) & \varphi_b(\mathbf{r}_2) \end{pmatrix}, \quad (8.20)$$

where

$$\varphi_a(\mathbf{r}) = \sum_{i=1}^{\alpha_{\max}} C_{a\alpha} \psi_i(\mathbf{r}) \quad (8.21)$$

is a so-called HF orbital, and $\{\psi_i(\mathbf{r})\}_{i=1}^{\alpha_{\max}}$ is the single-particle basis of harmonic oscillator functions. See Chapter 5 for a presentation of the HF method. Since each HF orbital is written as linear combination of harmonic oscillator functions, the HF wavefunction in Eq. (8.20) is a linear combination of 2×2 determinants. It can be shown that only one-particle one-hole (1p1h) excited determinants are included, i.e. determinants where only one particle is excited from a hole state i , to a particle state a . Therefore, in the 2-electron case, 2p2h excitations are not included in the HF wavefunction. In the general N -electron case, all excitation beyond 1p1h are excluded, i.e. 2p2p, 3p3h, and so forth up to NpNh. Turning back to the 2-electron case, when $R^b = 1$, we have that $R^b = R^f$. This means that

$$\Phi_{\text{HF}}(\mathbf{r}_1, \mathbf{r}_2) = \Phi_0(\mathbf{r}_1, \mathbf{r}_2), \quad (8.22)$$

where $\Phi_0(\mathbf{r}_1, \mathbf{r}_2)$ is the non-interacting ground state, and

$$E_{\text{HF}} = E_{\text{ref}} = \langle \Phi_0 | \hat{H} | \Phi_0 \rangle = 3.253314, \quad (8.23)$$

where E_{HF} is the HF energy, and E_{ref} is the non-interacting ground state energy. When we increase our basis to $R^b = 2$, we open for the possibility to include 1p1h excitations in the HF wavefunction. The non-interacting ground state of the 2-electron systems reads

$$\Phi_0(\mathbf{r}_1, \mathbf{r}_2) = \begin{pmatrix} \psi_0(\mathbf{r}_1) & \psi_0(\mathbf{r}_2) \\ \psi_1(\mathbf{r}_1) & \psi_1(\mathbf{r}_2) \end{pmatrix}, \quad (8.24)$$

where the harmonic oscillator functions are given in Table 8.1. In the bra-ket notation, the following two states are occupied (hole states),

$$|0\rangle = |0, 0, -1\rangle \quad (8.25)$$

$$|1\rangle = |0, 0, 1\rangle, \quad (8.26)$$

where $|\alpha\rangle = |n, m, m_s\rangle$. When $R^b = 2$, we include

$$|2\rangle = |0, -1, -1\rangle \quad (8.27)$$

$$|3\rangle = |0, -1, 1\rangle \quad (8.28)$$

$$|4\rangle = |0, 1, -1\rangle \quad (8.29)$$

$$|5\rangle = |0, 1, 1\rangle, \quad (8.30)$$

in the basis. Since the Coulomb interaction is independent of the angular momentum and the spin, the *total* angular momentum

$$M \equiv m_\alpha + m_\beta, \quad (8.31)$$

and *total* spin

$$M_s \equiv m_{s_\alpha} + m_{s_\beta}, \quad (8.32)$$

must be conserved. For example, assume the electrons are in the non-interacting ground state in Eq. (8.24). The occupied states are given in Eqs. (8.25) and (8.26), with total angular momentum $M = 0$ and total spin $S = 0$. We propose the 1p1h excitation

$$\begin{pmatrix} \psi_0(\mathbf{r}_1) & \psi_0(\mathbf{r}_2) \\ \psi_2(\mathbf{r}_1) & \psi_2(\mathbf{r}_2) \end{pmatrix}, \quad (8.33)$$

i.e. an electron excited into state $|2\rangle$, with $m = -1$ and $m_s = -1$. The total angular momentum and spin is -1 and -2 , respectively. Hence this is not an allowed excitation. All 1p1h excitations that do not conserve M and S , are not allowed. When $R^b = 2$, we cannot construct any 1p1h excited determinant that has $M = 0$ and $M_s = 0$. This is clearly seen in Eqs. (8.27), (8.28), (8.29) and (8.30). No more correlations are therefore included when we increase the basis from $R^b = 1$ to $R^b = 2$, and the energy remains the same. In all the other cases, when R^b increases from 3 to 4, 5 to 6, and so forth, no “new” 1p1h excitations are allowed, and the energies thus remain constant. For systems containing 6, 12 and 20 electrons, we observe from Tables 8.5-8.6 that the HF energies are different for all R^b . Thus by increasing R^b we include “new” allowed 1p1h correlations.

The HF method is variational, i.e. the HF energy overestimates the exact ground state energy. By looking at Tables 8.5-8.8, we conclude that increasing R^b yields a better energy, viz.

$$E_0 < E_{\text{HF}}(R^b + 1) \leq E_{\text{HF}}(R^b), \quad (8.34)$$

with equality for certain values of R^b in the 2-electron system. This is what we expect. For the 2-electron system, we observe that the HF energy converges rapidly for all frequencies. We have in Figure 8.1 and 8.2 plotted the HF energy as function of R^b . The energy changes only by approximately 10^{-5} when R^b increases from 8 to 10. For systems containing 6, 12 and 20 electrons, the HF energy also converges relatively rapidly. When R^b increases from 9 to 10, the energy changes approximately $10^{-3} - 10^{-5}$. The HF results for $R^b = 10$ are therefore good estimates of the HF limits, i.e.

$$\lim_{R^b \rightarrow \infty} E_{\text{HF}}(R^b), \quad (8.35)$$

We conclude that the most important 1p1h excitations are included when $R^b = 10$. When the system contains 2 electrons, the most important correlations are 1p1h excitations into shell 3. These are included when $R^b = 3$. When $\omega = 0.2$,

$$E_{\text{HF}}(R^b = 10) - E_{\text{HF}}(R^b = 3) = -0.000283, \quad (8.36)$$

and when $\omega = 50.0$,

$$E_{\text{HF}}(R^b = 10) - E_{\text{HF}}(R^b = 3) = -0.006131. \quad (8.37)$$

For systems containing 6, 12 and 20 electrons, 1p1h excitations in higher shells yield considerably contributions. For a system containing N electrons, we observe that we have relatively good energy estimates when

$$R^b = R^f + 4, \quad (8.38)$$

relative to the HF energies for $R^b = 10$, where R^f is the Fermi shell.

Consider the CCSD results in Tables 8.5-8.8. We observe that

$$E_{\text{CCSD}}(R^b) \leq E_{\text{HF}}(R^b), \quad (8.39)$$

for all frequencies. We obtain equality when $R^b = R^f$, where R^f is the Fermi shell. The CCSD method is not variational. Thus we cannot, in principle, conclude *with certainty* whether HF or CCSD yields the best energy estimate. By this we mean the energy that is closest to the exact value. In order to decide the best estimate, results from other variational methods, such as Full Configuration Interaction (FCI) [38], Variational Monte Carlo (VMC) [25] or Diffusion Monte Carlo (DMC) [25], are needed. That said, the CCSD energies are *more likely* better estimates. Since CCSD includes more correlations than HF, we should obtain a much better energy. We now choose to anticipate the course of events. For the 2-electron system, the CCSD with effective interaction yields *exact* energies (see Sec. 8.2). We observe that the results with standard interaction are always higher than the exact energies, i.e.

$$E_{\text{CCSD}}^{\text{std}}(R^b) > E_0 = E_{\text{CCSD}}^{\text{eff}}(R^b), \quad (8.40)$$

where “std” denotes standard interaction, and “eff” denotes effective interaction. We conclude that with standard interaction, the CCSD energies are better estimates than the HF energies. This is what we expect. For systems containing 6, 12 and 20 electrons, however, the exact ground state energies are unknown. Since CCSD yields better results than HF in the 2-electron case, it is probable that it also yields better estimates for larger systems. We emphasize that, in principle, we cannot say anything with certainty before comparing with other variational methods. Table ?? shows results from other many-body methods. Comparing with the CCSD results, we conclude that for $\omega = 1.0$ and $N = 6, 12$ and 20 , the CCSD energies are better estimates than the HF energies. This is what we expect since CCSD includes excitations from 1p1h up to NpNh. Excitations beyond 2p2h are obtained with combinations of \hat{T}_1 and \hat{T}_2 . For example, 3p3h excitations are obtained by

$$\hat{T}_1 \hat{T}_2 |\Phi_0\rangle, \quad (8.41)$$

where $|\Phi_0\rangle$ is the reference determinant. Therefore, since CCSD includes *much* more correlations than HF, the results should be better. Since CCSD yields better results in the 2-electron case (all frequencies) and for larger systems (6, 12 and 20 electrons) with $\omega = 1.0$, it is reasonable to believe that the CCSD energies are better estimates than HF for all frequencies ($\omega = 0.2 - 50.0$) and electron number ($N = 2, 6, 12$ and 20).

Consider the 2-electron system. We observe that the energy changes for every value of R^b , in contrast to the HF energy. This is a direct consequence of 2p2h excitations. As we discussed earlier, when $R^b = 2$, 1p1h excitations are not allowed. However, there exist two 2p2h excitations that conserve total angular momentum M and spin M_s . We see from Table 8.1 that the determinants

$$\begin{pmatrix} \psi_3(\mathbf{r}_1) & \psi_3(\mathbf{r}_2) \\ \psi_4(\mathbf{r}_1) & \psi_4(\mathbf{r}_2) \end{pmatrix}, \quad (8.42)$$

and

$$\begin{pmatrix} \psi_3(\mathbf{r}_1) & \psi_3(\mathbf{r}_2) \\ \psi_4(\mathbf{r}_1) & \psi_4(\mathbf{r}_2) \end{pmatrix}, \quad (8.43)$$

have $M = 0$ and $M_s = 0$. Since the reference state in Eq. (8.24) has $M = 0$ and $M_s = 0$, these 2p2h excitations are allowed. Thus the energy changes when we increase R^b from 1 to 2. In general, increasing R^b will always yield “new” allowed excitations. Furthermore, we observe that CCSD with $\omega = 0.2 - 5.0$ and $R^b = 2$ gives a better energy than HF with $R^b = 10$. This means that the allowed 2p2h excitations in Eqs. (8.42) and (8.43) are more important than 1p1h excitations in shell 2 – 10. The HF energy is practically converged for all frequencies, meaning that (at least for $\omega = 0.2 - 1.0$) the 2p2h excitations in Eqs. (8.42) and (8.43) describe the correlations in the system better than *all* 1p1h excitations beyond shell 2. For example, when

$\omega = 1.0$ and $R^b = 2$, the CCSD energy is 3.152329. The corresponding HF energy is 3.161909. We have that

$$E_{\text{HF}}(R^b = 10) - E_{\text{CCSD}}(R^b = 2) \approx 0.01, \quad (8.44)$$

and

$$E_{\text{HF}}(R^b = 8) - E_{\text{HF}}(R^b = 10) < 10^{-6}, \quad (8.45)$$

supporting the statement above.

Figure 8.1 and 8.2 show the HF energy and CCSD energy as function of the size of the model space (R^b) for 2, 6, 12 and 20 electrons. In addition, the relative error

$$\Delta E(R^b) \equiv \frac{E(R^b) - E(R^b = 10)}{E(R^b = 10)} \quad (8.46)$$

is plotted for the CCSD energy. We have chosen frequencies 0.4, 1.0 and 5.0 for the 2- and 6-electron system, 1.0 and 5.0 for the 12-electron system, and 2.0 and 5.0 for the 20-electron system. First, consider the HF energy. For the 2-electron system we observe that the energy is almost constant for $R^b \geq 3$. For the 6-electron system, the energy is almost constant for $R^b \geq 4$ when $\omega = 5.0$. Decreasing the frequency to $\omega = 0.4$ results in significant contributions from shell 5 and 6. Turning to the 12-electron system with $\omega = 5.0$, the most important excitations are included when $R^b = 5/6$. When the frequency is 0.4, we have important contributions from shells 6 and 7. For the 20-electron system, lowering the frequency from 5.0 to 2.0 makes the contributions from shells 6 and 7 more important. Thus in general, contributions from higher-lying shells tend to be important for low frequencies. Furthermore, consider the CCSD energy in Figure 8.1 and 8.2. For the 2-electron system, we clearly observe that when $R^b = 3$, important correlations are included. These correlations are particularly important when $\omega = 0.4$. Increasing the frequency leads to important contributions from higher-lying shells. When $\omega = 1.0$, contributions from shells 4 and 5 are more important than for $\omega = 0.4$. When $\omega = 5.0$, we also have important contributions from shells 6 and 7. Turning to the 6-electron system, we observe that the correlations included when $R^b = 4$ are particularly important. When $\omega = 0.4$, important contributions are also present in shells 5 and 6. Increasing the frequency to 1.0/5.0 leads to a slower convergence. For the 12-electron system, the correlations that are included when $R^b = 5$, are important. These correlations are particularly important when $\omega = 5.0$. Decreasing the frequency to 1.0 leads to a larger contributions from shells 5 and 6. Finally, for the 20-electron system, the same behaviour occurs. Important correlations are included when $R^b = 6$. When the frequency is lowered from 5.0 to 2.0, we obtain important contributions from shell 7. In general, when the frequency increases, the CCSD energy converges slower. Particularly important correlations are included when

$$R^b = R^f + 2. \quad (8.47)$$

Also, except for the 2-electron system, contributions from low-lying shells become more important when the frequency decreases.

Consider the relative error plots in Figure 8.1 and 8.2. The relative error can be approximated as

$$\Delta E(R^b) \approx A e^{aR^b}, \quad (8.48)$$

where A and a are constants. Both constants are dependent on the number of electrons and the frequency. We observe that the convergence rate is higher for larger systems. We therefore obtain that

$$|b_N| > |b_{N'}| \quad (8.49)$$

when $N > N'$.

8.1.3 Full Correlation Energy

We have in Table 8.9 tabulated energy results for $R^b = 10$ and different frequencies. For each electron number N and frequency ω , the table shows the non-interacting ground state energy $\langle \Phi_0 | \hat{H}_0 | \Phi_0 \rangle$, the HF energy, the CCSD energy, the difference between the CCSD energy and the HF energy, the reference expectation energy $\langle \Phi_0 | \hat{H} | \Phi_0 \rangle$, the \hat{T}_1 contribution $\langle \Phi_0 | \hat{H}_N \hat{T}_1 | \Phi_0 \rangle$, the \hat{T}_1^2 contribution $\langle \Phi_0 | \hat{H}_N \hat{T}_1^2 | \Phi_0 \rangle$, the \hat{T}_2 contribution $\langle \Phi_0 | \hat{H}_N \hat{T}_2 | \Phi_0 \rangle$, and the total contribution $\langle \Phi_0 | \hat{H}_N (\hat{T}_1 + \hat{T}_1^2 + \hat{T}_2) | \Phi_0 \rangle$ to the CCSD energy. First we observe that the non-interacting ground state energy increases when the frequency increases. This is what we expect since the single-particle energies are given by Eq. (8.16). Figure 8.1.3 shows the non-interacting energy, the CCSD energy, and the HF energy as function of frequency. We see that the energies are approximately linear functions. By taking the electron-electron repulsion into account, the energy increases more when the frequency is changed.

We define the *Full Correlation Energy* (FCE) as the difference between the exact ground state energy of the interacting system, and the non-interacting energy. The FCE is thus the contribution to the total energy from the electron-electron interaction. Therefore, the difference between the CCSD energy and the non-interacting energy gives us an approximation to the FCE. The Coulomb interaction is repulsive, meaning that the electrons repel each other. The repulsion should obviously give a positive contribution to the energy. We have in Figure 8.1.3 plotted the FCE as function of frequency. First we observe that the full correlation energy is positive, as expected. Furthermore, the contribution increases when the frequency increases. This can be understood by the following argument: When the frequency increases, the confinement potential

$$u(r) = \frac{1}{2}m^* \omega^2 r^2, \quad (8.50)$$

becomes steeper. When the potential well is steeper, the electrons are pushed harder together, yielding a stronger repulsion. Thus the Coulomb interaction contributes more to the total energy for higher frequencies. The full correlation energy can be approximated by

$$f_{\text{FCE}}(\omega) = BAe^{b\omega}, \quad (8.51)$$

where B and b are constants. We observe from Figure 8.1.3 that B depends on the number of electrons in the system, and that b is approximately independent of the electron number. We have calculated that $b \approx 1.6$. Furthermore, for a given frequency, a system containing more electrons than another has a larger contribution from the interaction. This is also what we expect. The more electrons that are present in the system, the larger is the number of interacting particles, obviously. Another important quantity is the fractional contribution to the CCSD energy. It is defined as

$$\Delta E_{\text{FCE}} \equiv \frac{E_{\text{CCSD}} - \langle \Phi_0 | \hat{H}_0 | \Phi_0 \rangle}{E_{\text{CCSD}}}. \quad (8.52)$$

The right plot of Figure 8.1.3 shows ΔE_{FCE} as function of frequency. For a given frequency, the fractional contribution is always larger for a system containing more electrons. Secondly, the contribution decreases when the frequency increases. We observe that

$$\Delta E_{\text{FCE}}(\omega) \approx Ce^{c\omega}, \quad (8.53)$$

where C and c are constants. This is a rough approximation. We observe that C is dependent on the number of electrons in the system, and c is approximately independent of the electron number. We have calculated $c \approx -5 \cdot 10^{-3}$. Let us now consider the changes in the fractional contribution to the CCSD energy when the frequency increases from the lowest to the highest value. For the 2-electron system, the contribution from FCE is approximately 48% of the CCSD energy when $\omega = 0.2$. When $\omega = 50.0$, the contribution is 8%. For the 6-electron system, the contribution is approximately 60% when $\omega = 0.4$, and 14% when $\omega = 50.0$. For the 12-electron system, the contribution is approximately 57% when $\omega = 1.0$, and 18% when $\omega = 50.0$.

For the 20-electron system, the contribution is approximately 54% when $\omega = 2.0$, and 21% when $\omega = 50.0$. In general, the fractional contribution to the CCSD energy decreases when the frequency increases. Thus the contribution from the electron-electron interaction is more important for low frequencies. We therefore conclude that the system is more correlated for low frequencies than for high frequencies. This may explain why the CCSD energy does not converge for low frequencies ($\omega < 0.4$ for $N = 6$, $\omega < 1.0$ for $N = 12$, and $\omega < 2.0$ for $N = 20$). We have also observed that the energy converges far more quickly (less iterations needed) for higher frequencies, i.e. for less correlated systems. This is what we intuitively expect.

8.1.4 Correlation Energy

The so-called Correlation Energy (CE) is normally defined as the difference between the HF limit and the exact ground state energy of the interacting system. This definition was introduced in [45]. The CE must not be confused with what we previously defined as the *full* correlation energy (FCE). While the FCE is a measurement of the total contribution from the electron-electron interaction, the CE is a measurement of the contribution from correlations beyond what are included in HF, i.e. 1p1h excitations. In Table 8.9, the difference between the CCSD energy and the HF energy is tabulated. Since the CCSD energy is not exact, and the single-particle basis is truncated in the HF calculation, the difference between the CCSD energy and the HF energy is an approximation to the CE. Figure 8.1.4 shows the CE (absolute value) as function of frequency. First we observe that the CE does not vary much. Nonetheless, it increases somewhat when the frequency increases, i.e.

$$f_{\text{CE}}(\omega) < f_{\text{CE}}(\omega'), \quad (8.54)$$

for $\omega > \omega'$, where f_{CE} is the CE. Remember that CE is defined to be negative. For the 2-electron system, the CE changes by approximately -0.09 when the frequency increases from 0.2 to 50.0. For the 6-electron system, it changes by approximately -0.19 when the frequency increases from 0.4 to 50.0. For the 12-electron system, the CE changes is approximately -0.13 when the frequency increases from 1.0 to 50.0. Finally, for the 20-electron system, we observe something else. The energy increases from $\omega = 2.0$ up to $\omega = 10.0$, and decreases from $\omega = 10.0$ up to $\omega = 50.0$. We first conclude that a system containing more electrons than another has a larger CE for all frequencies. This is what we expect. Compared to the FCE, however, the differences are relatively small, meaning that 1p1h correlations are important. The right plot in Figure 8.1.4 shows the fractional contribution from the CE to the CCSD energy. It is defined as

$$\Delta E_{\text{CE}} = \left| \frac{E_{\text{CCSD}} - E_{\text{HF}}}{E_{\text{CCSD}}} \right|. \quad (8.55)$$

The fractional contributions are in accordance with [23]. We observe that ΔE_{CE} can be approximated by an exponential function,

$$\Delta E_{\text{CE}}(\omega) \approx D e^{d\omega}, \quad (8.56)$$

where D and d are constants. We observe that D depends on the number of electrons in the system, and d is approximately independent of the electron number. We have calculated that $c \approx -9 \cdot 10^{-4}$. The fractional contribution from the CE to the CCSD energy decreases when the frequency increases. Let us for example consider the 2-electron system. When the frequency increases from 0.2 to 50.0, the fractional contribution changes from approximately 14% to 0.002%. The CE is therefore much more important for low frequencies. We conclude that when the frequency decreases, the system becomes more correlated. Furthermore, consider the fractional contribution from the CE and the FCE in Figure 8.1.4 and 8.1.3, respectively. We observe that both contributions decrease when the frequency increases. We have in Eqs. (8.53) and (8.56) approximated ΔE_{CE} and ΔE_{FCE} (see Eqs. 8.52 and 8.55) by the exponential function. The slopes were approximated to $c \approx -5 \cdot 10^{-3}$ (FCE) and $d \approx -9 \cdot 10^{-4}$ (CE). We

conclude that the fractional contribution from the FCE is much more sensitive to changes in the frequency. Also, the FCE is much larger than the CE, meaning that 1p1h excitations are very important. Furthermore, another clear difference between CE and FCE is that their fractional contributions depend differently on N . When the number of electrons in the system increases, the fractional contribution from FCE increases while the contribution from CE decreases. As pointed out before, CE is a measurement of the contribution from correlations beyond 1p1h. Increasing the size of the system lowers the fractional contribution from 2p2h, 3p3h, up to NpNh excitations. Thus the correlations beyond the HF approximation is less important when the size of the system increases, i.e. 1p1h excitations are important. This is what we would expect.

8.1.5 CCSD Correlation Energy

The CCSD energy can be written as (see Sec. 6.4.3)

$$E_{\text{CCSD}} = \langle \Phi_0 | \hat{H} | \Phi_0 \rangle + \langle \Phi_0 | \hat{H}_N \hat{T}_1 | \Phi_0 \rangle + \langle \Phi_0 | \hat{H}_N \hat{T}_1^2 | \Phi_0 \rangle + \langle \Phi_0 | \hat{H}_N \hat{T}_2 | \Phi_0 \rangle. \quad (8.57)$$

We define the CCSD correlation energy (CCSD-CE) as

$$\begin{aligned} f_{\text{CCSD-CE}} &\equiv E_{\text{CCSD}} - \langle \Phi_0 | \hat{H} | \Phi_0 \rangle \\ &= \langle \Phi_0 | \hat{H}_N \hat{T}_1 | \Phi_0 \rangle + \langle \Phi_0 | \hat{H}_N \hat{T}_1^2 | \Phi_0 \rangle + \langle \Phi_0 | \hat{H}_N \hat{T}_2 | \Phi_0 \rangle. \end{aligned} \quad (8.58)$$

We have in Table 8.9 tabulated $\langle \Phi_0 | \hat{H} | \Phi_0 \rangle$, $\langle \Phi_0 | \hat{H}_N \hat{T}_1 | \Phi_0 \rangle$, $\langle \Phi_0 | \hat{H}_N \hat{T}_1^2 | \Phi_0 \rangle$, $\langle \Phi_0 | \hat{H}_N \hat{T}_2 | \Phi_0 \rangle$ and $f_{\text{CCSD-CE}}$. Figure 8.6 shows the contribution from \hat{T}_1 , \hat{T}_1^2 and \hat{T}_2 to the CCSD-EC as function of frequency, for 2, 6, 12 and 20 electrons. First we observe that

$$\langle \Phi_0 | \hat{H}_N \hat{T}_1 | \Phi_0 \rangle < 0 \quad (8.59)$$

$$\langle \Phi_0 | \hat{H}_N \hat{T}_1^2 | \Phi_0 \rangle > 0 \quad (8.60)$$

$$\langle \Phi_0 | \hat{H}_N \hat{T}_2 | \Phi_0 \rangle < 0. \quad (8.61)$$

For the 2-electron system, the contribution from \hat{T}_2 is always larger than the contribution from \hat{T}_1 and \hat{T}_1^2 . This means that 2p2h excitations are important. It also explains why the HF energy is not a very good approximation to the exact energy in the 2-electron case. For example, when $\omega = 1.0$, the exact energy is 3, the CCSD energy is 3.006938, and the HF energy is 3.161909. Since the CCSD result is close to the exact value, the difference between the HF energy and the exact result is mainly because 2p2h correlations are not included. Furthermore, for larger systems (6, 12 and 20 electrons), we observe that

$$\left| \langle \Phi_0 | \hat{H}_N \hat{T}_1 | \Phi_0 \rangle \right| > \left| \langle \Phi_0 | \hat{H}_N \hat{T}_1^2 | \Phi_0 \rangle \right| \quad (8.62)$$

$$\left| \langle \Phi_0 | \hat{H}_N \hat{T}_1 | \Phi_0 \rangle \right| > \left| \langle \Phi_0 | \hat{H}_N \hat{T}_2 | \Phi_0 \rangle \right|, \quad (8.63)$$

i.e. the contribution from \hat{T}_1 is larger than both the contribution from \hat{T}_1^2 , and from \hat{T}_2 . When the size of the system increases from 6 to 12 electrons, the contribution from \hat{T}_1 increases by approximately a factor of 8, while the contribution from \hat{T}_1^2 and \hat{T}_2 roughly remains the same. When the size of the system increases from 12 to 20 electrons, the contribution from \hat{T}_1 and \hat{T}_2 still remains roughly the same. However, the contribution from \hat{T}_1 increases by roughly a factor of 3. We conclude that the single-particle field is stronger for a system containing more electrons than another. Furthermore, the contribution from \hat{T}_1 and \hat{T}_2 increases (absolute value) when the frequency increases. However, the contribution from \hat{T}_1 decreases. We also see that the contribution from \hat{T}_2 is less sensitive to changes in the frequency for larger systems. For the 20-electron system, the change is approximately 0.05 when the frequency increases from 2.0 to 50.0. For the 2-electron system, the change is approximately 0.1 when the frequency increases from 0.2 to 50.0.

We have in Figure 8.1.5 plotted the CCSD-CE (left plot) defined in Eq. (8.58), i.e. the total contributions from \hat{T}_1 , \hat{T}_1^2 and \hat{T}_2 , and the fractional contribution to the CCSD energy (right plot). The fractional contribution is defined as

$$\Delta E_{\text{CCSD-CE}} \equiv \left| \frac{f_{\text{CCSD-CE}}}{E_{\text{CCSD}}} \right|. \quad (8.64)$$

First we observe that the CCSD-EC increases (absolute value) when the size of the system increases. This is what we would expect. Moreover, when the frequency increases, the CCSD-EC also increases. However, the CCSD-EC is much more sensitive to changes in the frequency for larger systems. We observe that for the 2-electron system, the curve is flat compared to the 20-electron system. We conclude that when the frequency increases, the CCSD-EC (absolute value) increases more for a system containing more electrons than another. Furthermore, for a given frequency, the fractional contribution from the CCSD-EC increases when the size of the system increases. This is the same behaviour as the Full Correlation Energy (FCE). Even though the definitions of FCE and CCSD-EC are different, both quantities give information about the correlations in the system. We observe that when the frequency decreases, the fractional contribution from CCSD-EC increases. Thus the system is more correlated for low frequencies.

8.1.6 Analysis of the Amplitudes

We will in this section analyse the \hat{T}_1 and \hat{T}_2 amplitudes. We want to find out if it is possible to extract general tendencies for different system sizes and oscillator frequencies. We first define the total \hat{T}_1 contribution as

$$t_1(R) \equiv \sum_{i \leq i_f, a \in R} |t_i^a|^2, \quad (8.65)$$

where i_f is the Fermi state, and $a \in R$ means all orbitals within shell R (see Table 8.2). Remember that i denotes a hole state and a denotes a particle state. We see from the definition that $t_1(R)$ is the sum of all \hat{T}_1 amplitudes (squared) having contribution from shell R . This is an interesting quantity since it may reveal the shells that are most important. Figure 8.1.6 shows the plot of $t_1(R)$. We observe that for the 2-electron system,

$$t_1(R) \approx C e^{\varpi R}, \quad (8.66)$$

where C is a constant determined by the frequency, and ϖ is a constant that is approximately independent of the frequency. We observe that

$$\varpi \approx -0.05. \quad (8.67)$$

The \hat{T}_1 amplitudes are nonzero for odd shells. Stated differently, when we increase the basis from an even number to an odd number by one, we do not get additional 1p1h excitations. This is exactly what we observed for the HF energy in Table 8.5. This reflects that HF includes 1p1h excitations only.

Turning to systems containing 6, 12 and 20 electrons we see that $t_1(R)$ changes radically. Although it tends to decrease for higher shells, $t_1(R)$ can increase from one shell to another. For example, the contribution from shell 4 tends to be more important than the contribution from shell 3. For $\omega = 1.0$ we observe that $t_1(R_{\text{odd}})$ and $t_1(R_{\text{even}})$ are approximately exponential functions (straight lines in the plot) for systems containing 6 and 12 electrons. However, this is not true for other frequencies. It is important to note that the excitation amplitudes are *not* normalized. This follows from Eq. (6.51). Thus we cannot directly compare the quantitative values of $t_1(R)$ for different frequencies. Figure 8.1.6 can only be used to gain insight into how $t_1(R)$ depends on R for a given frequency. It is difficult to observe general tendencies in the figure. The “staggering-effect” is the reason for this.

We define the total \hat{T}_2 contribution as

$$t_2(R_1, R_2) \equiv \frac{1}{2} \sum_{ij \leq i_f, a \in R_1, b \in R_2} |t_{ij}^{ab}|^2, \quad (8.68)$$

where $a \in R_1$ means all orbitals within shell R_1 , and $b \in R_2$ means all orbitals within shell R_2 . We see from the definition that $t_2(R_1, R_2)$ is the sum of all \hat{T}_2 amplitudes (squared) having contribution from shell R_1 and R_2 . It gives an indication of which shells that are most important. Thus it is an interesting quantity to analyse. Figures 8.9 and 8.10 show the plot of

$$t_2^{R_1}(R_2) \equiv t_2(R_1, R_2), \quad (8.69)$$

for different values of R_1 . Note that the excitation amplitudes are not normalized. Consider the 2-electron system. We observe that

$$t_{ij}^{ab} = t_{ij}^{ba} = 0 \quad (8.70)$$

when

$$a \in R_{\text{odd}} \quad (8.71)$$

$$b \in R_{\text{even}}, \quad (8.72)$$

where R_{odd} is an odd shell, and R_{even} is an even shell. This is due to the fact that there are none 2p2h excitations that conserve total angular momentum and total spin. As we discussed previously for the 2-electron system, states that have

$$M = 0 \quad (8.73)$$

$$S = 0 \quad (8.74)$$

are allowed. Consider for example shell 3 and 4 with corresponding single-particle states in Table 8.2. The mapping scheme is given in Table 8.1. We see that orbitals within shell 3 have $m = -2, 0$ and 2 , and orbitals within shell 4 have $m = -3, -1, 1$ and 3 . Thus we cannot excite one electron into shell 3, and another electron into shell 4. This is what we observe in Figure 8.9. Furthermore, we observe that $t_2(R)$ decreases approximately exponentially. This indicates that low-lying shells are most important.

Turning to the system consisting of 6 electrons we observe that $t_2(R)$ changes radically. The “staggering-effect” makes it difficult to observe any general tendencies besides that $t_2(R)$ tend to decrease. When the system is larger (12 or 20 electrons) we observe that the “staggering-effect” is less present. Still we cannot draw any general conclusions.

8.1.7 Analysis of Basis Size

The accuracy of the CCSD results are obviously dependent on the size of the model space. Normally we obtain a better accuracy when the size of the model space increases. Thus we often like to run our calculations with a model space as large as possible. In wavefunction-based methods, such as Coupled-Cluster and Configuration Interaction [38], we quickly reach the maximum size of the model space due to computational limitations. It is therefore interesting to gain insight into how sensitive our results are on the size of the model space for different frequencies. In order to analyse this, we have in Figure 8.11 plotted

$$g_6(\omega) \equiv E_{R^b=6}(\omega) - E_{R^b=10}(\omega) \quad (8.75)$$

$$g_9(\omega) \equiv E_{R^b=9}(\omega) - E_{R^b=10}(\omega), \quad (8.76)$$

where E_{R^b} is the CCSD energy with model space R^b . The relative errors, defined as

$$\Delta E_6(\omega) \equiv \frac{g_6(\omega)}{E_{R^b=10}(\omega)} \quad (8.77)$$

$$\Delta E_9(\omega) \equiv \frac{g_9(\omega)}{E_{R^b=10}(\omega)}, \quad (8.78)$$

are also shown. First we observe that for a given frequency, both $g_6(\omega)$ and $g_9(\omega)$ increases when the size of the system increases, i.e.

$$g_6^N(\omega) > g_6^{N'}(\omega) \quad (8.79)$$

$$g_9^N(\omega) > g_9^{N'}(\omega), \quad (8.80)$$

when $N > N'$. This is an important similarity. Furthermore, we observe that $g_6(\omega)$ and $g_9(\omega)$ vary much more in the low-frequency region than in the high-frequency region. In the 2-electron case, $g_6(\omega)$ and $g_9(\omega)$ are roughly independent of the frequency. The curve is almost flat. Turning to the 6-electron system, both $g_6(\omega)$ and $g_9(\omega)$ increase somewhat in the low-frequency region, and then flatten out. In the case of 12 and 20 electrons, $g_6(\omega)$ and $g_9(\omega)$ depend quite differently on the frequency. We see that $g_6(\omega)$ decreases exponentially for systems containing 12 and 20 electrons. However, for the 12-electron system, $g_9(\omega)$ increases when the frequency increases. For the 20-electron system, $g_9(\omega)$ decreases when the frequency increases from 2.0 to 5.0, and then increases from 5.0 to 50.0. Both $g_6(\omega)$ and $g_9(\omega)$ tend to stabilize (converge) in the high-frequency region.

Consider the relative error plots in the second column of Figure 8.11. We see that the plots of $\Delta E_6(\omega)$ and $\Delta E_9(\omega)$ are relatively equal. For systems containing 2 and 6 electrons,

$$\frac{d}{d\omega} \Delta E_6(\omega) = \frac{d}{d\omega} \Delta E_9(\omega) = 0, \quad (8.81)$$

when $\omega \approx 0.8$. The errors increase up to $\omega \approx 0.8$, and then decrease for higher frequencies. For systems containing 12 and 20 electrons, the relative errors decrease exponentially. We observe that for low frequencies, both $\Delta E_6(\omega)$ and $\Delta E_9(\omega)$ depend strongly on the number of electrons. However, the relative errors converge in the high-frequency region. Moreover, here they are approximately independent of the electron number. We observe that $\Delta E_6(\omega)$ is approximately equal for 2, 6 and 12 electrons, and $\omega \geq 10$. When $20 \leq \omega \leq 50$,

$$\Delta E_6(20 \leq \omega \leq 50) \approx 5 \cdot 10^{-4}, \quad (8.82)$$

for 2, 6, 12 and 20 electrons. Since $\Delta E_9(\omega)$ is about a factor 1/10 lower than $\Delta E_6(\omega)$, it seems to converge somewhat slower. When $\omega \geq 20$, $\Delta E_9(\omega)$ is approximately equal for systems containing 2, 6, 12 and 20 electrons. When $\omega = 50$,

$$\Delta E_9(\omega = 50) \approx 5 \cdot 10^{-5}. \quad (8.83)$$

We conclude that in general, the size of the model space is more important for low frequencies than for high frequencies, except for $\omega \leq 0.8$ and $N = 2$ and 6. We also conclude that when the number of electrons in the system increases, the size of basis is more important. Thus in the low frequency region ($\omega \leq 10$), in order to obtain an accuracy for a system containing N electrons that is equal to the accuracy of a system containing N' electrons, where $N > N'$, the model space must be larger.

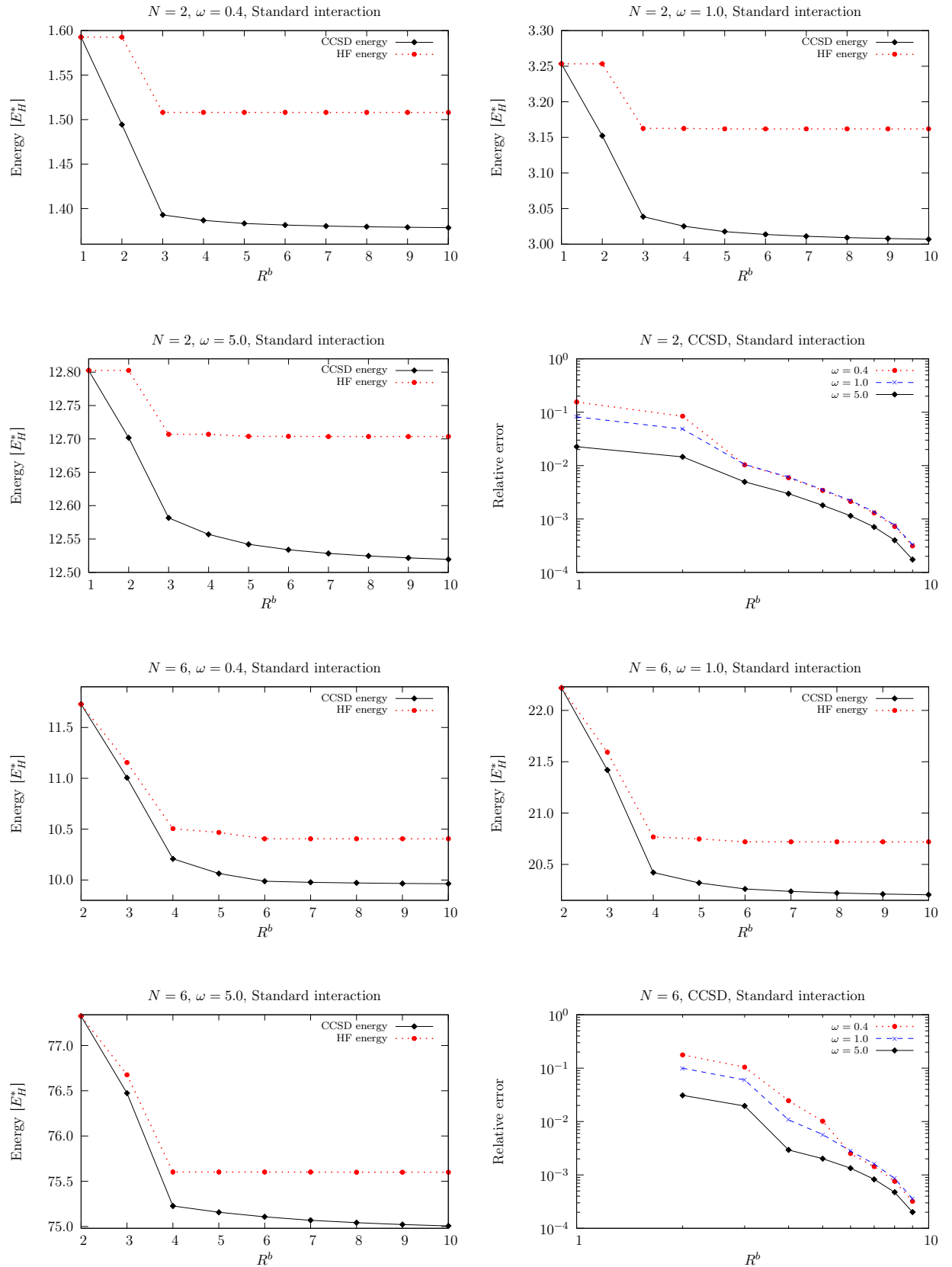


Figure 8.1: CCSD and HF energy as function of R^b (the size of the model space) for the 2– and 6-electron system with oscillator frequency $\omega = 0.4, 1.0$ and 5.0 . The energy is measured in effective Hartrees (E_H^*). For the CCSD energy, the relative error as function of R^b is also shown. The relative error is given by $[E(R^b) - E(10)] / E(10)$.

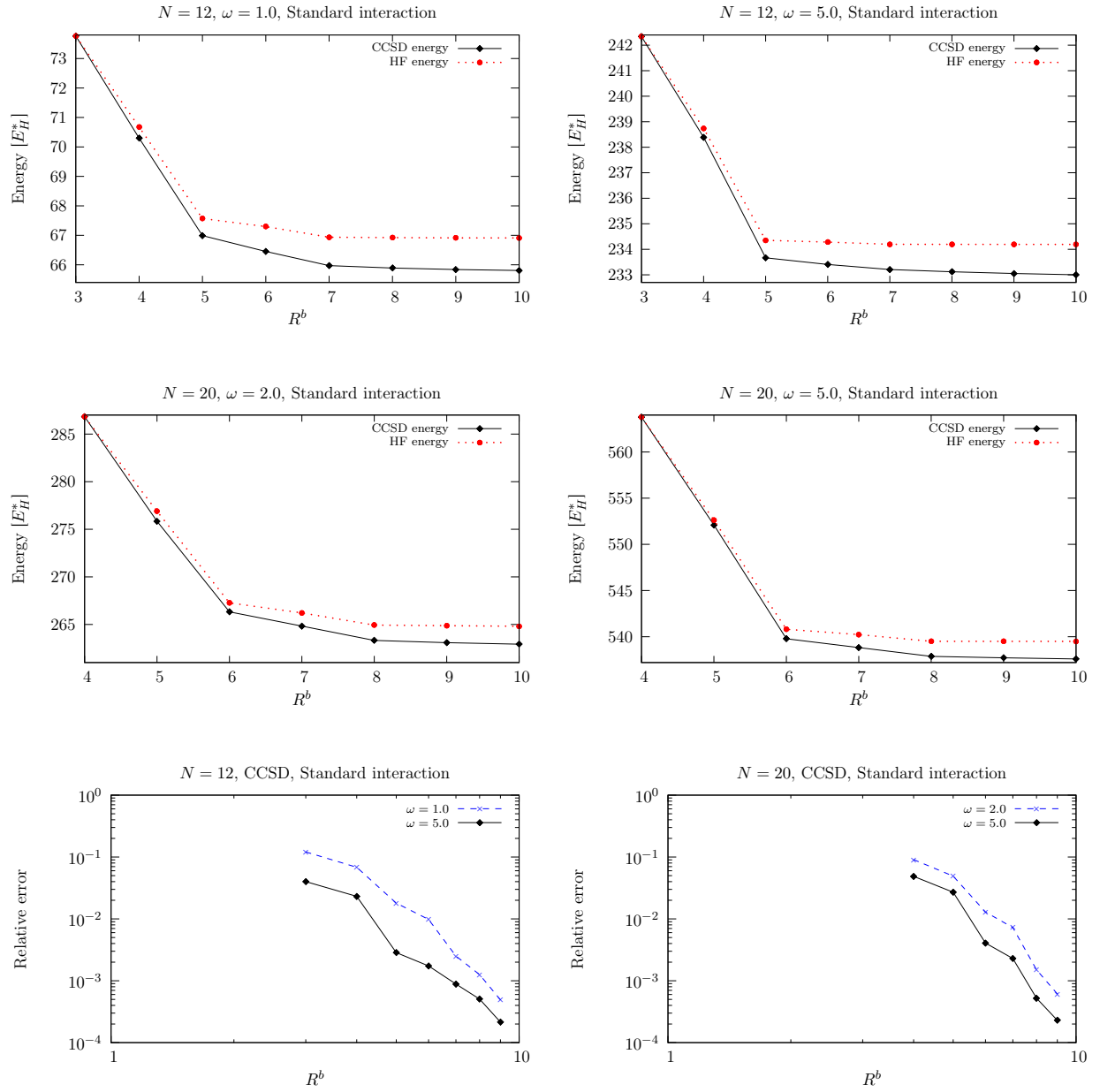


Figure 8.2: CCSD and HF energy as function of R^b (the size of the model space) for the 12– and 20-electron system. The energy is measured in effective Hartrees (E_H^*). With a harmonic oscillator basis, the CCSD energy does not converge for $\omega < 1.0$ ($N = 12$), and $\omega < 2$ ($N = 20$). We have therefore chosen $\omega = 1.0$ and 5.0 for $N = 12$, and $\omega = 2.0$ and 5.0 for $N = 20$. The relative error as function of R^b is also shown for the CCSD energy. The relative error is given by $[E(R^b) - E(10)] / E(10)$.

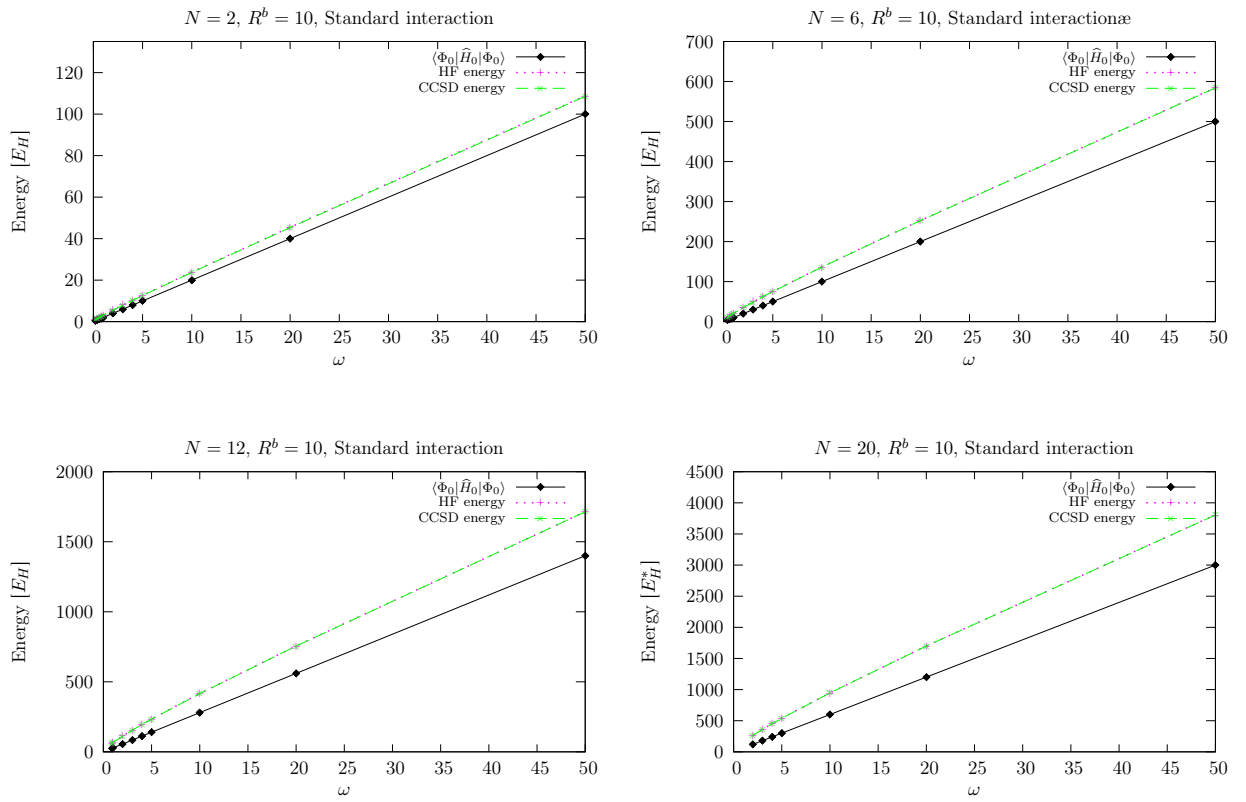


Figure 8.3: Non-interacting energy $\langle \Phi_0 | \hat{H}_0 | \Phi_0 \rangle$, HF energy, and CCSD energy as function of frequency. All calculations have been done with $R^b = 10$ and standard interaction. Energy is measured in units of effective Hartrees E_H^* .

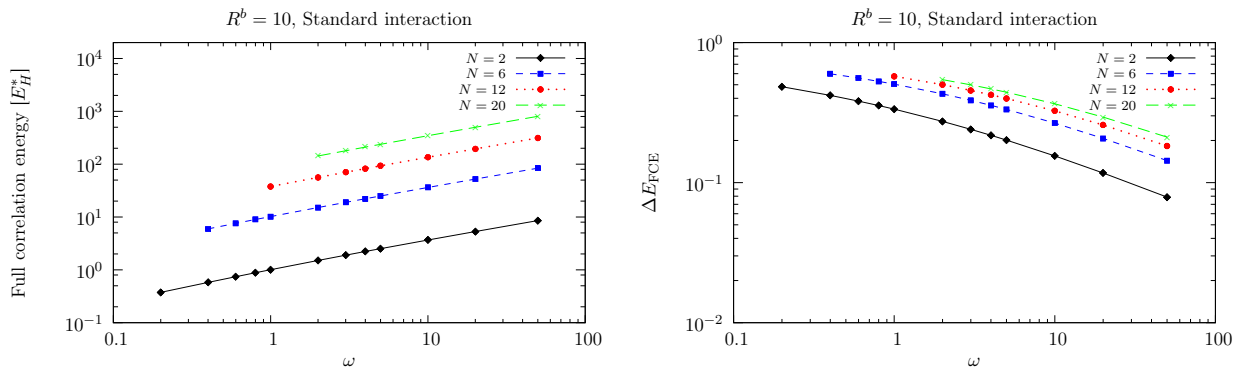


Figure 8.4: Full correlation energy (FCE) as function of frequency ω . The FCE is defined as the difference between the CCSD energy and the non-interacting ground state energy. In the right plot, the fractional contribution to the CCSD energy ΔE_{FCE} is shown. All calculations have been done with $R^b = 10$ and standard interaction. Energy is measured in effective Hartrees (E_H^*).

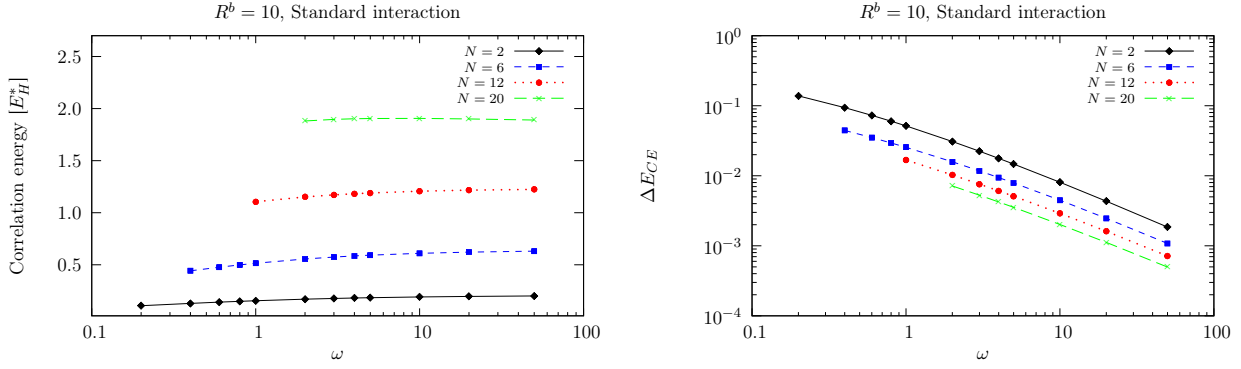


Figure 8.5: Correlation energy (absolute value) as function of oscillator frequency ω (left plot). The correlation energy is defined as the difference between the CCSD energy and HF energy. In the right plot, the fractional contribution from the correlation energy to the CCSD energy (see Eq. 8.52) is shown. All calculations have been done with model space $R^b = 10$. Energy is measured in effective Hartrees (E_H^*).

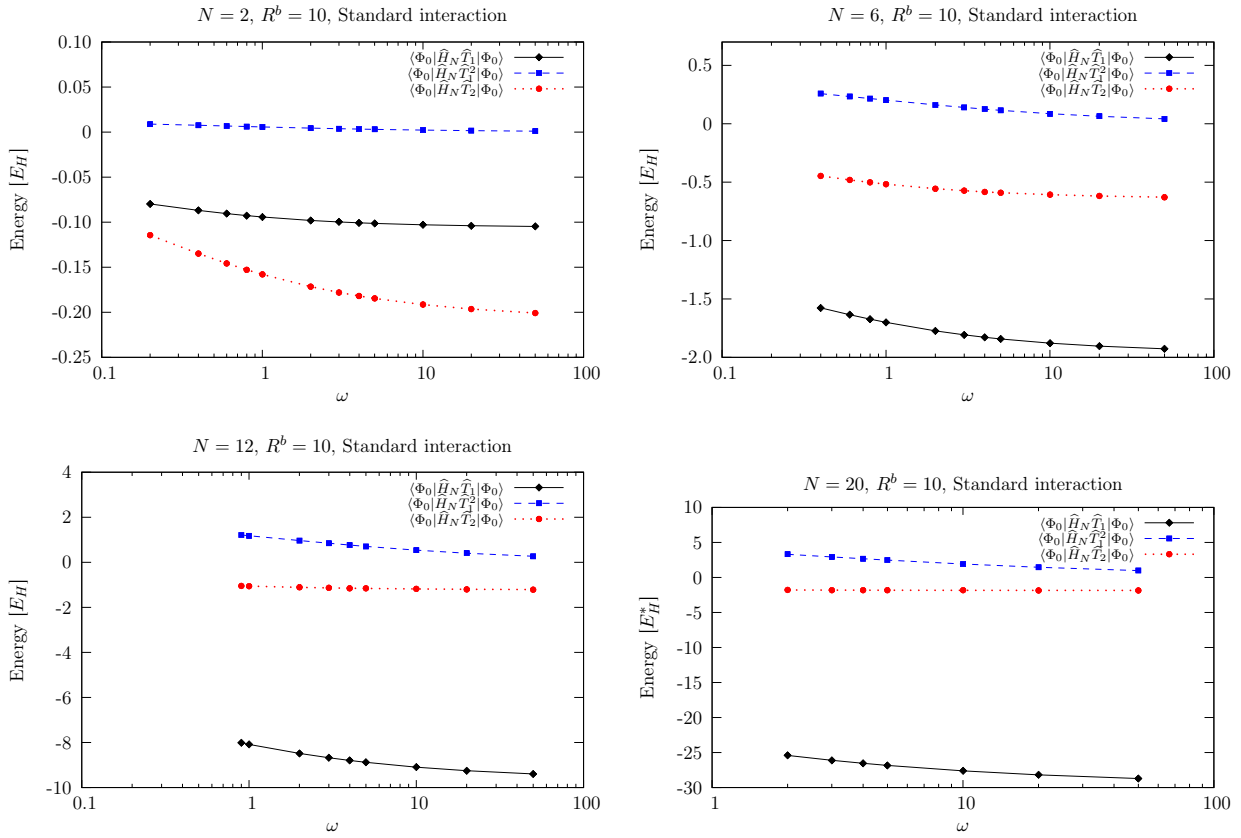


Figure 8.6: Contributions to the CCSD correlation energy (defined in Eq. 8.58) as function of frequency ω , for 2, 6, 12 and 20 electrons. The CCSD calculations have been done with model space $R^b = 10$, and standard interaction.

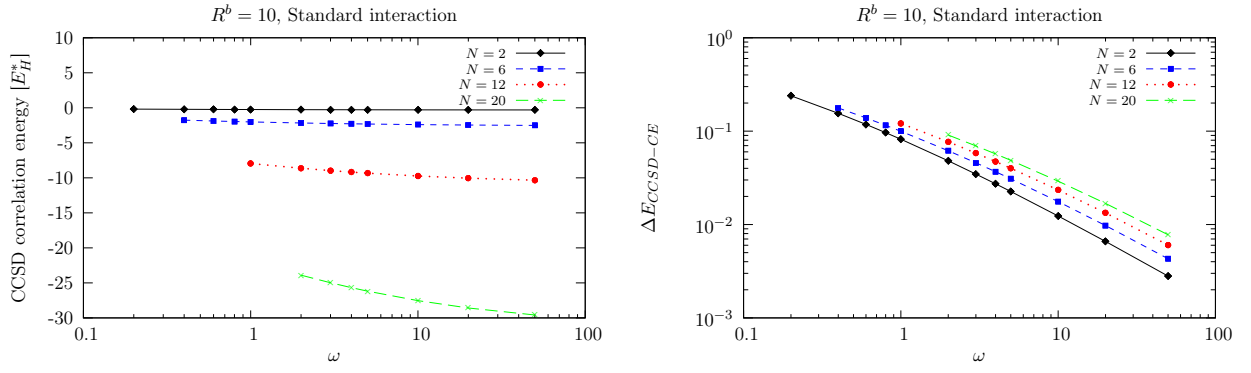


Figure 8.7: Left plot: CCSD correlation energy as function of frequency, for 2, 6, 12 and 20 electrons. The CCSD correlation energy is defined in Eq. (8.58). Right plot: Fractional contribution to the CCSD energy as function of frequency, defined in Eq. (8.64). The CCSD calculations have been done with model space $R^b = 10$, and standard interaction.

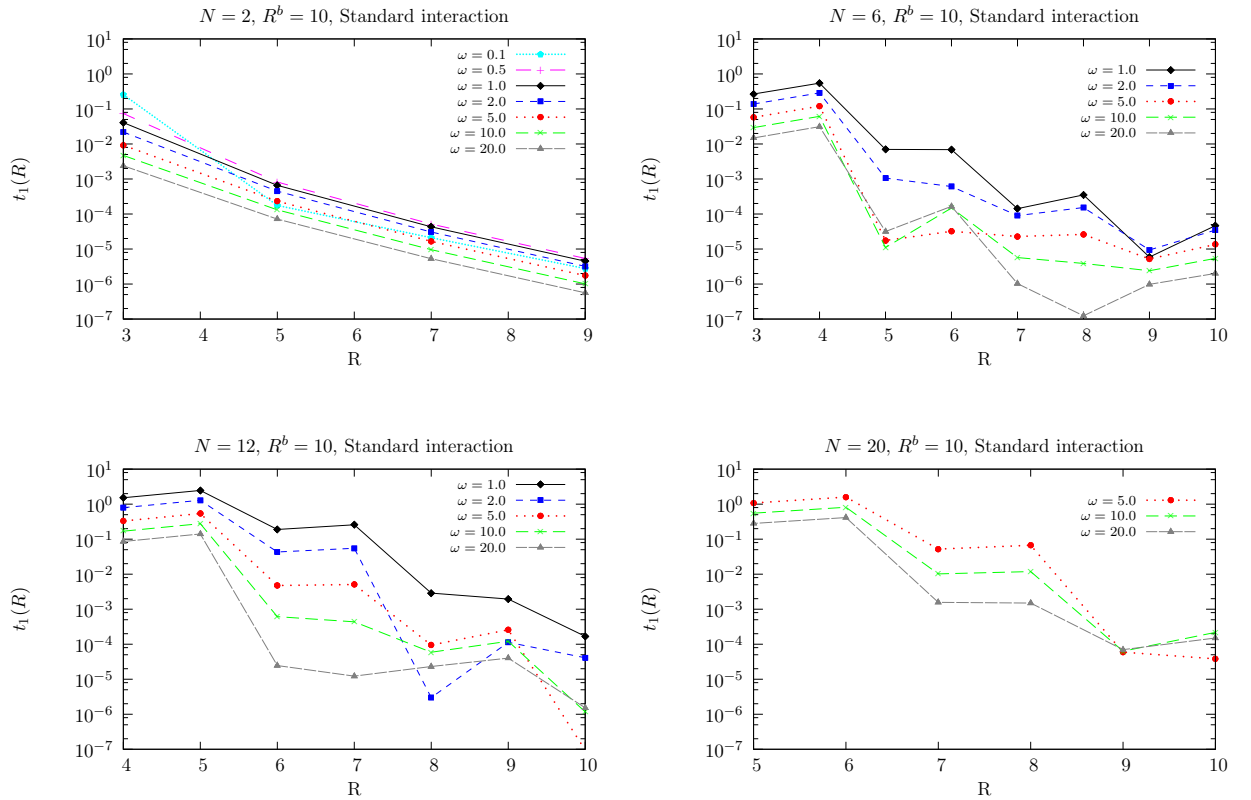


Figure 8.8: Total \hat{T}_1 contribution $t_1(R)$ (defined in Eq. 8.65) for systems with 2, 6, 12 and 20 electrons. The CCSD calculations have been done with model space $R^b = 10$ and for different frequencies ω . Note that the excitation amplitudes are not normalized.

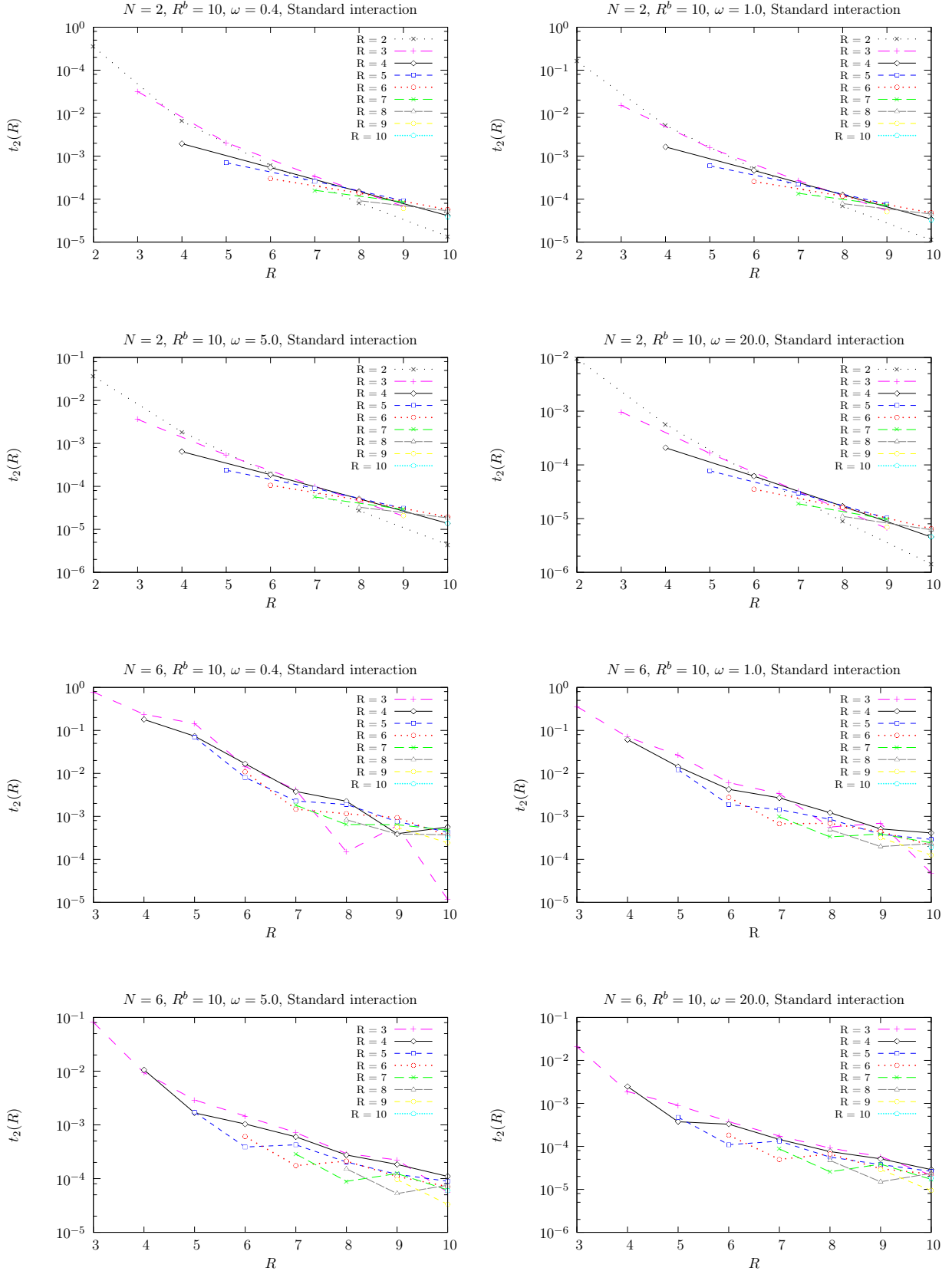


Figure 8.9: Total \hat{T}_2 contribution $t_2(R)$ (defined in Eqs. 8.68 and 8.69) for systems containing 2 and 6 electrons. The CCSD calculations have been done with model space $R^b = 10$ and for different frequencies ω . Note that the excitation amplitudes are not normalized.

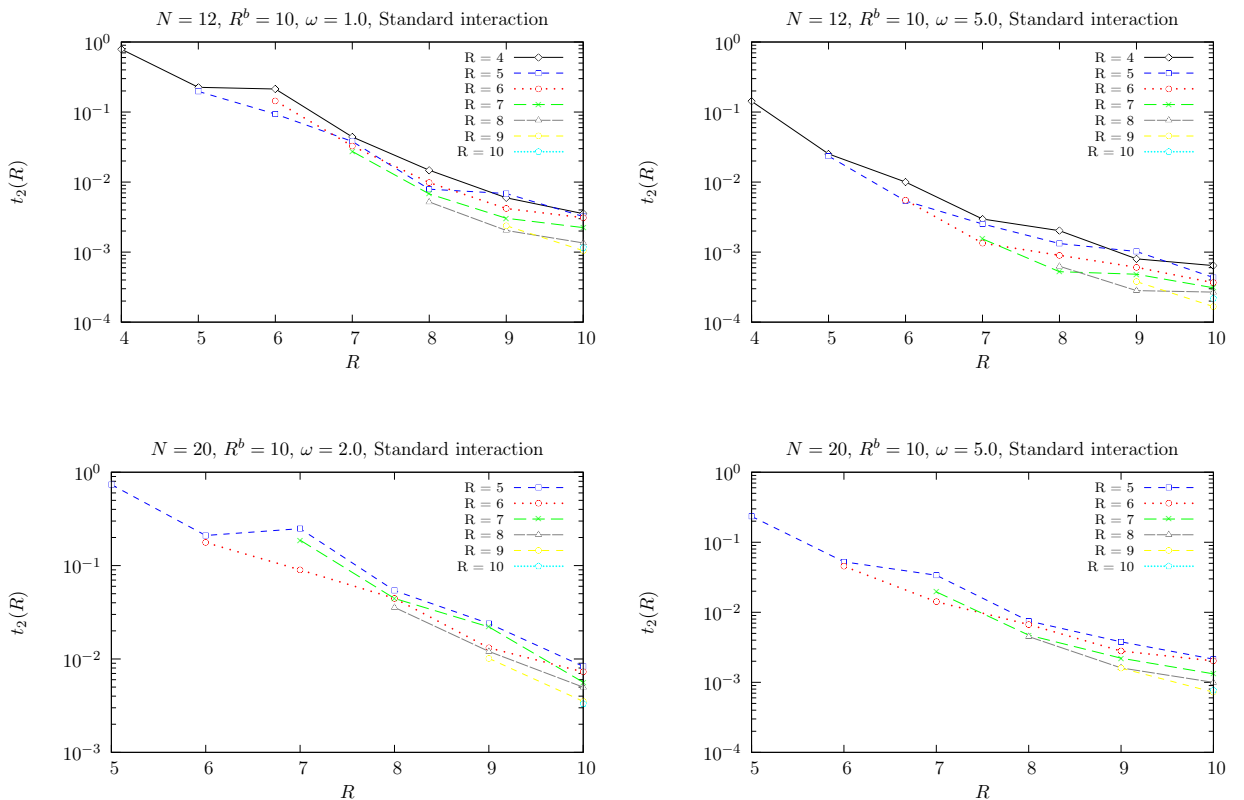


Figure 8.10: Total \hat{T}_2 contribution $t_2(R)$ (defined in Eqs. 8.68 and 8.69) for systems containing 12 and 20 electrons. The CCSD calculations have been done with model space $R^b = 10$ and for different frequencies ω . Note that the excitation amplitudes are not normalized.

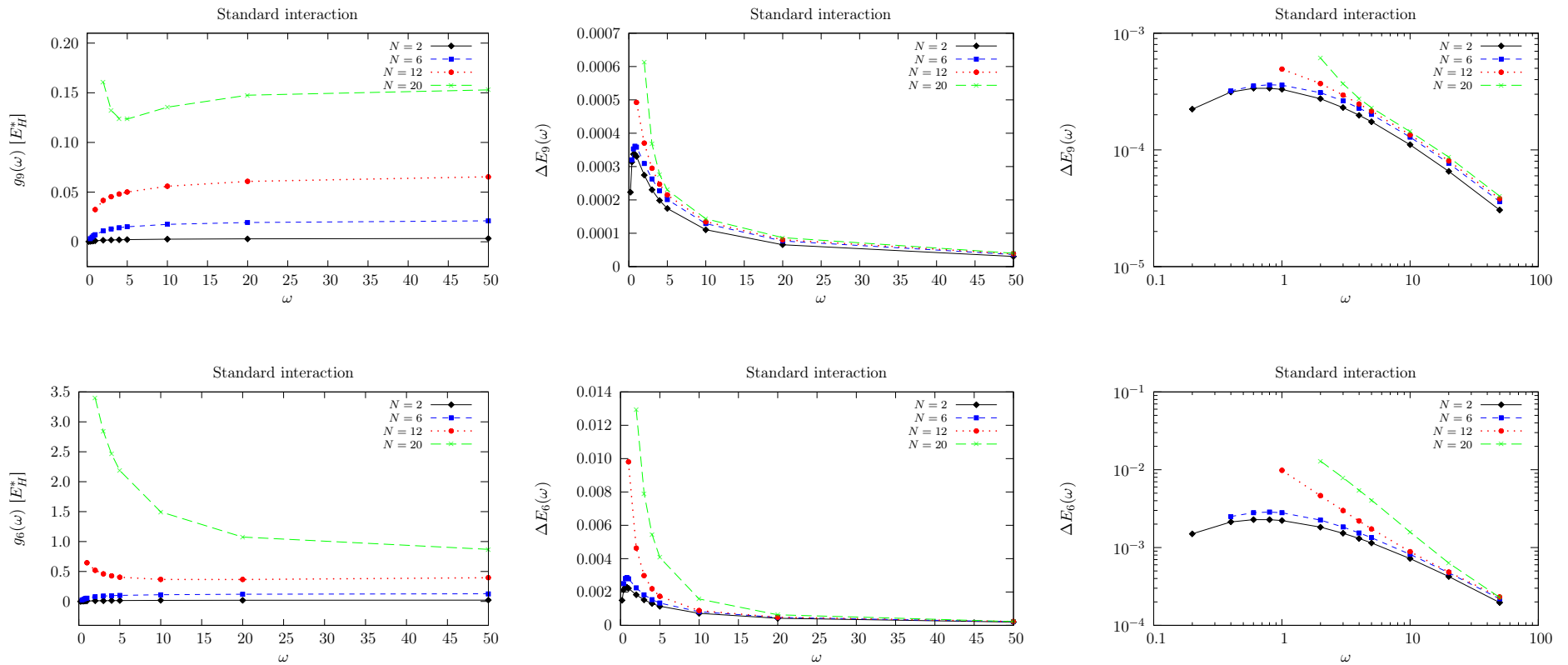


Figure 8.11: In the first column, the difference between the CCSD energy for $R^b = 10$ and $R^b = 6/R^b = 9$ as function of oscillator frequency ω is shown. See definitions of $g_6(\omega)$ and $g_9(\omega)$ in Eqs. (8.75) and (8.76). Energy is measured in effective Hartrees (E_H^*). The relative errors ($\Delta E_6(\omega)$ and $\Delta E_9(\omega)$) are defined in Eqs. 8.77 and 8.78, respectively) are shown in the second column, with corresponding logarithm plots in the third column.

8.1.8 Hartree-Fock Basis

We have till now used the harmonic oscillator functions as basis functions. These are given by Eq. (8.15). An other possibility is to use Hartree-Fock orbitals. The main idea is that we want to include some of the correlations in the basis. In order to generate a HF basis we first run a HF calculation yielding a set of orthonormal HF orbitals,

$$\mathcal{B}_{\text{HF}} = \{\varphi_a(\mathbf{r})\}_{a=1}^{d_b}, \quad (8.84)$$

where

$$\varphi_a(\mathbf{r}) = \sum_{\alpha=1}^{d_b} C_{a\alpha} \psi_{\alpha}(\mathbf{r}) \quad (8.85)$$

and

$$\mathcal{B}_1 = \{\psi_{\alpha}(\mathbf{r})\}_{\alpha=1}^{d_b} \quad (8.86)$$

are the harmonic oscillator functions. We donte the dimension of the model space by d_b . Using \mathcal{B}_{HF} as basis, the single-particle matrix elements are given as

$$\langle a|h|b \rangle = \sum_{\alpha\beta}^{d_b} {}^*_{a\alpha b\beta} \langle \alpha|h|\beta \rangle, \quad (8.87)$$

and the interaction elements as

$$\langle ab|v|cd \rangle = \sum_{\alpha\beta\gamma\delta}^{d_b} C_{a\alpha}^* C_{b\beta}^* C_{c\gamma} C_{d\delta} \langle \alpha\beta|v|\gamma\delta \rangle. \quad (8.88)$$

The expansion coefficients are determined by the HF calculation.

ω	R^b	$N = 2$	$N = 6$	$N = 12$	$N = 20$
0.4	2				
	4				
	6				
	8				
	10				
1.0	2				
	4				
	6				
	8				
	10				
5.0	2				
	4				
	6				
	8				
	10				

Table 8.10: CCSD results obtained for $N = 2, 6, 12$ and 20 by using Hartree-Fock basis (see Eq. 8.84). We have tabulated the energies for frequencies $\omega = 0.4, 1.0$ and 5.0 , and model space $R^b = 2, 4, 6, 8$ and 10 .

8.2 Effective Interaction

The two-body part of the Hamiltonian is given by the repulsive Coulomb interaction. Since our model space cannot include all possible single-particle states (harmonic oscillator functions), the basis must be truncated in CC calculations. This is the case for other wavefunction-based methods such as Hartree-Fock and Configuration Interaction (CI). The number of Slater

determinants increases exponentially with respect to the size of the basis. The number of available Slater determinants (n_S) is given by the binomial factor

$$n_S = \binom{n}{N}, \quad (8.89)$$

where n is the number of single-particle states, and N is the number of electrons. In Sec. 8.1 we saw that the energy converges relatively slow, meaning that we need a large model space in order to obtain an energy that is close to the exact value. However, as pointed out above, the dimensionalities of the Hilbert space must be reduced. A common way to circumvent the dimensionality problem is to introduce a renormalized Coulomb interaction, called effective interaction, that is defined in the model space. Effective Hamiltonians and interactions are commonly used in nuclear shell-model calculations [46, 47]. We will not give a profound presentation of the nuclear effective interaction theory. We refer to [47, 48, 49] for further reading. Put simply, an effective Hamiltonian is a Hamiltonian that reproduces exact eigenvalues of the full problem within a finite-dimensional model space [50]. We will in the following give a brief overview of the basic ideas.

Assume that the N -electron Hilbert space is finite-dimensional, i.e. $n = \dim(\mathcal{H}_N)$. The spectral decomposition of the Hamiltonian reads

$$\hat{H} = \sum_{k=1}^n E_k |\Psi_k\rangle\langle\Psi_k|, \quad (8.90)$$

where $\{|\Psi_k\rangle\}_{k=1}^n$ is the orthonormal set of energy eigenfunctions satisfying

$$\hat{H}|\Psi_k\rangle = E_k |\Psi_k\rangle, \quad (8.91)$$

where E_k is the energy eigenvalue that corresponds to $|\Psi_k\rangle$. We define the model space $\mathcal{P} \subset \mathcal{H}$ as

$$\mathcal{P} \equiv \text{span}\{|\epsilon_k\rangle : k = 1, 2, \dots, m\}, \quad (8.92)$$

where $\{|\epsilon_k\rangle\}_{k=1}^m$ is an orthonormal basis, and $m = \dim(\mathcal{P})$. Furthermore, we define the operator \hat{P} as the orthogonal projector of \mathcal{P} . Its spectral decomposition reads

$$\hat{P} = \sum_{i=1}^m |\epsilon_i\rangle\langle\epsilon_i|. \quad (8.93)$$

The orthogonal complement of \mathcal{P} is $\mathcal{Q} \subset \mathcal{H}_N$, which is often called the excluded space. Its orthogonal projector reads

$$\hat{Q} = 1 - \sum_{i=1}^m |\epsilon_i\rangle\langle\epsilon_i| \quad (8.94)$$

$$= \sum_{i=(m+1)}^n |\epsilon_i\rangle\langle\epsilon_i|, \quad (8.95)$$

The dimension of \mathcal{Q} is $l = \dim(\mathcal{Q}) = n - m$. We have now divided \mathcal{H}_N into \mathcal{P} and \mathcal{Q} . This division transfers to operators in \mathcal{H}_N . An arbitrary operator \hat{A} splits up in four parts, viz.

$$\hat{A} = (\hat{P} + \hat{Q}) \hat{A} (\hat{P} + \hat{Q}) = \hat{P}\hat{A}\hat{P} + \hat{P}\hat{A}\hat{Q} + \hat{Q}\hat{A}\hat{P} + \hat{Q}\hat{A}\hat{Q}, \quad (8.96)$$

since

$$\hat{P} + \hat{Q} = 1. \quad (8.97)$$

We see that $\widehat{P}\widehat{A}\widehat{P}$ maps \mathcal{P} into itself, $\widehat{P}\widehat{A}\widehat{Q}$ maps \mathcal{Q} into \mathcal{P} , and so forth. It is convenient to picture this in the following block (matrix) form:

$$\widehat{A} = \begin{pmatrix} \widehat{P}\widehat{A}\widehat{P} & \widehat{P}\widehat{A}\widehat{Q} \\ \widehat{Q}\widehat{A}\widehat{P} & \widehat{Q}\widehat{A}\widehat{Q} \end{pmatrix} \quad (8.98)$$

We define the similarity transformed Hamiltonian as

$$\widehat{H}' \equiv e^{-\widehat{S}}\widehat{H}e^{\widehat{S}}, \quad (8.99)$$

where \widehat{H} is the Hamiltonian of the system, and \widehat{S} is chosen such that

$$\widehat{Q}\widehat{H}'\widehat{P} = \widehat{P}\widehat{H}'\widehat{Q} = 0. \quad (8.100)$$

This is called the de-coupling equation. The effective Hamiltonian is defined as

$$\widehat{H}_{\text{eff}} \equiv \widehat{P}\widehat{H}'\widehat{P}. \quad (8.101)$$

Since similarity transformations preserve eigenvalues, the m eigenvalues of \widehat{H}_{eff} are identical to some of the n eigenvalues of \widehat{H} . We assume that the eigenvalues of E_k in Eq. (8.90) are arranged so that E_k ($k = 1, \dots, m$) are reproduced by \widehat{H}_{eff} . Furthermore, we define the effective interaction as

$$\widehat{V}_{\text{eff}} = \widehat{H}_{\text{eff}} - \widehat{P}\widehat{H}_0\widehat{P}, \quad (8.102)$$

where \widehat{H}_0 is the Hamiltonian of the non-interacting system. Here we assume that

$$[\widehat{H}_0, \widehat{P}] = 0, \quad (8.103)$$

which is satisfied when the model space is spanned by the eigenvectors (Slater determinants) of \widehat{H}_0 .

We have calculated a 2-particle effective interaction for the parabolic quantum dot by [51]. Calculating the effective interaction for the N -electron system in a large basis would not bring in computational advantages. The diagonalization problem is therefore solved for a sub-cluster Hamiltonian consisting of 2 electrons, leading to missing many-body correlations for $N > 2$. The diagonalization is done by first defining the relative coordinates as

$$\mathbf{r} \equiv \mathbf{r}_1 - \mathbf{r}_2, \quad (8.104)$$

and the centre-of-mass coordinates as

$$\mathbf{R} \equiv \frac{1}{2}(\mathbf{r}_1 + \mathbf{r}_2), \quad (8.105)$$

where \mathbf{r}_1 and \mathbf{r}_2 are the position vector of electron 1 and 2, respectively. The time-independent Schrödinger equation

$$\left[-\frac{\hbar^2}{2m^*} \nabla_1^2 - \frac{\hbar^2}{2m^*} \nabla_2^2 + \frac{1}{2}m^*\omega^2 r_1^2 + \frac{1}{2}m^*\omega^2 r_2^2 + \frac{e^2}{4\pi\epsilon_0\epsilon_r} \frac{1}{r_{12}} \right] \Psi(\mathbf{r}_1, \mathbf{r}_2) = E \Psi(\mathbf{r}_1, \mathbf{r}_2) \quad (8.106)$$

is separable in \mathbf{r} and \mathbf{R} . Inserting

$$\Psi(\mathbf{R}, \mathbf{r}) \equiv f_1(\mathbf{R})f_2(\mathbf{r}) \quad (8.107)$$

into the equation yields

$$\left[\frac{\hbar^2}{4m^*} \nabla_{\mathbf{R}}^2 + m^*\omega^2 \mathbf{R}^2 \right] f_1(\mathbf{R}) = E_1 f_1(\mathbf{R}) \quad (8.108)$$

$$\left[\frac{\hbar^2}{m^*} \nabla_{\mathbf{r}}^2 + \frac{1}{4} \omega^2 r^2 + \frac{e^2}{4\pi\epsilon_0\epsilon_r} \frac{1}{r} \right] f_2(\mathbf{r}) = E_2 f_2(\mathbf{r}). \quad (8.109)$$

The center-of-mass problem is trivial. The relative coordinate problem is solved by using the so-called generalized half-range Hermite functions (see [51]). The m eigenvalues of \hat{H}' will therefore be equal to some of the n eigenvalues of \hat{H} for the 2-electron system.

Using effective interaction in a CCSD calculation means that the standard interaction v is replaced by an effective interaction v_{eff} , viz.

$$\langle \alpha\beta | v | \gamma\delta \rangle \rightarrow \langle \alpha\beta | v_{\text{eff}} | \gamma\delta \rangle. \quad (8.110)$$

In order to obtain a well-defined effective interaction we must work with the energy cut model space (EC). This is because EC contains all the symmetries of the interaction. By using the DP model space we would break essential symmetries such as conservation of center-of-mass momentum.

8.2.1 Tables of Numerical Results

The HF and CCSD results obtained with effective interaction are tabulated in Tables 8.5-8.8. We have done calculations for systems containing 2, 6, 12 and 20 electrons, and frequencies $\omega = 0.2 - 50.0$. The CCSD energy with $R^b = 10$ does not converge for $\omega = 0.2$ ($N = 6$), $\omega = 0.2 - 0.8$ ($N = 12$) and $\omega = 0.2 - 1.0$ ($N = 20$).

Appendix A

Mathematical Derivations

A.1 Solution of the Single-Electron Schrödinger Equation

We will now derive the solution of

$$-\frac{\hbar^2}{2m^*} \left(\frac{d^2}{dr^2} + \frac{1}{r} \frac{d}{dr} - \frac{m^2}{r^2} + \frac{emB_0}{\hbar} \right) R(r) + \left(\frac{1}{2} m^* \omega^2 r^2 - \varepsilon_r \right) R(r) = 0, \quad (\text{A.1})$$

where $R(r)$ is the radial part of the energy eigenfunction, and ε_r is the energy eigenvalue (spatial contribution). See Sec. 4.3). This is the radial Schrödinger equation for a single-electron parabolic quantum dot subjected to a constant magnetic field in the z-direction. The idea is to build up an ansatz by considering the limits $r \rightarrow 0$ and $r \rightarrow \infty$. When $r \rightarrow 0$, m^2/r^2 dominates completely, and Eq. (A.1) reduces to

$$r^2 \frac{d^2 R(r)}{dr^2} + r \frac{dR(r)}{dr} - m^2 R(r) = 0. \quad (\text{A.2})$$

We make the ansatz

$$R(r) = r^s, \quad (\text{A.3})$$

and insert this expression into Eq. (A.2), yielding

$$s(s-1)r^s + sr^s - m^2 r^s = 0.$$

We thus obtain that

$$s = |m|, \quad (\text{A.4})$$

leading to

$$\lim_{r \rightarrow 0} R(r) = r^{absm}, \quad (\text{A.5})$$

where $R(r)$ is the solution of Eq.(A.1). Furthermore, in the limit $r \rightarrow \infty$, $\frac{1}{2}m^*\omega^2r^2$ dominates, and Eq. (A.1) reduces to

$$\frac{d^2 R(r)}{dr^2} + \frac{1}{r} \frac{dR(r)}{dr} - \frac{m^{*2}\omega^2r^2}{\hbar^2} R(r) = 0. \quad (\text{A.6})$$

We make the ansatz

$$R(r) = e^{tr^2}, \quad (\text{A.7})$$

where t is a constant, and insert this expression into Eq. (A.6), yielding

$$4t^2r^2 + 4t - \frac{m^{*2}\omega^2r^2}{\hbar^2} = 0. \quad (\text{A.8})$$

We obtain that

$$t = \pm \frac{m^* \omega}{2\hbar}. \quad (\text{A.9})$$

Mathematics allow both negative and positive values of t . However, a positive value leads to a wavefunction that cannot be normalized. Thus we choose the negative value. We obtain that

$$\lim_{r \rightarrow \infty} R(r) = e^{-\frac{m^* \omega}{2\hbar} r^2}. \quad (\text{A.10})$$

We now make the following ansatz to the solution of Eq. (A.6),

$$R(r) = r^{|m|} e^{-\frac{m^* \omega}{2\hbar} r^2} g(r), \quad (\text{A.11})$$

where $g(r)$ is a function that must satisfy

$$\lim_{r \rightarrow 0} g(r) = 1 \quad (\text{A.12})$$

$$\lim_{r \rightarrow \infty} g(r) = \frac{1}{r^{|m|}}. \quad (\text{A.13})$$

Inserting the ansatz into Eq. (A.1) yields

$$\begin{aligned} -\frac{\hbar^2}{2m^*} \left[\frac{d^2 g(r)}{dr^2} + \left(1 + 2|m| - \frac{2m^* \omega}{\hbar} r^2 \right) \frac{1}{r} \frac{dg(r)}{dr} - \frac{2m^* \omega}{\hbar} (1 + |m|) g(r) + \frac{m^{*2} \omega^2}{\hbar^2} r^2 g(r) \right] \\ + \left(\frac{1}{2} m^* \omega^2 r^2 - \varepsilon_r - \frac{em\hbar B_0}{2m^*} \right) g(r) = 0. \end{aligned} \quad (\text{A.14})$$

We define

$$\Lambda \equiv \frac{2m^* \varepsilon_r}{\hbar^2} + \frac{emB_0}{\hbar}, \quad (\text{A.15})$$

and

$$\beta \equiv \frac{m^* \omega}{\hbar}. \quad (\text{A.16})$$

By using the definitions above we obtain

$$\frac{d^2 g(r)}{dr^2} + (1 + 2|m| - 2\beta r^2) \frac{1}{r} \frac{dg(r)}{dr} - 2\beta (1 + |m|) g(r) + \Lambda g(r) = 0. \quad (\text{A.17})$$

Furthermore, we define

$$x = \beta r^2 \quad (\text{A.18})$$

$$\lambda = \frac{1}{2} \left(\frac{\Lambda}{2\beta} - |m| - 1 \right), \quad (\text{A.19})$$

leading to

$$x \frac{d^2 g(x)}{dx^2} + (1 + |m| - x) \frac{dg(x)}{dx} + \lambda g(x) = 0. \quad (\text{A.20})$$

This equation is called the associated Laguerre differential equation, and the solutions are the Laguerre polynomials. We assume $g(x)$ is analytic in the region $0 < x < \infty$. The Laurent series is given as [6]

$$g(x) = \sum_{n=0}^{\infty} a_n x^{n+s}, \quad (\text{A.21})$$

where s is real number and $a_0 \neq 0$. Inserting Eq. (A.21) into Eq. (A.20), yields

$$\begin{aligned} & x \sum_{n=0}^{\infty} a_n (n+s)(n+s-1) x^{n+s-2} \\ & g + (1+|m|-x) \sum_{n=0}^{\infty} a_n (n+s) x^{n+s-1} \\ & + \lambda \sum_{n=0}^{\infty} a_n x^{n+s} = 0. \end{aligned} \quad (\text{A.22})$$

After changing some dummy indices we obtain

$$\begin{aligned} & \sum_{n=0}^{\infty} a_n (n+s)(n+s-1) x^{n+s-1} \\ & + (1+|m|) \sum_{n=0}^{\infty} a_n (n+s) x^{n+s-1} \\ & - \sum_{n=1}^{\infty} a_{n-1} (n+s-1) x^{n+s-1} \\ & + \lambda \sum_{n=1}^{\infty} a_{n-1} x^{n+s-1} = 0. \end{aligned} \quad (\text{A.23})$$

For $n = 0$ we obtain

$$a_0 s(s-1) + a_0 s(1+|m|) = 0$$

leading to

$$s(s+|m|) = 0. \quad (\text{A.24})$$

Thus we have two possibilities: $s = 0$ and $s = -|m|$. However, when $s = -|m|$, the eigenvectors diverge at $x = 0$. We must therefore choose $s = 0$. The equation reduces to

$$\begin{aligned} & \sum_{n=0}^{\infty} a_n n(n-1) x^{n-1} \\ & + (1+|m|) \sum_{n=0}^{\infty} a_n n x^{n-1} \\ & - \sum_{n=1}^{\infty} a_{n-1} (n-1) x^{n-1} \\ & + \lambda \sum_{n=1}^{\infty} a_{n-1} x^{n-1} = 0. \end{aligned} \quad (\text{A.25})$$

For $n \geq 1$ we obtain the following recurrence relation

$$a_{n+1} = \frac{n-\lambda}{(n+1)(1+|m|+n)} a_n. \quad (\text{A.26})$$

Given a boundary condition, the constant a_0 can be determined, yielding a_n for $n \geq 1$. Thus have found the the solution of Eq. (A.1). It is given by Eqs. (A.11) and (A.21), with $s = 0$ and a_n determined by Eq. (A.21). We obtain the following expression for $g(x)$,

$$g(x) = \left[1 - \frac{\lambda}{1+|m|} x - \frac{(1-\lambda)\lambda}{2(1+|m|)(2+|m|)} x^2 + \dots \right] a_0. \quad (\text{A.27})$$

We observe that the series converges when $\lambda \geq 0$. The normalization condition requires that the series terminate after a certain n . This is obtained when

$$n = \lambda. \quad (\text{A.28})$$

We end up with the following allowed values for n (and λ),

$$n = 0, 1, 2, 3, 4, \dots \quad (\text{A.29})$$

Since Eq. (A.20) can be written as

$$\hat{D}g(x) = 0, \quad (\text{A.30})$$

where

$$\hat{D} = x \frac{d^2}{dx^2} + (1 + |m| - x) + \lambda, \quad (\text{A.31})$$

we can remove a_0 from Eq. (A.27). The solutions of Eq. (A.20) are the associated Laguerre polynomials $L_n^{|m|}$. The Rodrigues representation is given as

$$L_n^{|m|}(x) = \frac{e^x x^{-|m|}}{n!} \frac{d^2}{dx^2} \left(e^{-x} x^{n+|m|} \right). \quad (\text{A.32})$$

The polynomials can also be written as a finite series,

$$\sum_{k=0}^n (-1)^k \frac{(n+|m|)!}{(n-k)!(|m|+k)!k!} x^k. \quad (\text{A.33})$$

We finally obtain the solutions of Eq. (A.1),

n	$L_n^{ m }(x)$
0	1
1	$1 + m - x$
2	$\frac{1}{2} (1 + m) (2 + m) - 2 (2 + m) x + x^2$

Table A.1: Lowest order associated Laguerre polynomials.

$$R(r)_{nm} = \mathcal{K}_{nm} r^{|m|} e^{-\frac{1}{2}\beta r^2} L_n^{|m|}(\beta r^2), \quad (\text{A.34})$$

where \mathcal{K}_{nm} is the normalization constant determined by

$$1 = \mathcal{K}^2 \int_0^\infty \left| r^{|m|} e^{-\frac{1}{2}\beta r^2} L_n^{|m|}(\beta r^2) \right|^2 r dr. \quad (\text{A.35})$$

The spatial part of the eigenfunctions reads (see Sec. 4.3)

$$\phi_{nm}(r) = \sqrt{\frac{n!}{\pi(n+|m|)!}} \beta^{\frac{1}{2}(1+|m|)} r^{|m|} e^{-\frac{1}{2}\beta r^2} L_n^{|m|}(\beta r^2) e^{im\phi}, \quad (\text{A.36})$$

where

$$n = 0, 1, 2, 3, \dots \quad (\text{A.37})$$

$$m = 0, \pm 1, \pm 2, \pm 3, \dots \quad (\text{A.38})$$

The energy eigenvalue ε_r is determined by combining Eqs. (A.28) and (A.19) into

$$\Lambda_{nm} = 2\beta (1 + |m| + 2n). \quad (\text{A.39})$$

Inserting the in Eq. (A.15) finally yields

$$\varepsilon_{r,nm} = (1 + |m| + 2n) \hbar\omega + m\hbar\omega_B, \quad (\text{A.40})$$

where ω_B is defined in (4.47).

Bibliography

- [1] P. C. Hemmer, *Kvantemekanikk*. Tapir Akademisk Forlag, fifth ed., 2005.
- [2] D. J. Griffiths, *Introduction to Quantum Mechanics*. Pearson Prentice Hall, first ed., 2005.
- [3] R. Shankar, *Principles of Quantum Mechanics*. Plenum Press, 1994.
- [4] D. C. Lay, *Linear Algebra*. Pearson, 2006.
- [5] E. Merzbacher, *Quantum Mechanics*. Wiley, 1970.
- [6] M. L. Boas, *Mathematical Methods in the Physical Sciences*. Wiley, 2006.
- [7] W. H. Dickhoff and D. V. Neck, *Many-Body Theory Exposed!* World Scientific, second ed., 2008.
- [8] F. Mandl and G. Shaw, *Quantum Field Theory*. Wiley, 1993.
- [9] R. M. Dreizler and E. K. U. Gross, *Density Functional Theory - An Approach to the Quantum Many-Body Problem*. Springer, 1990.
- [10] A. Kumar, S. E. Laux, and F. Stern, “Electron states in a gaas quantum dot in a magnetic field,” *Phys. Rev. B*, vol. 42, no. 8, p. 5166, 1990.
- [11] M. Macucci, K. Hess, and G. J. Iafrate, “Electronic energy spectrum and the concept of capacitance in quantum dots,” *Phys. Rev. B*, vol. 48, no. 23, p. 17354, 1993.
- [12] M. Macucci, K. Hess, and G. J. Iafrate, “Numerical simulation of shell-filling effects in circular quantum dots,” *Phys. Rev. B*, vol. 55, no. 8, p. R4879, 1997.
- [13] M. Stopa, “Quantum dot self-consistent electronic structure and the coulomb blockade,” *Phys. Rev. B*, vol. 54, no. 19, p. 13767, 1996.
- [14] D. Heitmann and J. P. Kotthaus, “The spectroscopy of quantum dot arrays,” *Physics Today*, vol. 46, p. 56, 1993.
- [15] D. Heitmann, “Far infrared spectroscopy of quantum-dots and antidot arrays,” *Physica B: Condensed Matter*, vol. 212, no. 3, p. 201, 1995.
- [16] W. Kohn, “Cyclotron resonance and de haas-van alphen oscillations of an interacting electron gas,” *Phys. Rev.*, vol. 123, no. 4, p. 1242, 1961.
- [17] L. Brey, N. F. Johnson, and B. I. Halperin, “Optical and magneto-optical absorption in parabolic quantum wells,” *Phys. Rev. B*, vol. 40, no. 15, p. 10647, 1989.
- [18] F. M. Peeters, “Magneto-optics in parabolic quantum dots,” *Phys. Rev. B*, vol. 42, no. 2, p. 1486, 1990.
- [19] C. Sikorski and U. Merkt, “Spectroscopy of electronic states in insb quantum dots,” *Phys. Rev. Lett.*, vol. 62, no. 18, p. 2164, 1989.

- [20] J. M. Leinaas, "Classical mechanics and electrodynamics." Lecture Notes FYS3120, University of Oslo, 2008.
- [21] M. B. Tavernier, E. Anisimovas, F. M. Peeters, B. Szafran, J. Adamowski, and S. Bednarek, "Four-electron quantum dot in a magnetic field," *Phys. Rev. B*, vol. 68, no. 20, p. 205305, 2003.
- [22] T. M. Henderson, K. Runge, and R. J. Bartlett, "Excited states in artificial atoms via equation-of-motion coupled cluster theory," *Phys. Rev. B*, vol. 67, no. 4, p. 045320, 2003.
- [23] I. Heidari, S. Pal, B. S. Pujari, and D. G. Kanhere, "Electronic structure of spherical quantum dots using coupled cluster method," *The Journal of Chemical Physics*, vol. 127, no. 11, p. 114708, 2007.
- [24] E. Rasanen, S. Pittalis, J. G. Vilhena, and M. A. L. Marques, "Semi-local density functional for the exchange-correlation energy of electrons in two dimensions," *ArXiv e-prints*, 2010.
- [25] J. M. Thijssen, *Computational Physics*. Cambridge University Press, 2007.
- [26] E. Schrödinger, "An undulatory theory of the mechanics of atoms and molecules," *Phys. Rev.*, vol. 28, no. 6, p. 1049, 1926.
- [27] J. C. Slater, "The theory of complex spectra," *Phys. Rev.*, vol. 34, no. 10, p. 1293, 1929.
- [28] M. P. Lohne, "Hartree-fock, improved variational monte carlo and density functional theory." Project FYS4410, University of Oslo, 2009.
- [29] M. P. Lohne, "Variational monte carlo studies of light atoms." Project FYS4410, University of Oslo, 2009.
- [30] E. K. U. Gross, L. N. Oliveira, and W. Kohn, "Rayleigh-ritz variational principle for ensembles of fractionally occupied states," *Phys. Rev. A*, vol. 37, no. 8, p. 2805, 1988.
- [31] R. van Leeuwen, "Density functional approach to the many-body problem: Key concepts and exact functionals," vol. 43, p. 25, Academic Press, 2003.
- [32] E. Clementi and C. Roetti, *Atomic Data and Nuclear Data Tables Volume 14 - Roothaan-Hartree-Fock Atomic Wavefunctions*. Academic Press, 1974.
- [33] J. Čížek, "On the correlation problem in atomic and molecular systems. calculation of wavefunction components in ursell-type expansion using quantum-field theoretical methods," *The Journal of Chemical Physics*, vol. 45, no. 11, p. 4256, 1966.
- [34] J. Čížek *Advances in Chemical Physics*, vol. 14, 1969.
- [35] A. C. Hurley, *Electron correlation in small molecules*. Academic Press, 1976.
- [36] H. J. Monkhorst *Int. J. Quantum Chem. Symp.*, vol. 11, no. 421, 1977.
- [37] G. D. P. III and R. J. Bartlett, "A full coupled-cluster singles and doubles model: The inclusion of disconnected triples," *The Journal of Chemical Physics*, vol. 76, no. 4, p. 1910, 1982.
- [38] F. E. Harris, H. J. Monkhorst, and D. L. Freeman, *Algebraic and diagrammatic methods in many-fermion theory*. Oxford University Press, 1992.
- [39] S. Raimes, *Many-Electron Theory*. North-Holland Publishing Company, 1972.
- [40] T. D. Crawford and H. F. Schaefer, "An introduction to coupled cluster theory for computational chemists," *Reviews in Computational Chemistry*, vol. 14, 2007.

-
- [41] D. Yang, *C++ and Object-Oriented Numeric Computing*. Springer, 2001.
 - [42] H. P. Langtangen, *Python Scripting for Computational Science*. Springer, 2008.
 - [43] P. Merlot, “Many-body approaches to quantum dots,” 2009.
 - [44] M. Rontani, *Electronic States in Semiconductor Quantum Dots*. PhD thesis, Universita degli Studi di Modena e Reggio Emilia, 1999.
 - [45] P.-O. Löwdin, “Quantum theory of many-particle systems. iii. extension of the hartree-fock scheme to include degenerate systems and correlation effects,” *Phys. Rev.*, vol. 97, no. 6, p. 1509, 1955.
 - [46] P. Navrátil, J. P. Vary, and B. R. Barrett, “Large-basis ab initio no-core shell model and its application to ^{12}c ,” *Phys. Rev. C*, vol. 62, no. 5, p. 054311, 2000.
 - [47] D. J. Dean, T. Engeland, M. Hjorth-Jensen, M. P. Kartamyshev, and E. Osnes, “Effective interactions and the nuclear shell-model,” *Prog. Part. Nucl. Phys.*, vol. 53, no. 419, 2004.
 - [48] P. J. Ellis and E. Osnes, “An introductory guide to effective operators in nuclei,” *Rev. Mod. Phys.*, vol. 49, no. 4, p. 777, 1977.
 - [49] M. Hjorth-Jensen, T. T. S. Kuo, and E. Osnes, “Realistic effective interactions for nuclear systems,” *Physics Reports*, vol. 261, no. 3-4, p. 125, 1995.
 - [50] S. Kvaal, *Analysis of many-body methods for quantum dots*. PhD thesis, University of Oslo, 2009.
 - [51] S. Kvaal, “Open source fci code for quantum dots and effective interactions,” *arXiv:0810.2644v1*, 2008.